DISEASE TRANSMISSION AND PERSISTENCE IN DYNAMIC LANDSCAPES

Tobias Kürschner

Univ.-Diss.

zur Erlangung des akademischen Grades
"doctor rerum naturalium" (Dr. rer. nat.)
in der Wissenschaftsdisziplin "Ökologie"

eingereicht als publikationsbasierte Dissertation an der
Mathematisch-Naturwissenschaftlichen Fakultät des
Instituts für Biochemie und Biologie
der Universität Potsdam

Ort und Tag der Disputation: Potsdam, 23.09.2022

1. Gutachter/in: Prof. Dr. Stephanie Kramer-Schadt

2. Gutachter/in: Prof. Dr. Volker Grimm

3. Gutachter/in: Prof. Dr. Uta Berger

Published online on the
Publication Server of the University of Potsdam:
https://doi.org/10.25932/publishup-56468
https://nbn-resolving.org/urn:nbn:de:kobv:517-opus4-564689

Abstract

Infectious diseases are an increasing threat to biodiversity and human health. Therefore, developing a general understanding of the drivers shaping host-pathogen dynamics is of key importance in both ecological and epidemiological research. Disease dynamics are driven by a variety of interacting processes such as individual host behaviour, spatiotemporal resource availability or pathogen traits like virulence and transmission. External drivers such as global change may modify the system conditions and, thus, the disease dynamics. Despite their importance, many of these drivers are often simplified and aggregated in epidemiological models and the interactions among multiple drivers are neglected.

In my thesis, I investigate disease dynamics using a mechanistic approach that includes both bottom-up effects - from landscape dynamics to individual movement behaviour - as well as top-down effects - from pathogen virulence on host density and contact rates. To this end, I extended an established spatially explicit individual-based model that simulates epidemiological and ecological processes stochastically, to incorporate a dynamic resource landscape that can be shifted away from the timing of host population-dynamics (chapter 2). I also added the evolution of pathogen virulence along a theoretical virulence-transmission trade-off (chapter 3). In chapter 2, I focus on bottom-up effects, specifically how a temporal shift of resource availability away from the timing of biological events of host-species - as expected under global change - scales up to host-pathogen interactions and disease dynamics. My results show that the formation of temporary disease hotspots in combination with directed individual movement acted as key drivers for pathogen persistence even under highly unfavourable conditions for the host. Even with drivers like global change further increasing the likelihood of unfavourable interactions between host species and their environment, pathogens can continue to persist with heir hosts. In chapter 3, I demonstrate that the top-down effect caused by pathogen-associated mortality on its host population can be mitigated by selection for lower virulent pathogen strains when host densities are reduced through mismatches between seasonal resource availability and host life-history events. I chapter 4, I combined parts of both theoretical models into a new model that includes individual host movement decisions and the evolution of pathogenic virulence to simulate pathogen outbreaks in realistic landscapes. I was able to match simulated patterns of pathogen spread to observed patterns from long-term outbreak data of classical swine fever in wild boar in Northern Germany. The observed disease course was best explained by a simulated high virulent strain, whereas sampling schemes and vaccination campaigns could explain differences in the age-distribution of infected hosts. My model helps to understand and disentangle how the combination of individual decision making and evolution of virulence can act as important drivers of pathogen spread and persistence.

As I show across the chapters of this thesis, the interplay of both bottom-up and top-down processes is a key driver of disease dynamics in spatially structured host populations, as they ultimately shape host densities and contact rates among moving individuals. My findings are an important step towards a paradigm shift in disease ecology away from simplified assumptions towards the inclusion of mechanisms, such as complex multi-trophic interactions, and their feedbacks on pathogen spread and disease persistence. The mechanisms presented here should be at the core of realistic predictive and preventive epidemiological models.

Zusammenfassung

Infektionskrankheiten stellen eine zunehmende Bedrohung für die biologische Vielfalt und die menschliche Gesundheit dar. Daher ist es sowohl für die epidemiologische als auch für die ökologische Forschung von zentraler Bedeutung, ein allgemeines Verständnis der Mechanismen, die die Wirts-Pathogen-Dynamik beeinflussen, zu entwickeln. Die Krankheitsausbrüche werden durch eine Vielzahl von interagierenden Prozessen angetrieben, wie unter anderem individuellem Wirtsverhalten, Ressourcenverfügbarkeit oder Erregermerkmale wie Virulenz. Externe Faktoren wie der globale Wandel können grundlegende Veränderungen dieser Prozesse verursachen und sich damit auch auf Krankheitsdynamiken auswirken. Trotz ihrer Bedeutung für Krankheitsausbrüche werden viele dieser Faktoren in epidemiologischen Modellen oft vereinfacht und die Wechselwirkungen zwischen den Faktoren vernachlässigt. In Anbetracht dessen, ist es sowohl für die ökologische als auch für die epidemiologische Forschung von zentraler Bedeutung, ein allgemeines Verständnis dafür zu entwickeln, wie mehrere interagierende Prozesse Wirts-Pathogen-Interaktionen beeinflussen können.

In meiner Dissertation untersuche ich die Krankheitsdynamik mittels eines mechanistischen Ansatzes, der sowohl Bottom-up-Effekte - von der Landschaftsdynamik bis zum individuellen Bewegungsverhalten - als auch Top-down-Effekte - von der Virulenz des Erregers auf die Wirtsdichte und die Kontaktraten - berücksichtigt. Zu diesem Zweck habe ich ein etabliertes, räumlich explizites, Individuen basiertes Modell, das epidemiologische und ökologische Prozesse stochastisch simuliert, um eine dynamische Ressourcenlandschaft erweitert, die zeitlich mit der Populationsdynamik der Wirte verschoben werden kann (Kapitel 2). Zusätzlich habe ich die Evolution der Virulenz von Krankheitserregern entlang eines theoretischen Verhältnisses zwischen Virulenz und Übertragung hinzugefügt (Kapitel 3). In Kapitel 2 konzentriere ich mich auf Bottom-up-Effekte, insbesondere auf die Frage, wie sich eine zeitliche Verschiebung der Ressourcenverfügbarkeit weg vom Zeitpunkt biologischer Ereignisse der Wirtsarten - wie sie im Rahmen des globalen Wandels erwartet wird - auf die Wirt-Pathogen-Interaktionen und Krankheitsdynamiken auswirkt. Meine Ergebnisse zeigen, dass die Bildung vorübergehender Krankheitsherde in Kombination mit gezielter individueller Wirtsbewegung als Schlüsselfaktoren für die Persistenz von Krankheitserregern selbst unter äußerst ungünstigen Bedingungen für den Wirt fungieren. Selbst wenn Faktoren wie der globale Wandel die Wahrscheinlichkeit ungünstiger Wechselwirkungen zwischen Wirtsarten und ihrer Umwelt weiter erhöhen, können Krankheitserreger weiterhin in ihren Wirten persistieren. In Kapitel 3 zeige ich, dass der Top-Down-Effekt, der durch die pathogen-assoziierte Mortalität verursacht wird, durch eine evolutionäre Selektion auf weniger virulente Erregerstämme abgeschwächt werden kann, wenn die Wirtsdichte durch eine zeitliche Verschiebung von saisonaler Ressourcenverfügbarkeit und dem Zeitpunkt von biologischen Ereignissen der Wirtsarten reduziert wird. In Kapitel 4 habe ich Teile der beiden theoretischen Modelle zu einem neuen Modell kombiniert, das individuelle Wirtsbewegungen und die Entwicklung der Virulenz von Krankheitserregern einbezieht, um Ausbrüche von Krankheitserregern in realistischen Landschaften zu simulieren. Es gelang mir, die simulierten Muster der Krankheitsausbreitung mit beobachteten Mustern von Langzeitausbrüchen der klassischen Schweinepest in Wildschweinen in Norddeutschland abzugleichen. Der beobachtete Krankheitsverlauf ließ sich am besten durch einen simulierten hochvirulenten Stamm erklären, während das Design der Probenentnahmen und Impfkampagnen Unterschiede in der Altersverteilung der infizierten Wirte erklären könnten. Mein Modell trägt dazu bei, zu verstehen, wie die Kombination aus individueller

Bewegung und der Evolution von Virulenz als wichtige Treiber für die Ausbreitung und Persistenz des Erregers wirken können.

Wie ich in den Kapiteln dieser Arbeit zeige, ist das Zusammenspiel von Bottom-up- und Top-down-Prozessen ein entscheidender Faktor für die Krankheitsdynamik in Wirtspopulationen, da sie letztlich die Wirtsdichte und den Kontakt zwischen sich bewegenden Individuen bestimmen. Meine Ergebnisse sind ein wichtiger Schritt auf dem Weg zu einem Paradigmenwechsel in der Krankheitsökologie, weg von vereinfachten Annahmen hin zur Einbeziehung von komplexen Interaktionen und deren Rückkopplungen auf die Ausbreitung und Persistenz von Krankheitserregern. Die hier vorgestellten Mechanismen sollten den Kern realistischer Vorhersage- und Präventivmodelle für die Epidemiologie bilden.

Contents

CHAPTER 1

GENERAL INTRODUCTION

1 General Introduction

Infectious diseases are a major threat to biodiversity and human health (Andersen et al., 2020; Patz et al., 2004; Reaser et al., 2021; Williams et al., 2021). Biodiversity loss is exemplified, among others, by the declining bird populations in north America caused by West Nile virus (LaDeau et al., 2007) or the global population decline of many amphibian species through chytridiomycosis infections (Fisher et al., 2009). Furthermore, more than half of the infectious diseases currently affecting humans are believed to be zoonotic in origin (Smith and Guégan, 2010), with the recent SARS-CoV-2 pandemic (Andersen et al., 2020) as a testament to how devastating emerging zoonotic diseases can be to human health.

Host-pathogen interactions at different spatial and temporal scales are the core drivers of disease dynamics. Here, global change (e.g. land-use change, climate change or habitat encroachment) has the potential to alter density, distribution and susceptibility of host individuals with strong implication for the severity and frequency of disease outbreaks (Patz et al., 2004; Wilcox and Gubler, 2005) and spillover events from wildlife to human populations (Allen et al., 2017; Morse et al., 2012; Rulli et al., 2017). Global change can increase spatial and temporal variation in environmental factors, such as the distribution of resources, and induce spatiotemporal mismatches between host life-history events and resource availability (Plard et al., 2014; Visser and Gienapp, 2019). Under the current context of global change, we need not only to understand disease dynamics but also how they might change in the future.

Movement is the prime adaptive trait of animals to track environmental changes (Nathan et al., 2008). At the same time, the decisions individuals make during movement lead to shifts in patterns of population density and distributions on a large scale (Hastings et al., 2011) as well as affecting contact rates at the local scale (Dougherty et al., 2018). For example, asymmetric contacts between infected individuals across age classes or space can lead to cycling of pathogens (Franz et al., 2018; Marescot et al., 2021). This in turn alters disease dynamics (Scherer et al., 2020).

The aim of this thesis is to investigate how movement decisions linked with spatial and temporal variability of resources that affect host population dynamics (e.g. a mismatch between environmental conditions and host life-history) translate into different patterns of spread,

persistence, and evolution of pathogens (Figure 1.1). Movement, as the central host process and adaptive response mechanism to biotic and abiotic changes can be bottom-up influenced from resource distribution as an individual reaction towards tracking environmental cues (Jeltsch et al., 2013; Nathan et al., 2008). In this context, variations in resource availability and abundance influence individual movement and therefore, higher levels such as disease dynamics (Jeltsch et al., 2013; McLeod and Leroux, 2021; Radchuk et al., 2019). On the other hand, the importance of cascading top-down effects on ecological communities is well known (Ripple et al., 2014). Host movement and densities can be top-down regulated by pathogen caused mortality or altering behaviours (Anderson and May, 1979; Lafferty et al., 2008). Therefore, it is not only important to understand the bottom-up regulation (e.g. through landscape configuration and associated movement decisions) of host-pathogen systems but also to understand the direct effect (top-down) that pathogens can exert on their host populations to gain a broader understanding of pathogen persistence and patterns of spread. However, the simultaneous inclusion of bottom-up and top-down processes is a host-pathogen system is a novelty in eco-epidemiological studies.

Many epidemiological models simplified important forces that are exerted on populations into a single transmission rate (Anderson and May, 1991) and neglected key processes such as spatial and temporal landscape variability or individual decision making. However, including complex processes and interactions is key to identify and disentangle important drivers of disease dynamics.

In the following, I am going to introduce the importance of individual host decision-making processes (e.g. movement behaviour) and environmental fluctuations (e.g. seasonality) for disease spread and persistence. Furthermore, I will analyse how the evolution of pathogenic traits, such as virulence and transmission, can exert a strong pressure on host-pathogen systems, and I will emphasize the need for incorporating empirical data into epidemiological models. Lastly, I will introduce the host-pathogen system used in the following chapters of my thesis.

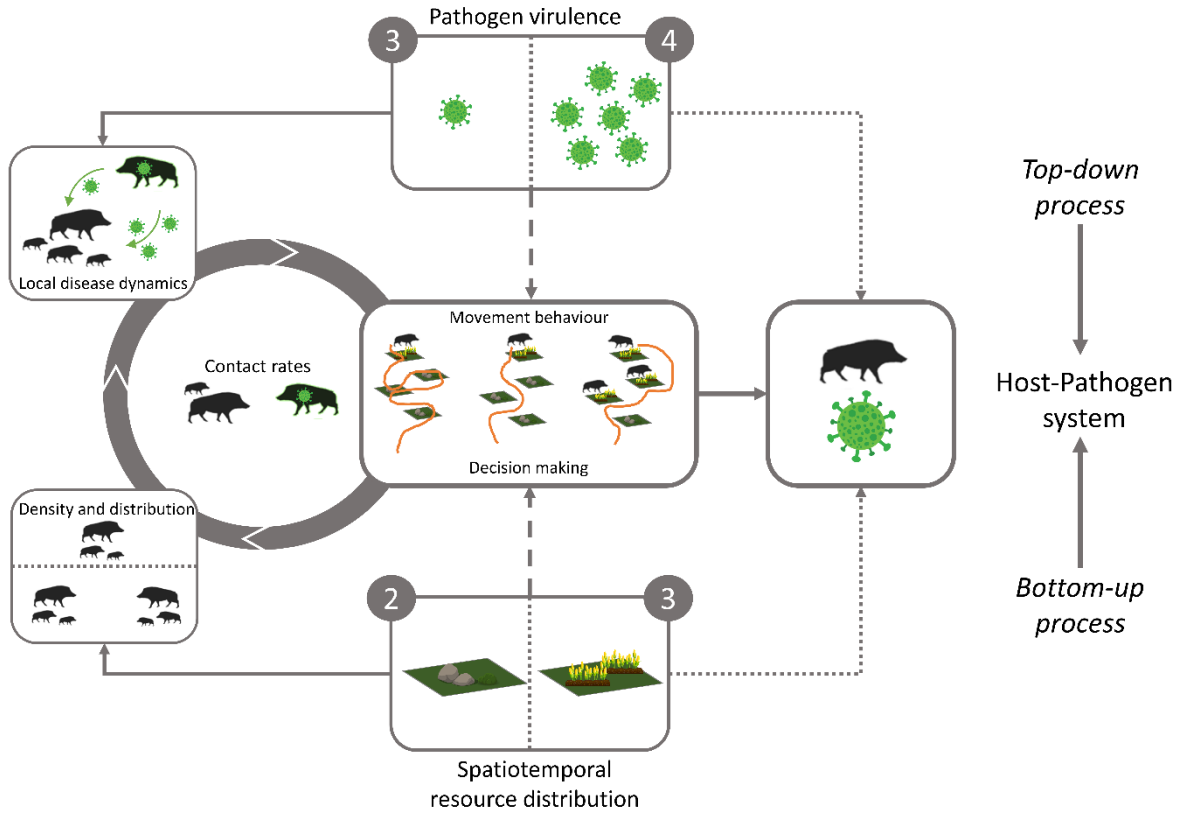

Figure 1.1: Conceptual framework of how bottom-up processes, such as seasonality and resource dynamics, feed back into individual movement decisions, and top-down processes, such as host mortality induced through varying levels of pathogenic virulence, also feed back into host movement decisions. Taken together, bottom-up and top-down processes affect the host-pathogen system and are mediated via movement in a complex interplay of contact rates, local disease dynamics and host density and distribution. Numbers indicate the chapter of this thesis focusing on these processes.

1.1 Moving forward: the relevance of individual-scale mechanisms for understanding infectious disease dynamics

Mathematical mean-field models that assume homogeneous mixing of susceptible and infectious hosts without including spatial factors in the disease transmission process have contributed substantially to our understanding of infectious disease dynamics (Anderson and May, 1982; Hethcote, 2000; Kermack and McKendrick, 1927). One of the best known examples is the classical 'SIR-model' that simulates the overall number of susceptible (S), infected (I), and recovered (R) individuals in the population (Kermack and McKendrick, 1927). Those models assumed that all individuals behave identical and have the same probability for infection. However, the probability of infection is the result of the complex interplay of pathogen and host dynamics (Lloyd-Smith et al., 2005) in heterogeneous landscapes that often feature heterogeneous contact rates (Craft, 2015). Particularly, the inclusion of individual movement

decisions into individual based eco-epidemiological models has shown to affect the predictions for pathogen spread and persistence in heterogenous landscapes (Scherer et al., 2020). The inclusion of individual movement in epidemiological models can decrease the possibility that pathogen transmission risk and epidemiological dynamics are mischaracterized and can therefore help to increase the predictability of future outbreaks (Wilber et al., 2022).

Simulation models that aim at predicting realistic host-pathogen dynamics need to include the individual behaviour and life-history of host individuals (Evans et al., 2013). Especially in heterogeneous landscapes the host's movement is decisive, because in the case of directly transmitted diseases, these infected host individuals can act as mobile links that connect separated sub-populations and transport the pathogen to and from those populations (Jeltsch et al., 2013).

1.2 Movement, seasonality, and the dynamics of host-pathogen systems

For the host individuals, the decision of when and where to move emerges from a complex combination of factors such as predator avoidance, resource availability or density of conspecifics (Nathan et al., 2008). The decision making process is, however, not uniform across a species but often shows remarkable individual plasticity due to differences in physiological condition, behaviour type or social status (Jeltsch et al., 2013; Morales et al., 2010; Nathan et al., 2008). Differences in individual's movement lead to variations in connectivity and contact networks of the host population (Taylor et al., 1993). Spatial and temporal heterogeneity of the landscape can restrict or facilitate movement between areas and result in a temporary increase in host density and subsequently contact rates under high resource conditions, or vice versa, when a lack of resources decreases host density (Altizer et al., 2006; Hossack et al., 2013; Meentemeyer et al., 2012). Hosts in heterogeneous landscapes move longer distances towards areas with higher resource availability and, after resources are no longer available due to seasonality, they move again to new areas (van Moorter et al. 2013).

Seasonality, meaning predictable and cyclic changes of environmental factors, have long been known to exert strong pressure on populations (Fretwell, 2020). In this context, resource variability is a key driver of the density and distribution of host individuals over space and time (Altizer et al., 2006). For many species, the need for seasonal dynamics is likely to be the result

of evolutionary processes that stemmed from regular changes in resource availability (e.g. migratory birds, Rappole and Jones, 2003). The timing of seasonal dynamics is linked to seasonal environmental fluctuations (e.g. temperature) that affect, for example, prey abundance (Christian et al., 2007; Sigler et al., 2009) or the mating season (Conaway, 1971). These seasonal dynamics affect pathogen transmission in wild populations (Tonkin et al., 2017). For example, seasonal aggregation of migratory birds can increase the risk of the individuals to contract infectious diseases at their overwintering sites (Krauss et al., 2010; Waldenstrom et al., 2002), as highlighted by an outbreak of avian influenza (H5N1) among the wintering common crane (*Grus grus*) population in Israel that killed around 6000 individuals during winter 2021 (Brainard, 2022).

Mismatches in the seasonal dynamics can occur when an environmental cue (e.g. temperature) no longer predicts the timing of the biological event and can lead to a temporal shift of the optimal environmental conditions away from the biological event (Altizer et al., 2006). There is mounting evidence for mismatches increasing fitness costs e.g. in seasonally breeding birds, particularly when life-history lags behind peak food availability (Durant et al., 2007). Mismatches are also observed between Caribou (*Rangifer tarandus*) migration and the onset of the plant growing season at their target location (Post and Forchhammer, 2008) and can cause changes in reproductive patterns (longer or shorter breeding seasons) in wild boar (*sus scrofa* L; Brogi et al., 2021). Consequently, mismatches are likely to feed back onto host-pathogen interactions.

Furthermore, environmental seasonal fluctuations have been shown to trigger outbreaks and range shifts in pathogens such as tick-borne pathogens, Zika virus or West-Nile virus (Marcantonio et al., 2015; Ostfeld and Brunner, 2015; Semenza and Suk, 2018). Global change drivers, like climate change or land use change, are likely to further increase the mismatches between resource availability and timing of the biological events (Durant et al., 2007) and can directly alter pathogen spread and persistence (Harvell, 2002).

Despite the importance of pathogens for the population dynamics of wild animals in terms of population viability and the possibility of extinctions, knowledge about how environmental variation in space and time affect host-pathogen interactions is sparse (Bauer et al., 2009;

Meentemeyer et al., 2012; Webb et al., 2007). More recent studies have shown that seasonally occurring stress and increased contact rates in the eastern deer mouse (*Peromyscus maniculatus*) decrease immune response and facilitate pathogen transmission (Eleftheriou et al., 2021). Identifying the mechanisms that link environmental fluctuations and seasonal mismatches to disease dynamics can help to create predictive models and management strategies for controlling disease outbreaks in wildlife and humans.

1.3 Where do we go from here? -or- the evolution of pathogenic virulence in a social host

Host-pathogen systems are not only bottom-up driven by resources of the host, but also through the top-down effects the pathogen itself exerts on the host population. While the spread of a pathogen within a landscape depends largely on biotic and abiotic landscape features and host contact rates with patterns arising from local transmission processes, density and distribution of susceptible hosts, or environmental variation (Lambin et al., 2010), theory also predicts a direct link from host spatial structure to the effectiveness of a pathogen and the evolutionary trajectory of pathogen traits, such as virulence and transmission (Parratt et al., 2016). The effectiveness of a pathogen can be described as the ability to persist and spread within its host population (Cressler et al., 2016). Pathogenic virulence is often defined as the ability of a pathogen to harm its hosts (Hudson, 2002). A natural conclusion would be that a most effective pathogen would not harm its host, i.e., become avirulent. However, virulence is subject to a variety of evolutionary trade-offs.

The transmission-virulence trade-off hypothesis states that an increase in strain transmission causes shorter infections due to higher lethality (Alizon and Michalakis, 2015; Anderson and May, 1982). Particularly the evolution of virulence along such trade-offs has received a tremendous amount of attention in the scientific literature (Cressler et al., 2016; Day, 2003; Day and Proulx, 2004). One important aspect when looking at the epidemiological dynamics of a pathogen is the dynamics of its resource, i.e., the host population itself. Epidemiological dynamics of a pathogen are closely related to those of its host (Cressler et al., 2016; Lion and Gandon, 2015). This is evident when looking at the early stages of an epidemic where the abundance of susceptible hosts is at its peak. Due to these high numbers, pathogenic virulence has shown to be at its peak because enough susceptible hosts are available, and tends to decrease

towards the end of the epidemic; or when reaching endemic equilibrium, i.e. a state where influx of new susceptible individuals is in balance with the mortality caused by a pathogen, which prevents the pathogen from becoming extinct (Alizon et al., 2009).

This linkage between susceptible host availability and mortality makes clear that spatial structuring of the underlying habitat also becomes an important factor in the evolution of virulence (Lion and Boots, 2010; Messinger and Ostling, 2009). Highly virulent pathogens can rapidly deplete the pool of susceptible host, decreasing their chance of further transmission and resulting in the local extinction of host clusters. Less virulent pathogens could increase in transmission capability when susceptible host clusters are depleted more slowly (Cressler et al. 2016; Lion and Boots 2010; Messinger and Ostling 2009).

Many theoretical models of virulence evolution in a classical adaptive dynamics framework rely on the assumption that mutation happens over evolutionary timescales and that new strains can only occur after a dominant strain has reached equilibrium (Dieckmann et al., 2005). However, those assumptions are rarely applicable to host-pathogen systems in nature due to their simplicity. Natural host-pathogen systems often undergo transient dynamics, for example through temporal and spatial changes in landscape structure that alter host contact rates. To understand how outbreaks progress through space and time, we need to account for the evolution of pathogen traits in combination with the dynamic processes in spatially structured host populations.

1.4 How past outbreaks can help to progress our predictions about future epidemics

While a lot of insight can be gained from studying past epidemics and pathogen outbreaks, it is often difficult to obtain long-term field data from such events. Tracking diseases in wildlife populations is an inherently difficult task. Wild animals are not constrained by borders and can move long distances, hence most infectious disease outbreaks are detected passively (e.g. through found carcasses or hunted individuals), usually after a large number of individuals has become infected (Morner et al., 2002). Even when such data can be obtained, it is very difficult to disentangle the complex interactions of animal movement decisions, density dependence, landscape heterogeneity, changing pathogenic virulence and human interference, like

vaccination. To address this issue, simulation models have been long since recognised as an important tool in epidemiology (Keeling and Rohani, 2008).

Data gathered from real outbreaks can provide patterns on which such simulation models can be tested and verified. Pattern oriented modelling is an approach that uses simulation models to explain an observed pattern at the population level that is based on underlying processes at a lower level of organisation, e.g. the individual (Grimm et al., 1996; Wiegand et al., 2003). The patterns and processes in observed outbreaks are often poorly understood due to fast pace, chaotic nature of the data and monitoring challenges during such disease outbreaks (Artois et al., 2009; Guberti et al., 2014). Pattern oriented modelling can help to retroactively fill knowledge gaps from past outbreaks by explaining how real systems respond to internal and external changes (Grimm et al., 2005). In consequence, insights gained from these models can help to create predictive models that could help preventing future epidemics through targeted management solutions.

1.5 Classical swine fever in wild boar – a dynamic model system with multiple interactive processes

The European wild boar is an ideal model species for disentangling the complex processes behind host-pathogen interactions. It is a group-living social species with sex- and age-differentiation in movement patterns and space use (Boitani et al., 1994; Morelle et al., 2015). Wild boars have a large distribution area across Eurasia with introduced populations in many other regions (Apollonio et al., 2010), and are currently increasing in numbers across Europe (Acevedo et al., 2006; Bieber and Ruf, 2005; Ruiz-Fons et al., 2008). They are considered a key reservoir species for a variety of infectious disease such as Classical SwineFfever (CSF), African Swine Fever (ASF), and diseases with zoonotic potential such as hepatitis E or brucellosis (Li et al., 2005; Melzer et al., 2007; Rossi et al., 2005; Ruiz-Fons et al., 2008). Due to the increasing density of wild boar, future outbreaks are likely to increase in frequency and severity. Although some pathogens, like CSF or ASF, are harmless to humans, transmission to domestic pigs can have profound socio-economic and ethical consequences (Halasa et al., 2016), and zoonotic transmission of other pathogens infecting humans has a direct effect on human health (Meng et al., 2009).

CSF is a highly-contagious directly-transmitted viral disease infecting animals of the *Suidae* family and is prevalent in many areas of the world that host wild boar (Paton and Greiser-Wilke, 2003). The risk of susceptible individuals to be infected with CSF is regulated through both host population-dynamics and viral properties. On the host population side, resources such as food or shelter shape wild boar density and distribution in space and time (Kramer-Schadt et al., 2007; Rossi et al., 2005). On the pathogen side, changes in virulence and transmission capacity of individual strains can alter host survival and pathogen persistence times (Blome et al., 2017; M. Lange et al., 2012). Additionally, demographic differences in susceptibility of host individuals (Artois et al., 2002) and individual movement behaviour (Scherer et al., 2020) shape and scale of outbreak dynamics. While the importance of these regulatory factors by themselves has been widely recognized, their combined effect and interactions, that ultimately explain pathogen persistence within a population, are not yet fully understood.

Many of the individual aspects of CFS persistence and spread in wild boars have been studied in the past. Scherer et al. (2020) have, for example, shown how feedback from the spatial configuration of landscapes through individual movement can drive pathogen persistence and spread. They were able to show how mechanistic movement rules, based on external factors such as resource heterogeneity, increased disease persistence. Furthermore, the existence of long-term data from a CSF outbreak in Mecklenburg-Vorpommern in norther Germany in the 1990's offers the rare opportunity to combine real epidemiological data with simulation studies. During this outbreak, seasonal reproductive peaks and demographic characteristics were shown to play an important role in CSF infection risk, with piglets suffering from higher incidence compared to older individuals (Scherer et al., 2019). However, due to wild boar social structure, piglets are not likely to spread CSF over large areas (Kramer-Schadt et al., 2007; Rossi et al., 2011), hence other factors drive the transmission and persistence of the disease. The combination of previous studies, both theoretical and empirical, on different aspects and drivers of CSF infection in wild boar populations, form an ideal starting point to expand upon and study the complex interactions in dynamic host-pathogen systems in depth.

1.6 Understanding how spatial and temporal variability of resources drive transmission, persistence, and evolution of pathogens

My thesis aims to investigate the drivers of disease dynamics in both theoretical and real settings using CSF in wild boar as a model system. Specifically, my research questions are how spatiotemporal variation on host population through synchronous and asynchronous resource seasonality and individual movement feed back onto host-pathogen interactions, and how the evolution of pathogen traits affect host-pathogen coexistence and pathogen patterns of spread. In the following chapters I will use a complex spatially explicit individual- based eco-epidemiological model in combination with long-term CSF outbreak data to answer the questions raised above.

In **chapter 2**, I analyse the bottom-up effects of spatiotemporal variation and temporal mismatches between biological events and resource availability in a social host on pathogen persistence and patterns of spread. To that end, I extended a single strain eco-epidemiological model that accounted for spatially-explicit host movement simulating the spread of CSF in a wild boar population (Kramer-Schadt et al., 2009; Lange et al., 2012a, b; Scherer et al., 2020) , to simulate seasonal landscape dynamics. Seasonality was included in the model through changing resource availability and associated processes, such as increased mortality of individuals under low resource conditions and movement away from low resource availability in certain movement types. I tested a range of temporal mismatch scenarios in complex landscapes from complete overlap of peak resource availability and the timing of biological events to complete mismatch between them, when peak resource availability was completely shifted away from the timing of biological events. Additionally, I imposed both mechanistic (e.g. movement dependent on the underlying resource landscape) and phenomenological (e.g. correlated random walk) host movement types (as in Scherer et al. 2020) on the study system.

In **chapter 3**, I address how the top-down process of pathogen trait evolution in spatially structured social host populations in dynamic resource landscapes affects host-pathogen coexistence in global change scenarios. I further extended the eco-epidemiological model used in **chapter 2** by adding a multi-strain outbreak system and the evolution of virulence along a theoretical virulence-transmission trade-off where high virulence (i.e., short host survival time) increases with transmission capability. I discuss how temporal mismatches between resource

availability and biological events affect host-pathogen coexistence and pathogen spread considering an evolving pathogen.

In **chapter 4**, I synthesize the knowledge gained from the previous chapters by comparing the outcomes of the eco-epidemiological model scenarios to patterns gathered from a CSF outbreak data analysis in the region of Mecklenburg-Vorpommern, North-East Germany (Scherer et al., 2019). Here, I evaluate the model scenarios against real data and analyse the development of the CSF outbreak. I further modified the model used in **chapter 3** by adding realistic landscape maps and accounting for individual movement in the evolution of virulence. I asses the effect of decision-making processes in host movement on disease outbreak patterns, persistence, and transmission on an individual and regional level based on a realistic scenario.

In **chapter 5**, I conclude with a general discussion where I synthesize the results of the chapters 2, 3 and 4 by integrating them into existing concepts and frameworks. I compare my findings to previous models in disease ecology and highlight my contribution the current knowledge in disease dynamics. I discuss the implications of my results regarding population-level consequences of host movement decisions and pathogen virulence for disease outbreaks, as well as how insights gained from disentangling the mechanisms behind host-pathogen interactions can help in predicting and preventing future zoonotic pandemics.

References

Acevedo, P., Escudero, M.A., Muńoz, R., Gortázar, C., 2006. Factors affecting wild boar abundance across an environmental gradient in Spain. Acta Theriol 51, 327–336. https://doi.org/10.1007/BF03192685

Alizon, S., Hurford, A., Mideo, N., van Baalen, M., 2009. Virulence evolution and the trade-off hypothesis: history, current state of affairs and the future. Journal of evolutionary biology 22, 245–259. https://doi.org/10.1111/j.1420-9101.2008.01658.x

Alizon, S., Michalakis, Y., 2015. Adaptive virulence evolution: the good old fitness-based approach. Trends in Ecology & Evolution 30, 248–254. https://doi.org/10.1016/j.tree.2015.02.009

Allen, T., Murray, K.A., Zambrana-Torrelio, C., Morse, S.S., Rondinini, C., Di Marco, M., Breit, N., Olival, K.J., Daszak, P., 2017. Global hotspots and correlates of emerging zoonotic diseases. Nat Commun 8, 1124. https://doi.org/10.1038/s41467-017-00923-8

Altizer, S., Dobson, A., Hosseini, P., Hudson, P., Pascual, M., Rohani, P., 2006. Seasonality and the dynamics of infectious diseases. Ecology letters 9, 467–484. https://doi.org/10.1111/j.1461-0248.2005.00879.x

Andersen, K.G., Rambaut, A., Lipkin, W.I., Holmes, E.C., Garry, R.F., 2020. The proximal origin of SARS-CoV-2. Nat Med 26, 450–452. https://doi.org/10.1038/s41591-020-0820-9

Anderson, R.M., May, R.M., 1991. Infectious diseases of humans: dynamics and control, Reprinted. ed, Oxford science publications. Oxford university press, New York.

Anderson, R.M., May, R.M., 1982. Coevolution of hosts and parasites. Parasitology 85, 411–426. https://doi.org/10.1017/S0031182000055360

Anderson, R.M., May, R.M., 1979. Population biology of infectious diseases: Part I. Nature 280, 361–367. https://doi.org/10.1038/280361a0

Apollonio, M., Andersen, R., Putman, R., 2010. European ungulates and their management in the 21st century. Cambridge University Press.

Artois, M., Bengis, R., Delahay, R.J., Duchêne, M.-J., Duff, J.P., Ferroglio, E., Gortazar, C., Hutchings, M.R., Kock, R.A., Leighton, F.A., Mörner, T., Smith, G.C., 2009. Wildlife Disease Surveillance and Monitoring, in: Delahay, R.J., Smith, G.C., Hutchings, M.R. (Eds.), Management of Disease in Wild Mammals. Springer Japan, Tokyo, pp. 187–213. https://doi.org/10.1007/978-4-431-77134-0_10

Artois, M., Depner, K.R., Guberti, V., Hars, J., Rossi, S., Rutili, D., 2002. Classical swine fever (hog cholera) in wild boar in Europe. Rev. Sci. Tech. OIE 21, 287–303. https://doi.org/10.20506/rst.21.2.1332

Bieber, C., Ruf, T., 2005. Population dynamics in wild boar *Sus scrofa* : ecology, elasticity of growth rate and implications for the management of pulsed resource consumers: *Population dynamics in wild boar*. Journal of Applied Ecology 42, 1203–1213. https://doi.org/10.1111/j.1365-2664.2005.01094.x

Blome, S., Staubach, C., Henke, J., Carlson, J., Beer, M., 2017. Classical Swine Fever—An Updated Review. Viruses 9, 86. https://doi.org/10.3390/v9040086

Boitani, L., Mattei, L., Nonis, D., Corsi, F., 1994. Spatial and Activity Patterns of Wild Boars in Tuscany, Italy. Journal of Mammalogy 75, 600–612. https://doi.org/10.2307/1382507

Brainard, J. (Ed.), 2022. News at a glance. Science 375, 6–8. https://doi.org/10.1126/science.acz9927

Brogi, R., Merli, E., Grignolio, S., Chirichella, R., Bottero, E., Apollonio, M., 2021. It is time to mate: population-level plasticity of wild boar reproductive timing and synchrony in a changing environment. Current Zoology zoab077. https://doi.org/10.1093/cz/zoab077

Christian, K., Webb, J.K., Schultz, T., Green, B., 2007. Effects of Seasonal Variation in Prey Abundance on Field Metabolism, Water Flux, and Activity of a Tropical Ambush Foraging Snake. Physiological and Biochemical Zoology 80, 522–533. https://doi.org/10.1086/519959

Conaway, C.H., 1971. Ecological Adaptation and Mammalian Reproduction. Biology of Reproduction 4, 239–247. https://doi.org/10.1093/biolreprod/4.3.239

Craft, M.E., 2015. Infectious disease transmission and contact networks in wildlife and livestock. Phil. Trans. R. Soc. B 370, 20140107. https://doi.org/10.1098/rstb.2014.0107

Cressler, C.E., McLEOD, D.V., Rozins, C., van den Hoogen, J., Day, T., 2016. The adaptive evolution of virulence: a review of theoretical predictions and empirical tests. Parasitology 143, 915–930. https://doi.org/10.1017/S003118201500092X

Day, T., 2003. Virulence evolution and the timing of disease life-history events. Trends in Ecology & Evolution 18, 113–118. https://doi.org/10.1016/S0169-5347(02)00049-6

Day, T., Proulx, S.R., 2004. A General Theory for the Evolutionary Dynamics of Virulence. The American Naturalist 163, E40–E63. https://doi.org/10.1086/382548

Dieckmann, U., Metz, J.A.J., Sabelis, M., W., Sigmund, K. (Eds.), 2005. Adaptive dynamics of infectious diseases: in pursuit of virulence management, 1st pbk. version. ed, Cambridge studies in adaptive dynamics. Cambridge University Press, New York.

Dougherty, E.R., Seidel, D.P., Carlson, C.J., Spiegel, O., Getz, W.M., 2018. Going through the motions: incorporating movement analyses into disease research. Ecol Lett 21, 588–604. https://doi.org/10.1111/ele.12917

Durant, J., Hjermann, D., Ottersen, G., Stenseth, N., 2007. Climate and the match or mismatch between predator requirements and resource availability. Clim. Res. 33, 271–283. https://doi.org/10.3354/cr033271

Eleftheriou, A., Kuenzi, A.J., Luis, A.D., 2021. Heterospecific competitors and seasonality can affect host physiology and behavior: key factors in disease transmission. Ecosphere 12. https://doi.org/10.1002/ecs2.3494

Evans, M.R., Grimm, V., Johst, K., Knuuttila, T., de Langhe, R., Lessells, C.M., Merz, M., O'Malley, M.A., Orzack, S.H., Weisberg, M., Wilkinson, D.J., Wolkenhauer, O., Benton, T.G., 2013. Do simple models lead to generality in ecology? Trends in Ecology & Evolution 28, 578–583. https://doi.org/10.1016/j.tree.2013.05.022

Fisher, M.C., Garner, T.W.J., Walker, S.F., 2009. Global Emergence of *Batrachochytrium dendrobatidis* and Amphibian Chytridiomycosis in Space, Time, and Host. Annu. Rev. Microbiol. 63, 291–310. https://doi.org/10.1146/annurev.micro.091208.073435

Franz, M., Kramer-Schadt, S., Greenwood, A.D., Courtiol, A., 2018. Sickness-induced lethargy can increase host contact rates and pathogen spread in water-limited landscapes. Funct Ecol 32, 2194–2204. https://doi.org/10.1111/1365-2435.13149

Fretwell, S.D., 2020. Populations in a Seasonal Environment. (MPB-5). Yale University Press. https://doi.org/10.12987/9780691209647

Grimm, V., Frank, K., Jeltsch, F., Brandl, R., Uchmański, J., Wissel, C., 1996. Pattern-oriented modelling in population ecology. Science of The Total Environment 183, 151–166. https://doi.org/10.1016/0048-9697(95)04966-5

Grimm, V., Revilla, E., Berger, U., Jeltsch, F., Mooij, W.M., Railsback, S.F., Thulke, H.-H., Weiner, J., Wiegand, T., DeAngelis, D.L., 2005. Pattern-Oriented Modeling of Agent-Based Complex Systems: Lessons from Ecology. Science 310, 987–991. https://doi.org/10.1126/science.1116681

Guberti, V., Stancampiano, L., Ferrari, N., 2014. Surveillance, monitoring and survey of wildlife diseases: a public health and conservation approach. Hystrix, the Italian Journal of Mammalogy 25. https://doi.org/10.4404/hystrix-25.1-10114

Halasa, T., Bøtner, A., Mortensen, S., Christensen, H., Toft, N., Boklund, A., 2016. Simulating the epidemiological and economic effects of an African swine fever epidemic in industrialized swine populations. Veterinary Microbiology 193, 7–16. https://doi.org/10.1016/j.vetmic.2016.08.004

Harvell, C.D., 2002. Climate Warming and Disease Risks for Terrestrial and Marine Biota. Science 296, 2158–2162. https://doi.org/10.1126/science.1063699

Hastings, A., Petrovskii, S., Morozov, A., 2011. Spatial ecology across scales. Biol. Lett. 7, 163–165. https://doi.org/10.1098/rsbl.2010.0948

Hethcote, H.W., 2000. The Mathematics of Infectious Diseases. SIAM Rev. 42, 599–653. https://doi.org/10.1137/S0036144500371907

Hossack, B.R., Lowe, W.H., Ware, J.L., Corn, P.S., 2013. Disease in a dynamic landscape: Host behavior and wildfire reduce amphibian chytrid infection. Biological Conservation 157, 293–299. https://doi.org/10.1016/j.biocon.2012.09.013

Hudson, P.J. (Ed.), 2002. The ecology of wildlife diseases. Oxford University Press, New York.

Jeltsch, F., Bonte, D., Pe'er, G., Reineking, B., Leimgruber, P., Balkenhol, N., Schröder, B., Buchmann, C.M., Mueller, T., Blaum, N., Zurell, D., Böhning-Gaese, K., Wiegand, T., Eccard, J.A., Hofer, H., Reeg, J., Eggers, U., Bauer, S., 2013. Integrating movement ecology with biodiversity research - exploring new avenues to address spatiotemporal biodiversity dynamics. Mov Ecol 1, 6. https://doi.org/10.1186/2051-3933-1-6

Keeling, M.J., Rohani, P., 2008. Modeling infectious diseases in humans and animals. Princeton University Press, Princeton.

Kermack, W.O., McKendrick, A.G., 1927. A Contribution to the Mathematical Theory of Epidemics. Proceedings of the Royal Society A: Mathematical, Physical and Engineering Sciences 115, 700–721. https://doi.org/10.1098/rspa.1927.0118

Kramer-Schadt, S., Fernández, N., Eisinger, D., Grimm, V., Thulke, H.-H., 2009. Individual variations in infectiousness explain long-term disease persistence in wildlife populations. Oikos 118, 199–208. https://doi.org/10.1111/j.1600-0706.2008.16582.x

Kramer-Schadt, S., Fernández, N., Thulke, H.-H., 2007. Potential ecological and epidemiological factors affecting the persistence of classical swine fever in wild boar *Sus scrofa* populations. Mammal Review 37, 1–20. https://doi.org/10.1111/j.1365-2907.2007.00097.x

Krauss, S., Stallknecht, D.E., Negovetich, N.J., Niles, L.J., Webby, R.J., Webster, R.G., 2010. Coincident ruddy turnstone migration and horseshoe crab spawning creates an ecological 'hot spot' for influenza viruses. Proc. R. Soc. B. 277, 3373–3379. https://doi.org/10.1098/rspb.2010.1090

LaDeau, S.L., Kilpatrick, A.M., Marra, P.P., 2007. West Nile virus emergence and large-scale declines of North American bird populations. Nature 447, 710–713. https://doi.org/10.1038/nature05829

Lafferty, K.D., Allesina, S., Arim, M., Briggs, C.J., De Leo, G., Dobson, A.P., Dunne, J.A., Johnson, P.T.J., Kuris, A.M., Marcogliese, D.J., Martinez, N.D., Memmott, J., Marquet, P.A., McLaughlin, J.P., Mordecai, E.A., Pascual, M., Poulin, R., Thieltges, D.W., 2008. Parasites in food webs: the ultimate missing links: Parasites in food webs. Ecology Letters 11, 533–546. https://doi.org/10.1111/j.1461-0248.2008.01174.x

Lambin, E.F., Tran, A., Vanwambeke, S.O., Linard, C., Soti, V., 2010. Pathogenic landscapes: Interactions between land, people, disease vectors, and their animal hosts. Int J Health Geogr 9, 54. https://doi.org/10.1186/1476-072X-9-54

Lange, M., Kramer-Schadt, S., Blome, S., Beer, M., Thulke, H.-H., 2012a. Disease severity declines over time after a wild boar population has been affected by classical swine fever—legend or actual epidemiological process? Preventive veterinary medicine 106, 185–195. https://doi.org/10.1016/j.prevetmed.2012.01.024.

Lange, M., Kramer-Schadt, S., Thulke, H.-H., 2012b. Efficiency of spatio-temporal vaccination regimes in wildlife populations under different viral constraints. Veterinary Research 43, 37. https://doi.org/10.1186/1297-9716-43-37

Li, T.-C., Chijiwa, K., Sera, N., Ishibashi, T., Etoh, Y., Shinohara, Y., Kurata, Y., Ishida, M., Sakamoto, S., Takeda, N., Miyamura, T., 2005. Hepatitis E Virus Transmission from Wild Boar Meat. Emerg. Infect. Dis. 11, 1958–1960. https://doi.org/10.3201/eid1112.051041

Lion, S., Boots, M., 2010. Are parasites "prudent" in space? Ecology letters 13, 1245–1255. https://doi.org/10.1111/j.1461-0248.2010.01516.x

Lion, S., Gandon, S., 2015. Evolution of spatially structured host-parasite interactions. Journal of evolutionary biology 28, 10–28. https://doi.org/10.1111/jeb.12551

Lloyd-Smith, J.O., Schreiber, S.J., Kopp, P.E., Getz, W.M., 2005. Superspreading and the effect of individual variation on disease emergence. Nature 438, 355–359. https://doi.org/10.1038/nature04153

Marcantonio, M., Rizzoli, A., Metz, M., Rosà, R., Marini, G., Chadwick, E., Neteler, M., 2015. Identifying the Environmental Conditions Favouring West Nile Virus Outbreaks in Europe. PLoS ONE 10, e0121158. https://doi.org/10.1371/journal.pone.0121158

Marescot, L., Franz, M., Benhaiem, S., Hofer, H., Scherer, C., East, M.L., Kramer-Schadt, S., 2021. 'Keeping the kids at home' can limit the persistence of contagious pathogens in social animals. J Anim Ecol 90, 2523–2535. https://doi.org/10.1111/1365-2656.13555

McLeod, A.M., Leroux, S.J., 2021. Incorporating abiotic controls on animal movements in metacommunities. Ecology 102. https://doi.org/10.1002/ecy.3365

Meentemeyer, R.K., Haas, S.E., Václavík, T., 2012. Landscape epidemiology of emerging infectious diseases in natural and human-altered ecosystems. Annual review of phytopathology 50, 379–402. https://doi.org/10.1146/annurev-phyto-081211-172938

Melzer, F., Lohse, R., Nieper, H., Liebert, M., Sachse, K., 2007. A serological study on brucellosis in wild boars in Germany. Eur J Wildl Res 53, 153–157. https://doi.org/10.1007/s10344-006-0072-0

Meng, X.J., Lindsay, D.S., Sriranganathan, N., 2009. Wild boars as sources for infectious diseases in livestock and humans. Phil. Trans. R. Soc. B 364, 2697–2707. https://doi.org/10.1098/rstb.2009.0086

Messinger, S.M., Ostling, A., 2009. The consequences of spatial structure for the evolution of pathogen transmission rate and virulence. The American naturalist 174, 441–454. https://doi.org/10.1086/605375

Morales, J.M., Moorcroft, P.R., Matthiopoulos, J., Frair, J.L., Kie, J.G., Powell, R.A., Merrill, E.H., Haydon, D.T., 2010. Building the bridge between animal movement and population dynamics. Phil. Trans. R. Soc. B 365, 2289–2301. https://doi.org/10.1098/rstb.2010.0082

Morelle, K., Podgórski, T., Prévot, C., Keuling, O., Lehaire, F., Lejeune, P., 2015. Towards understanding wild boar *Sus scrofa* movement: a synthetic movement ecology approach: A review of wild boar *Sus scrofa* movement ecology. Mammal Review 45, 15–29. https://doi.org/10.1111/mam.12028

Morner, T., Obendorf, D.L., Artois, M., Woodford, M.H., 2002. Surveillance and monitoring of wildlife diseases. Rev. Sci. Tech. OIE 21, 67–76. https://doi.org/10.20506/rst.21.1.1321

Morse, S.S., Mazet, J.A., Woolhouse, M., Parrish, C.R., Carroll, D., Karesh, W.B., Zambrana-Torrelio, C., Lipkin, W.I., Daszak, P., 2012. Prediction and prevention of the next pandemic zoonosis. The Lancet 380, 1956–1965. https://doi.org/10.1016/S0140-6736(12)61684-5

Nathan, R., Getz, W.M., Revilla, E., Holyoak, M., Kadmon, R., Saltz, D., Smouse, P.E., 2008. A movement ecology paradigm for unifying organismal movement research. Proceedings of the National Academy of Sciences 105, 19052–19059. https://doi.org/10.1073/pnas.0800375105

Ostfeld, R.S., Brunner, J.L., 2015. Climate change and *Ixodes* tick-borne diseases of humans. Phil. Trans. R. Soc. B 370, 20140051. https://doi.org/10.1098/rstb.2014.0051

Parratt, S.R., Numminen, E., Laine, A.-L., 2016. Infectious Disease Dynamics in Heterogeneous Landscapes. Annu. Rev. Ecol. Evol. Syst. 47, 283–306. https://doi.org/10.1146/annurev-ecolsys-121415-032321

Paton, D.J., Greiser-Wilke, I., 2003. Classical swine fever – an update. Research in Veterinary Science 75, 169–178. https://doi.org/10.1016/S0034-5288(03)00076-6

Patz, J.A., Daszak, P., Tabor, G.M., Aguirre, A.A., Pearl, M., Epstein, J., Wolfe, N.D., Kilpatrick, A.M., Foufopoulos, J., Molyneux, D., Bradley, D.J., Members of the Working Group on Land Use Change Disease Emergence, 2004. Unhealthy Landscapes: Policy Recommendations on Land Use Change and Infectious Disease Emergence. Environmental Health Perspectives 112, 1092–1098. https://doi.org/10.1289/ehp.6877

Plard, F., Gaillard, J.-M., Coulson, T., Hewison, A.J.M., Delorme, D., Warnant, C., Bonenfant, C., 2014. Mismatch Between Birth Date and Vegetation Phenology Slows the Demography of Roe Deer. PLoS Biol 12, e1001828. https://doi.org/10.1371/journal.pbio.1001828

Post, E., Forchhammer, M.C., 2008. Climate change reduces reproductive success of an Arctic herbivore through trophic mismatch. Phil. Trans. R. Soc. B 363, 2367–2373. https://doi.org/10.1098/rstb.2007.2207

Radchuk, V., Kramer-Schadt, S., Grimm, V., 2019. Transferability of Mechanistic Ecological Models Is About Emergence. Trends in Ecology & Evolution 34, 487–488. https://doi.org/10.1016/j.tree.2019.01.010

Rappole, J.H., Jones, P., 2003. Evolution of old and new world migration systems. Ardea 90, 525–537.

Reaser, J.K., Witt, A., Tabor, G.M., Hudson, P.J., Plowright, R.K., 2021. Ecological countermeasures for preventing zoonotic disease outbreaks: when ecological restoration is a human health imperative. Restor Ecol 29. https://doi.org/10.1111/rec.13357

Ripple, W.J., Estes, J.A., Beschta, R.L., Wilmers, C.C., Ritchie, E.G., Hebblewhite, M., Berger, J., Elmhagen, B., Letnic, M., Nelson, M.P., Schmitz, O.J., Smith, D.W., Wallach, A.D., Wirsing, A.J., 2014. Status and Ecological Effects of the World's Largest Carnivores. Science 343, 1241484. https://doi.org/10.1126/science.1241484

Rossi, S., Fromont, E., Pontier, D., Crucière, C., Hars, J., Barrat, J., Pacholek, X., Artois, M., 2005. Incidence and Persistence of Classical Swine Fever in Free-Ranging Wild Boar (*Sus scrofa*). Epidemiology and Infection 133, 559–568.

Rossi, S., Toigo, C., Hars, J., Pol, F., Hamann, J.-L., Depner, K., Le Potier, M.-F., 2011. New Insights on the Management of Wildlife Diseases Using Multi-State Recapture Models: The Case of Classical Swine Fever in Wild Boar. PLoS ONE 6, e24257. https://doi.org/10.1371/journal.pone.0024257

Ruiz-Fons, F., Segalés, J., Gortázar, C., 2008. A review of viral diseases of the European wild boar: Effects of population dynamics and reservoir rôle. The Veterinary Journal 176, 158–169. https://doi.org/10.1016/j.tvjl.2007.02.017

Rulli, M.C., Santini, M., Hayman, D.T.S., D'Odorico, P., 2017. The nexus between forest fragmentation in Africa and Ebola virus disease outbreaks. Sci Rep 7, 41613. https://doi.org/10.1038/srep41613

Scherer, C., Radchuk, V., Franz, M., Thulke, H., Lange, M., Grimm, V., Kramer–Schadt, S., 2020. Moving infections: individual movement decisions drive disease persistence in spatially structured landscapes. Oikos oik.07002. https://doi.org/10.1111/oik.07002

Scherer, C., Radchuk, V., Staubach, C., Müller, S., Blaum, N., Thulke, H., Kramer-Schadt, S., 2019. Seasonal host life-history processes fuel disease dynamics at different spatial scales. J Anim Ecol 88, 1812–1824. https://doi.org/10.1111/1365-2656.13070

Semenza, J.C., Suk, J.E., 2018. Vector-borne diseases and climate change: a European perspective. FEMS Microbiology Letters 365. https://doi.org/10.1093/femsle/fnx244

Sigler, M., Tollit, D., Vollenweider, J., Thedinga, J., Csepp, D., Womble, J., Wong, M., Rehberg, M., Trites, A., 2009. Steller sea lion foraging response to seasonal changes in prey availability. Mar. Ecol. Prog. Ser. 388, 243–261. https://doi.org/10.3354/meps08144

Smith, K.F., Guégan, J.-F., 2010. Changing Geographic Distributions of Human Pathogens. Annu. Rev. Ecol. Evol. Syst. 41, 231–250. https://doi.org/10.1146/annurev-ecolsys-102209-144634

Taylor, P.D., Fahrig, L., Henein, K., Merriam, G., 1993. Connectivity Is a Vital Element of Landscape Structure. Oikos 68, 571. https://doi.org/10.2307/3544927

Tonkin, J.D., Bogan, M.T., Bonada, N., Rios-Touma, B., Lytle, D.A., 2017. Seasonality and predictability shape temporal species diversity. Ecology 98, 1201–1216. https://doi.org/10.1002/ecy.1761

Visser, M.E., Gienapp, P., 2019. Evolutionary and demographic consequences of phenological mismatches. Nat Ecol Evol 3, 879–885. https://doi.org/10.1038/s41559-019-0880-8

Waldenstrom, J., Bensch, S., Kiboi, S., Hasselquist, D., Ottosson, U., 2002. Cross-species infection of blood parasites between resident and migratory songbirds in Africa. Mol Ecol 11, 1545–1554. https://doi.org/10.1046/j.1365-294X.2002.01523.x

Wiegand, T., Jeltsch, F., Hanski, I., Grimm, V., 2003. Using pattern-oriented modeling for revealing hidden information: a key for reconciling ecological theory and application. Oikos 100, 209–222. https://doi.org/10.1034/j.1600-0706.2003.12027.x

Wilber, M.Q., Yang, A., Boughton, R., Manlove, K.R., Miller, R.S., Pepin, K.M., Wittemyer, G., 2022. A model for leveraging animal movement to understand spatio-temporal disease dynamics. Ecology Letters ele.13986. https://doi.org/10.1111/ele.13986

Wilcox, B.A., Gubler, D.J., 2005. Disease ecology and the global emergence of zoonotic pathogens. Environ Health Prev Med 10, 263. https://doi.org/10.1007/BF02897701

Williams, P.C., Bartlett, A.W., Howard-Jones, A., McMullan, B., Khatami, A., Britton, P.N., Marais, B.J., 2021. Impact of climate change and biodiversity collapse on the global emergence and spread of infectious diseases. J Paediatr Child Health 57, 1811–1818. https://doi.org/10.1111/jpc.15681

CHAPTER 2

MOVEMENT CAN MEDIATE TEMPORAL MISMATCHES BETWEEN RESOURCE AVAILABILITY AND BIOLOGICAL EVENTS IN HOST-PATHOGEN INTERACTIONS

Authors:	Tobias Kürschner, Cédric Scherer, Viktoriia Radchuk, Niels Blaum, Stephanie Kramer-Schadt
Status:	Published
Journal:	Ecology and Evolution
Submission History:	Submitted: 01 October 2020, Published: 29 March 2021
Keywords:	classical swine fever, dynamic landscapes, global change, host-pathogen dynamics, individual-based model, movement ecology
Author contributions:	TK and SKS developed the core idea and designed the study. TK rewrote and modified the simulation model together with CS and SKS. TK, VR, and SKS analysed the simulation results. TK is the lead author and CS, VR, NB and SKS contributed substantially to the writing. All authors agreed to submission of the manuscript, and each author is accountable for the aspects of the conducted work.

2 Movement can mediate temporal mismatches between resource availability and biological events in host-pathogen interactions

Abstract: Global change is shifting the timing of biological events, leading to temporal mismatches between biological events and resource availability. These temporal mismatches can threaten species' populations. Importantly, temporal mismatches not only exert strong pressures on the population dynamics of the focal species, but can also lead to substantial changes in pairwise species interactions such as host-pathogen systems. We adapted an established individual-based model of host-pathogen dynamics. The model describes a viral agent in a social host, while accounting for the host's explicit movement decisions. We aimed to investigate how temporal mismatches between seasonal resource availability and host life-history events affect host-pathogen coexistence, that is, disease persistence. Seasonal resource fluctuations only increased coexistence probability when in synchrony with the hosts' biological events. However, a temporal mismatch reduced host-pathogen coexistence, but only marginally. In tandem with an increasing temporal mismatch, our model showed a shift in the spatial distribution of infected hosts. It shifted from an even distribution under synchronous conditions toward the formation of disease hotspots, when host life history and resource availability mismatched completely. The spatial restriction of infected hosts to small hotspots in the landscape initially suggested a lower coexistence probability due to the critical loss of susceptible host individuals within those hotspots. However, the surrounding landscape facilitated demographic rescue through habitat-dependent movement. Our work demonstrates that the negative effects of temporal mismatches between host resource availability and host life history on host-pathogen coexistence can be reduced through the formation of temporary disease hotspots and host movement decisions, with implications for disease management under disturbances and global change.

2.1 Introduction

Environmental fluctuations over time, like diurnal differences in temperature, seasonal changes of climate, or land-cover modifications due to agricultural practices, can affect species communities in many ways. Many species have adapted to these conditions, so that their biological events match the environmental fluctuations. For example, the onset of mating or breeding (Conaway, 1971), the timing of migration (La Sorte et al., 2015; Mayor et al., 2017), or the timing of prey occurrence (Christian et al., 2007; Sigler et al., 2009) is fundamentally linked to regularly occurring seasonal fluctuations in resource availability such as food or shelter. In many cases, such biological events of species match the regularly occurring changes in the environment, like the onset of spring, because they are triggered by a reliable environmental cue, for example, day length. Mismatches occur when the cue used no longer predicts the timing of the biological event. This mismatch leads to a steady temporal shift of the optimal environmental conditions away from the biological event and can exert strong pressures on population dynamics (Altizer et al., 2006). In marine ecology, mismatches have been found to affect stock recruitment (e.g., for Antarctic krill, Groeneveld et al., 2015). In terrestrial systems, mismatches were demonstrated to increase fitness costs as a result of hatching times (Thomas et al., 2001) and laying dates (Winkler et al., 2002), lagging behind the peak of food availability in seasonally breeding birds (Durant et al., 2007; Schweiger et al., 2008, 2012).

These mismatches affect not only individual species' performance but also pairwise or multispecies interactions such as the coexistence of a predator and its prey, or a host and its pathogen (Hossack et al., 2013; Kharouba et al., 2018; Mayor et al., 2017; Tonkin et al., 2017). With many species being unable to adapt quickly enough –if at all– to a shift of environmental conditions (Bellard et al., 2012; Radchuk et al., 2019; Visser, 2008), it becomes increasingly important to understand the long-term community consequences for interacting species under global change.

Within-year seasonality is one of the strongest and most-studied forms of periodically occurring environmental fluctuation affecting communities. Seasonality can be defined as an annually reoccurring change of one or more abiotic variables, such as temperature or precipitation (Kharin et al., 2013). These naturally occurring fluctuations are characterized by a positive

autocorrelation, meaning that the closer measurements are in time, the more similar will they be on average compared to temporally distant measurements (Dornelas et al., 2013; Koenig, 1999; Legendre, 1993). Temporal within-year seasonality is similar in its effects to spatial heterogeneity within landscapes as it creates temporary niches of varying levels of resource availability (Tonkin et al., 2017; Williams et al., 2017). While both temporal and spatial fluctuations can have stronger or weaker effects by themselves, they generally work in concert (Durant, 1998), leading to spatiotemporal autocorrelation in resources availability within years.

This spatiotemporal autocorrelation in the environment leads resource levels to vary across the year, and may increase population density when resource availability is highly coincident with a biological event, for example, the timing of birth peaks (Altizer et al., 2006; van Moorter et al., 2013). In this case, environmental and biological events are synchronized. Drivers like global change (e.g., climate or land-use change) can increase the mismatch between resource availability and timing of the biological event (Durant et al., 2007). A subsequent decline in population size could lead to a decreased coexistence of directly affected and any dependent species. In contrast, such an asynchronous temporal resource availability, if occurring on landscapes with heterogeneous resource availability, could offset the negative effect of the temporal mismatch on coexistence by creating local patches with suitable conditions. This could further lead to a metacommunity-like structure with increased metacommunity persistence (Duncan et al., 2013).

We here use host-pathogen interactions as a model system to explore the consequences of temporal mismatch on disease dynamics under global change. Global change increasingly affects the phenology of resources, with ensuing consequences for the host's life history and its large-scale movements and effects of pathogens on host survival and reproduction on the other hand (Semenza & Menne, 2009; Semenza & Suk, 2018).

Climactic fluctuations have triggered outbreaks and facilitated range shifts in pathogens such as West Nile virus, Zika virus, Borrelia bacteria, or other tick-borne pathogens (Marcantonio et al., 2015; Ostfeld & Brunner, 2015; Semenza & Suk, 2018, see also review in Altizeret al., 2013).

This highlights the importance of environmental conditions in understanding disease dynamics. In this context, resource variation is an essential driver of the distribution of

individuals within a host population over space and time. The transmission of many infectious agents depends on direct contact between infected and susceptible hosts, mediated by their movement decisions (Tracey et al., 2014). Hence, understanding how host-pathogen interactions are affected by mismatches on a local spatial and temporal scale is important to implement preventive strategies and develop predictive models.

While there have been studies tackling the effect of landscape heterogeneity on pathogen transmission where limited high-resource areas can lead to transmission hotspots (Benavides et al., 2012; Nunn et al., 2014) as well as studies considering individual movement (Lane-deGraaf et al., 2013; Scherer et al., 2020; Tracey et al., 2014), very few studies take asynchronous effects between resource levels and host life-history events into consideration. Additionally, these few exceptions mainly focus on the effects on vector lifecycles, for example, for ticks and mosquitoes (Estrada-Peña et al., 2014; Wang et al., 2016). Hence, there is a lack of theoretical studies linking the direct and indirect effects of global change-induced temporal mismatches on host-pathogen coexistence and dynamics through multiple scales, for example, spatial and temporal heterogeneity in resource availability and individual host movement (Meentemeyer et al., 2012; Rees et al., 2013; White et al., 2018a).

Mechanisms underlying such a mismatch could lead to an increase, but also to a decrease in host-pathogen coexistence: On the one hand, when applying autocorrelated temporal resource dynamics to a spatially heterogeneous landscape, transmission hotspots could form in areas that have higher resource availability than the surrounding landscape. This would facilitate pathogen persistence in those hotspots and subsequently enable the pathogen to be transferred back to other host subpopulations after they have recuperated from low resource conditions (Duncan et al., 2013). On the other hand, if the resource availability changes randomly, meaning there is neither spatial nor temporal correlation in resource availability, the reduction of resources can lead to an immediate and severe drop in host density. Subsequently, such a drop in host density could lead to pathogen extinction. (Altizer et al., 2006; Tonkin et al., 2017).

We investigated the effect of a temporal lag in resource availability leading to a temporal mismatch between resource availability and the host reproduction probability on pathogen persistence. Asynchrony between the resource availability and the host reproduction

probability effectively creates a cascading effect from the resource landscape through host survival, host movement decisions, and resulting host density to pathogen transmission and survival (Figure 2.1). We study this propagating effect of a temporal mismatch in a bottom-up driven, interdependent system where the pathogen is dependent on the host, which in turn is dependent on the resource. In detail, we investigate how a constantly shifting temporal lag in peak resource availability away from the timing of host birth events affects host-pathogen coexistence. To this end, we used a modified version of an existing spatially explicit individual-based host-pathogen model of a group-living social herbivore, that is, classical swine fever (CSF) virus in wild boar (*Sus scrofa*) (Kramer-Schadt et al., 2009; Scherer et al., 2020).

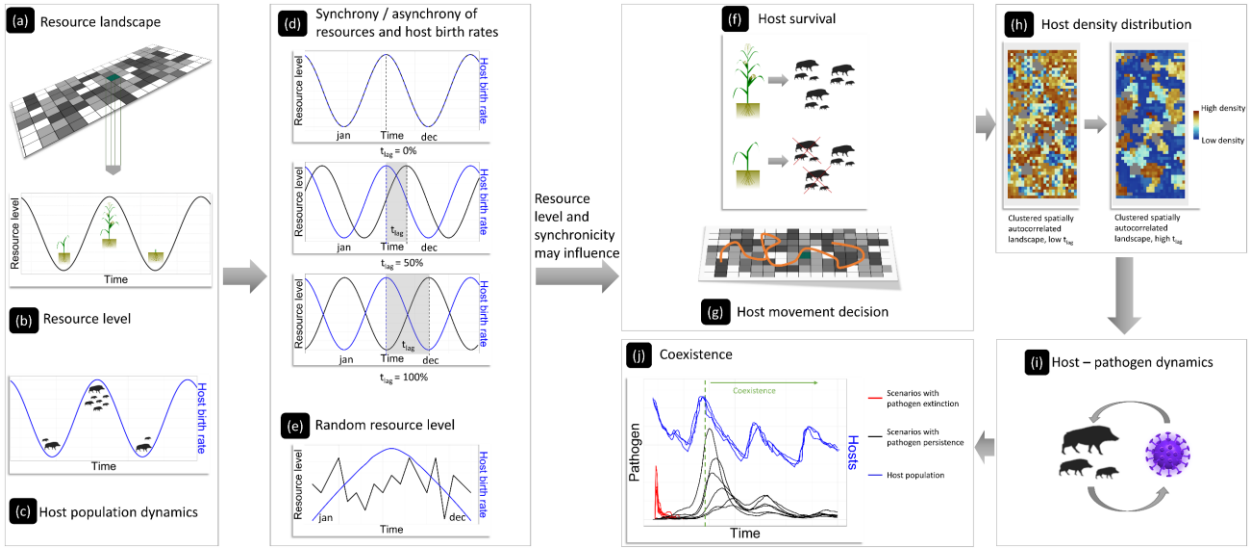

Figure 2.1: Cascading effect from the resource landscape (a) through the dynamic resource level of each single habitat cell (b) and the host population dynamics (c) that can be synchronous, asynchronous (shifted by t_{lag}) (d), or random (e) in time, respectively, to each other. The resource level at specific points in time may influence host survival (f) and movement decisions (g) that may alter host population density distribution (h) and subsequently host-pathogen interactions through contact rates and transmission (i) before ultimately accentuating scenarios that allow for coexistence (j).

We hypothesized that a temporal mismatch alters disease dynamics depending on the intensity of the mismatch between environmental resource availability and host life-history events and that movement can mediate or reverse the effects of asynchrony. In accordance with theory, we expect that unpredictable random changes in host resource availability over time, for example, induced by agricultural land-use practices like harvesting (Ullmann et al., 2018, 2020) or hunting, result in low coexistence probability due to increasing chance events, leading to higher

disease extinction (Melbourne & Hastings, 2008). In contrast, seasonality increases coexistence probability (Altizer et al., 2006). However, increasing asynchrony between seasonal resource availability and host life-history events will lead to a decrease in host-pathogen coexistence. Movement can reverse these processes by bridging spatiotemporal troughs in local host density, thereby increasing disease persistence. We discuss our results in terms of consequences for disease persistence under climate and land-use change conditions that may be provoked by increasing asynchrony of relevant time scales.

2.2 Methods

2.2.1 Model overview

We used a spatially explicit individual-based eco-epidemiological model developed by Scherer et al., (2020). It is based on earlier models only considering neighborhood infections developed by Kramer-Schadt et al., (2009) and Lange et al., (2012a,b). The model by Scherer et al., (2020) relies on individual movement decisions of host individuals, that is, long-distance roaming movement of males (hereafter termed "movement"), a process important for disease transmission. We further modified the model by adding spatiotemporal landscape dynamics representing changing resource availability, a response of movement decisions to that landscape and a resource-based mortality. A complete and detailed model description following the modified ODD (Overview, Design concepts, Detail) protocol (Grimm et al., 2006, 2020) is provided in the supplementary material (Appendix A1), and the model implementation is available in the Zenodo Database (Kürschner et al., 2021).

Overall, the model comprises two main components, a host life-history model and an epidemiological pathogen model. Host individuals are characterized by sex, age, location, demographic status (residential, group split of subadults and resource-based displacement to the neighbouring cells, and male long-distance roaming movement), and an epidemiological status. The latter is defined by an SIR epidemiological classification (susceptible, infected, and recovered; Kermack & McKendrick, 1927). Recovered individuals gain lifelong immunity and can pass on temporary immunity via maternal antibodies to their offspring. The pathogen model alters host survival rates, reproductive success, and infection length given its virulence.

2.2.2 Landscape structure

The landscape structure is comprised of a spatial grid of 1,250 2 km × 2 km cells each representing the average home range of a wild boar group (Kramer-Schadt et al., 2009), totalling a 100 km × 50 km landscape. The landscape is a self-contained system without any outside interaction or movement beyond the landscape border. Each cell is characterized by a variable resource availability (habitat quality) that is expressed as female host breeding capacity and that translates directly into possible group size, with the minimum being one breeding female per group to a maximum of nine. The initial resource availability was calibrated to achieve the reported average wild boar density of five breeding females per km2 (Howells & Edwards-Jones, 1997; Melis et al., 2006; Sodeikat & Pohlmeyer, 2003). We investigated several landscape scenarios of varying spatial complexity, ranging from a fully random landscape structure to different degrees of random landscape clusters generated in R (R Core team, 2019) using the NLMR package (Sciaini et al., 2018) while keeping the mean female breeding capacity constant at 4.5 females across the different landscapes, where all landscape cells, including the ones that are not suitable as habitat, are considered (Supplementary material Appendix A: Figure A4).

The spatiotemporal landscape dynamics are superimposed on the different types of landscapes, and the dynamics are designed to mimic seasonal changes by gradually increasing and decreasing resource availability. Resource availability in each cell increases in 5-week intervals for approximately 25 weeks from the beginning of the year and then declines in 5-week intervals for the following 25 weeks. Resource availability translates directly into the breeding capacity for each cell and cannot, during the increase, exceed the maximum breeding capacity of nine females and cannot decrease below one female during the decrease period. A breeding capacity < 1 could lead to inflated extinction scenarios, depending on the clustering of the landscape, through the creation of artificial barriers that would isolate host groups and prevent the pathogen from being spread. In case of wild boar, the increase or decrease of resource availability that occurs periodically throughout the year results in a variation of breeding females with an average over time being 4.5 females supported by one cell. Throughout each simulated year, resource availability changes in parallel to the host reproduction probability (Figure 2.1d). The resource availability is then temporally shifted (t_{lag}) away from the host reproduction probability by 25% increments up to a full mismatch at 100%. A higher level of

mismatch reflects an increase of severity in global change. Additionally, we implemented a nonseasonal, unpredictable landscape dynamic, where the resource availability changes randomly (a random integer between one and nine) every five weeks while maintaining a mean of 4.5 throughout the landscape (so-called "white noise," Figure 2.1e).

2.2.3 Process overview and scheduling

The temporal resolution equals the approximate CSF incubation time of one week (Artois et al., 2002). The following procedures were scheduled each step in the following order: pathogen transmission, male host roaming movement, natal host group split of subadult males and females and subsequent resource-based displacement to the neighbourhood, host reproduction, host mortality (disease-based and resource-based), host aging, and landscape dynamics. Group split of subadult males and females under no mismatch conditions was limited to week 17 and week 29 of the year, respectively, representing the typical dispersal time for each sex. The order of these procedures was established in previous versions of the models, and changes of the order were not shown to have significant implications to the model outcome.

2.2.4 Main processes

Pathogen transmission – All transmission processes remain unchanged from the model implementation by Scherer et al., (2020). The course of the disease is determined by an age-specific case fatality rate and an exponentially distributed infectious period for lethally infected individuals. Transient infected hosts have an infectious period of one week and gain lifelong immunity (Dahle & Liess, 1992). Infection dynamics emerge from multiple processes: within group transmission, movement-based transmission, and individual age-dependent courses of infection. Within groups, the density-dependent infection pressure is determined by transmission chance and the number of infectious group members. For roaming males, under movement-based scenarios, individual per-step transmission probability is calculated as the transmission rate divided by the movement distance the individual has travelled to account for the time an individual spends in each cell (Scherer et al., 2020).

Male host roaming movement – Our model uses two of the explicit intercell movement rules for males implemented in Scherer et al., (2020) (habitat-dependent movement: HDM; correlated random walk: CRW) as well as a setup without explicit movement (neighborhood

infection). Individuals performing a CRW display a general tendency to continue in the same direction as the previous movement without taking landscape structure or resource availability into consideration (Codling, Plank & Benhamou, 2008; Kareiva & Shigesada, 1983). The decision process of individuals following the HDM rule is related to the underlying landscape directly by tending to move toward landscape cells with higher resource availability. In general, individuals were moving up to an individual weekly maximum movement distance or supplementary rules led to the decision to stay in the current cell. Furthermore, individuals move from cell to cell without within-cell movement.

Group split of subadults – We implemented two distinct responses to changing resource availability. First, if the theoretical maximum number of individuals in a group is higher than the number of individuals currently present in the group, then the group does not split. However, if low resource availability reduces the theoretical maximum group size below the number of individuals currently in the group, individuals above the current capacity will try to leave the group and establish in an empty neighbouring cell based on resource availability. The selection of individuals to leave the group is dependent on the age of the individual, where young individuals will leave the group first.

Host reproduction – Female hosts reproduce once a year, depending on their age class. The number of breeding females is determined by each habitat cell's resource-dependent breeding capacity. Individual female hosts are checked for their breeding status on a weekly basis to then reproduce depending on the season with a peak in March and no reproduction in winter from October to December.

Host mortality – Another functional response to resource availability is increasing age-dependent mortality over time. Groups that exceed the theoretical maximum group size have increased mortality depending on the difference between actual group size (number of individuals) and theoretical maximum group size. Furthermore, the maximum survival time for adults in groups above their respective maximum group size was capped at assumed levels between 5 and 20 weeks (for details, see ODD Appendix A1).

Landscape dynamics with temporal lag – We modelled several levels of temporal lags (t_{lag}; Figure 2.1d). We gradually increased the level from 0% (no change) to 100% (full mismatch

between host population dynamics and resource availability) in 25% increments. Each 25% increment represents 5 weeks in the simulation. Therefore, the peak in resource availability is shifted 5 weeks away from the host species reproductive peak in each consecutive increment up to the maximum of approximately 25 weeks. The 25-week (or 100%) scenario represents the full mismatch of host population dynamics and resource availability. The scenario with 0% t_{lag} was used as control for temporal shift scenarios.

2.2.5 Model analysis

Each simulation was run for 50 years (2,600 weeks) in total, with the virus being randomly released in the second year (weeks 53-104). The virus was introduced to one out of a set of predefined cells in the centre of the upper row with a resource availability above the mean of 4.5 during time of release. We ran 25 repetitions per combination of movement rule (3 levels: CRW, HDM, and no roaming movement as a control scenario for movement rules), landscape scenario (4 levels: small clusters, medium clusters, large clusters, and random as a control scenario for the landscape structure), and degree of mismatch (5 levels: t_{lag} 25%, t_{lag} 50%, t_{lag} 75%, t_{lag} 100%, and t_{lag} 0% as a control for mismatch). We analysed proportional coexistence probability (P_{coex}) estimated over each block of 25 repetitions by counting the times both host and pathogen survived during the simulations. Furthermore, for simulations where coexistence was not achieved, we measured the time to pathogen extinction (t_{ext}). Due to the spatial variability of clusters throughout the landscape, the overall densities of hosts and pathogens varied too little across the different landscapes and scenarios to provide more detailed insight, while measuring local per-cell densities was beyond the scope of the study. Therefore, we also analysed the spatiotemporal distribution of infected hosts in the landscape by recording the number of timesteps an infected host was present in each landscape cell. Next, we applied the autocorrelation function (acf) at lag 2 to the frequency distribution of the cumulative time the pathogen was present in each landscape cell, so as to characterize the amount of time and proportion of the landscape with pathogen presence in the different scenarios. The higher the value of acf, the more similar is the cumulative time with pathogen presence across all the cells in the landscape. On the contrary, a low acf at the following timestep (lag 2) indicates that the cumulative time of pathogen presence differs among the cells across the landscape, more

precisely, that very few cells have the pathogen present, whereas the majority of cells never has an infected host present.

2.3 Results

2.3.1 Host-pathogen coexistence and disease persistence

The coexistence probability (P_{coex}) was lower in the two scenarios with roaming movement compared to the movement control (scenarios without roaming movement, Figure 2.2). Importantly, in both scenarios with movement the coexistence also decreased with increasing temporal mismatch (t_{lag}) and increasing landscape homogeneity (large clusters). That means, in contrast to our predictions, movement decreased coexistence or pathogen persistence. The decrease in P_{coex} was however, more severe in scenarios with random movement (CRW) where P_{coex} at t_{lag} 100% decreased to 24% from 96% in the control (t_{lag} 0%; i.e. no mismatch) in large-cluster landscapes compared to a P_{coex} decrease to 48% from 92% in the control in similar scenarios with habitat dependent movement (HDM). On average, over all landscape configurations, P_{coex} at t_{lag} 100% decreased to 45% with CRW, 73% with HDM and 91% in the movement control. In general, the control for temporal mismatch showed a P_{coex} between 100 and 92% for CRW, between 100 and 96% for HDM and 100% in movement control scenarios (no roaming movement). Random landscape dynamics yielded a P_{coex} of 0% in all landscape- and movement scenarios.

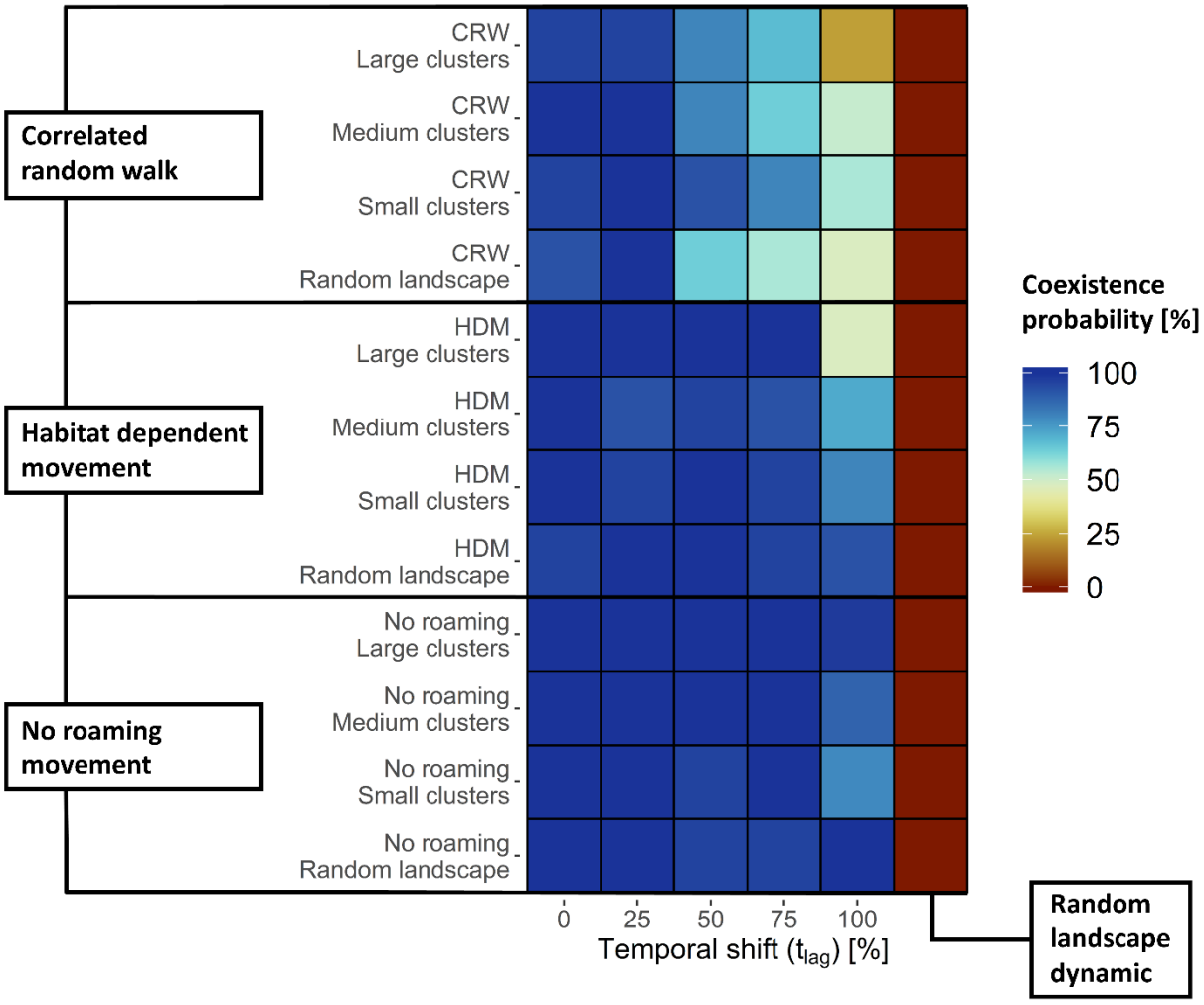

Figure 2.2: Coexistence probability (P_{coex}) estimated as the proportion of simulation runs in which both host and pathogen survived (color gradient). P_{coex} is grouped by three types of applied movement rules (correlated random walk–CRW, habitat-dependent movement–HDM, and no roaming movement (control)) and four different landscape configurations (large, medium, and small clusters and random configuration) along an increasing temporal mismatch (0%–100%) including a random dynamic (control)

2.3.2 Pathogen extinction time

We assessed the mean pathogen extinction time for simulations with P_{coex} below 100% (Figure 2.3). For most scenarios, the pathogen went extinct around the time of pathogen release. As an exception to that, the t_{lag} 75% scenarios with CRW movement had a higher t_{ext} then the other scenarios. Notably, for both types of movement (CRW and HDM) t_{ext} was shorter at t_{lag} 100% when compared with the other t_{lag} scenarios. That means, very restricted or directed movement as in the HDM does considerably delay pathogen extinction to high t_{lag} scenarios. Early onset of many disease clusters, as with CRW, again synchronized the outbreak temporally across the

landscape, leaving no high-density host cluster behind for bridging infections especially when the host peak density is completely mismatching peaks in resource availability (i.e. t_{lag} = 100%).

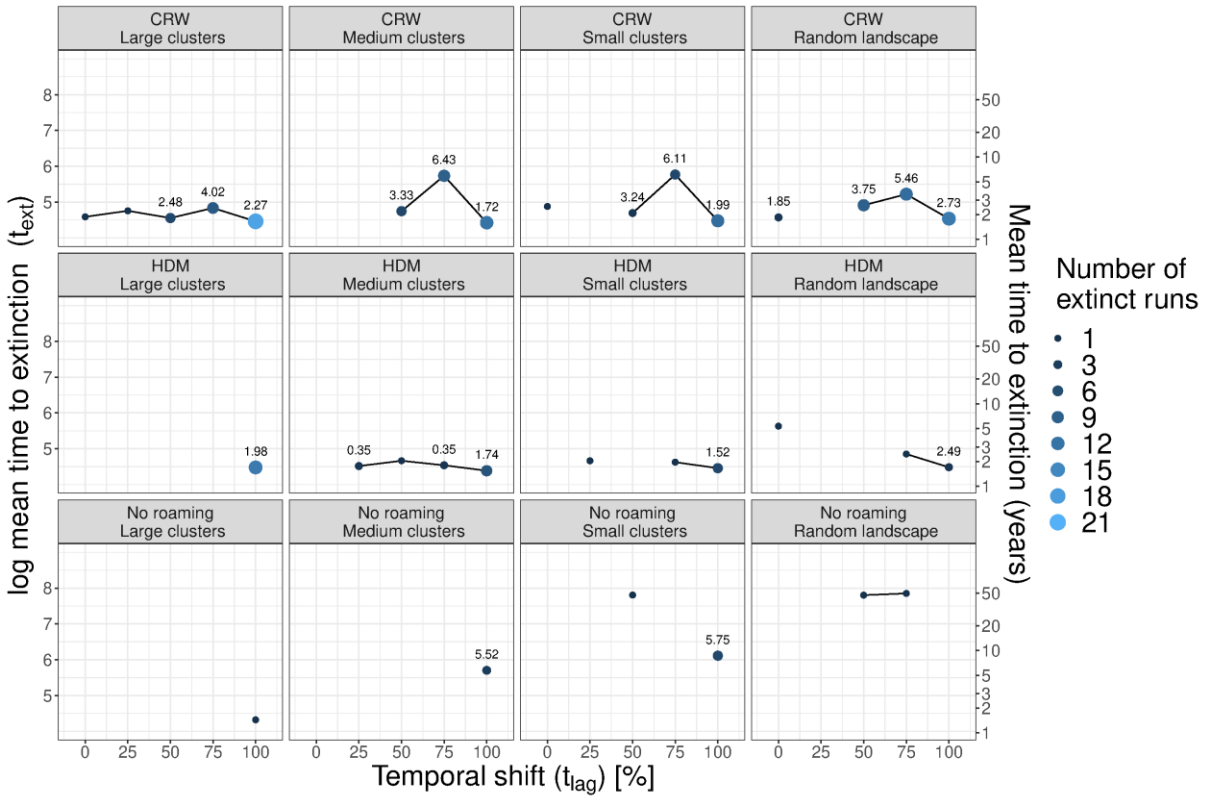

Figure 2.3: Mean log pathogen extinction times for all simulation scenarios where the pathogen went extinct separated for movement scenarios (CRW– correlated random walk, HDM– habitat-dependent movement, and no roaming movement (control)), landscape configuration, and temporal shift (tlag). The number of extinct runs (gradient and size) is relative to the 25 total runs that were conducted per combination of movement, landscape, and tlag. The number above the points is the standard deviation of the log mean pathogen extinction time, where applicable.

2.3.3 Spatial patterns in coexistence

To assess the effects of resource availability on host survival, host movement and pathogen survival, we explored the spatial distribution of infected hosts over the course of the simulations where coexistence was achieved. We found highly similar spatial patterns across all landscape scenarios, thus we here use the medium-cluster landscape as an example case in the following. For scenarios using the CRW movement rule we saw a decrease in acf (autocorrelation function) at lag 2 with increasing t_{lag} from 0.55 at t_{lag} 0% to 0.45 at t_{lag} 50% (Table 2.1). This decrease in acf means that with an increasing t_{lag} there were fewer cells with similar cumulative time of pathogen presence, i.e. the cumulative time with pathogen presence differed increasingly

among the cells. Such a difference among the cells in the cumulative time with pathogen presence increased further for the scenarios with t_{lag} 100% as indicated by acf 0.02, meaning that only a small fraction of the landscape carried the infected hosts, but a large number of the grid cells were either never infected or only for short periods of time. Figure 2.4 shows an example for the spatial clustering for the CRW movement scenario; more detailed figures for all movement and landscape scenarios can be found in the supplementary material (Appendix A2: Figure A5-A7). The frequency distribution of the cumulative time the pathogen was present in each landscape cell (Figure 2.5a) indicates that, in scenarios with t_{lag} 75 and 100% compared to the scenarios with low t_{lag}, the infected hosts were present in only a small fraction of the landscape for an extended period. In most of the other parts of the landscape, infected hosts were only present for a short duration, or were not present at all.

Table 2.1: Acf (autocorrelation function) values at lag 2 for all movement scenarios (CRW– correlated random walk, HDM–habitat dependent movement, and no roaming movement (control)), and temporal shift (t_{lag}) combinations including the 95% confidence interval (ci).

Movement	t_{lag}	ci +/-	acf lag 2
CRW	0	0.51	0.55
	25	0.46	0.49
	50	0.54	0.45
	75	0.51	0.32
	100	0.60	0.02
HDM	0	0.60	0.19
	25	0.49	0.25
	50	0.60	0.09
	75	0.60	0.13
	100	0.52	0.01
No roaming	0	0.60	0.12
	25	0.50	0.24
	50	0.54	0.34
	75	0.54	0.24
	100	0.52	-0.02

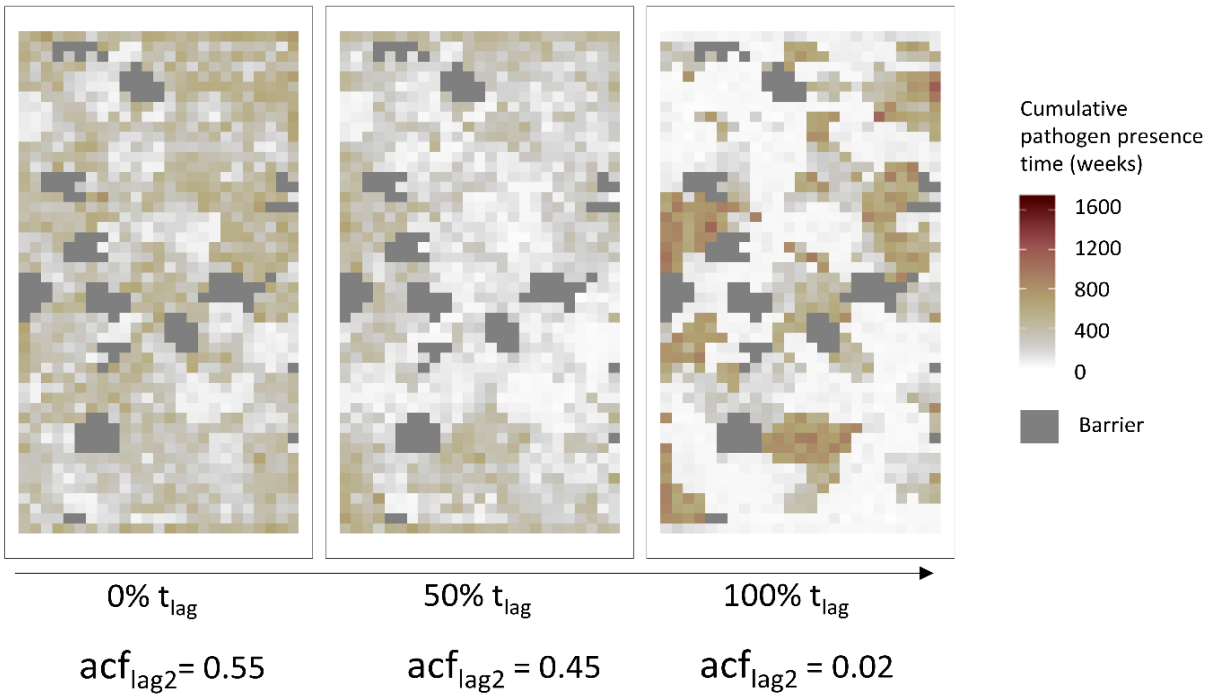

Figure 2.4: Spatial distribution of infected hosts in the correlated random walk movement scenario (CRW) applied to a landscape with medium clusters. The colour gradient shows the cumulative pathogen presence time in weeks, that is, how long the pathogen was present in a landscape cell including the acf (autocorrelation function) values at lag 2 for those scenarios. Each frame represents a single representative example run with increasing temporal shift (t_{lag}) from left to right

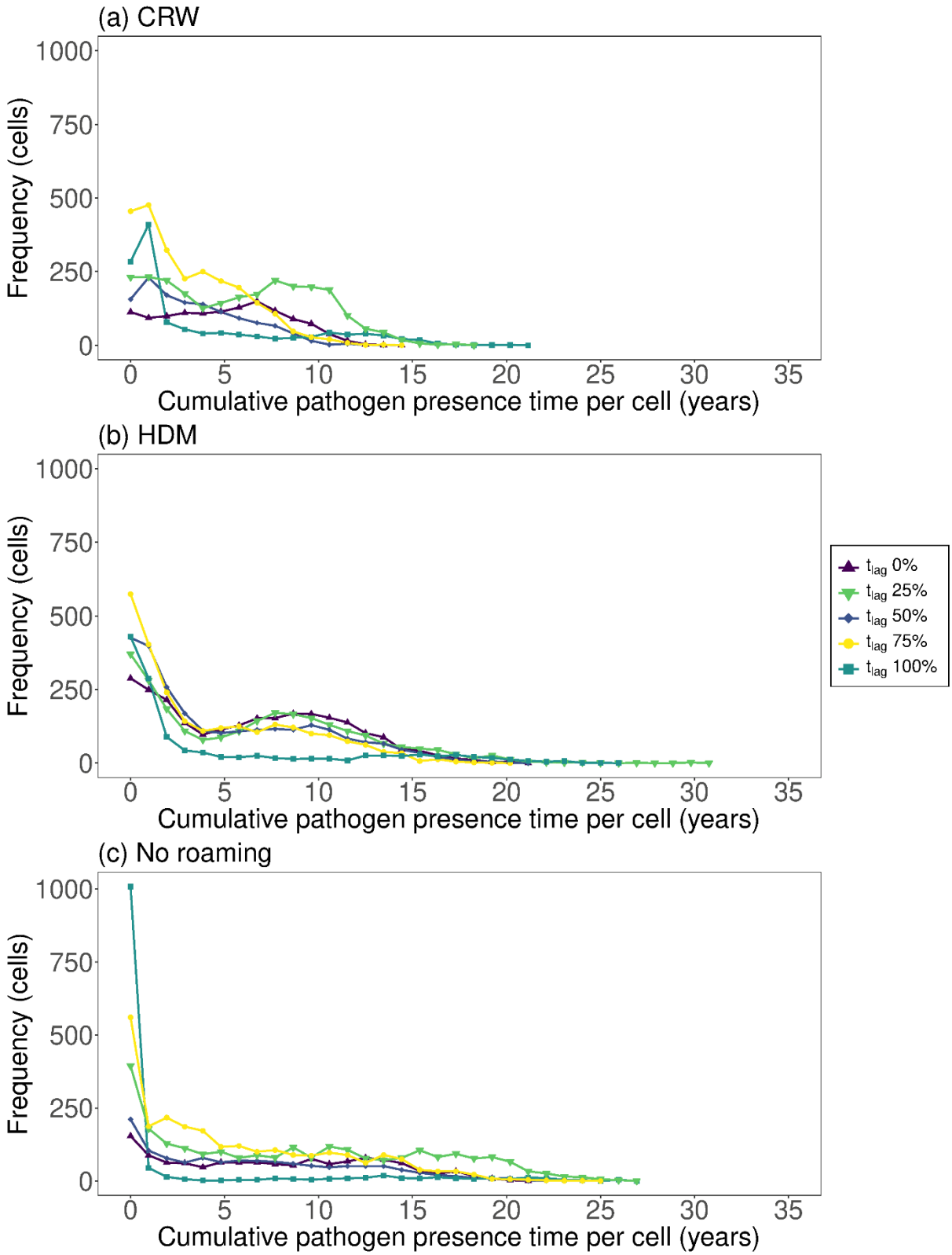

Figure 2.5: Frequency of cells with infected hosts throughout simulation runs with CRW movement (a), HDM movement (b), and no roaming movement (c) for all five t_{lag} scenarios. The cumulative pathogen presence time per landscape cell represents the total amount of time that a landscape cell had infected hosts occupying it, while frequency is the overall number of cells with the same pathogen presence time values at the end of the simulation

Within HDM scenarios (Table 2.1), while there was a lower acf at t_{lag} 100% (0.01) compared to t_{lag} 0% (0.19), there was no steady decrease in acf with increasing t_{lag} as found for CRW scenarios. Interestingly, however, the acf for HDM scenarios was on average lower than for CRW scenarios, indicating that under the HDM scenario the number of cells with a similar cumulative time of pathogen presence was lower than under the CRW. The frequency distributions of the cumulative time the pathogen was present in each landscape cell for HDM scenarios (Figure 2.5b) showed similar patterns to those found for CRW: in scenarios with high t_{lag} the pathogen was either absent from the majority of the cells, or present in a small fraction of the landscape.

Scenarios without roaming movement (control, Figure 2.5c) also showed the lowest acf at t_{lag} 100% with -0.02 when compared to all other t_{lag} scenarios (Table 1.1). The acf at t_{lag} 50% (0.34) was, however, higher than the acf at t_{lag} 75% (0.24), indicating that at this intermediate time lag we find the highest number of cells (i.e. larger proportion of the landscape) with similar cumulative time of pathogen presence. The t_{lag} 100% scenario showed 940 out of 1250 cells without infected hosts throughout the entire simulation and thus had no infected hosts in a large portion of the landscape while still having an 88% P_{coex}.

2.4 Discussion

While previous modelling approaches have theoretically demonstrated the importance of interactions between landscape structure, individual movement behaviour, and pathogen transmission for predicting and understanding disease dynamics (Scherer et al., 2020; White et al., 2018b), few studies have addressed how an increasing asynchrony between resource availability and dependent host biological processes influences host-pathogen coexistence. Given the current climate warming crisis with increased mismatch between resource availability and host phenological events (Plard et al., 2014; Post & Forchhammer, 2008; Visser & Gienapp, 2019), the knowledge on how disease dynamics might toss and turn in the future is of utmost importance for managing emerging and zoonotic diseases (White et al., 2018b). Also, tree mast years (Doublet et al., 2019) or land-use practices like harvesting, crop rotation, or asynchronous anthropogenic pressures such as hunting might lead to mismatches. While

climate warming might induce mismatch effects negatively affecting host life history, climate warming might have direct effects on the pathogen, too, amplifying either positive or negative consequences on the host. Indeed, it is reasonable to expect that some diseases will adapt to changing environmental conditions and potentially increase in prevalence (Rohr & Cohen, 2020; Thomas, 2020). However, here we focus on mismatch effects on host life history.

In accordance with theory, we found that random fluctuations of resources decreased coexistence, whereas occurrence of biological events in synchrony with resource seasonality increased coexistence (Altizer et al., 2006; Heino et al., 2000; Roy et al., 2005; Wichmann et al., 2003). This is underpinned by studies demonstrating that seasonality, for example, in transmission rates, can alter the dynamics of host-pathogen interaction and feed back to effects on the hosts density as demonstrated by Bolzoni et al., (2008) for rabies in several species. Other studies found similarly complex dynamics arising by applying seasonal dynamics to the host birth rate as done by Ireland et al., (2007) for rabies in foxes. However, for full mismatch conditions, our model yielded still rather high host-pathogen coexistence probabilities, contrary to our initial expectations.

2.4.1 Disease hotspots resulting from spatiotemporal asynchrony

One apparent factor for coexistence despite completely decoupled environmental and biological events, throughout all simulations, was the spatiotemporal clustering of infection hotspots with increasing mismatch, forming disease islands in the landscape. The emergence of disease islands due to asynchronous resource dynamics has also been shown experimentally by Duncan et al., (2013) and theoretically by Becker and Hall (2016). The spatial restrictions to relatively small infection hotspots suggest a lower coexistence probability, with small host populations not being able to sustain a prolonged disease outbreak. Usually, a disease outbreak within an island can lead to critical loss of host individuals up to the point where the population cannot recuperate on its own (Clifford et al., 2006; Walker et al., 2008). However, in our case those hotspots were not constantly isolated from each other or the surrounding landscape. In this case, theory predicts that asynchrony in resource availability throughout the landscape facilitates demographic rescue by movement or migration (Roy et al., 2005). Our model demonstrated this effect that subsidizes pathogen persistence and thus coexistence even when

the timing of resource scarcity coincided with the seasonal reproduction peak at a t_{lag} of 100%. Simulations of this "worst-case scenario" of resource mismatch showed that high-resource cells within the landscape that can support a higher population density were constantly recolonized if the pathogen depleted the host population in some of those cells during low resource conditions. On the other hand, during "high-resource periods," the entire remaining population could spread more evenly throughout the landscape. High-resource habitat clusters where the pathogen went temporarily extinct and thus harboured largely undisturbed host populations can function as partial refuges for many host individuals. Once the resource availability in the surrounding habitat becomes more favourable, these individuals can spread out and recolonize potentially depleted habitat cells and could subsequently come into contact with infected hosts. Respectively, high-resource habitat clusters where the pathogen was constantly present function as partial sources for the pathogen allowing it to be reintroduced into now susceptible or naïve subpopulations (Elkin & Possingham, 2008).

While metapopulation dynamics and source-sink dynamics have been well studied and documented (Bansaye & Lambert, 2013; Foppen et al., 2000; Nagatani et al., 2018), including the effect of temporal autocorrelation (Gonzalez & Holt, 2002; Roy et al., 2005), our model showed a metacommunity structure only under temporal mismatch scenarios. This reduces any negative effect a mismatch could have on coexistence, such as pathogen extinction through critically low host density. Only when the mismatch increased above 50%, did the distribution of infected hosts start to aggregate in certain parts of the landscape, forming a metacommunity structure with the pathogen.

Host density and connectivity are the two most important factors that determine contact rates and subsequent disease transmission in directly transmitted diseases (Parratt et al., 2016). The timing of the initial outbreak was variable between a burn-in phase of one year and the third year. This temporal variability of starting the initial outbreak might have led to the fact that in some simulations, the pathogen could never establish and invade the host population, leading to many extinction times shortly after pathogen introduction. This was especially prominent in mismatch scenarios. However, when the pathogen was able to establish in the host population beyond the initial outbreak and subsequently spread through the landscape, extinction became increasingly unlikely. The increase in early extinctions with increasing mismatch further

emphasizes an increasing importance of the timing of biological events. Pathogens are less likely to cause a widespread disease outbreak when being introduced into a susceptible population during a period of unfavourable environmental conditions.

2.4.2 Movement and decision-making in animals as key mechanism of coexistence

Spatially explicit host movement effectively mitigates some of the spatiotemporal restrictions a dynamic resource landscape can put on host and/or pathogen. As Scherer et al., (2020) have shown for static landscapes, explicit host movement can increase coexistence, and this also holds true for many instances within a spatiotemporally dynamic landscape. However, movement is also subject to a larger variability, for example, in distance moved or in timing of movement and can, in fact, become detrimental to coexistence under certain circumstances. There is, for example, the possibility that an infected host individual transports the pathogen to susceptible populations that have not fully recuperated from unfavourable habitat conditions and lack the population density to sustain the pathogen. This is especially prominent for nondirected movement such as correlated random walks, neglecting important species-landscape interactions (White et al., 2018b).

Particularly under random movement, there is a lower chance, compared to directed habitat-dependent movement, for infected host individuals to transmit the disease to susceptible hosts in high resource, high host density habitat clusters fast enough to allow for pathogen persistence. This is not apparent under habitat-dependent movement, due to directed movement toward high-resource areas. In consequence, under the directed habitat-dependent movement, the chance of coming into contact and infecting other hosts increases, while moving toward or through high-resource habitats. Hence, movement-induced species interactions could be a key mechanism promoting disease persistence, which is underpinned by studies on waterfowl (Figuerola & Green, 2000) or white-fronted geese (Kleijn et al., 2010). Also, White et al., (2018b) have demonstrated theoretically that decision-making of animals, here the decision to move toward high-quality habitat, might increase disease persistence.

2.4.3 The effect of landscape structure on coexistence

An increasing homogenization of the landscape particularly through anthropogenic land-use change, for example, deforestation or the increase in agricultural areas (Patz et al., 2004), can,

however, offset the pronounced effect of habitat-dependent movement on coexistence. Individuals within large clusters, comprised of the same level of resources, might not be able to find higher resource areas in time. In addition, a large proportion of the host population is situated in similar habitats and subjected to the same level of resource decrease simultaneously. Consequently, the loss of susceptible hosts due to death or immunization cannot be compensated with the influx of new susceptible hosts, for example, though birth or immigration, to sustain the pathogen (McCallum, 2012), causing it to go extinct in large parts of the landscape. Accordingly, our results demonstrate lower coexistence in landscapes with larger homogeneous habitat clusters.

Interestingly, while increasing spatial homogeneity of the landscape had a negative effect on pathogen persistence, we still found the formation of infection hotspots in scenarios with full temporal mismatch between host reproduction and resource peaks. Infection hotspots were, with varying degree, present across all tested landscape configurations in scenarios with full mismatch and across all tested movement scenarios. While the initial spatial resource structure might not be important when it comes to the emergence of infection hotspots, larger low-resource areas in more homogeneous landscape configurations can form temporary barriers, similar to seasonal landscape barriers (Mui et al., 2017). These temporary landscape barriers can restrict the pathogen to certain areas in scenarios where host individuals have no explicit long-distance movement (Appendix A2: Figure A7). While there was no strong effect of these temporary barriers on coexistence, this further highlights the role of explicit long-distance host movement in terms of disease transmission (see review in Altizer et al., 2011).

2.4.4 A reality check of our model assumptions

Our individual-based model here best described a group-living social animal conducting long-range movements acting autonomously, that is, deciding on movement directions, while demographic processes are also resource-dependent. On the other hand, it also considers viral traits like acute to chronic infections in a directly transmitted disease. Thus, our model is quite complex in terms of realistic processes and hence a template for many disease dynamics under temporal mismatch, induced, for example, by climate and land-use change. The spillover of Hendra virus from flying foxes to other animals (Martin et al., 2015; Plowright et al., 2015) or the

impact of the canine distemper virus on spotted hyenas (Benhaiem et al., 2018) or lions (Craft et al., 2011) could be amplified by climate and land-use change-induced temporal mismatches.

Climate change is altering environmental fluctuations that lead to increasing mismatches between resources and biological events (Durant et al., 2007). And, although some animal species may adapt to such temporal shifts in resource availability, they might respond too slowly to be able to persist (Radchuk et al., 2019). Yet, our results demonstrate that we could expect the emergence of disease hotspots under a full temporal mismatch of resource availability and the timing of host birth peaks, counteracting possible adverse effects of reduced host densities. Temporal shifts of the magnitude that were used in this work, that is, large shifts of multiple weeks up to a full mismatch, might not be as important for climate change in the near future, where temporal mismatches are expected to be smaller (Thackeray et al., 2016). However, climate change does not occur separately from other anthropogenically caused threats. Indeed, large-scale land-use changes can alter the resource distribution throughout a landscape in more drastic ways resulting in the possibility for stronger mismatches between available resources and host life history (Ullmann et al., ,2018, 2020). For example, changing natural habitats into agricultural areas could still provide resources, that is, food, but the peak availability might occur at drastically different times when compared to the natural environment.

The wild boar as our model host species is a long-lived mammal with seasonal breeding that has an annual peak and is currently profiting from climate warming-induced changes of the environment (Vetter et al., 2020). Pathogens will most probably profit most in species with multiple annual peaks of reproduction. Multiple reproductive events per year, like in hyenas (Kruuk, 1972), might mitigate effects of a mismatch on host-pathogen coexistence. While during one peak the resources might be scarce and the population size would be temporally reduced, the time between several birth peaks could be short enough to compensate the drop in host density and benefit host-pathogen coexistence. Subsequently, the more birth peaks a species has, the less it should be affected by temporal mismatches. In case of wild boar, if the species continues to benefit from the effects of climate and land-use change, the single birth peak dynamic might continue to change toward multiple reproductive peaks per year, further offsetting adverse effects on host-pathogen coexistence. This could lead to an upsurge in persistent viral outbreaks throughout wild boar populations, which might exacerbate currently

discussed processes like individual infection risk in piglets and movement (Scherer et al., ,2019, 2020). A prominent example is the persistence of African Swine Fever (ASF) in wild boar in Europe, which affects animal health more severely and can cause profound economic damages (Halasa et al., 2016) when coming into contact with domestic pigs.

Additionally, due to high mutation rates and short generation times, pathogens are likely to evolve, which can influence host as well as pathogen survival (Galvani, 2003) and might compensate for the response of the host species to changes in resource availability. Seasonal resource dynamics might strongly affect pathogen evolution if, during periods of high host densities, a particular strain of the pathogen has adapted to capitalize on the increased possibility for transmission or during periods of low host density if the pathogen has adapted to persist through those conditions (Altizer et al., 2006; Hite & Cressler, 2018; Koelle et al., 2005). A strong temporal mismatch that creates disease hotspots in combination with an even stronger system of alternating high and low host population densities than basic seasonality could further facilitate pathogen evolution. Furthermore, our model does not account for the host immune system, which can be impacted by a dynamic resource landscape. Long periods of resource scarcity and an expected poorer nutrition, as well as increased investment in movement to move toward higher resource areas, have been shown to negatively affect a host individual's ability to defend against infectious diseases (Altizer et al., 2006; Sheldon & Verhulst, 1996; White et al., 2018b). Subsequently, this could lead to further alterations of host-pathogen dynamics and coexistence.

In conclusion, our work has shown that temporary spatial hotspots of infectious hosts can emerge from a limited number of high-resource sites that are formed due to temporal mismatches between resource availability and host reproduction. Considering the increasing effect of climate and land-use change on resource availability and distribution, this will promote the understanding of how temporal resource variability and host movement affect host-pathogen systems.

2.5 Additional information

Acknowledgements

This work was supported by the German Research Foundation (DFG) in the framework of the BioMove Research Training Group (DFG-GRK 2118/1). We thank Volker Grimm for valuable comments on earlier drafts of this manuscript, Michael Crawford for helping with English language editing and Florian Jeltsch for helpful discussions.

Data availability

The model implementation in NetLogo is available on Zenodo (DOI:10.5281/zenodo.4593791).

Supplementary material

- Appendix A1: ODD protocol
- Appendix A2: Additional figures

References

Altizer, S., Bartel, R., Han, B.A., 2011. Animal Migration and Infectious Disease Risk. Science 331, 296–302. https://doi.org/10.1126/science.1194694

Altizer, S., Dobson, A., Hosseini, P., Hudson, P., Pascual, M., Rohani, P., 2006. Seasonality and the dynamics of infectious diseases. Ecology letters 9, 467–484. https://doi.org/10.1111/j.1461-0248.2005.00879.x

Altizer, S., Ostfeld, R.S., Johnson, P.T.J., Kutz, S., Harvell, C.D., 2013. Climate Change and Infectious Diseases: From Evidence to a Predictive Framework. Science 341, 514–519. https://doi.org/10.1126/science.1239401

Artois M., Depner K.R., Guberti V., Hars J., Rossi S., & Rutili D. (2002). Classical swine fever (hog cholera) in wild boar in Europe. Revue Scientifique et Technique de l'OIE, 21, 287–303. http://dx.doi.org/10.20506/rst.21.2.1332

Bansaye, V., Lambert, A., 2013. New approaches to source-sink metapopulations decoupling demography and dispersal. Theoretical Population Biology 88, 31–46. https://doi.org/10.1016/j.tpb.2013.06.003

Becker, D.J., Hall, R.J., 2016. Heterogeneity in patch quality buffers metapopulations from pathogen impacts. Theor Ecol 9, 197–205. https://doi.org/10.1007/s12080-015-0284-6

Bellard, C., Bertelsmeier, C., Leadley, P., Thuiller, W., Courchamp, F., 2012. Impacts of climate change on the future of biodiversity: Biodiversity and climate change. Ecology Letters 15, 365–377. https://doi.org/10.1111/j.1461-0248.2011.01736.x

Benavides, J., Walsh, P.D., Meyers, L.A., Raymond, M., Caillaud, D., 2012. Transmission of Infectious Diseases En Route to Habitat Hotspots. PLoS ONE 7, e31290. https://doi.org/10.1371/journal.pone.0031290

Benhaiem, S., Marescot, L., East, M.L., Kramer-Schadt, S., Gimenez, O., Lebreton, J.-D., Hofer, H., 2018. Slow recovery from a disease epidemic in the spotted hyena, a keystone social carnivore. Commun Biol 1, 201. https://doi.org/10.1038/s42003-018-0197-1

Bolzoni, L., Dobson, A.P., Gatto, M., De Leo, G.A., 2008. Allometric Scaling and Seasonality in the Epidemics of Wildlife Diseases. The American Naturalist 172, 818–828. https://doi.org/10.1086/593000

Christian, K., Webb, J.K., Schultz, T., Green, B., 2007. Effects of Seasonal Variation in Prey Abundance on Field Metabolism, Water Flux, and Activity of a Tropical Ambush Foraging Snake. Physiological and Biochemical Zoology 80, 522–533. https://doi.org/10.1086/519959

Clifford, D.L., Mazet, J.A.K., Dubovi, E.J., Garcelon, D.K., Coonan, T.J., Conrad, P.A., Munson, L., 2006. Pathogen exposure in endangered island fox (Urocyon littoralis) populations: Implications for conservation management. Biological Conservation 131, 230–243. https://doi.org/10.1016/j.biocon.2006.04.029

Codling E. A., Plank M. J., & Benhamou S. (2008). Random walk models in biology. Journal of The Royal Society Interface, 5, 813–834. http://dx.doi.org/10.1098/rsif.2008.0014

Conaway, C.H., 1971. Ecological Adaptation and Mammalian Reproduction. Biology of Reproduction 4, 239–247. https://doi.org/10.1093/biolreprod/4.3.239

Craft, M.E., Volz, E., Packer, C., Meyers, L.A., 2011. Disease transmission in territorial populations: the small-world network of Serengeti lions. J. R. Soc. Interface 8, 776–786. https://doi.org/10.1098/rsif.2010.0511

Dahle, J., Liess, B., 1992. A review on classical swine fever infections in pigs: Epizootiology, clinical disease and pathology. Comparative Immunology, Microbiology and Infectious Diseases 15, 203–211. https://doi.org/10.1016/0147-9571(92)90093-7

Dornelas, M., Magurran, A.E., Buckland, S.T., Chao, A., Chazdon, R.L., Colwell, R.K., Curtis, T., Gaston, K.J., Gotelli, N.J., Kosnik, M.A., McGill, B., McCune, J.L., Morlon, H., Mumby, P.J., Ovre\aas, L., Studeny, A.,

Vellend, M., 2013. Quantifying temporal change in biodiversity: challenges and opportunities. Proceedings. Biological sciences 280, 20121931. https://doi.org/10.1098/rspb.2012.1931

Doublet, V., Gidoin, C., Lefèvre, F., Boivin, T., 2019. Spatial and temporal patterns of a pulsed resource dynamically drive the distribution of specialist herbivores. Sci Rep 9, 17787. https://doi.org/10.1038/s41598-019-54297-6

Duncan, A.B., Gonzalez, A., Kaltz, O., 2013. Stochastic environmental fluctuations drive epidemiology in experimental host-parasite metapopulations. Proceedings. Biological sciences 280, 20131747. https://doi.org/10.1098/rspb.2013.1747

Durant, J., Hjermann, D., Ottersen, G., Stenseth, N., 2007. Climate and the match or mismatch between predator requirements and resource availability. Clim. Res. 33, 271–283. https://doi.org/10.3354/cr033271

Durant, S., 1998. Competition refuges and coexistence: an example from Serengeti carnivores. Journal of Animal Ecology 67, 370–386. https://doi.org/10.1046/j.1365-2656.1998.00202.x

Elkin, C.M., Possingham, H., 2008. The Role of Landscape-Dependent Disturbance and Dispersal in Metapopulation Persistence. The American Naturalist 172, 563–575. https://doi.org/10.1086/590962

Estrada-Peña, A., Carreón, D., Almazán, C., de la Fuente, J., 2014. Modeling the Impact of Climate and Landscape on the Efficacy of White Tailed Deer Vaccination for Cattle Tick Control in Northeastern Mexico. PLoS ONE 9, e102905. https://doi.org/10.1371/journal.pone.0102905

Figuerola, J., Green, A.J., 2000. Haematozoan Parasites and Migratory Behaviour in Waterfowl. Evolutionary Ecology 14, 143–153. https://doi.org/10.1023/A:1011009419264

Foppen, R.P.B., Chardon, J.P., Liefveld, W., 2000. Understanding the Role of Sink Patches in Source-Sink Metapopulations: Reed Warbler in an Agricultural Landscape. Conservation Biology 14, 1881–1892. https://doi.org/10.1111/j.1523-1739.2000.99022.x

Galvani, A.P., 2003. Epidemiology meets evolutionary ecology. Trends in Ecology & Evolution 18, 132–139. https://doi.org/10.1016/S0169-5347(02)00050-2

Gonzalez, A., Holt, R.D., 2002. The inflationary effects of environmental fluctuations in source-sink systems. Proceedings of the National Academy of Sciences 99, 14872–14877. https://doi.org/10.1073/pnas.232589299

Grimm, V., Berger, U., Bastiansen, F., Eliassen, S., Ginot, V., Giske, J., Goss-Custard, J., Grand, T., Heinz, S.K., Huse, G., Huth, A., Jepsen, J.U., Jørgensen, C., Mooij, W.M., Müller, B., Pe'er, G., Piou, C., Railsback, S.F., Robbins, A.M., Robbins, M.M., Rossmanith, E., Rüger, N., Strand, E., Souissi, S., Stillman, R.A., Vabø, R., Visser, U., DeAngelis, D.L., 2006. A standard protocol for describing individual-based and agent-based models. Ecological Modelling 198, 115–126. https://doi.org/10.1016/j.ecolmodel.2006.04.023

Grimm, V., Railsback, S.F., Vincenot, C.E., Berger, U., Gallagher, C., DeAngelis, D.L., Edmonds, B., Ge, J., Giske, J., Groeneveld, J., Johnston, A.S.A., Milles, A., Nabe-Nielsen, J., Polhill, J.G., Radchuk, V., Rohwäder, M.-S., Stillman, R.A., Thiele, J.C., Ayllón, D., 2020. The ODD Protocol for Describing Agent-Based and Other Simulation Models: A Second Update to Improve Clarity, Replication, and Structural Realism. JASSS 23, 7. https://doi.org/10.18564/jasss.4259

Groeneveld, J., Johst, K., Kawaguchi, S., Meyer, B., Teschke, M., Grimm, V., 2015. How biological clocks and changing environmental conditions determine local population growth and species distribution in Antarctic krill (Euphausia superba): a conceptual model. Ecological Modelling 303, 78–86. https://doi.org/10.1016/j.ecolmodel.2015.02.009

Halasa, T., Bøtner, A., Mortensen, S., Christensen, H., Toft, N., Boklund, A., 2016. Simulating the epidemiological and economic effects of an African swine fever epidemic in industrialized swine populations. Veterinary Microbiology 193, 7–16. https://doi.org/10.1016/j.vetmic.2016.08.004

Heino, M., Ripa, J., Kaitala, V., 2000. Extinction risk under coloured environmental noise. Ecography 23, 177–184. https://doi.org/10.1111/j.1600-0587.2000.tb00273.x

Hite, J.L., Cressler, C.E., 2018. Resource-driven changes to host population stability alter the evolution of virulence and transmission. Phil. Trans. R. Soc. B 373, 20170087. https://doi.org/10.1098/rstb.2017.0087

Hossack, B.R., Lowe, W.H., Ware, J.L., Corn, P.S., 2013. Disease in a dynamic landscape: Host behavior and wildfire reduce amphibian chytrid infection. Biological Conservation 157, 293–299. https://doi.org/10.1016/j.biocon.2012.09.013

Howells, O., Edwards-Jones, G., 1997. A feasibility study of reintroducing wild boar *Sus scrofa* to Scotland: Are existing woodlands large enough to support minimum viable populations. Biological Conservation 81, 77–89. https://doi.org/10.1016/S0006-3207(96)00134-6

Ireland, J.M., Mestel, B.D., Norman, R.A., 2007. The effect of seasonal host birth rates on disease persistence. Mathematical Biosciences 206, 31–45. https://doi.org/10.1016/j.mbs.2006.08.028

Kareiva P. M., & Shigesada N. (1983). Analyzing insect movement as a correlated random walk. Oecologia, 56, 234–238. http://dx.doi.org/10.1007/bf00379695

Kermack, W.O., McKendrick, A.G., 1927. A Contribution to the Mathematical Theory of Epidemics. Proceedings of the Royal Society A: Mathematical, Physical and Engineering Sciences 115, 700–721. https://doi.org/10.1098/rspa.1927.0118

Kharin, V.V., Zwiers, F.W., Zhang, X., Wehner, M., 2013. Changes in temperature and precipitation extremes in the CMIP5 ensemble. Climatic Change 119, 345–357. https://doi.org/10.1007/s10584-013-0705-8

Kharouba, H.M., Ehrlén, J., Gelman, A., Bolmgren, K., Allen, J.M., Travers, S.E., Wolkovich, E.M., 2018. Global shifts in the phenological synchrony of species interactions over recent decades. Proc Natl Acad Sci USA 115, 5211–5216. https://doi.org/10.1073/pnas.1714511115

Kleijn, D., Munster, V.J., Ebbinge, B.S., Jonkers, D.A., Müskens, G.J.D.M., Van Randen, Y., Fouchier, R.A.M., 2010. Dynamics and ecological consequences of avian influenza virus infection in greater white-fronted geese in their winter staging areas. Proc. R. Soc. B. 277, 2041–2048. https://doi.org/10.1098/rspb.2010.0026

Koelle, K., Pascual, M., Yunus, M., 2005. Pathogen adaptation to seasonal forcing and climate change. Proc. R. Soc. B 272, 971–977. https://doi.org/10.1098/rspb.2004.3043

Koenig, W.D., 1999. Spatial autocorrelation of ecological phenomena. Trends in Ecology & Evolution 14, 22–26. https://doi.org/10.1016/S0169-5347(98)01533-X

Kramer-Schadt, S., Fernández, N., Eisinger, D., Grimm, V., Thulke, H.-H., 2009. Individual variations in infectiousness explain long-term disease persistence in wildlife populations. Oikos 118, 199–208. https://doi.org/10.1111/j.1600-0706.2008.16582.x

Kruuk, H, 1972. The spotted hyena: a study of predation and social behavior. Univ. Chicago Press, xvi + 335 pp. https://doi.org/10.2307/1379154

Kürschner, T., Scherer, C., Radchuk, V., Blaum, N., & Kramer-Schadt, S. (2021). Data from: Movement can mediate temporal mismatches between resource availability and biological events in host-pathogen interactions. Zenodo Digital Repository. https://doi.org/10.5281/ZENODO.4593791L

La Sorte, F.A., Hochachka, W.M., Farnsworth, A., Sheldon, D., Fink, D., Geevarghese, J., Winner, K., Van Doren, B.M., Kelling, S., 2015. Migration timing and its determinants for nocturnal migratory birds during autumn migration. J Anim Ecol 84, 1202–1212. https://doi.org/10.1111/1365-2656.12376

Lane-deGraaf, K.E., Kennedy, R.C., Arifin, S., Madey, G.R., Fuentes, A., Hollocher, H., 2013. A test of agent-based models as a tool for predicting patterns of pathogen transmission in complex landscapes. BMC Ecol 13, 35. https://doi.org/10.1186/1472-6785-13-35

Lange, M., Kramer-Schadt, S., Blome, S., Beer, M., Thulke, H.-H., 2012a. Disease severity declines over time after a wild boar population has been affected by classical swine fever-legend or actual epidemiological process? Preventive veterinary medicine 106, 185–195. https://doi.org/10.1016/j.prevetmed.2012.01.024.

Lange, M., Kramer-Schadt, S., Thulke, H.-H., 2012b. Efficiency of spatio-temporal vaccination regimes in wildlife populations under different viral constraints. Veterinary Research 43, 37. https://doi.org/10.1186/1297-9716-43-37

Legendre, P., 1993. Spatial Autocorrelation: Trouble or New Paradigm? Ecology 74, 1659–1673. https://doi.org/10.2307/1939924

Marcantonio, M., Rizzoli, A., Metz, M., Rosà, R., Marini, G., Chadwick, E., Neteler, M., 2015. Identifying the Environmental Conditions Favouring West Nile Virus Outbreaks in Europe. PLoS ONE 10, e0121158. https://doi.org/10.1371/journal.pone.0121158

Martin, G., Plowright, R., Chen, C., Kault, D., Selleck, P., Skerratt, L.F., 2015. Hendra virus survival does not explain spillover patterns and implicates relatively direct transmission routes from flying foxes to horses. Journal of General Virology 96, 1229–1237. https://doi.org/10.1099/vir.0.000073

Mayor, S.J., Guralnick, R.P., Tingley, M.W., Otegui, J., Withey, J.C., Elmendorf, S.C., Andrew, M.E., Leyk, S., Pearse, I.S., Schneider, D.C., 2017. Increasing phenological asynchrony between spring green-up and arrival of migratory birds. Sci Rep 7, 1902. https://doi.org/10.1038/s41598-017-02045-z

McCallum, H., 2012. Disease and the dynamics of extinction. Phil. Trans. R. Soc. B 367, 2828–2839. https://doi.org/10.1098/rstb.2012.0224

Meentemeyer, R.K., Haas, S.E., Václavík, T., 2012. Landscape epidemiology of emerging infectious diseases in natural and human-altered ecosystems. Annual review of phytopathology 50, 379–402. https://doi.org/10.1146/annurev-phyto-081211-172938

Melbourne, B.A., Hastings, A., 2008. Extinction risk depends strongly on factors contributing to stochasticity. Nature 454, 100–103. https://doi.org/10.1038/nature06922

Melis, C., Szafranska, P.A., Jedrzejewska, B., Barton, K., 2006. Biogeographical variation in the population density of wild boar (*Sus scrofa*) in western Eurasia. J Biogeography 33, 803–811. https://doi.org/10.1111/j.1365-2699.2006.01434.x

Mui, A.B., Caverhill, B., Johnson, B., Fortin, M.-J., He, Y., 2017. Using multiple metrics to estimate seasonal landscape connectivity for Blanding's turtles (Emydoidea blandingii) in a fragmented landscape. Landscape Ecol 32, 531–546. https://doi.org/10.1007/s10980-016-0456-9

Nagatani, T., Ichinose, G., Tainaka, K., 2018. Heterogeneous network promotes species coexistence: metaopulation model for rock-paper-scissors game. Sci Rep 8, 7094. https://doi.org/10.1038/s41598-018-25353-4

Nunn, C.L., Thrall, P.H., Kappeler, P.M., 2014. Shared resources and disease dynamics in spatially structured populations. Ecological Modelling 272, 198–207. https://doi.org/10.1016/j.ecolmodel.2013.10.004

Ostfeld, R.S., Brunner, J.L., 2015. Climate change and Ixodes tick-borne diseases of humans. Phil. Trans. R. Soc. B 370, 20140051. https://doi.org/10.1098/rstb.2014.0051

Parratt, S.R., Numminen, E., Laine, A.-L., 2016. Infectious Disease Dynamics in Heterogeneous Landscapes. Annu. Rev. Ecol. Evol. Syst. 47, 283–306. https://doi.org/10.1146/annurev-ecolsys-121415-032321

Patz, J.A., Daszak, P., Tabor, G.M., Aguirre, A.A., Pearl, M., Epstein, J., Wolfe, N.D., Kilpatrick, A.M., Foufopoulos, J., Molyneux, D., Bradley, D.J., Members of the Working Group on Land Use Change Disease Emergence, 2004. Unhealthy Landscapes: Policy Recommendations on Land Use Change and Infectious Disease Emergence. Environmental Health Perspectives 112, 1092–1098. https://doi.org/10.1289/ehp.6877

Plard, F., Gaillard, J.-M., Coulson, T., Hewison, A.J.M., Delorme, D., Warnant, C., Bonenfant, C., 2014. Mismatch Between Birth Date and Vegetation Phenology Slows the Demography of Roe Deer. PLoS Biol 12, e1001828. https://doi.org/10.1371/journal.pbio.1001828

Plowright, R.K., Eby, P., Hudson, P.J., Smith, I.L., Westcott, D., Bryden, W.L., Middleton, D., Reid, P.A., McFarlane, R.A., Martin, G., Tabor, G.M., Skerratt, L.F., Anderson, D.L., Crameri, G., Quammen, D.,

Jordan, D., Freeman, P., Wang, L.-F., Epstein, J.H., Marsh, G.A., Kung, N.Y., McCallum, H., 2015. Ecological dynamics of emerging bat virus spillover. Proc. R. Soc. B 282, 20142124. https://doi.org/10.1098/rspb.2014.2124

Post, E., Forchhammer, M.C., 2008. Climate change reduces reproductive success of an Arctic herbivore through trophic mismatch. Phil. Trans. R. Soc. B 363, 2367–2373. https://doi.org/10.1098/rstb.2007.2207

R Core team, 2019. R: A Language and Environment for Statistical Computing. R Foundation for Statistical Computing.

Radchuk, V., Reed, T., Teplitsky, C., van de Pol, M., Charmantier, A., Hassall, C., Adamík, P., Adriaensen, F., Ahola, M.P., Arcese, P., Miguel Avilés, J., Balbontin, J., Berg, K.S., Borras, A., Burthe, S., Clobert, J., Dehnhard, N., de Lope, F., Dhondt, A.A., Dingemanse, N.J., Doi, H., Eeva, T., Fickel, J., Filella, I., Fossøy, F., Goodenough, A.E., Hall, S.J.G., Hansson, B., Harris, M., Hasselquist, D., Hickler, T., Joshi, J., Kharouba, H., Martínez, J.G., Mihoub, J.-B., Mills, J.A., Molina-Morales, M., Moksnes, A., Ozgul, A., Parejo, D., Pilard, P., Poisbleau, M., Rousset, F., Rödel, M.-O., Scott, D., Senar, J.C., Stefanescu, C., Stokke, B.G., Kusano, T., Tarka, M., Tarwater, C.E., Thonicke, K., Thorley, J., Wilting, A., Tryjanowski, P., Merilä, J., Sheldon, B.C., Pape Møller, A., Matthysen, E., Janzen, F., Dobson, F.S., Visser, M.E., Beissinger, S.R., Courtiol, A., Kramer-Schadt, S., 2019. Adaptive responses of animals to climate change are most likely insufficient. Nature Communications 10, 3109. https://doi.org/10.1038/s41467-019-10924-4

Rees, E.E., Pond, B.A., Tinline, R.R., Bélanger, D., 2013. Modelling the effect of landscape heterogeneity on the efficacy of vaccination for wildlife infectious disease control. J Appl Ecol 50, 881–891. https://doi.org/10.1111/1365-2664.12101

Rohr, J.R., Cohen, J.M., 2020. Understanding how temperature shifts could impact infectious disease. PLoS Biol 18, e3000938. https://doi.org/10.1371/journal.pbio.3000938

Roy, M., Holt, R.D., Barfield, M., 2005. Temporal Autocorrelation Can Enhance the Persistence and Abundance of Metapopulations Comprised of Coupled Sinks. The American Naturalist 166, 246–261. https://doi.org/10.1086/431286

Scherer, C., Radchuk, V., Franz, M., Thulke, H., Lange, M., Grimm, V., Kramer-Schadt, S., 2020. Moving infections: individual movement decisions drive disease persistence in spatially structured landscapes. Oikos oik.07002. https://doi.org/10.1111/oik.07002

Scherer, C., Radchuk, V., Staubach, C., Müller, S., Blaum, N., Thulke, H., Kramer-Schadt, S., 2019. Seasonal host life-history processes fuel disease dynamics at different spatial scales. J Anim Ecol 88, 1812–1824. https://doi.org/10.1111/1365-2656.13070

Schweiger, O., Heikkinen, R.K., Harpke, A., Hickler, T., Klotz, S., Kudrna, O., Kühn, I., Pöyry, J., Settele, J., 2012. Increasing range mismatching of interacting species under global change is related to their ecological c characteristics: Range mismatching of interacting species. Global Ecology and Biogeography 21, 88–99. https://doi.org/10.1111/j.1466-8238.2010.00607.x

Schweiger, O., Settele, J., Kudrna, O., Klotz, S., Kühn, I., 2008. Climate change can cause spatial mismatch of trophically interacting species. Ecology 89, 3472–3479. https://doi.org/10.1890/07-1748.1

Sciaini, M., Fritsch, M., Scherer, C., Simpkins, C.E., 2018. NLMR and landscapetools : An integrated environment for simulating and modifying neutral landscape models in R. Methods Ecol Evol 9, 2240–2248. https://doi.org/10.1111/2041-210X.13076

Semenza, J.C., Menne, B., 2009. Climate change and infectious diseases in Europe. The Lancet Infectious Diseases 9, 365–375. https://doi.org/10.1016/S1473-3099(09)70104-5

Semenza, J.C., Suk, J.E., 2018. Vector-borne diseases and climate change: a European perspective. FEMS Microbiology Letters 365. https://doi.org/10.1093/femsle/fnx244

Sheldon, B.C., Verhulst, S., 1996. Ecological immunology: costly parasite defences and trade-offs in evolutionary ecology. Trends in Ecology & Evolution 11, 317–321. https://doi.org/10.1016/0169-5347(96)10039-2

Sigler, M., Tollit, D., Vollenweider, J., Thedinga, J., Csepp, D., Womble, J., Wong, M., Rehberg, M., Trites, A., 2009. Steller sea lion foraging response to seasonal changes in prey availability. Mar. Ecol. Prog. Ser. 388, 243–261. https://doi.org/10.3354/meps08144

Sodeikat, G., Pohlmeyer, K., 2003. Escape movements of family groups of wild boar *Sus scrofa* influenced by drive hunts in Lower Saxony, Germany. Wildlife Biology 9, 43–49. https://doi.org/10.2981/wlb.2003.063

Thackeray, S.J., Henrys, P.A., Hemming, D., Bell, J.R., Botham, M.S., Burthe, S., Helaouet, P., Johns, D.G., Jones, I.D., Leech, D.I., Mackay, E.B., Massimino, D., Atkinson, S., Bacon, P.J., Brereton, T.M., Carvalho, L., Clutton-Brock, T.H., Duck, C., Edwards, M., Elliott, J.M., Hall, S.J.G., Harrington, R., Pearce-Higgins, J.W., Høye, T.T., Kruuk, L.E.B., Pemberton, J.M., Sparks, T.H., Thompson, P.M., White, I., Winfield, I.J., Wanless, S., 2016. Phenological sensitivity to climate across taxa and trophic levels. Nature 535, 241–245. https://doi.org/10.1038/nature18608

Thomas, D.W., Blondel, J., Perret, P., Lambrechts, M. M., Speakman, J. R., 2001. Energetic and Fitness Costs of Mismatching Resource Supply and Demand in Seasonally Breeding Birds. Science 291, 2598–2600. https://doi.org/10.1126/science.1057487

Thomas, M.B., 2020. Epidemics on the move: Climate change and infectious disease. PLoS Biol 18, e3001013. https://doi.org/10.1371/journal.pbio.3001013

Tonkin, J.D., Bogan, M.T., Bonada, N., Rios-Touma, B., Lytle, D.A., 2017. Seasonality and predictability shape temporal species diversity. Ecology 98, 1201–1216. https://doi.org/10.1002/ecy.1761

Tracey, J.A., Bevins, S.N., VandeWoude, S., Crooks, K.R., 2014. An agent-based movement model to assess the impact of landscape fragmentation on disease transmission. Ecosphere 5, art119. https://doi.org/10.1890/ES13-00376.1

Ullmann, W., Fischer, C., Kramer-Schadt, S., Pirhofer-Walzl, K., Glemnitz, M., Blaum, N., 2020. How do agricultural practices affect the movement behaviour of European brown hares (*Lepus europaeus*)? Agriculture, Ecosystems & Environment 292, 106819. https://doi.org/10.1016/j.agee.2020.106819

Ullmann, W., Fischer, C., Pirhofer-Walzl, K., Kramer-Schadt, S., Blaum, N., 2018. Spatiotemporal variability in resources affects herbivore home range formation in structurally contrasting and unpredictable agricultural landscapes. Landscape Ecol 33, 1505–1517. https://doi.org/10.1007/s10980-018-0676-2

van Moorter, B., Bunnefeld, N., Panzacchi, M., Rolandsen, C.M., Solberg, E.J., Sæther, B.-E., 2013. Understanding scales of movement: animals ride waves and ripples of environmental change. The Journal of animal ecology 82, 770–780. https://doi.org/10.1111/1365-2656.12045

Vetter, S.G., Puskas, Z., Bieber, C., Ruf, T., 2020. How climate change and wildlife management affect population structure in wild boars. Sci Rep 10, 7298. https://doi.org/10.1038/s41598-020-64216-9

Visser, M.E., 2008. Keeping up with a warming world; assessing the rate of adaptation to climate change. Proc. R. Soc. B 275, 649–659. https://doi.org/10.1098/rspb.2007.0997

Visser, M.E., Gienapp, P., 2019. Evolutionary and demographic consequences of phenological mismatches. Nat Ecol Evol 3, 879–885. https://doi.org/10.1038/s41559-019-0880-8

Walker, S.F., Bosch, J., James, T.Y., Litvintseva, A.P., Oliver Valls, J.A., Piña, S., García, G., Rosa, G.A., Cunningham, A.A., Hole, S., Griffiths, R., Fisher, M.C., 2008. Invasive pathogens threaten species recovery programs. Current Biology 18, R853–R854. https://doi.org/10.1016/j.cub.2008.07.033

Wang, H.-H., Teel, P.D., Grant, W.E., Schuster, G., Pérez de León, A.A., 2016. Simulated interactions of white-tailed deer (Odocoileus virginianus), climate variation and habitat heterogeneity on southern cattle tick (Rhipicephalus (Boophilus) microplus) eradication methods in south Texas, USA. Ecological Modelling 342, 82–96. https://doi.org/10.1016/j.ecolmodel.2016.10.001

White, L.A., Forester, J.D., Craft, M.E., 2018a. Dynamic, spatial models of parasite transmission in wildlife: Their structure, applications and remaining challenges. J Anim Ecol 87, 559–580. https://doi.org/10.1111/1365-2656.12761

White, L.A., Forester, J.D., Craft, M.E., 2018b. Disease outbreak thresholds emerge from interactions between movement behavior, landscape structure, and epidemiology. Proc Natl Acad Sci USA 115, 7374–7379. https://doi.org/10.1073/pnas.1801383115

Wichmann, M.C., Johst, K., Moloney, K.A., Wissel, C., Jeltsch, F., 2003. Extinction risk in periodically fluctuating environments. Ecological Modelling 167, 221–231. https://doi.org/10.1016/S0304-3800(03)00136-4

Williams, C.M., Ragland, G.J., Betini, G., Buckley, L.B., Cheviron, Z.A., Donohue, K., Hereford, J., Humphries, M.M., Lisovski, S., Marshall, K.E., Schmidt, P.S., Sheldon, K.S., Varpe, Ø., Visser, M.E., 2017. Understanding Evolutionary Impacts of Seasonality: An Introduction to the Symposium. Integrative and comparative biology 57, 921–933. https://doi.org/10.1093/icb/icx122

Winkler, D.W., Dunn, P.O., McCulloch, C.E., 2002. Predicting the effects of climate change on avian life-history traits. Proceedings of the National Academy of Sciences 99, 13595–13599. https://doi.org/10.1073/pnas.21225199

CHAPTER 3

RESOURCE ASYNCHRONY AND LANDSCAPE HOMOGENIZATION AS DRIVERS OF VIRULENCE EVOLUTION

Authors:	Tobias Kürschner, Cédric Scherer, Viktoriia Radchuk, Niels Blaum, Stephanie Kramer-Schadt
Status:	in revision
Journal:	Proceedings of the Royal Society B
Submission History:	Submitted: 16 November 2021
Keywords:	virulence, evolution, host-pathogen dynamics, dynamic landscapes, global change
Author contributions:	TK and SKS developed the core idea and designed the study. TK rewrote and modified the simulation model together with CS and SKS. TK, VR, and SKS analysed the simulation results. TK is the lead author and CS, VR, NB and SKS contributed substantially to the writing. All authors agreed to submission of the manuscript, and each author is accountable for the aspects of the conducted work.

---

3 Resource asynchrony and landscape homogenization as drivers of virulence evolution

Abstract: In the last years, the emergence of zoonotic diseases and the frequency of disease outbreaks have increased substantially, fuelled by habitat encroachment and asynchrony of biological cycles due to global change. Disease outbreaks are driven by virulence evolution. In order to understand the complex processes of pathogen virulence evolution in the global change context, we adapted an established individual-based model of host-pathogen dynamics. Our model simulates a population of social hosts affected by an evolving pathogen in a dynamic landscape. Pathogen virulence evolution is explored by the inclusion of multiple strains in the model that differ in their transmission capability and lethality. Simultaneously, the host's resource landscape is subjected to spatial and temporal dynamics, emulating effects of global change.

We found an increase in pathogenic virulence and a shift in strain dominance with increasing landscape homogenisation. Our model further shows a trend to lower virulence pathogens being dominant in fragmented landscapes, although pulses of highly virulent strains are expected under resource asynchrony. While all landscape scenarios favour coexistence of low and high virulent strains, when host density increases, the high virulence strains capitalize on the high possibility for transmission and are likely to become dominant.

3.1 Introduction

Novel pathogens like emerging zoonotic diseases such as Ebola or SARS-CoV-2, are often associated with high virulence (Visher et al., 2021), i.e. the ability of the pathogen to quickly kill its host and spread quickly. The frequency and severity of infectious diseases have increased substantially over the past two decades. This trend is expected to continue in the near future facilitated by global change aspects, like land-use change, habitat encroachment, or climate change (CDC, 2020; Patz et al., 2004; Wilcox and Gubler, 2005), which will severely influence disease outbreaks by changes in the density and availability of hosts.

This will change disease dynamics in unprecedented ways, which will cascade down to pathogen traits such as virulence and transmission ability. Neglecting the complex interactions of resource availability in space and time and host life history could hinder the success of preventive measures aimed at reducing infection probability. Therefore, it is imperative to understand the pathways via which pathogens spread across a host population and the interaction between environmental conditions, host movement and pathogen traits. This is of paramount importance for example when it comes to understanding the triggers that lead to spillover effects or emerging zoonotic outbreaks (Allen et al., 2017; Andersen et al., 2020; Kumar et al., 2020; Morse et al., 2012; Rulli et al., 2017).

In this context, it is particularly important to understand factors that govern the spread and the persistence of pathogens in changing landscapes to put counteractive measures in place (Griette et al., 2015). While theoretical studies focus on long-term predictions of strains with evolutionarily stable virulence at equilibrium (Osnas et al., 2015), there is a poor understanding of how virulence evolves through space and time during an epidemic, especially under complex dynamics arising under global change (Lebarbenchon et al., 2008).

Virulence evolution is often highly accelerated during the emergence stage of an epidemic (Geoghegan and Holmes, 2018; Griette et al., 2015). The emergence stage is characterized by a high number of susceptible –and later infected– host individuals and subsequently high mutation rates in the high number of infected hosts (Galvani, 2003). Since the distributions of host individuals in a landscape determines the number of susceptible individuals, local and regional host densities are important factors in the evolution of virulence (Boots, 2004). With global change further altering the resource distribution in space and time, subsequent changes in the spatiotemporal density and distribution of host individuals (Boots, 2004; Galvani, 2003; Geoghegan and Holmes, 2018) could influence the evolution of virulence. Density changes could for example be induced via mismatches between the host's life history such as reproduction and host resource availability at that time. Understanding how pathogen virulence responds to global change will increase our ability to deal with it in the future. This is especially relevant, as ultimately, host-pathogen coexistence will increase the chance events for pathogens to spill over from wildlife to human populations either directly or via intermediary species (Plowright et al., 2021).

Theory predicts an evolution towards low virulence or even avirulence (Alizon et al., 2009), as observed in rabbit hemorrhagic disease virus in Australia (Cressler et al., 2016; Kamo et al., 2007). Virulence has been shown to be adaptive if there is a correlation with other pathogenic traits, which is known as virulence-transmission trade-off hypothesis. The transmission-virulence trade-off hypothesis states that an increase in strain transmission causes shorter infections through higher lethality (Alizon and Michalakis, 2015; Anderson and May, 1982). In other words, pathogen virulence is subject to a variety of evolutionary trade-offs (Cressler et al., 2016; Kamo et al., 2007; Messinger and Ostling, 2009). Pathogens, in particular viruses, possess an extraordinary plasticity that facilitates adaptations to novel conditions (Messinger and Ostling, 2009). This plasticity is a key component of emergence of new viral strains or re-emergence and the persistence of various viral strains. The constant emergence, re-emergence, and extinctions of viral strains will result in an overlap and possible coexistence between different viral strains, all competing for the same resource (Choua and Bonachela, 2019).

Understanding the transmission and persistence of pathogens in group living or social host species is of high importance for human health and wildlife conservation. Social hosts often form closely connected subgroups in a network of connected hosts (Nunn et al., 2015; Sah et al., 2017). Pathogen spread in such networks strongly depends on between-group and within-group interactions on pathogen spread, which are modulated by the underlying landscape. Prominent examples are outbreaks of classical swine fever in wild boars (*Sus scrofa*) (Artois et al., 2002) and canine distemper virus in spotted hyenas (*Crocuta crocuta*) (Benhaiem et al., 2018) and can be extended to humans that are living together in households (Buckee et al., 2021).

The theoretical models of virulence evolution, particularly the classical adaptive dynamics framework, rely on the assumption that mutation of pathogens happens very slowly and that mutations towards new strains can only occur after the dominant strain has reached equilibrium (Dieckmann et al., 2002). However, such simplified assumptions are rarely applicable to pathogens in nature, which often undergo transient dynamics, for example due to temporal and spatial changes in the landscape structure. Due to temporal variation in the landscape, the formation of spatial (Figure 3.1A) and or temporal (Figure 3.1B) host niches can cascade through the density distribution of potential hosts onto host-pathogen interactions (Figure 3.1C, D). The formation of niches with varying beneficial or detrimental properties for

host and pathogen could facilitate different viral strains at specific times or locations. The result can be a complex system of different competing and coexisting pathogen strains (Figure 3.1E) with their own spatial and temporal dynamics.

Here, we investigated the evolution of pathogen virulence in spatially structured social host populations in different dynamic resource landscapes. We were particularly interested in how temporal mismatches between optimal resource availability and biological events affect host-pathogen coexistence and pathogen spread. Our mismatch scenarios consider global change induced temporal shifts in optimal environmental conditions away from biological events relying on these conditions, like reproduction.

To this end, we modified an existing spatially-explicit individual-based host-pathogen model of a group-living social herbivore (Kramer-Schadt et al., 2009; Kürschner et al., 2021; Lange et al., 2012a, b; Scherer et al., 2020) and added evolution in pathogen traits leading to multi-strain outbreak scenarios. We hypothesized that dynamic landscapes induce evolution in pathogenic virulence to facilitate host-pathogen coexistence. In more detail, we expect pathogenic virulence to evolve into a system of different viral strains that will coexist and persist within the host population. Furthermore, we expect increasing landscape homogenization and related contact homogenization to facilitate evolution towards higher pathogenic virulence. By condensing a large number of susceptible host individuals into patches of high habitat suitability, thereby increasing the availability of hosts for highly virulent strains. Additionally, we expect a temporal asynchrony of resources and host population dynamics to shift evolution of virulence towards lower virulence during unfavourable environmental conditions.

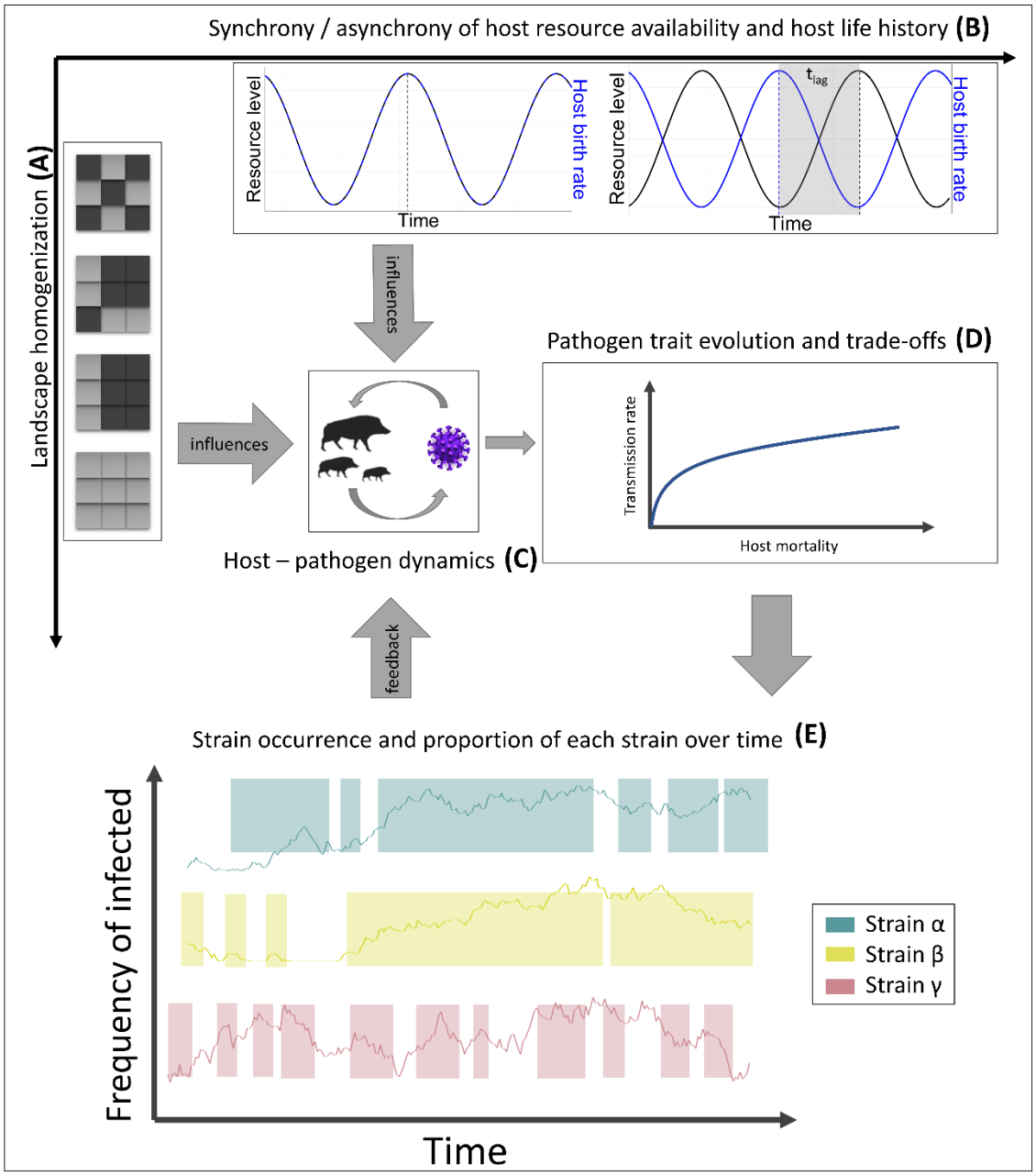

Figure 3.1: Landscape homogenization (A) and synchrony/asynchrony (t_{lag}) of host life-history and host-resource availability (B) influence host-pathogen dynamics (C) and subsequently the evolution of pathogenic traits (D) that will affect strain occurrence over time where gaps in the background line are times when the strain did not occur in the landscape (E).

3.2 Methods

3.2.1 Model overview

We modified a spatially explicit individual-based, eco-epidemiological model developed by Kürschner et al. (2021). It is based on earlier models considering neighbourhood infections only that was developed by Kramer-Schadt et al. (2009), Lange et al. (2012a,b) and Scherer et al. (2020)

and includes spatiotemporal landscape dynamics representing changing resource availability, coupled with resource-based mortality. We incorporated evolution of viral traits such as virulence and corresponding trade-offs with viral transmission (see below). A complete and detailed model description following the modified ODD (Overview, Design concepts, Detail) protocol (Grimm et al., 2020, 2006)is provided in the supplementary material (Appendix B1) and the model (implementation) in the Zenodo Database and on GitHub (links provided on acceptance).

The model comprises three main components, a host model depending on underlying landscape features, an epidemiological pathogen model and a pathogen evolutionary model. Host individuals are characterised by sex, age, location, demographic status (residential, dispersing) and epidemiological status (susceptible, infected, immune). The epidemiological status of the individuals is defined by an SIR epidemiological classification (susceptible, infected, and recovered; Kermack and McKendrick, 1927). The pathogen is characterized by strain type, virulence and transmission. The pathogen model alters host survival rates and infection length depending on the pathogen's virulence, while the dynamic landscape features determine host reproductive success. We record strain occurrences as the number of infected individuals carrying a specific strain and pathogen persistence, measured at the level of simulation runs (see below).

3.2.2 Pathogen dynamics

We determined the course of the disease by an age-specific case fatality rate and a strain-specific infectious period. Transiently infected hosts shed the pathogen for one week and gain lifelong immunity (Dahle and Liess, 1992). Infection dynamics emerge from multiple processes: within-group transmission and individual age-dependent courses of infection. Within groups, the density-dependent infection pressure (i.e. the chance of a host individual to become infected) is determined by a transmission chance and the number of infectious group members carrying the same strain. In this model we included the dependence of the transmission chance on the strain's virulence T_s, so that the strains with higher virulence have higher transmission chance. The original model based on a single pathogen strain used the density of infected individuals in a cell to infer the likelihood for a susceptible host in that cell to become infected based on a

binomial model. Our model allows the evolution into 12 (arbitrarily categorized) different viral strains. The infection pressure λ, i.e. the probability of pathogen transmission to a susceptible host individual, is therefore determined for each strain individually . The probability λ_{is} of an individual *i* of being infected by a specific strain *s* is calculated as

$$\lambda_{is} = 1 - (1 - (\beta_w + T_s))^{I_{js}} * (1 - \frac{(\beta_w + T_s)}{10})^{\Sigma_i I_{js}} \quad \text{(eq. 1)}$$

with β_w being the individual probability of transmission to the power of all infected individuals *Ijs* in a group *j* per strain *s* as well as a reduced transmission probability between groups (i.e. cells) $\frac{\beta_w}{10}$ to the power of all infected individuals in neighboring groups $\Sigma_i I_{js}$.

The strain virulence translates directly into infection length, i.e., host survival time, where a high virulence results in shorter survival times for the host compared to low-virulence. Consequently, the shorter lifetime of a highly virulent pathogen results in a shorter reproductive time span, while making the pathogen highly infective.

Evolution of pathogenic traits – Virulence and transmission are emergent properties and are evolving in the model. This means, there are no fixed positions for each strain on the transmission/virulence trade-off curve. Instead, such positions of each strain can change via evolution. Our trade-off curve is modelled to follow theoretical transmission-virulence trade-off curves (Alizon et al., 2009) and is applied for each infected host individually. During a transmission event, a strain can, with a mutation rate of 0.01, mutate into a new strain with a different virulence. The virulence of the new strain is selected from a normal distribution with a standard deviation σ = 1 around the virulence value of the originally transmitted strain, meaning that the new strain will be closely related to the parental strain.

3.2.3 Landscape structure and dynamics

The tested landscapes consist of a spatial grid of 1.250 2 km x 2 km cells, each representing the average home range of a social host, e.g. a wild boar group (Kramer-Schadt et al., 2009), totalling a 100 km x 50 km landscape. The landscapes are self-contained systems without any outside interaction. Each cell is characterized by a variable resource availability that represents host breeding capacity and translates directly into host group size, with the minimum being one

breeding female per group to a maximum of nine. Resource availability was adapted to achieve the average wild boar density of five breeding females per km² (Howells and Edwards-Jones, 1997; Melis et al., 2006; Sodeikat and Pohlmeyer, 2003). We investigated several landscape scenarios of varying spatial complexity, ranging from a fully random landscape structure to different degrees of random landscape clusters generated in R (R Core team, 2020) using the NLMR package (Sciaini et al., 2018) up to a fully homogeneous landscape. To exclude any biases that could stem from different host densities, the mean female breeding capacity was kept constant at five females per km² across the different landscape types (Appendix B2: Figure B4). The spatiotemporal landscape dynamics that were designed to mimic seasonal changes in resource availability by gradually increasing and decreasing resource availability were kept unchanged from the previous model implementation by Kürschner et al. (2021).

3.2.4 Process overview and scheduling

The temporal resolution of the model equals the approximate pathogen incubation time of one week (Artois et al., 2002). The model procedures were scheduled each step in the following order: pathogen transmission, pathogen evolution, natal host group split of subadult males and females, resource-based host dispersal, host reproduction, baseline host mortality, strain-based host mortality, resource-based host mortality, host ageing and landscape dynamics. Natal group split of males and females was limited to week 17 and week 29 of each year, respectively, representing the observed dispersal time for each sex.

Host mortality – Mortality in response to resource availability remained unchanged to the previous model implementation (for details see ODD; Appendix B1). Additionally, we added a fixed, strain-specific mortality for each strain that affects the host population.

Landscape dynamics with temporal lag – We modelled two levels of temporal lag (t_{lag}) implemented in Kürschner et al. (2021). We focus on the level 0% (synchrony between host population dynamics and resource availability) to 100% (asynchrony between host population dynamics and resource availability), with the latter simulating phenological mismatch between the resources and hosts reproduction potentially due to climate change. The extreme values were chosen because previous studies investigating temporal lag did not show strong effects in the intermediary steps (Kürschner et al., 2021).

3.2.5 Model analysis

Each simulation was run for 100 years in total, with the virus released in a randomly taken week of the second year (week 53-104), to allow the population to stabilize after initialization. The virus was introduced to a set of multiple predefined cells in the centre of the landscape to ensure an outbreak. The virus was released in a low virulence variant. We ran 25 repetitions per combination of landscape scenarios (5 levels: small clusters, medium clusters, large clusters, homogenous landscape and random) and asynchrony (2 levels: t_{lag} 0%, t_{lag} 100%). We also analysed the strain occurrence (i.e., if a strain was present in any landscape cell, recorded at every timestep) and number of infected hosts per strain at every timestep to measure strain extinction as well as reappearance through mutation. We further recorded the proportion that each strain contributed to the pool of infected hosts by calculating the ratio of the hosts infected with each strain to the total number of hosts infected with all strains, at each time step. To highlight differences in strain composition in those scenarios, we subtracted the strain proportion in asynchronous scenarios from the proportion in synchronous scenarios. We categorized all viral strains into three categories: low virulence strains; medium virulence strains; high virulence strains, each compartment summing the outcomes of 4 of the 12 strains modelled.

3.3 Results

3.3.1 Host-pathogen coexistence

Overall, host pathogen coexistence P_{coex} was very high in almost all tested scenarios. Due to a collapse of the host population in asynchronous scenarios in homogeneous landscapes, host-pathogen coexistence was not achievable in the current model-framework and therefore excluded. We did not find notable differences in the scenarios (Appendix B2: Figure B5).

3.3.2 Categorized infection trends

Our model showed that in synchronous scenarios, highly virulent strains were the least abundant ones among the three strain categories during the early stages of the epidemic. However, these strains became dominant in the later stages of the epidemic in homogeneous

and large clustered landscapes (Figure 3.2, left). With increasing landscape homogenization, medium virulence strains in the later stages of the epidemic were usually dominating along with high virulence strains. Across all landscapes, low virulent strains only occurred in high prevalence in the early stages of the epidemic but reached higher prevalence in less heterogeneous landscapes.

In scenarios with asynchrony, low virulent strains occurred over a longer time period and were more prevalent in the host population, while medium and highly virulent strains occurred later at high prevalence (Figure 3.2, right). Furthermore, prevalence of all strain categories was lower throughout the simulations when directly compared to the 'synchronous' scenarios. A clear shift towards a dominance of highly virulent strains only occurred in the less heterogeneous, large clustered landscapes.

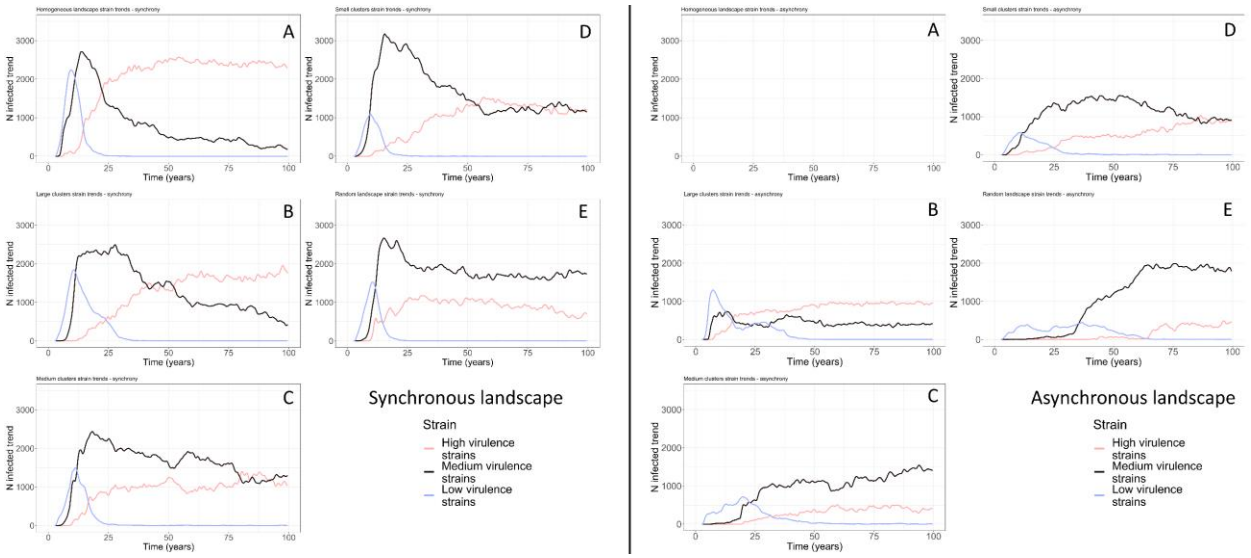

Figure 3.2: Temporal trends of the number of hosts infected with the strains of three virulence categories, low (blue) medium (black) and high (red) virulence over time. The left half shows the trends for synchronous host reproduction (t_{lag} = 0) and the right half for asynchronous host reproduction (t_{lag} = 100) scenarios. The landscape configuration is A- Homogenous, B- Large clusters, C- Medium clusters, D- Small clusters and E- Random landscape.

3.3.3 Strain specific occurrence and dominance over time

Strain occurrence and dominance of high virulent strains increased with increasing landscape heterogenization in dynamic landscapes in combination with synchronous scenarios (Figure 3.3 top). In the highly heterogeneous random landscape, low virulent strains persisted longer while higher virulent strains occurred much later in time (around year 40), compared to the same

landscape in synchronous scenarios. After its appearance through mutations around year 45, the medium virulent strain 7 became dominant for the course of the epidemic. As landscape homogeneity increased (from random landscapes to small clustered landscapes), lower virulent strains occurred on much shorter time spans. The high virulent strains appeared much earlier around year 10 of the epidemic and remained present in the landscape for the duration of the simulation. A further increase in homogenization towards medium-sized patches showed overall similar patterns as the small clustered landscape with the exception of the strain 7 peak prevalence, which shifted towards the end of the epidemic. In the highly homogenous large clustered landscapes, the lower virulent strains persisted for a longer period, while medium virulent strains were represented during the full period of the epidemic. Contrary to the more heterogeneous landscapes, strain 7 did not become the dominant strain despite high prevalence in the host population. As indicated by the larger proportion of hosts infected with higher virulent strains, overall, in synchronous scenarios (Figure 3.3), virulence of occurring strains increased over time and with increasing landscape homogenization. In asynchronous scenarios we observed a similar increase in strain occurrence with landscape homogenization, even though the temporal rate of increase was smaller compared to synchronous scenarios. Furthermore, there was a temporal variation of strain occurrence within the more homogenous landscape between synchronous and asynchronous scenarios, as can be seen in a direct comparison of the per strain infection counts and wavelets of synchronous and asynchronous scenarios over time (Figure 3.4). A general comparison of the proportional strain contribution in asynchronous vs synchronous scenarios further showed that the occurring strains were of lower virulence in asynchronous scenarios in case of the more heterogeneous landscapes (Appendix B2: Figure B6).

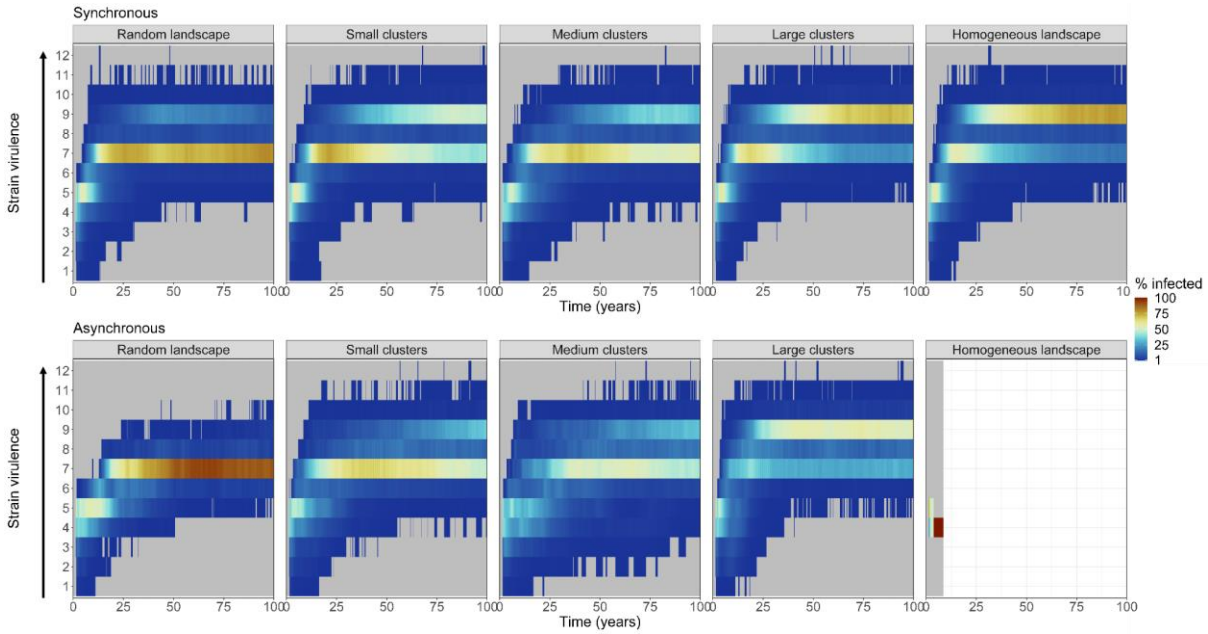

Figure 3.3: Occurrence and dominance of the different virulence strains in synchronous (t_{lag} = 0, top row) and asynchronous (t_{lag} = 100, bottom row) scenarios. Colour gradient represents the proportion of infected individuals with each strain in the landscape. Grey areas represent zero occurrence of the strains.

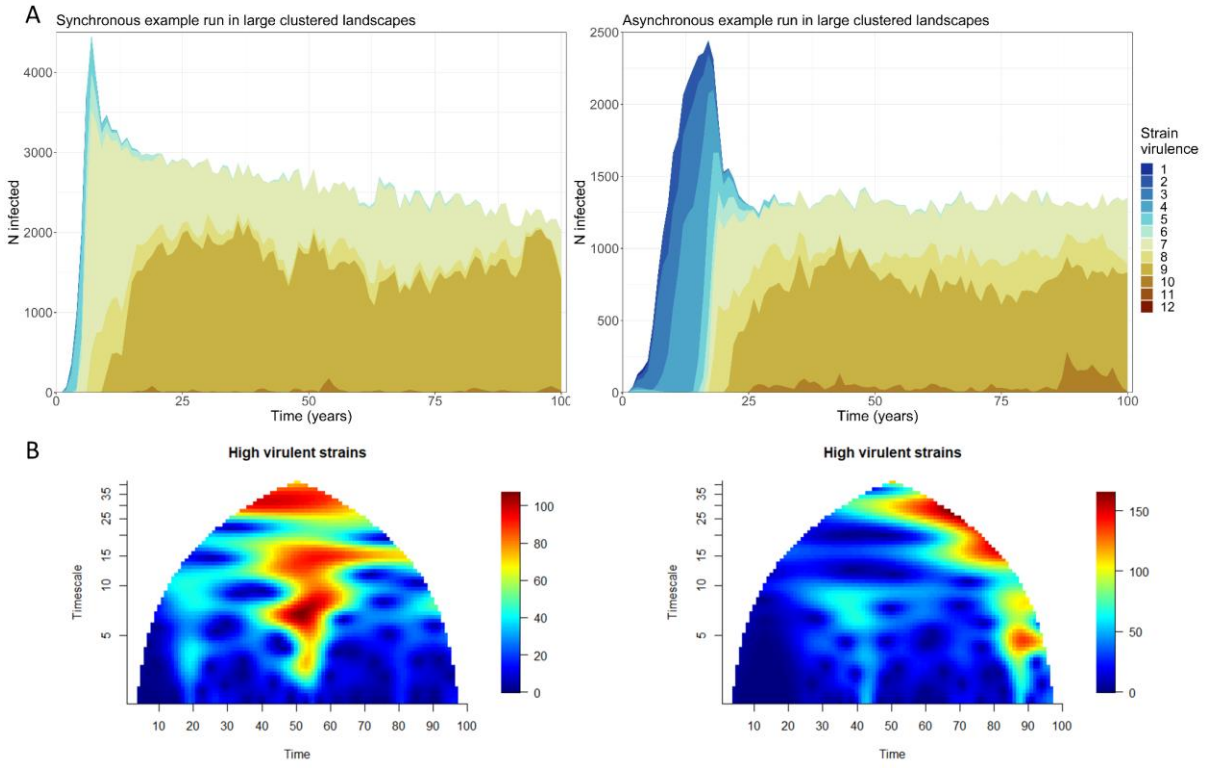

Figure 3.4: **A–** Muller plot for a single example run in a large clustered landscape in synchronous (left) and asynchronous (right) scenarios, showing the number of infected individuals for each strain (colour) over time aggregated as annual mean. **B–** Wavelet analysis of high virulent strains in synchronous (left) and asynchronous (right) scenarios of a single example run in a large clustered landscape using the R package "wsyn" (Reuman et al., 2021).

3.4 Discussion

To extend the understanding of pathogen evolution and spread during epidemics, we implemented virulence evolution in an individual-based model simulating an interdependent, tri-trophic system (landscape resources-host-pathogen) under the effects of global change. In accordance with our hypothesis, we found an increase in pathogenic virulence and a shift in strain dominance with increasing landscape homogenisation.

Landscape homogenisation alters the density distribution of susceptible host individuals by increasing host connectivity, which subsequently can lead to more infection events and viral mutations. The detrimental effect that density, connectivity and contact rates can have on viral mutations and infection events can also be observed in "superspreader"-events of the current SARS-CoV-2 pandemic (Tasakis et al., 2021). Our results support that host density and connectivity are the most important factors that affect evolution of high virulence in directly transmitted diseases under transmission/virulence trade-offs (Castillo-Chavez and Velasco-Hernández, 1998). While we found lower mean virulence in scenarios with asynchronous host resources, the landscape heterogeneity was the main driver of virulence evolution. Interestingly, under asynchrony, we found higher proportions of low and high strains coexisting in homogeneous landscapes, indicating that isolated disease hotspots (Kürschner et al., 2021) could facilitate different viral strains.

As long as host populations in our model are distributed heterogeneously, mean pathogenic virulence remains similar, with little change from completely heterogeneous, i.e., random landscapes, to the less heterogeneous medium habitat clusters. However, in large clusters, a clear increase in mean virulence was apparent, showing that there is a threshold in landscape homogeneity not only enhancing disease spread, but also evolution towards higher virulence. These modelling findings are consistent with previous research on thresholds in disease transmission and functional connectivity. For example, homogenous landscapes have been shown to facilitate the spread of rabies in raccoons (*Procyon lotor*) (Brunker et al., 2012) or tuberculosis in badgers (*Meles meles*) (Acevedo et al., 2019), while more heterogeneous landscapes have been shown to limit the spread of highly virulent pathogens (Lane-deGraaf et al., 2013). Host-pathogen interactions –in directly transmitted diseases– occur at specific

locations and points in time, with the availability of susceptible hosts being the governing factor of a successful transmission (Hudson, 2002; Ostfeld et al., 2005; Real and Biek, 2007). Consequently, homogenous landscapes and their lack of barriers allow more virulent pathogen strains to infect a sufficient number of hosts to persist in those landscapes. On the contrary, in heterogeneous landscapes, small clusters of high host density in a matrix of low density cause the extinction of highly virulent strains. This pattern can be explained by the short survival time of individuals in the matrix that form an immunity belt around the clusters and prevent spread between clusters (Marescot et al., 2021).

Increasing landscape homogenisation also resulted in higher mean virulence in scenarios with asynchrony between host life-history and resource availability. Even though overall susceptible host density was lower in asynchronous scenarios, the homogenous landscape's increased connectivity allowed for higher virulent strains to persist at high prevalence. In the homogenous landscape, composed of large habitat clusters, the virulence of occurring strains was similar between the scenarios with and without synchrony. This indicates a strong effect of landscape configuration.

Interestingly, in our previous study (Kürschner et al., 2021), we showed that increasing spatial homogeneity of the landscape affected pathogen persistence negatively without pathogen virulence evolution. One reason behind this difference lies in the temporal differentiation of the strains within the landscapes. During the beginning of an outbreak, the pathogen strains with low virulence are able to spread across the landscape into larger habitat clusters due to the long survival times they impose on their hosts. Once the susceptible host density in one of the neighbouring areas is high enough, highly virulent strains that previously only occurred in low prevalence outcompete the low virulent strains and increase in prevalence. In other words, when host density increases, the high virulence strains capitalize on the high possibility for transmission and are likely to become dominant (Altizer et al., 2006; Hite and Cressler, 2018). However, although highly virulent strains became more dominant, lower virulent strains continued to persist within the host population. In line with our findings, the coexistence of high and low virulent strains was also shown for rabbit haemorrhagic disease in the United Kingdom (Forrester et al., 2009) as well as influenza A in wild birds (Olsen et al., 2006).

Furthermore, our results show that, independent of landscape heterogeneity, a single, low virulent strain of a pathogen is able to evolve into a complex system of multiple coexisting strains with varying virulence. However, while multiple strains coexisted at any given time throughout all tested scenarios, we demonstrated that some strains likely become dominant. Similarly, a system of coexisting low and highly virulent strains was reported by empirical studies of the African swine fever virus in wild boar (Portugal et al., 2015), a pathogen causing severe diseases with huge economic impact (Artois et al., 2002). In this system the carriers of low virulent strains could remain infectious over long periods of time (de Carvalho Ferreira et al., 2012) increasing the chance of the pathogen transmission and its mutation into higher virulent strains, which could become dominant over time. In our study, the virulence of the dominant strain was intrinsically linked to the degree of landscape homogenisation, but was also variable in time. Our findings are consistent with theoretical models that showed an increase of pathogenic virulence over time (Osnas et al., 2015). However, while Osnas et al. (2015) assumed a direct trade-off between virulence and host movement in homogenous landscapes, here we show that different landscape configurations may lead to the same patterns of increasing virulence without the necessity of such a trade-off.

On the one hand, our results show that with natural landscapes becoming more fragmented and resources becoming more asynchronous due to global change, a shift towards lower virulent pathogens could be expected. As a consequence, some diseases may become endemic in their respective host populations. The longer a pathogen is able to persist within its host population the higher the risk for spontaneous mutations and the possibility of spillovers to other species. On the other hand, global change will lead to increasing homogenisation within those fragments (Patz et al., 2004) and has the potential to increase the average pathogenic virulence with possibly catastrophic effects on wildlife communities. A large variance in virulence has been shown among infected host individuals, where the infection can range from severe to asymptomatic. This variation can be the result of a variety of factors, including genetic variation or intraspecific host interactions but also environmental conditions (Ebert and Bull, 2003). Furthermore, an increase in virulence will go hand in hand with higher transmission rates in many diseases (Alizon and Michalakis, 2015; Messinger and Ostling, 2009) that will further increase the probability of pathogen spillovers. While pathogen spillovers to other wild or

domestic animal populations can have profound social or economic effects (Kamo et al., 2007), the possibly detrimental effects on human health can not be underestimated. The current SARS-CoV-2 pandemic clearly highlights the importance of understanding which factors govern the spread of diseases in wildlife populations and how anthropogenic changes may alter those in the future.

3.5 Additional information

Acknowledgements

This work was supported by the German Research Foundation (DFG) in the framework of the BioMove Research Training Group (DFG-GRK 2118/1). We thank Volker Grimm for valuable comments on earlier drafts of this manuscript and Florian Jeltsch and Heribert Hofer for helpful discussions.

Supplementary material

- Appendix B1: ODD protocol
- Appendix B2: Additional figures

References

Acevedo, P., Prieto, M., Quirós, P., Merediz, I., de Juan, L., Infantes-Lorenzo, J.A., Triguero-Ocaña, R., Balseiro, A., 2019. Tuberculosis Epidemiology and Badger (*Meles meles*) Spatial Ecology in a Hot-Spot Area in Atlantic Spain. Pathogens 8, 292. https://doi.org/10.3390/pathogens8040292

Alizon, S., Hurford, A., Mideo, N., van Baalen, M., 2009. Virulence evolution and the trade-off hypothesis: history, current state of affairs and the future. Journal of evolutionary biology 22, 245–259. https://doi.org/10.1111/j.1420-9101.2008.01658.x

Alizon, S., Michalakis, Y., 2015. Adaptive virulence evolution: the good old fitness-based approach. Trends in Ecology & Evolution 30, 248–254. https://doi.org/10.1016/j.tree.2015.02.009

Allen, T., Murray, K.A., Zambrana-Torrelio, C., Morse, S.S., Rondinini, C., Di Marco, M., Breit, N., Olival, K.J., Daszak, P., 2017. Global hotspots and correlates of emerging zoonotic diseases. Nat Commun 8, 1124. https://doi.org/10.1038/s41467-017-00923-8

Altizer, S., Dobson, A., Hosseini, P., Hudson, P., Pascual, M., Rohani, P., 2006. Seasonality and the dynamics of infectious diseases. Ecology letters 9, 467–484. https://doi.org/10.1111/j.1461-0248.2005.00879.x

Andersen, K.G., Rambaut, A., Lipkin, W.I., Holmes, E.C., Garry, R.F., 2020. The proximal origin of SARS-CoV-2. Nat Med 26, 450–452. https://doi.org/10.1038/s41591-020-0820-9

Anderson, R.M., May, R.M., 1982. Coevolution of hosts and parasites. Parasitology 85, 411–426. https://doi.org/10.1017/S0031182000055360

Artois, M., Depner, K.R., Guberti, V., Hars, J., Rossi, S., Rutili, D., 2002. Classical swine fever (hog cholera) in wild boar in Europe. Rev. Sci. Tech. OIE 21, 287–303. https://doi.org/10.20506/rst.21.2.1332

Benhaiem, S., Marescot, L., East, M.L., Kramer-Schadt, S., Gimenez, O., Lebreton, J.-D., Hofer, H., 2018. Slow recovery from a disease epidemic in the spotted hyena, a keystone social carnivore. Commun Biol 1, 201. https://doi.org/10.1038/s42003-018-0197-1

Boots, M., 2004. Large Shifts in Pathogen Virulence Relate to Host Population Structure. Science 303, 842–844. https://doi.org/10.1126/science.1088542

Brunker, K., Hampson, K., Horton, D.L., Biek, R., 2012. Integrating the landscape epidemiology and genetics of RNA viruses: rabies in domestic dogs as a model. Parasitology 139, 1899–1913. https://doi.org/10.1017/S003118201200090X

Buckee, C., Noor, A., Sattenspiel, L., 2021. Thinking clearly about social aspects of infectious disease transmission. Nature 595, 205–213. https://doi.org/10.1038/s41586-021-03694-x

Castillo-Chavez, C., Velasco-Hernández, J.X., 1998. On the Relationship Between Evolution of Virulence and Host Demography. Journal of Theoretical Biology 192, 437–444. https://doi.org/10.1006/jtbi.1998.0661

CDC – Emerging Infectious Diseases [WWW Document], 2020. URL https://web.archive.org/web/20200418131812/https:/www.cdc.gov/niosh/topics/emerginfectdiseases/default.html (accessed 12.11.20).

Choua, M., Bonachela, J.A., 2019. Ecological and Evolutionary Consequences of Viral Plasticity. The American Naturalist 193, 346–358. https://doi.org/10.1086/701668

Cressler, C.E., McLEOD, D.V., Rozins, C., van den Hoogen, J., Day, T., 2016. The adaptive evolution of virulence: a review of theoretical predictions and empirical tests. Parasitology 143, 915–930. https://doi.org/10.1017/S003118201500092X

Dahle, J., Liess, B., 1992. A review on classical swine fever infections in pigs: Epizootiology, clinical disease and pathology. Comparative Immunology, Microbiology and Infectious Diseases 15, 203–211. https://doi.org/10.1016/0147-9571(92)90093-7

Reuman, D.C., Anderson T.L., Walter, J.A., Zhao, L., Sheppard, L.W., 2021. wsyn: Wavelet Approaches to Studies of Synchrony in Ecology and Other Fields. https://CRAN.R-project.org/package=wsyn

de Carvalho Ferreira, H.C., Weesendorp, E., Elbers, A.R.W., Bouma, A., Quak, S., Stegeman, J.A., Loeffen, W.L.A., 2012. African swine fever virus excretion patterns in persistently infected animals: A quantitative approach. Veterinary Microbiology 160, 327–340. https://doi.org/10.1016/j.vetmic.2012.06.025

Dieckmann, U., International Institute for Applied Systems Analysis (Eds.), 2002. Adaptive dynamics of infectious diseases: in pursuit of virulence management, Cambridge studies in adaptive dynamics. IIASA : Cambridge University Press, [Laxenburg] : Cambridge ; New York.

Ebert, D., Bull, J.J., 2003. Challenging the trade-off model for the evolution of virulence: is virulence management feasible? Trends in Microbiology 11, 15–20. https://doi.org/10.1016/S0966-842X(02)00003-3

Forrester, N.L., Boag, B., Buckley, A., Moureau, G., Gould, E.A., 2009. Co-circulation of widely disparate strains of Rabbit haemorrhagic disease virus could explain localised epidemicity in the United Kingdom. Virology 393, 42–48. https://doi.org/10.1016/j.virol.2009.07.008

Galvani, A.P., 2003. Epidemiology meets evolutionary ecology. Trends in Ecology & Evolution 18, 132–139. https://doi.org/10.1016/S0169-5347(02)00050-2

Geoghegan, J.L., Holmes, E.C., 2018. The phylogenomics of evolving virus virulence. Nat Rev Genet 19, 756–769. https://doi.org/10.1038/s41576-018-0055-5

Griette, Q., Raoul, G., Gandon, S., 2015. Virulence evolution at the front line of spreading epidemics. Evolution 69, 2810–2819. https://doi.org/10.1111/evo.12781

Grimm, V., Berger, U., Bastiansen, F., Eliassen, S., Ginot, V., Giske, J., Goss-Custard, J., Grand, T., Heinz, S.K., Huse, G., Huth, A., Jepsen, J.U., Jørgensen, C., Mooij, W.M., Müller, B., Pe'er, G., Piou, C., Railsback, S.F., Robbins, A.M., Robbins, M.M., Rossmanith, E., Rüger, N., Strand, E., Souissi, S., Stillman, R.A., Vabø, R., Visser, U., DeAngelis, D.L., 2006. A standard protocol for describing individual-based and agent-based models. Ecological Modelling 198, 115–126. https://doi.org/10.1016/j.ecolmodel.2006.04.023

Grimm, V., Railsback, S.F., Vincenot, C.E., Berger, U., Gallagher, C., DeAngelis, D.L., Edmonds, B., Ge, J., Giske, J., Groeneveld, J., Johnston, A.S.A., Milles, A., Nabe-Nielsen, J., Polhill, J.G., Radchuk, V., Rohwäder, M.-S., Stillman, R.A., Thiele, J.C., Ayllón, D., 2020. The ODD Protocol for Describing Agent-Based and Other Simulation Models: A Second Update to Improve Clarity, Replication, and Structural Realism. JASSS 23, 7. https://doi.org/10.18564/jasss.4259

Hite, J.L., Cressler, C.E., 2018. Resource-driven changes to host population stability alter the evolution of virulence and transmission. Phil. Trans. R. Soc. B 373, 20170087. https://doi.org/10.1098/rstb.2017.0087

Howells, O., Edwards-Jones, G., 1997. A feasibility study of reintroducing wild boar *Sus scrofa* to Scotland: Are existing woodlands large enough to support minimum viable populations. Biological Conservation 81, 77–89. https://doi.org/10.1016/S0006-3207(96)00134-6

Hudson, P.J. (Ed.), 2002. The ecology of wildlife diseases. Oxford University Press, New York.

Kamo, M., Sasaki, A., Boots, M., 2007. The role of trade-off shapes in the evolution of parasites in spatial host populations: An approximate analytical approach. Journal of Theoretical Biology 244, 588–596. https://doi.org/10.1016/j.jtbi.2006.08.013

Kermack, W.O., McKendrick, A.G., 1927. A Contribution to the Mathematical Theory of Epidemics. Proceedings of the Royal Society A: Mathematical, Physical and Engineering Sciences 115, 700–721. https://doi.org/10.1098/rspa.1927.0118

Kramer-Schadt, S., Fernández, N., Eisinger, D., Grimm, V., Thulke, H.-H., 2009. Individual variations in infectiousness explain long-term disease persistence in wildlife populations. Oikos 118, 199–208. https://doi.org/10.1111/j.1600-0706.2008.16582.x

Kumar, V., Ramkumar, Pruthvishree, B.S., Pande, T., Sinha, D.K., Singh, B.R., Dhama, K., Malik, Y.S., 2020. SARS-CoV-2 (COVID-19): Zoonotic Origin and Susceptibility of Domestic and Wild Animals. J. Pure Appl. Microbiol. 14, 741–747. https://doi.org/10.22207/JPAM.14.SPL1.11

Kürschner, T., Scherer, C., Radchuk, V., Blaum, N., Kramer-Schadt, S., 2021. Movement can mediate temporal mismatches between resource availability and biological events in host-pathogen interactions. Ecol. Evol. 11, 5728–5741. https://doi.org/10.1002/ece3.7478

Lane-deGraaf, K.E., Kennedy, R.C., Arifin, S., Madey, G.R., Fuentes, A., Hollocher, H., 2013. A test of agent-based models as a tool for predicting patterns of pathogen transmission in complex landscapes. BMC Ecol 13, 35. https://doi.org/10.1186/1472-6785-13-35

Lange, M., Kramer-Schadt, S., Blome, S., Beer, M., Thulke, H.-H., 2012. Disease severity declines over time after a wild boar population has been affected by classical swine fever-legend or actual epidemiological process? Preventive veterinary medicine 106, 185–195. https://doi.org/10.1016/j.prevetmed.2012.01.024.

Lange, Martin, Kramer-Schadt, S., Thulke, H.-H., 2012. Efficiency of spatio-temporal vaccination regimes in wildlife populations under different viral constraints. Veterinary Research 43, 37. https://doi.org/10.1186/1297-9716-43-37

Lebarbenchon, C., Brown, S.P., Poulin, R., Gauthier-Clerc, M., Thomas, F., 2008. Evolution of pathogens in a man-made world. Molecular Ecology 17, 475–484. https://doi.org/10.1111/j.1365-294X.2007.03375.x

Marescot, L., Franz, M., Benhaiem, S., Hofer, H., Scherer, C., East, M.L., Kramer-Schadt, S., 2021. 'Keeping the kids at home' can limit the persistence of contagious pathogens in social animals. J Anim Ecol 90, 2523–2535. https://doi.org/10.1111/1365-2656.13555

Melis, C., Szafranska, P.A., Jedrzejewska, B., Barton, K., 2006. Biogeographical variation in the population density of wild boar (*Sus scrofa*) in western Eurasia. J Biogeography 33, 803–811. https://doi.org/10.1111/j.1365-2699.2006.01434.x

Messinger, S.M., Ostling, A., 2009. The consequences of spatial structure for the evolution of pathogen transmission rate and virulence. The American naturalist 174, 441–454. https://doi.org/10.1086/605375

Morse, S.S., Mazet, J.A., Woolhouse, M., Parrish, C.R., Carroll, D., Karesh, W.B., Zambrana-Torrelio, C., Lipkin, W.I., Daszak, P., 2012. Prediction and prevention of the next pandemic zoonosis. The Lancet 380, 1956–1965. https://doi.org/10.1016/S0140-6736(12)61684-5

Nunn, C.L., Jordán, F., McCabe, C.M., Verdolin, J.L., Fewell, J.H., 2015. Infectious disease and group size: more than just a numbers game. Phil. Trans. R. Soc. B 370, 20140111. https://doi.org/10.1098/rstb.2014.0111

Olsen, B., Munster, V.J., Wallensten, A., Waldenström, J., Osterhaus, A.D.M.E., Fouchier, R.A.M., 2006. Global Patterns of Influenza A Virus in Wild Birds. Science 312, 384–388. https://doi.org/10.1126/science.1122438

Osnas, E.E., Hurtado, P.J., Dobson, A.P., 2015. Evolution of Pathogen Virulence across Space during an Epidemic. The American Naturalist 185, 332–342. https://doi.org/10.1086/679734

Ostfeld, R., Glass, G., Keesing, F., 2005. Spatial epidemiology: an emerging (or re-emerging) discipline. Trends in Ecology & Evolution 20, 328–336. https://doi.org/10.1016/j.tree.2005.03.009

Patz, J.A., Daszak, P., Tabor, G.M., Aguirre, A.A., Pearl, M., Epstein, J., Wolfe, N.D., Kilpatrick, A.M., Foufopoulos, J., Molyneux, D., Bradley, D.J., Members of the Working Group on Land Use Change Disease Emergence, 2004. Unhealthy Landscapes: Policy Recommendations on Land Use Change and Infectious Disease Emergence. Environmental Health Perspectives 112, 1092–1098. https://doi.org/10.1289/ehp.6877

Plowright, R.K., Reaser, J.K., Locke, H., Woodley, S.J., Patz, J.A., Becker, D.J., Oppler, G., Hudson, P.J., Tabor, G.M., 2021. Land use-induced spillover: a call to action to safeguard environmental, animal, and human health. The Lancet Planetary Health 5, e237–e245. https://doi.org/10.1016/S2542-5196(21)00031-0

Portugal, R., Coelho, J., Höper, D., Little, N.S., Smithson, C., Upton, C., Martins, C., Leitão, A., Keil, G.M., 2015. Related strains of African swine fever virus with different virulence: genome comparison and analysis. Journal of General Virology 96, 408–419. https://doi.org/10.1099/vir.0.070508-0

R Core team, 2020. R: A Language and Environment for Statistical Computing. R Foundation for Statistical Computing.

Real, L.A., Biek, R., 2007. Spatial dynamics and genetics of infectious diseases on heterogeneous landscapes. J. R. Soc. Interface. 4, 935–948. https://doi.org/10.1098/rsif.2007.1041

Rulli, M.C., Santini, M., Hayman, D.T.S., D'Odorico, P., 2017. The nexus between forest fragmentation in Africa and Ebola virus disease outbreaks. Sci Rep 7, 41613. https://doi.org/10.1038/srep41613

Sah, P., Leu, S.T., Cross, P.C., Hudson, P.J., Bansal, S., 2017. Unraveling the disease consequences and mechanisms of modular structure in animal social networks. Proc Natl Acad Sci USA 114, 4165–4170. https://doi.org/10.1073/pnas.1613616114

Scherer, C., Radchuk, V., Franz, M., Thulke, H., Lange, M., Grimm, V., Kramer-Schadt, S., 2020. Moving infections: individual movement decisions drive disease persistence in spatially structured landscapes. Oikos oik.07002. https://doi.org/10.1111/oik.07002

Sciaini, M., Fritsch, M., Scherer, C., Simpkins, C.E., 2018. NLMR and landscapetools : An integrated environment for simulating and modifying neutral landscape models in R. Methods Ecol Evol 9, 2240–2248. https://doi.org/10.1111/2041-210X.13076

Sodeikat, G., Pohlmeyer, K., 2003. Escape movements of family groups of wild boar *Sus scrofa* influenced by drive hunts in Lower Saxony, Germany. Wildlife Biology 9, 43–49. https://doi.org/10.2981/wlb.2003.063

Tasakis, R.N., Samaras, G., Jamison, A., Lee, M., Paulus, A., Whitehouse, G., Verkoczy, L., Papavasiliou, F.N., Diaz, M., 2021. SARS-CoV-2 variant evolution in the United States: High accumulation of viral mutations over time likely through serial Founder Events and mutational bursts. PLoS ONE 16, e0255169. https://doi.org/10.1371/journal.pone.0255169

Visher, E., Evensen, C., Guth, S., Lai, E., Norfolk, M., Rozins, C., Sokolov, N.A., Sui, M., Boots, M., 2021. The three Ts of virulence evolution during zoonotic emergence. Proc. R. Soc. B. 288, 20210900. https://doi.org/10.1098/rspb.2021.0900

Wilcox, B.A., Gubler, D.J., 2005. Disease ecology and the global emergence of zoonotic pathogens. Environ Health Prev Med 10, 263. https://doi.org/10.1007/BF02897701

CHAPTER 4

THE EFFECT OF SPATIAL DECISION-MAKING PROCESSES OF MOVING HOSTS ON PATHOGEN TRANSMISSION AND PATTERNS OF SPREAD IN A SOCIAL HOST

Authors:	Tobias Kürschner, Cédric Scherer, Aimara Planillo, Viktoriia Radchuk, Niels Blaum, Christoph Staubach, Hans-Hermann Thulke, Volker Grimm, Stephanie Kramer-Schadt

Status:	ready for submission
Keywords:	virulence, evolution, host-pathogen dynamics, classical swine fever, individual movement, wildlife disease
Author contributions:	TK and SKS developed the core idea and designed the study. TK rewrote and modified the simulation model together with CS and SKS. TK, VR, AP and SKS analysed the simulation results. TK is the lead author and CS, AP, VR, HHT, CSt, NB and SKS contributed substantially to the writing.

---

4 The effect of spatial decision-making processes of moving hosts on pathogen transmission and patterns of spread in a social host

Abstract: Understanding the drivers of disease dynamics, like spread and persistence, is a major challenge in disease ecology, due to the complex interactions of the major players, host and pathogen, and their intertwined reaction towards landscape structure. Therefore, individual host decision-making processes depending on both landscape structure and host population density in combination with pathogen properties such as virulence, are important factors that need to be taken into account when disentangling complex disease dynamics. In this study, we used a spatially explicit eco-epidemiological individual-based model to investigate the effect of decision-making processes in host movement on disease outbreak patterns, persistence, and transmission. We matched our simulated patterns to observed patterns from a long term outbreak of classical swine fever in wild boar in Northern Germany where despite a large-scale vaccination campaign, classical swine fever persisted for seven years.

We found that explicit host movement increased the speed of pathogen spread. Additionally, the simulation results showed a strong shift in the age-class distribution towards a higher proportion of infected adult hosts compared to the real outbreak data that could be explained through sampling or detection biases as well as the effectiveness of the vaccination, which targeted adult individuals. The trajectory of the simulated highly virulent strain, however, corresponded well with observed patterns and support from the field where three different strain types were found. We could further demonstrate how the evolution of virulence in combination with density-driven movement acted as an important driver of disease persistence.

4.1 Introduction

Social host species often form a network of interconnected groups in the landscape that come in contact via roaming individuals or random group encounters (Nunn et al., 2015; Sah et al., 2017), which can also become a source of disease transmission. In this context, density-dependent effects in the host population primarily drive the spread of directly transmitted pathogens as they affect contact rates between groups. Higher host densities can force single individuals to avoid high-density areas through movement to escape competition, carrying the pathogen from group to group, and increasing contact chances between susceptible and infected host individuals (Hu et al., 2013). In addition to conspecific's density, landscape composition also affects the decision making process of moving individuals due to resource allocation or habitat quality cues (van Moorter et al., 2013). Therefore, to fully understand pathogen spread in social host populations, we need to account for the roaming individuals' spatial decision-making process associated with both habitat quality and population density (Gupte et al., 2022).

The spatial structure of the host population also influences pathogen spread (Kokko and López-Sepulcre, 2007), together with host-specific demographics (e.g., seasonal breeding peak) or pathogen properties such as virulence, particularly if virulence causes a reduction in host movement through for example lethargy (Franz et al., 2018). Another reason could be the evolution of virulence over time and associated evolutionary trade-offs such as the trade-off between virulence and transmission (Alizon et al., 2009; Cressler et al., 2016; Messinger and Ostling, 2009). Therefore, the initial outbreak strain could vary through time, hence space might not represent the entire outbreak pattern (Osnas et al., 2015). In this context, the range of host dispersal or roaming movements, particularly if the decision-making process is associated with the landscape structure, is an important aspect of host-pathogen dynamics (Hu et al., 2013; Messinger and Ostling, 2009; Scherer et al., 2020) and virulence management of infectious diseases. If host movement aggregates individuals in areas with high resource availability, this may put a halt to long distance transmission, because individuals do not need to disperse or migrate anymore. Such an aggregation could effectively quarantine large landscape areas, preventing the pathogens from being transported across distant groups. On the contrary, when density or resource availability changes in the landscape and forces individuals to aggregate in

new areas, it acts as a source for transmission of pathogens in previously naïve sub-populations (Paull et al., 2012).

Classical swine fever (CSF) infection in European wild boar (*Sus scrofa* L.) forms an ideal model system to study pathogen dynamics and patterns of spread on social hosts, as wild boar individuals exhibit both social behaviour and capacity for long-distance movement (Morelle et al., 2015), combined with the current increasing wild boar population density in Europe (Ruiz-Fons et al., 2008). Spillover from CSF (Edwards et al., 2000) to domestic pigs or the current outbreak of African swine fever (ASF) in Europe with their profound social, ethical and economic impact, highlight the importance of understanding the drivers of disease persistence and spread (Edwards et al., 2000; Woźniakowski et al., 2021). Despite the vast knowledge on wild boar host characteristics as well as previous studies both from theoretical approaches (Kramer-Schadt et al., 2009; Lange et al., 2012a; Lange et al., 2012b) and from real outbreak analyses across several years (Scherer et al., 2019), many dynamics of CSF virus cycling are still not fully understood. The outbreak showed a fast pathogen spread in the population during the beginning of the epidemic and strong density-dependent effects, i.e., the number of susceptible conspecifics in the surrounding area. The study of this outbreak suggested that contact rates may be positively associated with increased movement of host individuals (Scherer et al., 2019). Despite a heavy vaccination campaign, CSF persisted in the German wild boar population for seven years (Scherer et al., 2019). The outbreak affected mainly the piglet age class with approximately 8% of sampled piglets being infected, followed by the subadult and adult age class with 2 and 1%, respectively, and was characterised by an initial outbreak and a constant increase in immune individuals up to around 30% that decreased after 4 years, with wave-like patterns (Scherer et al. 2019). After a steep increase in area covered by infected, the speed of spread levelled off, having infected nearly half the area. Adult animals mostly seroconverted (60%), followed by subadults (30%) and piglets (20%).

Next to changes in virulence over time (Lange et al., 2012a), invasions of different strains (Blome et al., 2017), particularly host movement behaviour and associated spatial decision-making have been linked to outbreaks of a similar pathogen (African Swine Fever, ASF) in wild boar populations in the recent past (Halasa et al., 2016; Podgórski et al., 2013). While previous studies focus mainly on transmission through host density (homogenous mixing), it is expected that

changes in behaviour, for example during mating season, can alter the contact patterns in the host population. However, disentangling the single factors –landscape heterogeneity, density dependence, and movement decisions of hosts along with possible changes in pathogen virulence–, and ranking their effects on explaining disease persistence is nearly impossible from sparse and messy field data of outbreaks in the wild.

In this context, stochastic individual-based simulation models help to understand dynamics and patterns that arise from real outbreak data by making single processes associated with infectious disease outbreaks tractable and. First mathematical mean-field models assumed homogeneous mixing of susceptible and infectious hosts without explicitly including spatial factors in the disease transmission process (Anderson and May, 1982; Hethcote, 2000; Kermack and McKendrick, 1927). While those models have contributed significantly to understanding infectious disease dynamics, they assume that all individuals behave identically; in contrast, real individuals in heterogeneous landscapes often feature heterogeneous contact rates (Craft, 2015). However, individuals can have various reasons to move to a different location, such as resource abundance, predator avoidance, or density of conspecifics (Nathan et al., 2008). Local spatiotemporal conditions exert a strong influence on the movement decisions of individuals. Pattern oriented approaches uses multiple observed patterns simultaneously to characterize a system and its dynamics. In order to understand and predict disease outbreaks in realistic landscapes, data gathered from past outbreaks provide patterns against which we can test the simulation models and increase their accuracy to reproduce realistic results and infer the potential mechanism behind the observed patterns (Grimm et al., 2005).

In this study, we investigate and assess the effect of decision-making processes in host movement on disease outbreak patterns, persistence, and transmission. Through individual based models, we simulate a disease outbreak based on a realistic scenario and we compare our simulated spatiotemporal outbreak patterns to the observed patterns during the CSF outbreak in northern Germany. Specifically, we use an established spatially explicit individual based host-pathogen model Kramer-Schadt et al., 2009; Kürschner et al., 2021, 2022 (under review); Lange et al., 2012a, b; Scherer et al., 2020) to impose different mechanisms behind individual movement behaviours (habitat driven, density/competition driven and habitat-biased correlated random walk), on the host-pathogen system in Mecklenburg-Vorpommern. Our

model investigates how these different movement behaviours affect (1) the different proportion of affected individuals within each age class, (2) the speed and patterns of pathogen spread over time in the landscape through the host population, and (3) the temporal change in the epidemiological status of affected individuals in the host population (susceptible, infected, recovered) at the landscape-scale. Finally, by comparing model results with real data we further develop our understanding of host-pathogen dynamics in real landscapes.

4.2 Methods

4.2.1 Model overview

We modified a spatially explicit individual-based, eco-epidemiological model developed by Kürschner et al. (2021, 2022). It is based on earlier models considering neighbourhood infections only that were developed by Kramer-Schadt et al. (2009) and Lange et al. (2012a, b), and the addition of spatially explicit host movement implemented in Scherer et al. (2020). The current model includes spatiotemporal landscape dynamics representing changing resource availability, coupled with resource-based mortality as well as the evolution of pathogenic traits. We ran all previously developed model components on the wild boar (*Sus scrofa*) habitat suitability map of the German federal state of Mecklenburg-Vorpommern (Fernández et al., 2006; Scherer et al., 2019) representing resource availability. A complete and detailed model description of the dynamic processes following the modified ODD (Overview, Design concepts, Detail) protocol (Grimm et al., 2020, 2006) is provided in the supplementary material (Appendix C) and the model (implementation) in the Zenodo Database and on GitHub (links provided on acceptance).

The dynamic model comprises three main components, an epidemiological pathogen model, a pathogen evolutionary model, and a host model depending on underlying landscape features. Host individuals are characterised by sex, age, location, demographic (residential, dispersing), and epidemiological (susceptible, infected, immune) status. The epidemiological status of the individuals is defined by an SIR epidemiological classification (susceptible, infected, and recovered; Kermack & McKendrick, 1927).

4.2.2 Pathogen dynamics

The course of the disease is determined through an age-specific case fatality rate, a strain-specific transmission rate, and a strain-specific infectious period. Transiently infected hosts shed the pathogen for one week and gain lasting immunity. We adapted the in Kürschner et al. (2022, under review) developed evolution of pathogenic traits and strain-specific transmission/virulence trade-offs to fit transmission via moving host individuals. We further implemented a vaccination regime akin to the one used at the beginning of the MVP outbreak (Scherer et al., 2019); for details, see ODD protocol.

4.2.3 Host movement

We adapted four inter-cell explicit movement rules implemented in Scherer et al. (2020). In habitat driven-movement (HDM) moving host individuals directly reference the underlying landscape as a basis for their decision-making process by tending to move towards landscape cells with higher resource availability or habitat suitability, respectively. With competition-driven movement (CDM) moving host individuals reference the underlying landscape indirectly through the number of conspecifics and avoid areas of high densities. We also adapted a biased correlated random walk (HDCRW) defined by movement decision of host individuals is based on resource availability (local behaviour) while following performing a correlated random walk. The difference to HDM is that HDCRW has directional persistence in the decision making, i.e., moving to the best possible habitat within a certain direction. The difference in all adapted movement rules is in the decision-making process of moving individuals, i.e., into which cell to move, while other movement-related parameters (e.g., movement distance) remain the same. Regardless of the applied movement rule, all movement decisions include 30% stochasticity, meaning that 30% of all movement decisions are made randomly. As a control, we included a scenario without spatially explicit host movement.

We adapted all movement rules to include the strain-specific transmission trade-off implemented in Kürschner et al. (2022; under review) by adding the respective transmission increase per strain to the individual probability of transmission. Furthermore, we added a strain-specific trade-off between the strain virulence and maximum movement distance per timestep (week). While the average movement distance for roaming male wild boar is around

22 km per week, they can cover up to 84 km per week in search of resources (Morelle et al., 2015; Podgórski et al., 2013). The implemented trade-off (for details see ODD protocol) strongly reduces the capability of long-distance movement in case an individual is carrying a highly virulent strain. The maximum movement distance of an individual is reduced by 5% increments depending on the virulence of the affecting strain.

4.2.4 Process overview and scheduling

The temporal resolution of the model equals the approximate pathogen incubation time of one week (Artois et al., 2002). The model procedures were scheduled for each step in the following order: pathogen transmission, pathogen evolution, natal host group split of subadult males and females, resource-based host dispersal, host reproduction, host mortality and host ageing. The general group split of subadult females and males was limited to week 17 and week 29 of the year, respectively, representing the typical dispersal time for each sex.

4.2.5 Pathogen transmission

In all scenarios with spatially-explicit host movement, pathogen transmission between landscape cells occurs exclusively through moving individuals. In scenarios without host movement (control), inter-cell transmission occurs through neighbourhood infection (see ODD protocol for details).

4.2.6 Landscape structure

The tested landscape includes the federal state of Mecklenburg-Vorpommern (MVP) and surrounding area in a 2 km by 2 km grid, represented by 11,520 individual landscape cells with 5363 cells (21,452 km^2) that are habitable for wild boar. The implemented wild boar habitat suitability map is translated into the number of breeding females per cell, representing host breeding capacity and translating directly into host group size, and is a proxy of resource availability (Fernández et al., 2006; Scherer et al., 2019).

4.2.7 Model analysis

Each simulation lasted approximately 11 years, around two years of population "burn-in", 9 years from the time of the disease outbreak. The simulation time was chosen to represent the same timeframe as the recorded outbreak in MVP with an added buffer of two years both at the

beginning and end. We ran 10 repetitions per scenario due to computational limitations. For each of the 4 movement-related parameters (HDM, CDM, HDCRW, and no movement), different sampling designs (5 individuals per landscape cell with infected or immune individuals, 5 individuals per municipality with infected or immune individuals (N_sampled) and recording all individuals), amounting to 120 individual simulations. We recorded and analysed both on a landscape-wide level and on an individual cell level and municipality level. On the landscape-wide level, we recorded every alive individual that was either currently infected, immune or susceptible, the respective age class (adult, subadult, piglet), as well as how many individuals carry each strain of the pathogen. On the individual landscape cell level, we employed a sampling design to mimic the data from the real outbreak. In each cell, we selected a number (N_sampled) of recently (at the end of each time step, i.e., week) deceased individual and recorded its status at the time (infected, immune, other) and age class.

The simulations were done using the package "nlrx" (Salecker et al., 2019) to access the NetLogo (Wilensky, 1999) implementation through R (R Core team, 2020). We subsequently analysed the data on a municipality level regarding pathogen prevalence in the host population, the age class of the sampled individuals, and speed of spreading through the landscape, recorded as area in km^2 with infected host individuals over time. For pattern 1 (SIR per age class), we recorded (depending on the sampling design) the number of either infected or immune individuals and their respective age class in cells or municipalities. For pattern 2 (speed of pathogen spread) we recorded municipalities with active cases over time and for pattern 3 (epidemiological status at landscape scale) we recorded all either infected or immune individuals. Finally, the data was compared to their respective counterparts in the outbreak data used in Scherer et al. (2019).

4.3 Results

The simulated outbreak data has shown that of all tested movement scenarios, HDCRW spread through the landscape the fastest by affecting almost the entire study area after one year. A noticeable difference in the effect of sampling design was only apparent in HDM where with a sampling design of five individuals per municipality the affected area was smaller when compared to five individuals per landscape cell or all individuals. The overall proportion of

individuals classified into SIR (pattern 1) did not vary noticeably between sampling or movement scenarios, with the most sampled individuals being infected (between 75 and 95%). In comparison the MVP outbreak data showed the opposite distribution, where infected made up the lowest proportion of tested individuals (Figure 4.1).

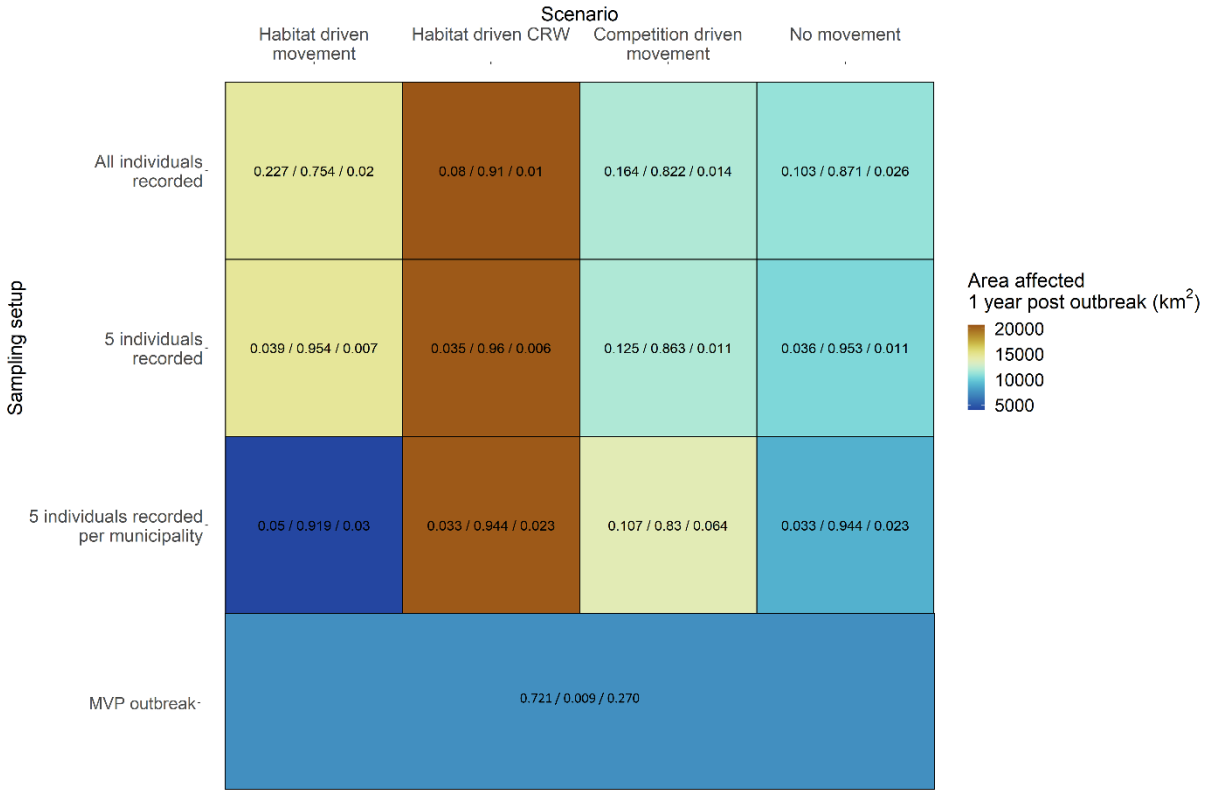

Figure 4.1: Overview of the comparison of simulated data and real outbreak data with the total area with infected individuals (colour gradient), separated for sampling design and movement scenario. Additionally, the MVP outbreak data (Scherer et al., 2019) was added for reference. Each tile contains the S / I / R classification of the sampled individuals (proportion). Each tile represents the average of five separate repetitions.

4.3.1 Speed of pathogen spread (pattern 2)

In the sampling design based on five individuals per municipality, the speed of pathogen spread varied strongly across the different simulated movement rules (Figure 4.2A). Habitat driven correlated random walk (HDCRW) scenarios showed the fastest spatial spread of all tested scenarios by reaching almost landscape wide-spread around quarter 15 (i.e., three and a half years, Figure 4.2A, Figure 4.3A). The pathogen spread in habitat driven movement (HDM) scenarios was slower, covering noticeably less area at quarter 15, and only reached high

landscape-wide spread around quarter 20 (i.e., five years, Figure 4.2A, Figure 4.3B). In this scenario, a strong increase in rate of spread happened around quarter 20 (Figure 4.2A), compared to the other scenarios with explicit host movement where the initial strong increase in speed of spread occurred shortly after the pathogen was introduced. Competition driven movement (CDM) showed the slowest rate of spread of all the scenarios with explicit host movement and the pathogen did not reach landscape-wide spread until quarter 25 (i.e., six years and 4 months, Figure 4.2A), with noticeably low area of spread around quarter 15 (Figure 4.3C). The scenarios without explicit host movement showed an overall different pattern in the speed of spread (Figure 4.2A). Instead of a strong increase in the affected area over a short period of time that was present in all the scenarios with explicit host movement, the increase in area was more gradual over time. The landscape-wide spread around quarter 15 was however, slightly larger compared to CDM (Figure 4.3D). In comparison with the MVP outbreak data from Scherer et al. (2019) (Figure 4.2, red line) the simulated data showed a similar pattern of speed of spread relative to the maximum affected area across all tested scenarios. However, the absolute values for the total affected area were noticeably higher in the simulated data. At the end of the simulated time, the movement scenarios reached an affected area of approximately 20000 km^2, which is almost the entirety of MVP region (approximately 24000 km^2), while the real outbreak data peaked at around 8000 km^2.

When all individuals were sampled or five individuals per landscape cell were sampled, (Figure 4.2B, Figure 4.2C), the observed patterns remained similar to the ones in the five individuals per municipality sampling except habitat driven movement which showed a faster increase in affected area compared to the municipality based sampling.

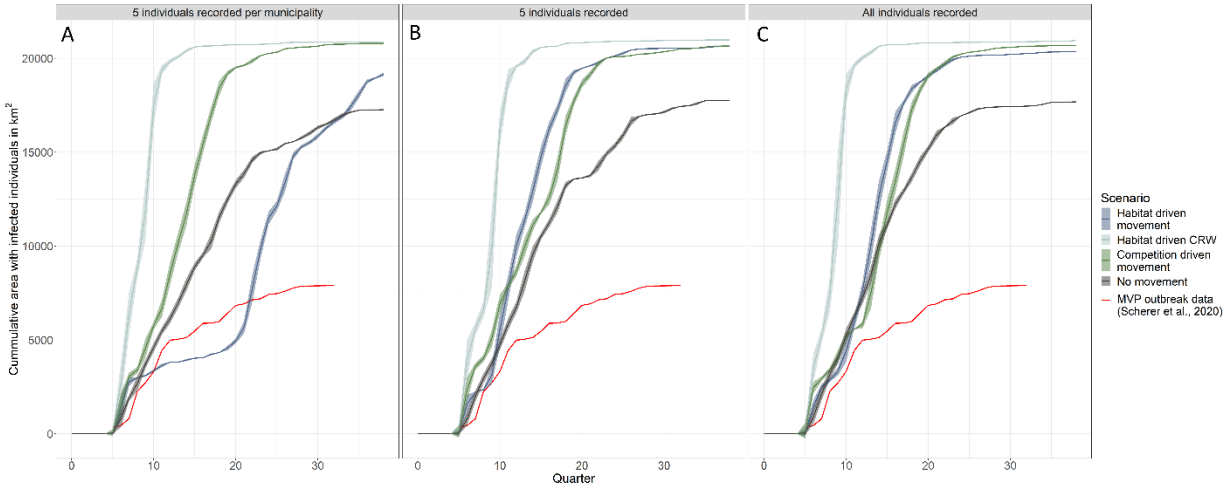

Figure 4.2: Speed of pathogen spread, recorded as number of municipalities with infected host individuals over time for the applied movement rules: habitat-driven correlated random walk (HDCRW), Habitat-driven movement (HDM), competition driven movement (CDM) and scenarios without movement (colour) and their respective standard deviation (coloured ribbon) within a sampling design of all individuals recorded (A) 5 sampled individuals per municipality (B) and 5 individuals sampled per landscape cell (C). All sampling scenarios have the original MVP outbreak data (Scherer et al., 2019) added as a red line.

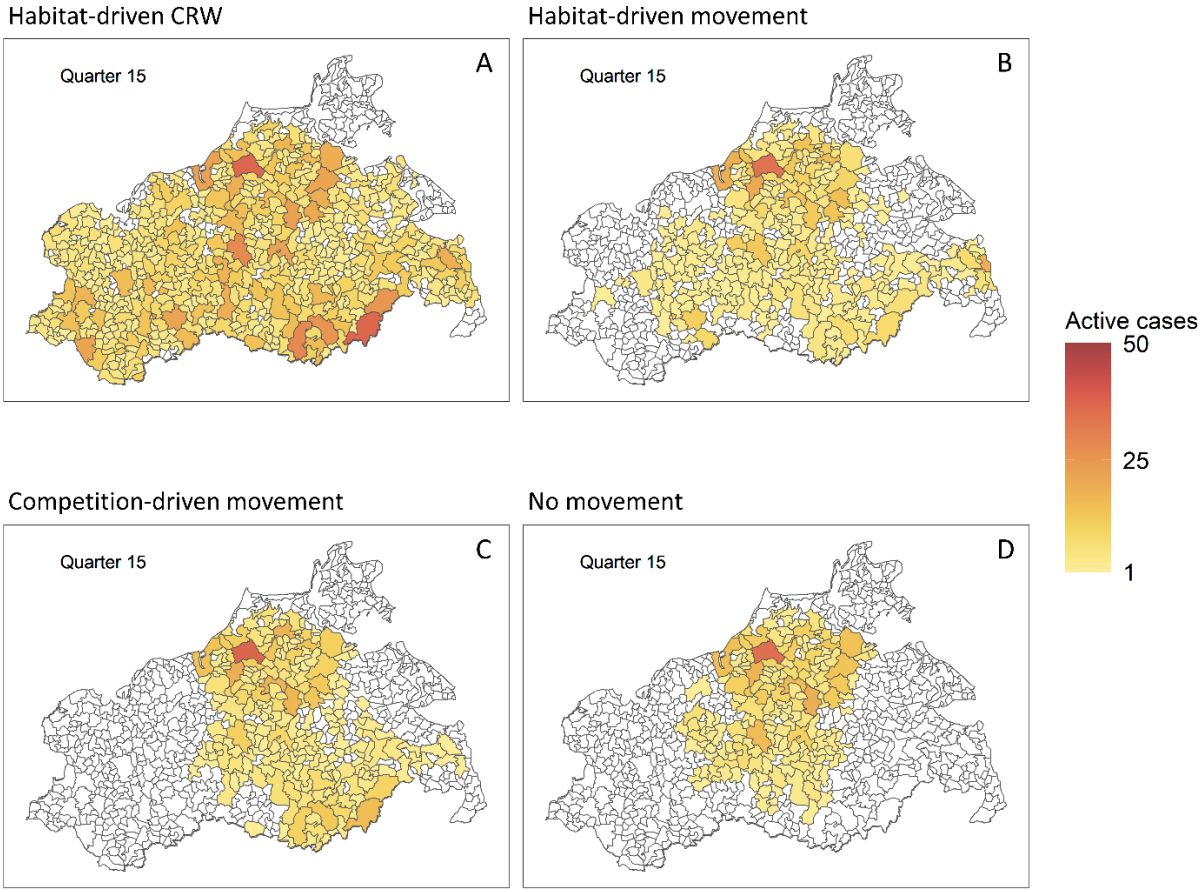

Figure 4.3: Municipality map of MVP at quarter 15 showing the number of infected host individuals (colour gradient) in A– HDCRW, B– HDM, C– CDM and D– no movement scenarios with all individuals sampled.

4.3.2 Relative comparison of host individuals per age class (pattern 1)

We recorded the age class of all sampled individuals, namely adults (age > 2 years), subadults (age > .5 years) ang piglets (age < .5 years). All the scenarios with explicit movement presented very similar results, thus here we use the HDM scenario with all tested individuals to represent movement scenarios and compare it to the no movement scenario (see supplementary material Appendix C2: Figures C5 – C8 for a full list of figures and table 4.1 for the SIR classification per age class). The proportion of sampled individuals in each age class in both HDM (Figure 4.4A) and no movement (Figure 4.4D) was similar, with piglets as the most sampled individuals. Sampled immune individuals also showed a similar age class distribution between both movement rules, although the proportion of piglets was higher in the no movement scenario at the beginning of the outbreak (Figure 4.4C, Figure 4.4F). However, there was a clear difference in the proportion of infected individuals of each age class between both scenarios. In HDM scenarios adults made up the largest proportion of sampled infected individuals (Figure 4.4B) while noticeably more sampled infected subadults and piglets were found in the scenarios without explicit host movement (Figure 4.4E). These results were consistent when all individuals were included and when only five individuals per landscape cell or per municipality were included.

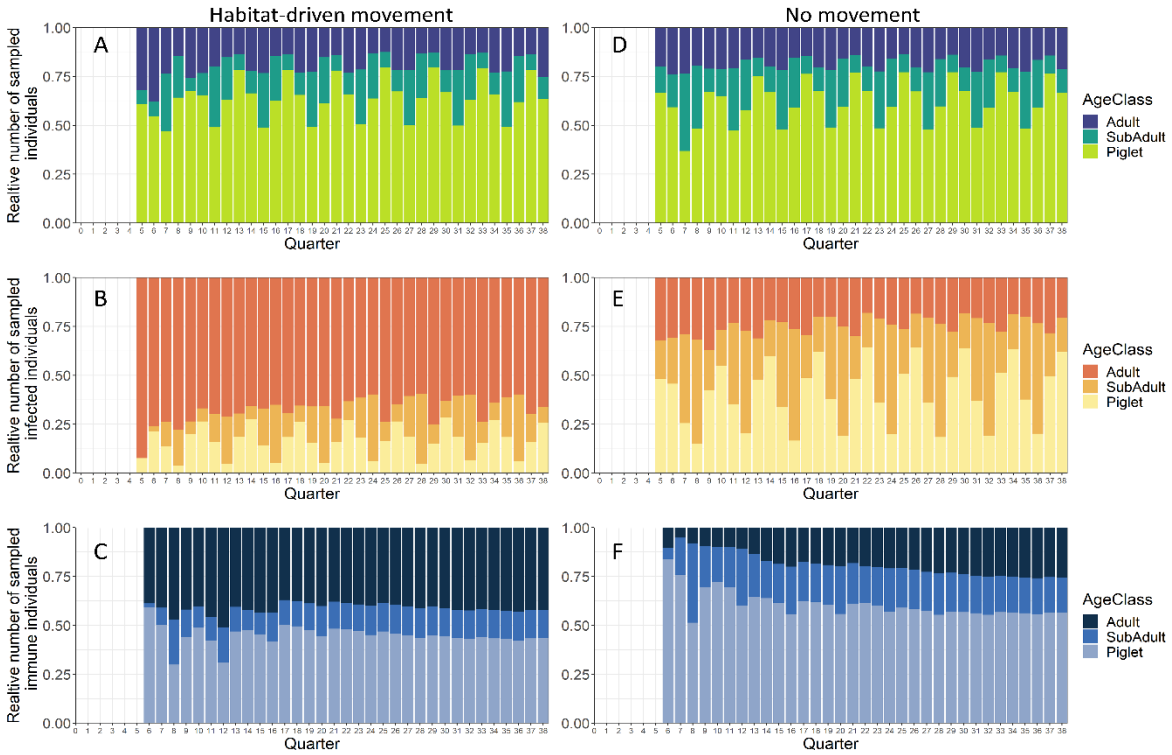

Figure 4.4: Relative number of sampled individuals per age class (adult, subadult, piglet, colour) in the HDM scenarios with all individuals (left) and no explicit host movement scenarios (right) for all sampled individuals (A and D), Infected individuals (B and E) and immune (i.e., recovered) individuals (C and F). Only individuals of municipalities with either active (i.e., infected) or immune (i.e., recovered) samples were included.

Table 4.1: Proportional SIR (susceptible, infected, recovered) classification for the movement scenarios (HDM, HDCRW, CDM and no movement) and sampling designs (All individuals sampled, 5 individuals per landscape cell sampled and 5 individuals per municipality sampled). Separated for the age class of the individuals (Adult, Subadult, Piglet) in form of S / I / R.

	S / I / R	Habitat driven movement	Habitat driven CRW	Competition driven movement	No movement
All individuals	Adult	0.019 / 0.961 / 0.02	0.012 / 0.973 / 0.015	0.042 / 0.907 / 0.051	0.038 / 0.944 / 0.018
	Subadult	0.098 / 0.874 / 0.028	0.066 / 0.928 / 0.006	0.189 / 0.764 / 0.048	0.03 / 0.954 / 0.016
	Piglet	0.108 / 0.829 / 0.063	0.083 / 0.866 / 0.052	0.263 / 0.615 / 0.122	0.033 / 0.937 / 0.03
5 individuals per cell	Adult	0.015 / 0.982 / 0.004	0.012 / 0.985 / 0.003	0.049 / 0.943 / 0.007	0.042 / 0.947 / 0.011
	Subadult	0.07 / 0.922 / 0.007	0.065 / 0.915 / 0.02	0.222 / 0.769 / 0.009	0.033 / 0.959 / 0.008
	Piglet	0.091 / 0.892 / 0.017	0.09 / 0.896 / 0.015	0.317 / 0.655 / 0.028	0.035 / 0.952 / 0.013
5 individuals per municipality	Adult	0.078 / 0.909 / 0.013	0.023 / 0.972 / 0.005	0.055 / 0.937 / 0.009	0.115 / 0.855 / 0.029
	Subadult	0.405 / 0.572 / 0.023	0.158 / 0.829 / 0.013	0.294 / 0.692 / 0.014	0.082 / 0.898 / 0.02
	Piglet	0.508 / 0.456 / 0.036	0.266 / 0.706 / 0.028	0.494 / 0.473 / 0.033	0.11 / 0.861 / 0.029

Compared to the simulated data, the MVP outbreak data (Figure 4.5) showed changing proportions of sampled individuals for each age class over time. The proportion of sampled adults decreased with time and, although the piglet numbers increased slightly, they were always lower than those in the simulated data (Figure 4.5A). Within the group of infected individuals, piglets dominated the proportions in most quarters followed by subadults, while only very few adult individuals were sampled that were currently infected (Figure 4.5B). The distribution of immune individuals by age class in the MVP outbreak data was almost identical to the age class distribution of all sampled individuals (Figure 4.5C).

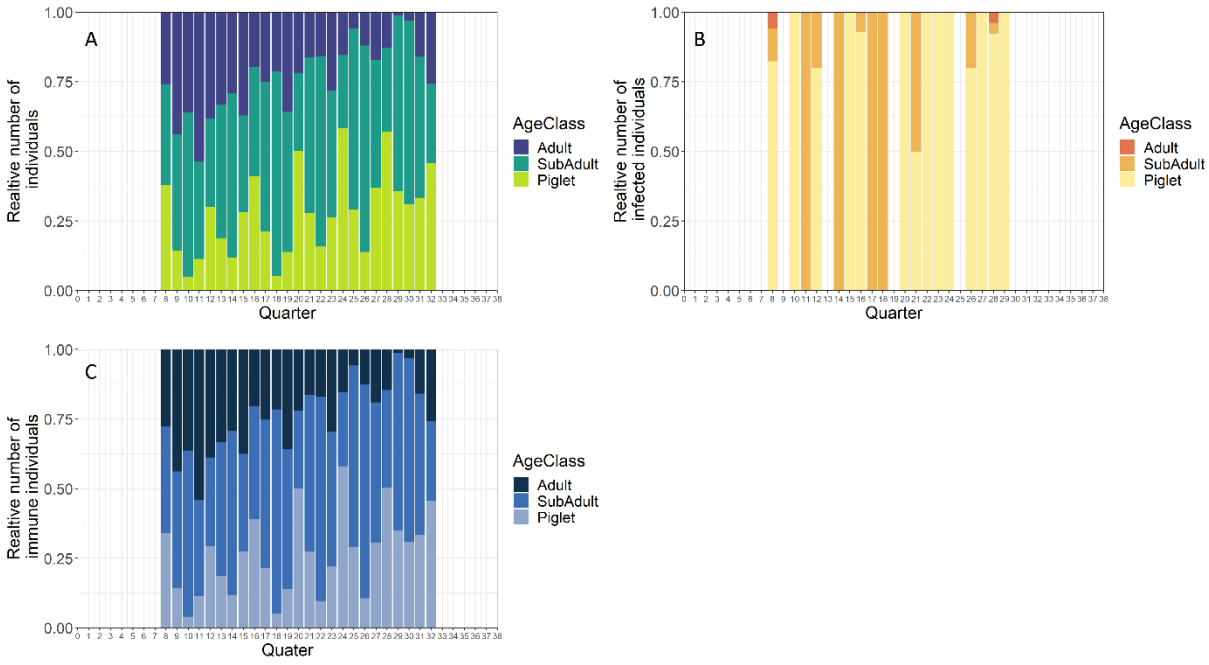

Figure 4.5: Relative number of sampled individuals per age class (adult, subadult, piglet, colour) for all sampled individuals (A), Infected individuals (B) and immune (i.e., recovered) individuals (C) in the MVP outbreak (Scherer et al., 2019).

4.3.3 Epidemiological status of all individuals at landscape scale (pattern 3)

The global infection status showed (Figure 4.6A) only slight differences between the tested movement scenarios especially after quarter 15, however, habitat driven correlated random walk HDCRW showed high peaks already at the beginning of the outbreak (Figure 4.6A). Habitat driven HDM and competition driven CDM movement showed slightly lower infected peaks while the control scenario of only neighbourhood infection showed the lowest number of infected over time. The number of immune individuals (Figure 4.6B) showed a similar difference in peak numbers in movement scenarios, however, in habitat driven HDCRW the number of

immune individuals increased more slowly compared to the habitat driven movement. A noticeable difference was seen in the control with a faster increase in number of immunes as well as higher peak numbers.

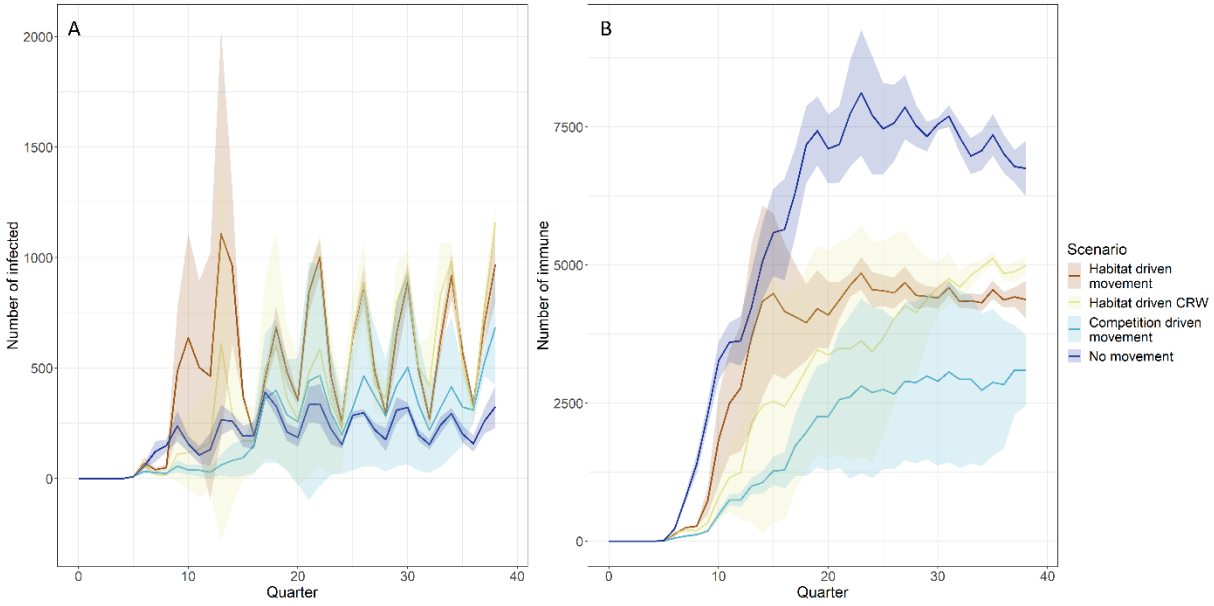

Figure 4.6: Epidemiological status of all individuals that were either infected (A) or immune (B) (for visibility at different scales) over time for Habitat-driven movement, Habitat-driven correlated random walk, competition-driven movement and no movement (colour).

4.3.4 Landscape-wide distribution of infected individuals separated by pathogen strains

We recorded how many individuals were infected by each pathogen strain classified from 1 to 12 different strains (Figure 4.7). The classification included differences in host survival time for each strain as well as transmission probability. For example, the strain with a virulence of one was characterized by a long host survival time and a low probability of transmission and the strain with a virulence of 12 was characterized by a very short host survival time and a high probability of transmission. All tested movement scenarios showed a shift in strain composition over time. The released high virulent strain dominated the infection process for the first years, followed by a shift towards medium and lower virulent strains. After this shift, the number of infected individuals increased substantially, particularly initially in both habitat-driven movement scenarios (HDCRW, HDM) (Figure 4.7A,B). Competition driven movement (CDM, Figure 4.7C) showed a similar shift in strain composition but with lower overall numbers of

infected compared to habitat driven CRW. In the scenario without host movement, there was no shift in the composition of strains or number of infected over time. The initial highly virulent strain as well as strains of similar high virulence remained dominant over the course of the epidemic, while medium and lower virulent strains only occurred in very low proportions (Figure 4.7D).

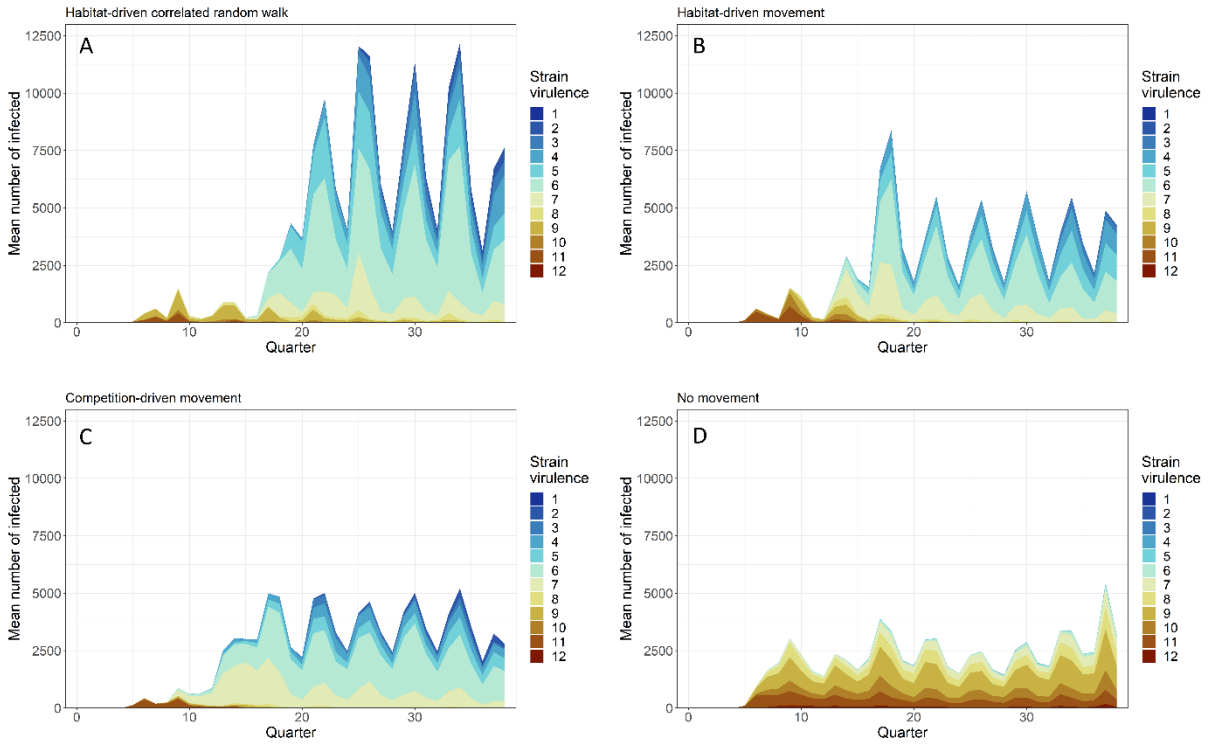

Figure 4.7: Mueller plots of the landscape-wide number of infected individuals separated for each strain, classified as strain virulence (colour) with 1– low virulence strain (long host survival time, low probability of transmission) to 12– highly virulent strain (short host survival time, high probability of transmission) in A– Habitat-driven CRW, B– Habitat-driven movement, C– Competition-driven movement and D– no movement (control).

4.4 Discussion

By applying an individual-based spatially-explicit model to real landscapes and comparing it to long-term outbreak data, we were able to gain insight into the complex dynamics of host pathogen systems. We were specifically interested in how adding movement behaviour and adaptive pathogen virulence can mimic real outbreaks, and we investigated this by adopting different sampling schemes or virtual observers (Zurell et al., 2010) on the simulations that could have biased the pattern match. Pattern oriented modelling can help to fill knowledge gaps

from past epidemics by explaining how real systems respond to external and internal changes. It is a robust method to reduce uncertainties when analysing multiple patterns simultaneously and helps to reveal cascading effects of processes (Grimm et al., 2005).

In our simulations, including explicit host movement always increased the speed of pathogen spread with variations between the processes behind the decision-making of host individuals. However, a sampling design that focused only on a small number of individuals per municipality underestimated the speed of spread.

4.4.1 Disease course of infected and immune over time (pattern 1)

Higher percentages of infected in all three age classes of infected individuals in both simulated and MVP data may be explained through the applied sampling design and sampling as well as detection biases. At the same time the immune age class was underrepresented, this might be an indication that the difference in infectiousness between young and old in the model could be much larger. While the MVP outbreak showed for example only 1% of adults infected, the model showed 70% infected (Figure 4.4, 4.5 for reference). During the MVP outbreak only individuals that were found dead or had been hunted were sampled; of these, hunted individuals were the most prevalent ones and only a small sample size of tested individuals was found actually infected (Scherer et al., 2019), which, however, is understandable from the fact that the proof of virus presence via PCR is not easy in wildlife, as samples are not always fresh and the detection of the virus in infected tissue is only possible during a short time window (David et al., 2002; Gal et al., 2008).

4.4.2 Match and mismatch of simulated spatiotemporal patterns with real outbreak data (pattern 2)

The speed of the pathogen spread in our simulations was similar a short period after emergence but kept increasing at high speed while there was a noticeable reduction in speed of spread in the MVP outbreak data. All our tested movement scenarios overestimated the area affected by the pathogen by a factor of around 2.5. However, during the MVP outbreak, a complex vaccination regime was established on a municipality level to prevent further spread of the pathogen (Artois et al., 2002; Moennig, 2015). Such vaccination regimes have been shown to reduce the number of susceptible individuals enough to slow down pathogen spread (Lange et

al., 2012b; Rossi et al., 2010). This could be responsible for the mismatch of the spatiotemporal speed of spread pattern in the epidemic phase and could be an indirect proof of how even an incomplete vaccination regime that might have reached only a fraction of mostly adult individuals (Rossi et al., 2010) might still work well in containing the disease.

4.4.3 Sampling scheme and the importance of standardized wildlife health monitoring

Without pre-emptive monitoring and testing, the likelihood of detecting emerging diseases is often too low to implement management strategies early enough to halt a larger outbreak, especially if the dynamics of the disease are not fully understood. This is further facilitated by the fact that wild animals are not constrained by borders and have the ability to move long distances or for migratory movements (Morner et al., 2002). Additionally, hunting-based approaches have been shown to be not fully random, for example in sampling for chronic wasting disease in mule deer (Conner et al., 2000) and feline immunodeficiency virus in domestic cats (Courchamp et al., 2000). On the one hand, host movement and space use can, as well as hunting associated behaviours such as avoidance, influence the pool of tested individuals. On the other hand, disease-related changes in behaviour such as reduced or severely altered movement behaviour (Franz et al., 2018), could select against the detection of infected individuals through hunting. Furthermore, sampling and testing during the MVP outbreak varied significantly between municipalities and over time, even at the height of the epidemic. To avoid further biases and to be able to implement proactive management strategies, a large scale and continuous wildlife monitoring is needed. Such a monitoring scheme will not only benefit wildlife populations, but it is likely to also benefit human health. A recent study found that more than half (58%) of the reporting 107 countries and territories did not have functional wildlife health surveillance programmes for health security planning, including pandemic prevention (Machalaba et al., 2021). Emerging or re-emerging zoonotic diseases such as severe acute respiratory syndrome, influenza or Ebola with pandemic potential can have a profound social, economic or health effect on human populations (Binder et al., 1999).

4.4.4 Strain differentiation and pathogenic virulence over time

Interestingly, our results showed a distinct change in prevalent viral strains over time with explicit host movement (Figure 4.6 for reference). Initially, the release strain of high virulence

(as well as closely related strains) dominated the outbreak but were replaced by strains of low and medium virulence between two and three years after the initial outbreak with habitat driven movement behaviours and between one and two years with a density (of conspecifics)-driven movement behaviour. Contrary, high virulence was largely maintained without explicit host movement.

To turn this around and compare back to the MVP outbreak, during the emergence of the simulated pathogen, the initial outbreak was characterised by a highly virulent strain and a low number of infected individuals. It is unclear at what point in time the MVP outbreak was first detected and when the intensive monitoring started. Very little is known about how the pathogen entered the wider area and how it spread pre monitoring. Some theories suggest a clustering of multiple separate and overlapping outbreaks were responsible, which might be supported by the occurrence of different CSF strains in the landscape, since all isolates of CSF-Viruses in Europe belonged to the subgroups 2.1, 2.2 or 2.3 (Blome et al., 2017). Our results could partially substantiate the assumption of multiple strains occurring simultaneously. However, in our simulation these were not necessarily caused by different outbreaks but were caused by the evolution of the initial strain. Furthermore, initial passive detection of a pathogen can require a high pathogen prevalence in the host population (Guberti et al., 2014). Our results showed a noticeably higher number of infected individuals once lower virulent strains became dominant. The real pattern of infected over time corresponds well with the pattern of the highly virulent strains in the simulations with movement. When infected with the low virulent strains (this could have been the introduction of subtype 2.2 or 2.3 in the real outbreak data) the infection could have been undetected and might explain the high ratio of immune individuals. In our model, the evolution of virulence had a similar effect as the vaccination applied in the field.

A variety of theoretical and empirical studies have shown that reducing host density will select for lower pathogen transmission, and a trade-off between transmission and virulence will subsequently select for lower virulence (as reviewed in Cressler et al., 2016). Our study further supports those findings by showing that explicit host movement is a key driver for virulence evolution in a realistic landscape. Disregarding animal movements in real landscapes can misrepresent infection risk and epidemiological dynamics (Wilber et al., 2022). While habitat

or resource-based movement decisions initially suggest an aggregation or clustering of susceptible hosts, those spatial clusters may be temporarily isolated from each other. Such clusters could however, due to a highly virulent strain, run the risk of local extinction before transmitting the pathogen to a large enough number of susceptible hosts (Messinger and Ostling, 2009). However, the occurrence of a pathogen could also induce adaptations in the movement behaviour of the host-species, such as avoidance of infected conspecifics that would impact the transmission risk of the pathogen (Gupte et al., 2022).

We found further evidence for a selection towards lower virulence in our simulations resulting from competition-driven movement behaviour of host individuals. Under those conditions, host individuals tended to avoid large clusters of conspecifics and used the density of close by conspecifics as a basis for their movement decision. This would subsequently alter the density and distribution of moving host individuals, the sole transmission factor in our simulations. This avoidance behaviour may have exerted a stronger selection pressure on lower virulent / less transmissible strains and resulted in a faster shift from high to medium and low virulent strains. Our simulations of different movement scenarios were mutually exclusive, while the decision making process behind animal movement is based on a complex interaction of extrinsic and intrinsic factors (Morales et al., 2010). Furthermore, considering the capacity for spatial memory in Suidae (Mendl et al., 1997) it is likely that the process behind the decision making of host individuals to be more dynamic and therefore less restrictive than our model assumptions.

In conclusion, we were able to recreate spatial patterns of disease transmission observed during an outbreak of classical swine fever in wild boar in Mecklenburg-Vorpommern with a spatially explicit eco-epidemiological model. In particular, the pattern of infected over time with the simulated highly virulent strain corresponded well with observed patterns. However, some restrictions such as a strong sampling bias or a complex vaccination regime may have led our model to overestimate parameters such as the overall affected area. We could, however, demonstrate that host movement and movement-induced species interactions are a key mechanism for prolonged disease persistence, especially under the assumption of an evolving pathogen.

4.5 Additional information

Supplementary material

- Appendix C1: ODD protocol
- Appendix C2: Additional figures

References

Alizon, S., Hurford, A., Mideo, N., van Baalen, M., 2009. Virulence evolution and the trade-off hypothesis: history, current state of affairs and the future. Journal of evolutionary biology 22, 245–259. https://doi.org/10.1111/j.1420-9101.2008.01658.x

Anderson, R.M., May, R.M., 1982. Coevolution of hosts and parasites. Parasitology 85, 411–426. https://doi.org/10.1017/S0031182000055360

Artois, M., Depner, K.R., Guberti, V., Hars, J., Rossi, S., Rutili, D., 2002. Classical swine fever (hog cholera) in wild boar in Europe. Rev. Sci. Tech. OIE 21, 287–303. https://doi.org/10.20506/rst.21.2.1332

Binder, S., Levitt, A.M., Sacks, J.J., Hughes, J.M., 1999. Emerging Infectious Diseases: Public Health Issues for the 21st Century. Science 284, 1311–1313. https://doi.org/10.1126/science.284.5418.1311

Blome, S., Staubach, C., Henke, J., Carlson, J., Beer, M., 2017. Classical Swine Fever–An Updated Review. Viruses 9, 86. https://doi.org/10.3390/v9040086

Conner, M.M., McCarty, C.W., Miller, M.W., 2000. Detection of bias in harvest-based estimates of chronic wasting disease prevalence in mule deer. Journal of Wildlife Diseases 36, 691–699. https://doi.org/10.7589/0090-3558-36.4.691

Courchamp, F., Say, L., Pontier, D., 2000. Detection, identification, and correction of a bias in an epidemiological study. Journal of Wildlife Diseases 36, 71–78. https://doi.org/10.7589/0090-3558-36.1.71

Craft, M.E., 2015. Infectious disease transmission and contact networks in wildlife and livestock. Phil. Trans. R. Soc. B 370, 20140107. https://doi.org/10.1098/rstb.2014.0107

Cressler, C.E., McLEOD, D.V., Rozins, C., van den Hoogen, J., Day, T., 2016. The adaptive evolution of virulence: a review of theoretical predictions and empirical tests. Parasitology 143, 915–930. https://doi.org/10.1017/S003118201500092X

David, D., Yakobson, B., Rotenberg, D., Dveres, N., Davidson, I., Stram, Y., 2002. Rabies virus detection by RT-PCR in decomposed naturally infected brains. Veterinary Microbiology 87, 111–118. https://doi.org/10.1016/S0378-1135(02)00041-X

Edwards, S., Fukusho, A., Lefèvre, P.-C., Lipowski, A., Pejsak, Z., Roehe, P., Westergaard, J., 2000. Classical swine fever: the global situation. Veterinary Microbiology 73, 103–119. https://doi.org/10.1016/S0378-1135(00)00138-3

Fernández, N., Kramer-Schadt, S., Thulke, H.-H., 2006. Viability and Risk Assessment in Species Restoration: Planning Reintroductions for the Wild Boar, a Potential Disease Reservoir. E&S 11, art6. https://doi.org/10.5751/ES-01560-110106

Franz, M., Kramer-Schadt, S., Greenwood, A.D., Courtiol, A., 2018. Sickness-induced lethargy can increase host contact rates and pathogen spread in water-limited landscapes. Funct Ecol 32, 2194–2204. https://doi.org/10.1111/1365-2435.13149

Gal, A., Loeb, E., Yisaschar-Mekuzas, Y., Baneth, G., 2008. Detection of Ehrlichia canis by PCR in different tissues obtained during necropsy from dogs surveyed for naturally occurring canine monocytic ehrlichiosis. The Veterinary Journal 175, 212–217. https://doi.org/10.1016/j.tvjl.2007.01.013

Grimm, V., Berger, U., Bastiansen, F., Eliassen, S., Ginot, V., Giske, J., Goss-Custard, J., Grand, T., Heinz, S.K., Huse, G., Huth, A., Jepsen, J.U., Jørgensen, C., Mooij, W.M., Müller, B., Pe'er, G., Piou, C., Railsback, S.F.,

Robbins, A.M., Robbins, M.M., Rossmanith, E., Rüger, N., Strand, E., Souissi, S., Stillman, R.A., Vabø, R., Visser, U., DeAngelis, D.L., 2006. A standard protocol for describing individual-based and agent-based models. Ecological Modelling 198, 115–126. https://doi.org/10.1016/j.ecolmodel.2006.04.023

Grimm, V., Railsback, S.F., Vincenot, C.E., Berger, U., Gallagher, C., DeAngelis, D.L., Edmonds, B., Ge, J., Giske, J., Groeneveld, J., Johnston, A.S.A., Milles, A., Nabe-Nielsen, J., Polhill, J.G., Radchuk, V., Rohwäder, M.-S., Stillman, R.A., Thiele, J.C., Ayllón, D., 2020. The ODD Protocol for Describing Agent-Based and Other Simulation Models: A Second Update to Improve Clarity, Replication, and Structural Realism. JASSS 23, 7. https://doi.org/10.18564/jasss.4259

Grimm, V., Revilla, E., Berger, U., Jeltsch, F., Mooij, W.M., Railsback, S.F., Thulke, H.-H., Weiner, J., Wiegand, T., DeAngelis, D.L., 2005. Pattern-Oriented Modeling of Agent-Based Complex Systems: Lessons from Ecology. Science 310, 987–991. https://doi.org/10.1126/science.1116681

Guberti, V., Stancampiano, L., Ferrari, N., 2014. Surveillance, monitoring and survey of wildlife diseases: a public health and conservation approach. Hystrix, the Italian Journal of Mammalogy 25. https://doi.org/10.4404/hystrix-25.1-10114

Gupte, P.R., Albery, G.F., Gismann, J., Sweeny, A.R., Weissing, F.J., 2022. Novel pathogen introduction rapidly alters evolved movement strategies, restructuring animal societies (preprint). Ecology. https://doi.org/10.1101/2022.03.09.483239

Halasa, T., Bøtner, A., Mortensen, S., Christensen, H., Toft, N., Boklund, A., 2016. Simulating the epidemiological and economic effects of an African swine fever epidemic in industrialized swine populations. Veterinary Microbiology 193, 7–16. https://doi.org/10.1016/j.vetmic.2016.08.004

Hethcote, H.W., 2000. The Mathematics of Infectious Diseases. SIAM Rev. 42, 599–653. https://doi.org/10.1137/S0036144500371907

Hu, H., Nigmatulina, K., Eckhoff, P., 2013. The scaling of contact rates with population density for the infectious disease models. Mathematical Biosciences 244, 125–134. https://doi.org/10.1016/j.mbs.2013.04.013

Kermack, W.O., McKendrick, A.G., 1927. A Contribution to the Mathematical Theory of Epidemics. Proceedings of the Royal Society A: Mathematical, Physical and Engineering Sciences 115, 700–721. https://doi.org/10.1098/rspa.1927.0118

Kokko, H., López-Sepulcre, A., 2007. The ecogenetic link between demography and evolution: can we bridge the gap between theory and data? Ecol Letters 10, 773–782. https://doi.org/10.1111/j.1461-0248.2007.01086.x

Kramer-Schadt, S., Fernández, N., Eisinger, D., Grimm, V., Thulke, H.-H., 2009. Individual variations in infectiousness explain long-term disease persistence in wildlife populations. Oikos 118, 199–208. https://doi.org/10.1111/j.1600-0706.2008.16582.x

Kürschner, T., Scherer, C., Radchuk, V., Blaum, N., Kramer-Schadt, S., 2021. Movement can mediate temporal mismatches between resource availability and biological events in host-pathogen interactions. Ecol. Evol. 11, 5728–5741. https://doi.org/10.1002/ece3.7478

Lange, M., Kramer-Schadt, S., Blome, S., Beer, M., Thulke, H.-H., 2012a. Disease severity declines over time after a wild boar population has been affected by classical swine fever-legend or actual epidemiological process? Preventive veterinary medicine 106, 185–195. https://doi.org/10.1016/j.prevetmed.2012.01.024.

Lange, M., Kramer-Schadt, S., Thulke, H.-H., 2012b. Efficiency of spatio-temporal vaccination regimes in wildlife populations under different viral constraints. Veterinary Research 43, 37. https://doi.org/10.1186/1297-9716-43-37

Machalaba, C., Uhart, M., Ryser-Degiorgis, M.-P., Karesh, W.B., 2021. Gaps in health security related to wildlife and environment affecting pandemic prevention and preparedness, 2007–2020. Bull. World Health Organ. 99, 342-350B. https://doi.org/10.2471/BLT.20.272690

Messinger, S.M., Ostling, A., 2009. The consequences of spatial structure for the evolution of pathogen transmission rate and virulence. The American naturalist 174, 441–454. https://doi.org/10.1086/605375

Moennig, V., 2015. The control of classical swine fever in wild boar. Front. Microbiol. 6. https://doi.org/10.3389/fmicb.2015.01211

Morelle, K., Podgórski, T., Prévot, C., Keuling, O., Lehaire, F., Lejeune, P., 2015. Towards understanding wild boar *Sus scrofa* movement: a synthetic movement ecology approach: A review of wild boar *Sus scrofa* movement ecology. Mammal Review 45, 15–29. https://doi.org/10.1111/mam.12028

Morner, T., Obendorf, D.L., Artois, M., Woodford, M.H., 2002. Surveillance and monitoring of wildlife diseases. Rev. Sci. Tech. OIE 21, 67–76. https://doi.org/10.20506/rst.21.1.1321

Nathan, R., Getz, W.M., Revilla, E., Holyoak, M., Kadmon, R., Saltz, D., Smouse, P.E., 2008. A movement ecology paradigm for unifying organismal movement research. Proceedings of the National Academy of Sciences 105, 19052–19059. https://doi.org/10.1073/pnas.0800375105

Nunn, C.L., Jordán, F., McCabe, C.M., Verdolin, J.L., Fewell, J.H., 2015. Infectious disease and group size: more than just a numbers game. Phil. Trans. R. Soc. B 370, 20140111. https://doi.org/10.1098/rstb.2014.0111

Osnas, E.E., Hurtado, P.J., Dobson, A.P., 2015. Evolution of Pathogen Virulence across Space during an Epidemic. The American Naturalist 185, 332–342. https://doi.org/10.1086/679734

Paull, S.H., Song, S., McClure, K.M., Sackett, L.C., Kilpatrick, A.M., Johnson, P.T., 2012. From superspreaders to disease hotspots: linking transmission across hosts and space. Frontiers in Ecology and the Environment 10, 75–82. https://doi.org/10.1890/110111

Podgórski, T., Baś, G., Jędrzejewska, B., Sönnichsen, L., Śnieżko, S., Jędrzejewski, W., Okarma, H., 2013. Spatiotemporal behavioral plasticity of wild boar (*Sus scrofa*) under contrasting conditions of human pressure: primeval forest and metropolitan area. Journal of Mammalogy 94, 109–119. https://doi.org/10.1644/12-MAMM-A-038.1

R Core team, 2020. R: A Language and Environment for Statistical Computing. R Foundation for Statistical Computing. https://www.R-project.org/

Rossi, S., Pol, F., Forot, B., Masse-provin, N., Rigaux, S., Bronner, A., Le Potier, M.-F., 2010. Preventive vaccination contributes to control classical swine fever in wild boar (*Sus scrofa* sp.). Veterinary Microbiology 142, 99–107. https://doi.org/10.1016/j.vetmic.2009.09.050

Ruiz-Fons, F., Segalés, J., Gortázar, C., 2008. A review of viral diseases of the European wild boar: Effects of population dynamics and reservoir rôle. The Veterinary Journal 176, 158–169. https://doi.org/10.1016/j.tvjl.2007.02.017

Sah, P., Leu, S.T., Cross, P.C., Hudson, P.J., Bansal, S., 2017. Unraveling the disease consequences and mechanisms of modular structure in animal social networks. Proc Natl Acad Sci USA 114, 4165–4170. https://doi.org/10.1073/pnas.1613616114

Salecker, J., Sciaini, M., Meyer, K.M., Wiegand, K., 2019. The nlrx r package: A next-generation framework for reproducible NetLogo model analyses. Methods in Ecololgy and Evolution 00, 2041–210X. https://doi.org/10.1111/2041-210X.13286

Scherer, C., Radchuk, V., Franz, M., Thulke, H., Lange, M., Grimm, V., Kramer-Schadt, S., 2020. Moving infections: individual movement decisions drive disease persistence in spatially structured landscapes. Oikos oik.07002. https://doi.org/10.1111/oik.07002

Scherer, C., Radchuk, V., Staubach, C., Müller, S., Blaum, N., Thulke, H., Kramer-Schadt, S., 2019. Seasonal host life-history processes fuel disease dynamics at different spatial scales. J Anim Ecol 88, 1812–1824. https://doi.org/10.1111/1365-2656.13070

van Moorter, B., Bunnefeld, N., Panzacchi, M., Rolandsen, C.M., Solberg, E.J., Sæther, B.-E., 2013. Understanding scales of movement: animals ride waves and ripples of environmental change. The Journal of animal ecology 82, 770–780. https://doi.org/10.1111/1365-2656.12045

Wilber, M.Q., Yang, A., Boughton, R., Manlove, K.R., Miller, R.S., Pepin, K.M., Wittemyer, G., 2022. A model for leveraging animal movement to understand spatio-temporal disease dynamics. Ecology Letters ele.13986. https://doi.org/10.1111/ele.13986

Wilensky, U., 1999. NetLogo (http://ccl.northwestern.edu/netlogo/). Center for Connected Learning and Computer-Based Modeling, Northwestern University, Evanston, IL.

Woźniakowski, G., Pejsak, Z., Jabłoński, A., 2021. Emergence of African Swine Fever in Poland (2014-2021). Successes and Failures in Disease Eradication. Agriculture 11, 738. https://doi.org/10.3390/agriculture11080738

Zurell, D., Berger, U., Cabral, J.S., Jeltsch, F., Meynard, C.N., Münkemüller, T., Nehrbass, N., Pagel, J., Reineking, B., Schröder, B., Grimm, V., 2010. The virtual ecologist approach: simulating data and observers. Oikos 119, 622–635. https://doi.org/10.1111/j.1600-0706.2009.18284.x

CHAPTER 5

GENERAL DISCUSSION

5 General Discussion

Wildlife disease dynamics are created by a complex web of interlinked processes, both on the side of the host-species as well as on the side of the pathogen. While the importance of single processes, such as host-population dynamics (Anderson and May, 1978; Hudson, 2002), host movement behaviour (Scherer et al., 2020) or pathogen virulence (Cressler et al., 2016), has been profusely studied, their combined effects and the interactions of those processes are often neglected (Turner et al., 2021). Furthermore, interactions such as host movement decisions based on dynamic landscape resource availability are likely susceptible to global change drivers, such as land-use changes or climate warming, that will ultimately modify and feed back into disease dynamics (Semenza and Menne, 2009; Semenza and Suk, 2018).

Epidemiological models have evolved from more simple mathematical mean-field approaches (Anderson and May, 1982) to complex tools, capable of capturing interactions on multiple trophic levels. Particularly, the integration of individual decision making processes such as movement (Manlove et al., 2021; Wilber et al., 2022) as a bottom-up regulation of host density and distribution through heterogenous and dynamic resource landscapes has seen more and more recognition. On the other hand, host-pathogen systems are also top-down regulated through the pathogen that, through transmission and mortality, will feed back onto the density and distribution of host individuals (Alizon et al., 2009; Cressler et al., 2016). The interplay of these complex and interlinked processes on multiple trophic levels and their importance for wildlife and human health is the current frontier of disease ecology.

Across the chapters of my thesis, I used **theoretical** and **pattern oriented** modelling approaches to investigate these interactions. I used theoretical models (chapters 2 and 3) to explore the effects of changing environmental conditions on disease dynamics. In the first **theoretical** part of my thesis (chapter 2), I investigated how temporal mismatches between seasonal resource availability and host life-history events affect host-pathogen dynamics and disease persistence in the landscape, in conjunction with host movement decision making, by modifying an established eco-epidemiological, individual-based model. I showed that the formation of temporary disease hotspots in combination with host movement decisions increases pathogen

persistence and therefore host-pathogen coexistence. Even under extreme conditions, such as a full temporal mismatch between host resource availability and host life-history, I showed a remarkable resilience of the host-pathogen system that prevented the pathogen from going extinct. In the second **theoretical** part of my thesis (chapter 3), I further modified the eco-epidemiological, individual-based model to illuminate the top-down effects of pathogens on host density and distribution and analysed pathogen virulence evolution in spatially structured host-populations and under global change scenarios. I demonstrated that mismatches between seasonal resource availability and host life-history facilitated pathogen persistence by favouring lower virulent strains, while landscape homogenization favoured higher virulent strains, capitalizing on higher host densities for transmission. In the **pattern oriented** approach of my thesis (chapter 4), I applied the newly developed theoretical model including host movement decision making and adaptive pathogen virulence to assess patterns of disease outbreak, persistence and transmission in a real population. Then I matched those patterns to observations from long-term outbreak data of a classical swine fever outbreak in wild boar in Northern Germany. I showed that the patterns associated with the simulated highly virulent strain corresponded well with the observed pattern, and I demonstrated how the evolution of virulence in combination with movement-induced individual interactions act as key drivers of prolonged disease persistence.

In the following I will synthesize my findings within the current framework of existing concepts and theories in disease dynamics. First, I will discuss key bottom-up drivers of disease dynamics and the importance of their interactions. Afterwards, I will emphasize the importance of including top-down processes in epidemiological models, followed by an assessment of disease drivers in the broader context of global change. Furthermore, I will discuss how the combination of empirical data and eco-epidemiological models can help to identify key drivers of disease dynamics under realistic conditions. Finally, I will conclude with an outlook of possible future developments to create accurate predictive frameworks for pathogen persistence and spread.

5.1 Movement, seasonality, spatial structure and dynamic host density

Chapter 2 highlighted how considering explicit host movement decisions and temporal mismatches of resources in the landscape resulted on different outcomes for pathogen persistence in hot-pathogen systems. Under host life history and resource availability mismatch

conditions, undirected random movement strategies, such as a correlated random walk, decreased the probability for pathogen persistence compared to directed host movements, such as habitat-driven movement strategies. One key aspect of the spread and persistence of directly transmitted infectious diseases is the contact rate of infected and susceptible host individuals (Craft, 2015; Eames et al., 2015; Heesterbeek et al., 2015). When host individuals move directly towards a resource such as food, shelter or mates, they aggregate in dense groups which are known to increase pathogen spread and persistence through increased contact rates (Altizer et al., 2006; Roy et al., 2005; Wichmann et al., 2003). My results illustrate this effect and support previous findings, e.g. seasonal dynamics in house finches (*Carpodacus mexicanus*) that promote species aggregation have been shown to greatly increase pathogen persistence (Hosseini et al., 2004). While contact rates and spatial heterogeneity have been studied extensively in compartmental metapopulation models (Kermack and McKendrick, 1927; Lloyd and May, 1996), temporal variability such as seasonal effects or explicit host movement are often neglected.

The study of temporal mismatches becomes especially relevant due to the current global change crisis that will potentially increase mismatch between resource availability and host phenological events (Plard et al., 2014; Visser and Gienapp, 2019) and the inability of many species to adapt to the new conditions in time (Radchuk et al., 2019). In chapter 2 I found that mismatches (or asynchrony) between resource availability and host life-history events slightly decreased pathogen persistence. A higher asynchrony forced spatiotemporal clustering of the host population into high resource habitats, forming disease islands within the landscape. While host population clustering under asynchrony is expected (Becker and Hall, 2016; Duncan et al., 2013), the presumed host population decline and subsequent pathogen extinction (Clifford et al., 2006) did not occur. During times of high resource availability, different clusters can be temporarily connected, allowing for demographic rescue of the host populations through individual movement (Roy et al., 2005), as opposed to spatially isolated and small host populations that are generally not able to sustain a prolonged disease outbreak (Clifford et al., 2006; Walker et al., 2008). As shown in my model, in the spatially structured populations, accounting for individual effects is key to understand the disease dynamics and movement behaviour played an important role that allowed for disease persistence.

Individual movement decisions played an important role in both connecting subpopulations and transporting the pathogen among them. For a pathogen to spread and persist within a population, a high host density (Parratt et al., 2016) and in case of an SIR-system where recovered individuals gain life-long immunity (Kermack and McKendrick, 1927), a high contact rate with susceptible hosts (Craft, 2015; Eames et al., 2015; Lloyd-Smith et al., 2005) is critical. There is clear evidence, both theoretical and empirical (Figuerola and Green, 2000; Kleijn et al., 2010; White et al., 2018; Wilber et al., 2022), that host movement might increase disease persistence. The results from my simulations suggest that movement decisions of the hosts in relation to resource availability in the landscape increase the chance of either coming into contact with infected conspecifics or transmitting the pathogen to susceptible hosts while moving through high resource areas that also attract other conspecifics. For example, the aggregation of otherwise unconnected cattle-herds around water resources in Kenya has shown to greatly increase that chance of disease transmission between herds (VanderWaal et al., 2017). Due to metapopulation-like structures, disease management and control become more complex and need to be adjusted to also account for areas with low infection density (Rowthorn et al., 2009). Understanding where and under what conditions those structures arise is an important step in moving towards predictive and preventive frameworks for disease control and management. Simultaneously, when a pathogen invades a group of low host density, members can be more vulnerable to mortality and ultimately, group extinction occurred.

Another important result is the effect of landscape homogenization on pathogen persistence under asynchronous conditions. Homogenous landscapes can increase hosts contact rates and pathogen transmission. Simultaneously, seasonal mismatches between food sources and life history events are increasingly common due to climate change (e.g. birds, Visser et al., 2012) and a general lower resource availability can additionally impair a host species immune response (Strandin et al., 2018). A subsequently higher susceptibility and increased pathogen spread can not only directly affect host populations but also could lead to zoonotic spillovers to other species, including humans in case of pathogen with high host-plasticity (Kreuder Johnson et al., 2015) such as the West-Nile virus (Marm Kilpatrick et al., 2006).

Even without the inclusion of explicit host movement, disease hotspots formed in high resource areas based of the initial landscape configuration. In return, there will be a high contact rate

and high number of pathogen transmission events within those hotspots (Paull et al., 2012) once a pathogen initially invades or emerges. Once emerged, there is evidence, that host-pathogen interactions can evolve rapidly (Hawley et al., 2013), with strong implications for disease persistence and spread. This highlights the importance of the pathogen effects as top-down forces shaping disease outbreaks that also need to be taken into account for understanding disease dynamics.

5.2 Pathogens in space and time – The evolution of virulence in spatially structured host populations

Pathogens have the potential to rapidly adapt due to high population sizes, high mutation rates and short generation times (Geoghegan and Holmes, 2018). Particularly, when landscape structure and dynamics facilitate the formation of spatiotemporally isolated pathogen hotspots with high host densities, a large number of transmission events (Paull et al., 2012) within those might drive pathogen evolution. A key aspect of pathogen evolution is virulence (i.e., a pathogens ability to cause harm to its host through for example mortality), which is subject to a variety of evolutionary trade-offs. One well known trade-off is the transmission-virulence trade-off hypothesis, which states that an increase in a strains transmission rate can cause shorter infections due to higher lethality (Alizon et al., 2009; Alizon and Michalakis, 2015; Cressler et al., 2016; Kamo et al., 2007).

Exploring how spatial structure impacts the evolution of pathogen virulence has been subject of both theoretical (Lion and Boots, 2010; Lion and Gandon, 2015; Webb et al., 2007) and empirical studies (Boots and Mealor, 2007). In chapter 3, I was able to show a threshold in the degree of landscape homogenization where higher levels of homogenization not only enhanced pathogen spread, but also evolution towards higher virulence. My results show that the spatial structure, configuration and dynamic of the landscape will impact the evolution of pathogen virulence in specific ways; while low virulence will be the norm in heterogeneous landscapes, we expect an increase of average pathogen virulence as landscapes become more homogeneous. This pattern is consistent with field observations, for example in the spread of tuberculosis in badgers (*Meles meles*) (Acevedo et al., 2019). By incorporating pathogen virulence evolution in the model, I built up upon the results in chapter 2, where pathogen virulence was fixed and landscape homogenization resulted in lower pathogen persistence, and I could show a clear

temporal differentiation in the virulence (and subsequent transmissibility) of the occurring pathogen strains that further facilitated pathogen persistence. As shown in my model, during the emergence of the pathogen, low virulent strains spread throughout the landscape over time. When host density increases at times of high resource availability, so do contact and transmission rates, and sporadically occurring higher virulent strains were able to capitalize on the high number of susceptible hosts (Altizer et al., 2006; Hite and Cressler, 2018). High host density and even distribution in homogenous landscapes can cause a rapid spread of a pathogen that could lead to host extinction through the pathogen or pathogen extinction through "self-shading", i.e. depleting the pool of susceptible individuals (Boots and Mealor, 2007). However, my model showed that pathogen-host coexistence can be achieved through virulence evolution. Both effects, host and pathogen extinction, can be mitigated through the evolution of lower virulence which allows the pathogen either to persist long enough until new susceptible individuals are available or spread slowly enough to not deplete the existing pool of susceptible individuals.

An additional key finding from chapter 3 was that although only one low virulent strain was released into the population it quickly evolved into a complex system of coexisting strains with varying virulence, resembling observed patterns, such as the ASF-virus in wild boar (Portugal et al., 2015). While the coexistence of multiple strains was apparent through all levels of landscape homogenization the likelihood of a strain to dominate the outbreak with high prevalence varied strongly with the level of landscape homogenization and time. Whereas theory predicts an evolution of virulence towards an optimal point along the virulence-transmission trade-off (Bonneaud and Longdon, 2020; Cressler et al., 2016), the presence and persistence of non-dominant strains could indicate a spatial differentiation of strains within the landscape. Lower virulent strains could persist within low density host clusters over time. Even if management efforts such as large-scale vaccination campaigns are undertaken, they would most likely target on high density host aggregations (Joseph et al., 2013). This would drastically reduce the prevalence of the highly virulent strains found in those areas, but lower virulent strains may escape management efforts and become endemic. As a result, a re-emergence of a pathogen and subsequent re-appearance of higher virulent strains through evolution from surviving low virulent strains could keep an outbreak active within a population over a long period of time,

especially if host movement can quickly and efficiently transport the pathogen over large distances. For example, one of the hypothesized causes of chytridiomycosis and the global population decline of many amphibian species, is a shift from an endemic low virulent strain towards a highly virulent variant (Rachowicz et al., 2005).

The results of the two previous models showed that long term pathogen persistence in the host population can be achieved in multiple ways. Directed host movement towards concentrated resources facilitates pathogen spread and persistence in the landscape (chapter 2), as well as the evolution of low virulent strains ensure pathogen persistence when host populations are isolated (chapter 3). Taken together, these results further highlight the critical importance of the interplay between resource landscape, seasonal dynamics, pathogen evolution and temporal asynchrony between host life history events and resource availability for pathogen persistence and host-pathogen coexistence and provide new insides on the mechanisms that allow for pathogen persistence, which ultimately opens up new avenues for emerging infectious diseases and spillover events to other species. There is evidence that habitat loss and increasing human-wildlife contacts are related to the emergence of viruses such as Hendra or Nipah (Patz et al., 2004; Plowright et al., 2021). Furthermore, increases in human-livestock-wildlife contacts, facilitated through seasonal changes in wildlife aggregation, can not only directly affect pathogen persistence and spread (Altizer et al., 2006; Roy et al., 2005; Wichmann et al., 2003), but can also lead to multi-directional spillover events (Fagre et al., 2022).

5.3 Implications of global change for pathogen persistence and spread

That global change, through mechanism like climate change or land-use change, can lead to environmental fluctuations and to an increase of mismatches between resources and biological events and feedback onto disease dynamics is one of the key results of both chapter 2 and 3. For example, large scale land use changes such as converting natural habitats into agricultural areas affected the density and distribution of many species, including wild boar, by aggregating them in agricultural areas (Acevedo et al., 2011) which can lead to novel contact points within and between species. The density, distribution and timing of those novel resources is likely to be vastly different from natural systems, resulting in the possibility for stronger temporal mismatches (Ullmann et al., 2020, 2018). Additionally, while landscapes are becoming more and more fragmented on a large scale, the structure within the suitable habitat fragments might

become more homogenous and subsequently, contact rates and pathogen transmission might increases locally (Patz et al., 2004).

The wild boar, as my model host species, is currently benefiting from landscape changes induced by global change (Vetter et al., 2020). Agricultural intensification and land-use change provide ample resources for wild boar populations to continue to increase in numbers across Europe (Acevedo et al., 2006; Ruiz-Fons et al., 2008). I demonstrated that, even under extreme global change scenarios such as a complete mismatch of host life-history and resource availability, host and pathogen had a high probability of coexisting, therefore ensuring disease persistence. If landscape fragments become more isolated from each other but internally become more homogenous, a potential increase in average pathogenic virulence within those fragments could have catastrophic effects on wildlife communities. On the other hand, if global change would result in a reduction of host density in certain areas, some diseases may become endemic in their respective host populations. I have shown that low virulent strains could continue to persist in these populations, and they could act as pathogen sources for re-occurring larger outbreaks through spontaneous mutation into more virulent strains and transport into areas of higher host density through host movement. Additionally, for many diseases an increase in virulence can coincide with an increase in transmissibility (Alizon and Michalakis, 2015; Messinger and Ostling, 2009), even though host survival times are generally shorter when infected with a highly virulent strain. As a result, the chance of spillover events to other wild or domesticated animals increases (Plowright et al., 2021). Furthermore, habitat encroachment and destruction will not only bring different wildlife species closer together but could facilitate selection of viruses with high host plasticity that could include human populations (Rulli et al., 2021). There is evidence that pathogens in domestic animals had a significantly wider host variety than pathogens that are not shared with domestic animals (Kreuder Johnson et al., 2015). Not only can zoonotic spillovers to humans have a detrimental effect on human health, but if host density becomes high enough a pathogen can be transmitted back to wildlife populations, potentially becoming endemic and creating long-term reservoirs. Subsequently, if contact rates between human and animal population continue to increase, integrating humans as part of a metapopulation of hosts, it may be inevitable to account for bidirectional pathogen transmission from humans to animals and vice versa (Fagre et al., 2022). This is evident in a

recent study that showed SARS-CoV-2 in white-tailed deer (*Odocoileus virginianus*) resulted from a spillover from humans and continued to spread directly within the white-tailed deer population (Kuchipudi et al., 2022). In the case of wild boar, that already hosts a variety of pathogens with implications for human health (e.g., hepatitis E or brucellosis; Li et al., (2005), Melzer et al. (2007)), the species might continue to benefit from the effects of climate and land use change, and contacts with human populations could increase in frequency. How my theoretical findings of bottom-up and top-down processes behave in a real system and translate into host-pathogen dynamics and large-scale patterns at the landscape and host population scale is the subject of chapter 4.

5.4 Patterns, processes and the effect of spatial decision-making

Disentangling the complex interactions of host-pathogen systems and resource landscapes in real outbreak data is often challenging. To that end, identifying the processes that drive real host-pathogen systems such as feedbacks from a heterogenous resource landscape to pathogen persistence through movement decisions is a natural first step. Incorporating patterns that arose from the interplay of individual movement and landscape into individual-based models can help to gain a mechanistic understanding of how pathogen spread and persistence are influenced by the external and internal components behind the decision making process of individual hosts (Dougherty et al., 2018; Grimm et al., 2005). Individual-based approaches can be used to include variation into the movement process of individuals such as distance or environmental and behavioral cues (Coulon et al., 2015; Grimm and Railsback, 2005). Even though complex transmission networks could be the result of moving individuals along internal or external drivers and could prove beneficial in understanding disease dynamics most epidemiological models used phenomenological approaches up until recently when mechanistic movement models became more common (e.g., Manlove et al., 2021; Scherer et al., 2020; Tardy et al., 2021; Wilber et al., 2022). For example, a broader understanding of why, when and where individuals exhibit specific movement patterns (Nathan et al., 2008) and technologies such as high-resolution animal tracking (Kays et al., 2015) have contributed substantially to the inclusion of mechanistic decision making processes into epidemiological models. The complex patterns that emerge from the interplay of animal movement and disease

dynamics, can be utilised for identifying implications for wildlife and human health (Dougherty et al., 2018).

Here, pattern-oriented modelling can help explaining how real systems respond to external and internal drivers by matching simulations to observed patterns from real outbreak data (Grimm et al., 2005). In chapter 4, I used my spatially explicit simulation model to match observed patterns in data gathered from a Classical Swine Fever (CSF) outbreak in Mecklenburg-Vorpommern (MVP). The outbreak was characterized by an initial peak of infected hosts and strong increase in infections although at low absolute numbers that decreased after a few years and sporadically reappeared in wave-like patterns. Despite a large-scale vaccination regime, CSF persisted in the wild boar population for seven years (Scherer et al., 2019). In the simulated outbreak I found that the trajectory of a simulated strain with high virulence matched well with observed patterns and was supported from the field data, where three different strain types were found. Interestingly, the highly virulent strain dominated the outbreak initially but was replaced by strains of low and medium virulence between two- and three-years post outbreak. In the context of the results from chapter 3, in which I showed that not only can multiple strains evolve from a single strain, but also that lower host density could likely favor less virulent strain, two interesting implications arise from that: firstly, the pathogen could over this period of time persist mostly through low density within subpopulations infected with low virulence strains, with sporadic surges of higher virulent strains when individual movement re-introduced the pathogen to higher density areas. During the MVP outbreak, CSF infection was detected in very few sampled individuals (0.5 to 1% post initial outbreak) while after the initial outbreak, around 30 to 40% of the sampled individuals were classified as immune (Scherer et al., 2019). However, a strict vaccination scheme was put into effect shortly after the outbreak (Artois et al., 2002; Moennig, 2015) and a differentiation between immune individuals that were vaccinated and those that gained natural immunity was not possible (Moennig, 2015; Scherer et al., 2019). Despite that, the pathogen continued to persist and new actively infected individuals were found throughout the seven year course of the outbreak (Scherer et al., 2019), indicating that undetected low virulent strains could have contributed to long duration of the MVP outbreak. Secondly, the detectability of pathogens in wildlife populations is inherently difficult and proof of virus presence through PCR (polymerase chain reaction) is only viable for limited amount of

time (David et al., 2002; Gal et al., 2008). Furthermore, most of the samples taken during the MVP outbreak were collected from hunted wild boar (Scherer et al., 2019). Hunting-based samplings have been shown to be not fully random and biased towards a subset of individuals, usually from high density areas (Conner et al., 2000; Courchamp et al., 2000). However, the pathogen could persist either at low virulence in low density areas (as shown in chapter 3), or the pathogen could be distributed more evenly through a landscape without asynchronous spatiotemporal variation forcing high density pathogen clusters (as shown in chapter 2). In both cases, a host-density biased sampling might underestimate the pathogen prevalence in the landscape and could misrepresent infection risk and epidemiological dynamics. Simulation studies, generally, are not subject to such strong biases and give us the opportunity to virtually observe the outbreak dynamics as a whole (Zurell et al., 2010). However, to better match the observed patterns in the MVP outbreak I included a municipality-based sampling design in chapter 4, where five deceased individuals (in affected municipalities) were chosen at random and sampled to mimic the limited often lower sample sizes of real data. I could demonstrate that under certain conditions, such as habitat-driven individual movement decisions, the sampling design underestimated the actual course of the disease.

Recalling from chapter 2, mechanistic host individual movement towards higher resource habitats, allowed for a pathogen to coexist with the host population at high probabilities. This is especially true when compared to a less targeted type of host movement such as the correlated random walk, where the probability of coexistence for host and pathogen was lower not only during periods of overall unfavourable habitat conditions, but also during periods of less extreme conditions. In addition, it was shown in chapter 4 that movement decisions in realistic landscapes based on conspecific density (avoidance) lead to earlier evolution of the pathogen toward less virulent strains than under directed movement into more resource-rich habitats. Excluding explicit host movement in the simulations in chapter 4 did not lead to a strong differentiation in pathogen strains, and lower virulent strains remained absent from the landscape. This is particularly interesting due to that fact that the CSF outbreak in MVP has in part been related to a change from a highly virulent strain to a strain of lower virulence (Lange et al., 2012; Mittelholzer et al., 2000). Taken together, the complementary use of mechanistic decision making processes and evolving pathogens is likely to increase in importance for disease

ecology, especially when external factors such as global change increase and alter the dynamic processes that drive individual movement.

5.5 Conclusion and outlook

Bottom-up and top-down processes and their interactions play an important role in shaping host densities and contact rates among moving individuals, two factors at the core of disease ecology. While bottom-up effects such as individual movement in response to a heterogeneous resource landscape as well as top-down processes, like varying levels of mortality caused by different virulent strains, have been well studied individually, their interaction is often missing in most epidemiological studies. Therefore, a general understanding of the interplay between spatiotemporal heterogeneity and the evolution of virulence is a key goal in disease ecology.

In my thesis, I focused on how explicit individual movement (chapter 2) and the evolution of pathogenic virulence (chapter 3) shape density, distribution and contact rates and subsequently feed back into pathogen transmission and persistence within a social host. I applied key insights from both processes with data from an outbreak of CSF in wild boar to identify drivers behind large-scale long-term disease outbreaks (chapter 4). By modifying an agent-based eco-epidemiological model I have shown that directed, decision-based individual movement led to higher probabilities of disease persistence in dynamic landscapes while in return, dynamic landscapes and mismatches between resources and host life-history selected for lower virulent viral strains. I was able to highlight important bottom-up mechanisms, such as the formation of disease hotspots under asynchronous resource conditions that facilitated pathogen persistence, even in scenarios with extremely unfavourable conditions for the host population. Secondly, I showed that the selection for low virulent strains under these unfavourable conditions can counteract some of the top-down effects that pathogens exert on their hosts through mortality and facilitated continuous pathogen persistence. Furthermore, I was able to recreate observed patterns in a long-term CSF outbreak and demonstrated how directed host movement and the evolution of virulence act as important drivers of pathogen persistence and spread.

Taken together, the complementary use of theoretical and pattern-oriented modelling in my thesis highlights the importance of spatiotemporal autocorrelations within the landscape

structure, plasticity in viral traits such a virulence and their interactions for long-term disease persistence and patterns of spread. My findings are an important step towards the inclusion of complex multi-trophic interactions both on a pathogen and on a host level in eco-epidemiological approaches to understand feedbacks on pathogen spread and disease persistence. The increasing rate of zoonotic spillovers with pandemic potential as well as the ongoing SARS-CoV-2 pandemic not only highlight the importance of understanding these complex interactions but are a warning for researchers to further investigate the causes and consequences behind disease dynamics to create predictive and preventive frameworks.

References

Acevedo, P., Escudero, M.A., Muńoz, R., Gortázar, C., 2006. Factors affecting wild boar abundance across an environmental gradient in Spain. Acta Theriol 51, 327–336. https://doi.org/10.1007/BF03192685

Acevedo, P., Farfán, M.Á., Márquez, A.L., Delibes-Mateos, M., Real, R., Vargas, J.M., 2011. Past, present and future of wild ungulates in relation to changes in land use. Landscape Ecology 26, 19–31. https://doi.org/10.1007/s10980-010-9538-2

Acevedo, P., Prieto, M., Quirós, P., Merediz, I., de Juan, L., Infantes-Lorenzo, J.A., Triguero-Ocaña, R., Balseiro, A., 2019. Tuberculosis Epidemiology and Badger (*Meles meles*) Spatial Ecology in a Hot-Spot Area in Atlantic Spain. Pathogens 8, 292. https://doi.org/10.3390/pathogens8040292

Alizon, S., Hurford, A., Mideo, N., van Baalen, M., 2009. Virulence evolution and the trade-off hypothesis: history, current state of affairs and the future. Journal of evolutionary biology 22, 245–259. https://doi.org/10.1111/j.1420-9101.2008.01658.x

Alizon, S., Michalakis, Y., 2015. Adaptive virulence evolution: the good old fitness-based approach. Trends in Ecology & Evolution 30, 248–254. https://doi.org/10.1016/j.tree.2015.02.009

Altizer, S., Dobson, A., Hosseini, P., Hudson, P., Pascual, M., Rohani, P., 2006. Seasonality and the dynamics of infectious diseases. Ecology letters 9, 467–484. https://doi.org/10.1111/j.1461-0248.2005.00879.x

Anderson, R.M., May, R.M., 1982. Coevolution of hosts and parasites. Parasitology 85, 411–426. https://doi.org/10.1017/S0031182000055360

Anderson, R.M., May, R.M., 1978. Regulation and Stability of Host-Parasite Population Interactions: I. Regulatory Processes. Journal of Animal Ecology 47, 219–247.

Artois, M., Depner, K.R., Guberti, V., Hars, J., Rossi, S., Rutili, D., 2002. Classical swine fever (hog cholera) in wild boar in Europe. Rev. Sci. Tech. OIE 21, 287–303. https://doi.org/10.20506/rst.21.2.1332

Becker, D.J., Hall, R.J., 2016. Heterogeneity in patch quality buffers metapopulations from pathogen impacts. Theor Ecol 9, 197–205. https://doi.org/10.1007/s12080-015-0284-6

Bonneaud, C., Longdon, B., 2020. Emerging pathogen evolution: Using evolutionary theory to understand the fate of novel infectious pathogens. EMBO Rep 21. https://doi.org/10.15252/embr.202051374

Boots, M., Mealor, M., 2007. Local Interactions Select for Lower Pathogen Infectivity. Science 315, 1284–1286. https://doi.org/10.1126/science.1137126

Clifford, D.L., Mazet, J.A.K., Dubovi, E.J., Garcelon, D.K., Coonan, T.J., Conrad, P.A., Munson, L., 2006. Pathogen exposure in endangered island fox (Urocyon littoralis) populations: Implications for conservation management. Biological Conservation 131, 230–243. https://doi.org/10.1016/j.biocon.2006.04.029

Conner, M.M., McCarty, C.W., Miller, M.W., 2000. Detection of bias in harvest-based estimates of chronic wasting disease prevalence in mule deer. Journal of Wildlife Diseases 36, 691–699. https://doi.org/10.7589/0090-3558-36.4.691

Coulon, A., Aben, J., Palmer, S.C.F., Stevens, V.M., Callens, T., Strubbe, D., Lens, L., Matthysen, E., Baguette, M., Travis, J.M.J., 2015. A stochastic movement simulator improves estimates of landscape connectivity. Ecology 96, 2203–2213. https://doi.org/10.1890/14-1690.1

Courchamp, F., Say, L., Pontier, D., 2000. detection, identification, and correction of a bias in an epidemiological study. Journal of Wildlife Diseases 36, 71–78. https://doi.org/10.7589/0090-3558-36.1.71

Craft, M.E., 2015. Infectious disease transmission and contact networks in wildlife and livestock. Phil. Trans. R. Soc. B 370, 20140107. https://doi.org/10.1098/rstb.2014.0107

Cressler, C.E., McLEOD, D.V., Rozins, C., van den Hoogen, J., Day, T., 2016. The adaptive evolution of virulence: a review of theoretical predictions and empirical tests. Parasitology 143, 915–930. https://doi.org/10.1017/S003118201500092X

David, D., Yakobson, B., Rotenberg, D., Dveres, N., Davidson, I., Stram, Y., 2002. Rabies virus detection by RT-PCR in decomposed naturally infected brains. Veterinary Microbiology 87, 111–118. https://doi.org/10.1016/S0378-1135(02)00041-X

Dougherty, E.R., Seidel, D.P., Carlson, C.J., Spiegel, O., Getz, W.M., 2018. Going through the motions: incorporating movement analyses into disease research. Ecol Lett 21, 588–604. https://doi.org/10.1111/ele.12917

Duncan, A.B., Gonzalez, A., Kaltz, O., 2013. Stochastic environmental fluctuations drive epidemiology in experimental host-parasite metapopulations. Proceedings. Biological sciences 280, 20131747. https://doi.org/10.1098/rspb.2013.1747

Eames, K., Bansal, S., Frost, S., Riley, S., 2015. Six challenges in measuring contact networks for use in modelling. Epidemics 10, 72–77. https://doi.org/10.1016/j.epidem.2014.08.006

Fagre, A.C., Cohen, L.E., Eskew, E.A., Farrell, M., Glennon, E., Joseph, M.B., Frank, H.K., Ryan, S.J., Carlson, C.J., Albery, G.F., 2022. Assessing the risk of human-to-wildlife pathogen transmission for conservation and public health. Ecology Letters n/a, 1–16. https://doi.org/10.1111/ele.14003

Figuerola, J., Green, A.J., 2000. Haematozoan Parasites and Migratory Behaviour in Waterfowl. Evolutionary Ecology 14, 143–153. https://doi.org/10.1023/A:1011009419264

Gal, A., Loeb, E., Yisaschar-Mekuzas, Y., Baneth, G., 2008. Detection of Ehrlichia canis by PCR in different tissues obtained during necropsy from dogs surveyed for naturally occurring canine monocytic ehrlichiosis. The Veterinary Journal 175, 212–217. https://doi.org/10.1016/j.tvjl.2007.01.013

Geoghegan, J.L., Holmes, E.C., 2018. The phylogenomics of evolving virus virulence. Nat Rev Genet 19, 756–769. https://doi.org/10.1038/s41576-018-0055-5

Grimm, V., Railsback, S.F., 2005. Individual-based Modeling and Ecology: Princeton University Press. https://doi.org/10.1515/9781400850624

Grimm, V., Revilla, E., Berger, U., Jeltsch, F., Mooij, W.M., Railsback, S.F., Thulke, H.-H., Weiner, J., Wiegand, T., DeAngelis, D.L., 2005. Pattern-Oriented Modeling of Agent-Based Complex Systems: Lessons from Ecology. Science 310, 987–991. https://doi.org/10.1126/science.1116681

Hagenaars, T.J., Donnelly, C.A., Ferguson, N.M., 2004. Spatial heterogeneity and the persistence of infectious diseases. Journal of Theoretical Biology 229, 349–359. https://doi.org/10.1016/j.jtbi.2004.04.002

Hawley, D.M., Osnas, E.E., Dobson, A.P., Hochachka, W.M., Ley, D.H., Dhondt, A.A., 2013. Parallel Patterns of Increased Virulence in a Recently Emerged Wildlife Pathogen. PLoS Biol 11, e1001570. https://doi.org/10.1371/journal.pbio.1001570

Heesterbeek, H., Anderson, R.M., Andreasen, V., Bansal, S., De Angelis, D., Dye, C., Eames, K.T.D., Edmunds, W.J., Frost, S.D.W., Funk, S., Hollingsworth, T.D., House, T., Isham, V., Klepac, P., Lessler, J., Lloyd-Smith, J.O., Metcalf, C.J.E., Mollison, D., Pellis, L., Pulliam, J.R.C., Roberts, M.G., Viboud, C., Isaac Newton Institute IDD Collaboration, 2015. Modeling infectious disease dynamics in the complex landscape of global health. Science 347, aaa4339. https://doi.org/10.1126/science.aaa4339

Hite, J.L., Cressler, C.E., 2018. Resource-driven changes to host population stability alter the evolution of virulence and transmission. Phil. Trans. R. Soc. B 373, 20170087. https://doi.org/10.1098/rstb.2017.0087

Hosseini, P.R., Dhondt, A.A., Dobson, A., 2004. Seasonality and wildlife disease: how seasonal birth, aggregation and variation in immunity affect the dynamics of Mycoplasma gallisepticum in house finches. Proceedings. Biological sciences 271, 2569–2577. https://doi.org/10.1098/rspb.2004.2938

Hudson, P.J. (Ed.), 2002. The ecology of wildlife diseases. Oxford University Press, New York.

Joseph, M.B., Mihaljevic, J.R., Arellano, A.L., Kueneman, J.G., Preston, D.L., Cross, P.C., Johnson, P.T.J., 2013. Taming wildlife disease: bridging the gap between science and management. J Appl Ecol 50, 702–712. https://doi.org/10.1111/1365-2664.12084

Kamo, M., Sasaki, A., Boots, M., 2007. The role of trade-off shapes in the evolution of parasites in spatial host populations: An approximate analytical approach. Journal of Theoretical Biology 244, 588–596. https://doi.org/10.1016/j.jtbi.2006.08.013

Kays, R., Crofoot, M.C., Jetz, W., Wikelski, M., 2015. Terrestrial animal tracking as an eye on life and planet. Science 348, aaa2478. https://doi.org/10.1126/science.aaa2478

Kermack, W.O., McKendrick, A.G., 1927. A Contribution to the Mathematical Theory of Epidemics. Proceedings of the Royal Society A: Mathematical, Physical and Engineering Sciences 115, 700–721. https://doi.org/10.1098/rspa.1927.0118

Kleijn, D., Munster, V.J., Ebbinge, B.S., Jonkers, D.A., Müskens, G.J.D.M., Van Randen, Y., Fouchier, R.A.M., 2010. Dynamics and ecological consequences of avian influenza virus infection in greater white-fronted geese in their winter staging areas. Proc. R. Soc. B. 277, 2041–2048. https://doi.org/10.1098/rspb.2010.0026

Kreuder Johnson, C., Hitchens, P.L., Smiley Evans, T., Goldstein, T., Thomas, K., Clements, A., Joly, D.O., Wolfe, N.D., Daszak, P., Karesh, W.B., Mazet, J.K., 2015. Spillover and pandemic properties of zoonotic viruses with high host plasticity. Sci Rep 5, 14830. https://doi.org/10.1038/srep14830

Kuchipudi, S.V., Surendran-Nair, M., Ruden, R.M., Yon, M., Nissly, R.H., Vandegrift, K.J., Nelli, R.K., Li, L., Jayarao, B.M., Maranas, C.D., Levine, N., Willgert, K., Conlan, A.J.K., Olsen, R.J., Davis, J.J., Musser, J.M., Hudson, P.J., Kapur, V., 2022. Multiple spillovers from humans and onward transmission of SARS-CoV-2 in white-tailed deer. Proc. Natl. Acad. Sci. U.S.A. 119, e2121644119. https://doi.org/10.1073/pnas.2121644119

Lange, M., Kramer-Schadt, S., Blome, S., Beer, M., Thulke, H.-H., 2012. Disease severity declines over time after a wild boar population has been affected by classical swine fever—legend or actual epidemiological process? Preventive veterinary medicine 106, 185–195. https://doi.org/10.1016/j.prevetmed.2012.01.024.

Li, T.-C., Chijiwa, K., Sera, N., Ishibashi, T., Etoh, Y., Shinohara, Y., Kurata, Y., Ishida, M., Sakamoto, S., Takeda, N., Miyamura, T., 2005. Hepatitis E Virus Transmission from Wild Boar Meat. Emerg. Infect. Dis. 11, 1958–1960. https://doi.org/10.3201/eid1112.051041

Lion, S., Boots, M., 2010. Are parasites "prudent" in space? Ecology letters 13, 1245–1255. https://doi.org/10.1111/j.1461-0248.2010.01516.x

Lion, S., Gandon, S., 2015. Evolution of spatially structured host-parasite interactions. Journal of evolutionary biology 28, 10–28. https://doi.org/10.1111/jeb.12551

Lloyd, A.L., May, R.M., 1996. Spatial Heterogeneity in Epidemic Models. Journal of Theoretical Biology 179, 1–11. https://doi.org/10.1006/jtbi.1996.0042

Lloyd-Smith, J.O., Schreiber, S.J., Kopp, P.E., Getz, W.M., 2005. Superspreading and the effect of individual variation on disease emergence. Nature 438, 355–359. https://doi.org/10.1038/nature04153

Manlove, K., Wilber, M., White, L., Bastille-Rousseau, G., Yang, A., Gilbertson, M., Craft, M., Cross, P., Wittemyer, G., Pepin, K., 2021. Defining an epidemiological landscape by connecting host movement to pathogen transmission (preprint). Preprints. https://doi.org/10.22541/au.163458112.22651398/v1

Marm Kilpatrick, A., Daszak, P., Jones, M.J., Marra, P.P., Kramer, L.D., 2006. Host heterogeneity dominates West Nile virus transmission. Proceedings of the Royal Society B: Biological Sciences 273, 2327–2333. https://doi.org/10.1098/rspb.2006.3575

Melzer, F., Lohse, R., Nieper, H., Liebert, M., Sachse, K., 2007. A serological study on brucellosis in wild boars in Germany. Eur J Wildl Res 53, 153–157. https://doi.org/10.1007/s10344-006-0072-0

Messinger, S.M., Ostling, A., 2009. The consequences of spatial structure for the evolution of pathogen transmission rate and virulence. The American naturalist 174, 441–454. https://doi.org/10.1086/605375

Mittelholzer, C., Moser, C., Tratschin, J.-D., Hofmann, M.A., 2000. Analysis of classical swine fever virus replication kinetics allows differentiation of highly virulent from avirulent strains. Veterinary Microbiology 74, 293–308. https://doi.org/10.1016/S0378-1135(00)00195-4

Moennig, V., 2015. The control of classical swine fever in wild boar. Front. Microbiol. 6. https://doi.org/10.3389/fmicb.2015.01211

Nathan, R., Getz, W.M., Revilla, E., Holyoak, M., Kadmon, R., Saltz, D., Smouse, P.E., 2008. A movement ecology paradigm for unifying organismal movement research. Proceedings of the National Academy of Sciences 105, 19052–19059. https://doi.org/10.1073/pnas.0800375105

Parratt, S.R., Numminen, E., Laine, A.-L., 2016. Infectious Disease Dynamics in Heterogeneous Landscapes. Annu. Rev. Ecol. Evol. Syst. 47, 283–306. https://doi.org/10.1146/annurev-ecolsys-121415-032321

Patz, J.A., Daszak, P., Tabor, G.M., Aguirre, A.A., Pearl, M., Epstein, J., Wolfe, N.D., Kilpatrick, A.M., Foufopoulos, J., Molyneux, D., Bradley, D.J., Members of the Working Group on Land Use Change Disease Emergence, 2004. Unhealthy Landscapes: Policy Recommendations on Land Use Change and Infectious Disease Emergence. Environmental Health Perspectives 112, 1092–1098. https://doi.org/10.1289/ehp.6877

Paull, S.H., Song, S., McClure, K.M., Sackett, L.C., Kilpatrick, A.M., Johnson, P.T., 2012. From superspreaders to disease hotspots: linking transmission across hosts and space. Frontiers in Ecology and the Environment 10, 75–82. https://doi.org/10.1890/110111

Plard, F., Gaillard, J.-M., Coulson, T., Hewison, A.J.M., Delorme, D., Warnant, C., Bonenfant, C., 2014. Mismatch Between Birth Date and Vegetation Phenology Slows the Demography of Roe Deer. PLoS Biol 12, e1001828. https://doi.org/10.1371/journal.pbio.1001828

Plowright, R.K., Reaser, J.K., Locke, H., Woodley, S.J., Patz, J.A., Becker, D.J., Oppler, G., Hudson, P.J., Tabor, G.M., 2021. Land use-induced spillover: a call to action to safeguard environmental, animal, and human health. The Lancet Planetary Health 5, e237–e245. https://doi.org/10.1016/S2542-5196(21)00031-0

Portugal, R., Coelho, J., Höper, D., Little, N.S., Smithson, C., Upton, C., Martins, C., Leitão, A., Keil, G.M., 2015. Related strains of African swine fever virus with different virulence: genome comparison and analysis. Journal of General Virology 96, 408–419. https://doi.org/10.1099/vir.0.070508-0

Rachowicz, L.J., Hero, J.-M., Alford, R.A., Taylor, J.W., Morgan, J.A.T., Vredenburg, V.T., Collins, J.P., Briggs, C.J., 2005. The Novel and Endemic Pathogen Hypotheses: Competing Explanations for the Origin of Emerging Infectious Diseases of Wildlife. Conservation Biology 19, 1441–1448. https://doi.org/10.1111/j.1523-1739.2005.00255.x

Radchuk, V., Reed, T., Teplitsky, C., van de Pol, M., Charmantier, A., Hassall, C., Adamík, P., Adriaensen, F., Ahola, M.P., Arcese, P., Miguel Avilés, J., Balbontin, J., Berg, K.S., Borras, A., Burthe, S., Clobert, J., Dehnhard, N., de Lope, F., Dhondt, A.A., Dingemanse, N.J., Doi, H., Eeva, T., Fickel, J., Filella, I., Fossøy, F., Goodenough, A.E., Hall, S.J.G., Hansson, B., Harris, M., Hasselquist, D., Hickler, T., Joshi, J., Kharouba, H., Martínez, J.G., Mihoub, J.-B., Mills, J.A., Molina-Morales, M., Moksnes, A., Ozgul, A., Parejo, D., Pilard, P., Poisbleau, M., Rousset, F., Rödel, M.-O., Scott, D., Senar, J.C., Stefanescu, C., Stokke, B.G., Kusano, T., Tarka, M., Tarwater, C.E., Thonicke, K., Thorley, J., Wilting, A., Tryjanowski, P., Merilä, J., Sheldon, B.C., Pape Møller, A., Matthysen, E., Janzen, F., Dobson, F.S., Visser, M.E., Beissinger, S.R., Courtiol, A., Kramer-Schadt, S., 2019. Adaptive responses of animals to climate change are most likely insufficient. Nature Communications 10, 3109. https://doi.org/10.1038/s41467-019-10924-4

Rowthorn, R.E., Laxminarayan, R., Gilligan, C.A., 2009. Optimal control of epidemics in metapopulations. Journal of The Royal Society Interface 6, 1135–1144. https://doi.org/10.1098/rsif.2008.0402

Roy, M., Holt, R.D., Barfield, M., 2005. Temporal Autocorrelation Can Enhance the Persistence and Abundance of Metapopulations Comprised of Coupled Sinks. The American Naturalist 166, 246–261. https://doi.org/10.1086/431286

Ruiz-Fons, F., Segalés, J., Gortázar, C., 2008. A review of viral diseases of the European wild boar: Effects of population dynamics and reservoir rôle. The Veterinary Journal 176, 158–169. https://doi.org/10.1016/j.tvjl.2007.02.017

Rulli, M.C., D'Odorico, P., Galli, N., Hayman, D.T.S., 2021. Land-use change and the livestock revolution increase the risk of zoonotic coronavirus transmission from rhinolophid bats. Nat Food 2, 409–416. https://doi.org/10.1038/s43016-021-00285-x

Scherer, C., Radchuk, V., Franz, M., Thulke, H., Lange, M., Grimm, V., Kramer–Schadt, S., 2020. Moving infections: individual movement decisions drive disease persistence in spatially structured landscapes. Oikos oik.07002. https://doi.org/10.1111/oik.07002

Scherer, C., Radchuk, V., Staubach, C., Müller, S., Blaum, N., Thulke, H., Kramer-Schadt, S., 2019. Seasonal host life-history processes fuel disease dynamics at different spatial scales. J Anim Ecol 88, 1812–1824. https://doi.org/10.1111/1365-2656.13070

Semenza, J.C., Menne, B., 2009. Climate change and infectious diseases in Europe. The Lancet Infectious Diseases 9, 365–375. https://doi.org/10.1016/S1473-3099(09)70104-5

Semenza, J.C., Suk, J.E., 2018. Vector-borne diseases and climate change: a European perspective. FEMS Microbiology Letters 365. https://doi.org/10.1093/femsle/fnx244

Strandin, T., Babayan, S.A., Forbes, K.M., 2018. Reviewing the effects of food provisioning on wildlife immunity. Philos Trans R Soc Lond B Biol Sci 373. https://doi.org/10.1098/rstb.2017.0088

Tardy, O., Bouchard, C., Chamberland, E., Fortin, A., Lamirande, P., Ogden, N.H., Leighton, P.A., 2021. Mechanistic movement models reveal ecological drivers of tick-borne pathogen spread. J. R. Soc. Interface. 18, 20210134. https://doi.org/10.1098/rsif.2021.0134

Turner, W.C., Kamath, P.L., Van Heerden, H., Huang, Y.H., Barandongo, Z.R., Bruce, S.A., Kausrud, K., 2021. The roles of environmental variation and parasite survival in virulence-transmission relationships. Royal Society Open Science 8. https://doi.org/10.1098/rsos.210088

Ullmann, W., Fischer, C., Kramer-Schadt, S., Pirhofer-Walzl, K., Glemnitz, M., Blaum, N., 2020. How do agricultural practices affect the movement behaviour of European brown hares (*Lepus europaeus*)? Agriculture, Ecosystems & Environment 292, 106819. https://doi.org/10.1016/j.agee.2020.106819

Ullmann, W., Fischer, C., Pirhofer-Walzl, K., Kramer-Schadt, S., Blaum, N., 2018. Spatiotemporal variability in resources affects herbivore home range formation in structurally contrasting and unpredictable agricultural landscapes. Landscape Ecol 33, 1505–1517. https://doi.org/10.1007/s10980-018-0676-2

VanderWaal, K., Gilbertson, M., Okanga, S., Allan, B.F., Craft, M.E., 2017. Seasonality and pathogen transmission in pastoral cattle contact networks. R. Soc. open sci. 4, 170808. https://doi.org/10.1098/rsos.170808

Vetter, S.G., Puskas, Z., Bieber, C., Ruf, T., 2020. How climate change and wildlife management affect population structure in wild boars. Sci Rep 10, 7298. https://doi.org/10.1038/s41598-020-64216-9

Visser, M.E., Gienapp, P., 2019. Evolutionary and demographic consequences of phenological mismatches. Nat Ecol Evol 3, 879–885. https://doi.org/10.1038/s41559-019-0880-8

Visser, M.E., te Marvelde, L., Lof, M.E., 2012. Adaptive phenological mismatches of birds and their food in a warming world. J Ornithol 153, 75–84. https://doi.org/10.1007/s10336-011-0770-6

Walker, S.F., Bosch, J., James, T.Y., Litvintseva, A.P., Oliver Valls, J.A., Piña, S., García, G., Rosa, G.A., Cunningham, A.A., Hole, S., Griffiths, R., Fisher, M.C., 2008. Invasive pathogens threaten species recovery programs. Current Biology 18, R853–R854. https://doi.org/10.1016/j.cub.2008.07.033

Webb, S.D., Keeling, M.J., Boots, M., 2007. Host-parasite interactions between the local and the mean-field: how and when does spatial population structure matter? Journal of theoretical biology 249, 140–152. https://doi.org/10.1016/j.jtbi.2007.06.013

White, L.A., Forester, J.D., Craft, M.E., 2018. Disease outbreak thresholds emerge from interactions between movement behavior, landscape structure, and epidemiology. Proc Natl Acad Sci USA 115, 7374–7379. https://doi.org/10.1073/pnas.1801383115

Wichmann, M.C., Johst, K., Moloney, K.A., Wissel, C., Jeltsch, F., 2003. Extinction risk in periodically fluctuating environments. Ecological Modelling 167, 221–231. https://doi.org/10.1016/S0304-3800(03)00136-4

Wilber, M.Q., Yang, A., Boughton, R., Manlove, K.R., Miller, R.S., Pepin, K.M., Wittemyer, G., 2022. A model for leveraging animal movement to understand spatio-temporal disease dynamics. Ecology Letters ele.13986. https://doi.org/10.1111/ele.13986

Zurell, D., Berger, U., Cabral, J.S., Jeltsch, F., Meynard, C.N., Münkemüller, T., Nehrbass, N., Pagel, J., Reineking, B., Schröder, B., Grimm, V., 2010. The virtual ecologist approach: simulating data and observers. Oikos 119, 622–635. https://doi.org/10.1111/j.1600-0706.2009.182

Acknowledgements

First, I want to thank my supervisor Stephanie Kramer-Schadt for her amazing support, all the helpful discussions, giving inspiring feedback and always having an open door or "zoom-link" to listen to problems. I also want to thank my co-supervisors, Niels Blaum and Volker Grimm, for their support on the concepts and designs of my project and the invaluable feedback and great scientific advice during the writing of the manuscripts. I am thankful to all my co-authors for helping to realize all my projects and all the extra help during my PhD.

Special thanks to Florian Jeltsch for establishing the research training group, introducing me to BioMove and giving us the opportunity to work with a diverse group of scientists with various specializations. Further, I am grateful for the DFG for funding the BioMove research training group (DFG-GRK 2118/1) which allowed me not only to fulfill my research but also to participate in conferences and summer schools. I also would like to thank all my fellow BioMovers, I really enjoyed vivid discussions with every one of you during BioMove seminars, workshops, or retreats. I am grateful to all my lab colleagues who have supported me throughout my PhD and all the relaxing strolls through the Tierpark to get lunch. Very special thanks go to Aimara Planillo for always being there, no matter if I needed help with R, writing manuscripts or just a hug. I also like to thank all my other colleagues from the Leibniz Institute for Zoo and Wildlife Research for all the lively discussion about work or life.

Heartfelt thanks also go to all my family and friends apart from work for supporting and distracting me continuously throughout my PhD, I couldn't have done it without you.

APPENDIX A
SUPPLEMENTARY MATERIAL FOR CHAPTER 2

A1 Model description (ODD protocol)

The classical swine fever (CSF) wild boar model is a combination of a spatially explicit, stochastic, agent-based model for wild boars (*Sus scrofa* L.) and an epidemiological model for the CSF virus. The model was implemented in NetLogo (Wilensky, 1999) and is documented following the ODD protocol (Grimm et al., 2006, 2010, 2020).

The ODD protocol below includes changes in model description across two wild boar / CSF eco-epidemiological models. The first model SwiFCoIBMove (M1 and black text throughout, Scherer et al. 2020) was developed to assess the effects of host movement and landscape structure on disease dynamics and the one described here, SwiFCoIBM_dynamic (M2 and blue text throughout) was developed to assess the role of a dynamic resource landscape and temporal mismatches on disease dynamics. As a note, while in some instance (as seen for example in 1. Purpose) parts of the original model are replaced, in other instances and submodels (as seen in 4 – *Emergence*) M2 is a mixture of old and new versions.

1 Purpose

[1]M1: The model aims to assess the role of host movement based on individual movement decisions (imposed, i.e. a correlated random walk, or based on external factors such as habitat and conspecifics) and landscape structure in driving on-going disease dynamics as pathogen persistence and patterns of spread. Specifically, the question will be addressed to what degree a high-resolution representation of the interaction between moving vectors and landscape features is required to capture spatio-temporal disease dynamics in a predictive way.

M2: The model aims to assess the role of a dynamic resource landscape and temporal shifts in resources on disease dynamics as pathogen persistence and patterns of spread through individual movement. Specifically, how seasonal resource availability and the decoupling of resource availability and reproduction alter disease dynamics.

2 Entities, state variables and scales

The model entities are spatial units, or grid cells, and wild boars. Grid cells are characterized by habitat quality in terms of breeding capacity, i.e. the number of female boars that are allowed to have offspring (Jedrzejewska et al., 1997). Thereby, local host density is in the model, i.e. increasing numbers of fertile

[1]This ODD describes M2, so that 'Purpose' for M1 is obsolete. It is kept in the ODD to better understand how the design of the model developed

females can breed only until breeding capacity is reached. A grid cell represents about 2 km × 2 km, encompassing an average home range area of a boar group (Leaperet al., 1999).

Wild boars are characterized by sex, age in weeks, location, demographic status (e.g. breeding, dispersing and ranging) and health status. Three age classes are distinguished: piglet (< 34 weeks), subadult (between 34 weeks and < 1 year for females and < 2 years for males) and adult. Location is defined by the grid cell the wild boar inhabits. The health status of the individuals is described by an SIR epidemiological classification (susceptible; transiently infected; lethally infected with individual infectious period; immune by surviving the infection or by maternal antibodies). Females, which are at least subadult, may be assigned as breeders according to the breeding capacity of their family group's cell. Subadult wild boars may disperse during the dispersal period dependent on their sex and demographic status (disperser or non-disperser). In the model versions simulating explicit movement, males become ranging individuals (i.e. move solely) once they are adult and thereby change their locations every time step.

M1 & M2: One time step corresponds to the approximate CSF incubation time of one week (Artois et al., 2002; Moennig et al., 2003) while simulations usually run for 12 years (624 weeks) or 50 years (2600 weeks) with the virus being released in the second year (week 53–104) to a defined boar group to ensure the same distance to the model borders and an established spatial population structure. The model landscape consists of 100 km × 50 km (50 × 25 grid cells).

3 Process overview and scheduling

[1]M1: Each time step, the following procedures are executed by the wild boars in the given order: pathogen transmission, ranging movement, natal dispersal of males and females, respectively, reproduction, mortality, ageing, and disease course (Figure A1)

In the first week of each year, females are assigned to breed. Natal dispersal of males and females was limited to week 17 and week 29 of the year, respectively.

M2: Each time step, the following procedures are executed by the wild boars in the given order: pathogen transmission, ranging movement, natal dispersal of males and females, resource-based host movement, host reproduction, general host mortality, resource-based host mortality, ageing, and disease course (Figure A1.1).

[1] This ODD describes M2, so that 'Process overview and scheduling' for M1 is obsolete. It is kept in the ODD to better understand how the design of the model developed

M2: Females are assigned to breed on a week to week basis, with the prerequisite that they have not bred previously in the current year.

4 Design concepts

Basic principles

M1 & M2: Both processes of the host and the pathogen are simulated with a given stochasticity which resembles natural conditions. Disease transmission for groups is modelled density-dependent (see Eq. A1 and A2). Heterogeneous landscape scenarios were simulated using neutral landscape model algorithms.

Emergence

M1 & M2: Wild boar population dynamics emerge from individual behaviour, resulting from age- and sex-dependent movement behaviours (natal dispersal and ranging) as well as age-dependent seasonal reproduction, survival probabilities and is shaped by the underlying dynamic resource landscape. The epidemic course emerges from different virus transmission probabilities, wild boar movement behaviours as well as individual stochastic disease courses and infectious periods.

Adaptation

M1 & M2: Movement rules either reproduce observed movement behaviours (phenomenological approach, e.g. correlated random walk with a given directional persistence) or are based on decisions in response to spatial structure or conspecifics (mechanistic approach, e.g. the competition-driven movement rule implicitly seeks to increase habitat quality in relation to conspecifics). The number of breeding females per cell is determined by (a) the habitat quality of the cell and (b) the number and age of the reproductive females within the cell.

Objectives

M1 & M2: The exact way individuals decide where to move depend on the applied movement rule (see section "Ranging movement"). In general, ranging individuals (i.e. adult males) using decision-based movement rules move into the neighbouring cell with the highest weight (which is defined by the applied movement rule). Individuals' decisions are not perfect but may be a random direction depending on the directional persistence ρ (probability to move randomly = 1 - ρ, set to 0.7).

Dispersing individuals search for empty (unoccupied) cells (in case of female dispersers) or join other groups that are below their cells' carrying capacity (in case of male dispersers).

Learning

M1 & M2: There is no learning implemented in our model.

Prediction

M1 & M2: There is no need to predict future environmental conditions.

Sensing

M1 & M2: Individuals moving through the landscape may base their decisions on the underlying landscape structure in terms of habitat quality (or, synonymously, breeding capacity B) or number of conspecifics. Moving individuals can sense all that information from their own cell and surrounding cells but the decision might be random (implicitly due to insufficient information) depending on the assumed directional persistence ρ.

Interaction

M1 & M2: Based on the transmission rates, interactions between individuals might lead to virus transmission from an infected to a susceptible individual. Reproduction is density-and age-dependent with the oldest females giving birth first. Thus, if the number of reproducible females exceeds a cell's breeding capacity, interaction leads to repressed reproduction.

Stochasticity

M1 & M2: Demographic and behavioural parameters are imposed via probability distributions to account for variation in the biological processes. Stochastic individual disease courses and infectious periods are modelled explicitly because variation in the disease outcome between individuals was identified to be essential for virus endemicity without reservoirs (Kramer-Schadt et al., 2009). Movement decisions are based on a random component (with 30% of the decisions being random).

Collectives

M1 & M2: Individuals that are not ranging between home ranges (i.e. all individuals but adult males) form groups within their cell that experience density-dependent transmission probabilities. These groups are formed by reproducible females and their offspring. During natal dispersal, male subadults may join those groups while female subadults may form new groups.

Observation

M1 & M2: To evaluate model outcomes, we measure several properties of the host-virus system at each time step of the simulation. These outputs include number of individuals for each class of age (piglet, subadult, adult), demographic (resident, ranging) and health status (susceptible, infected, recovered) and their combinations. Furthermore, sex ratio, number of new infections (transient and lethal), number of cells with infectious individuals, the last week of infection and the cumulative time (i.e. how many weeks in total) of infected hosts per habitat cell are recorded. From this output, duration of an outbreak, probability of disease persistence (i.e. the virus being present in the system until the end of simulations), outbreak size for different classes, as well as density distribution of infected hosts can be estimated.

5 Initialization

M1 & M2: We simulate landscapes with four different levels of spatial heterogeneity in habitat quality: homogeneous (only M1), random, and two or four clustered landscape scenarios using an random cluster algorithm (very small, small, medium and large clusters, respectively; Saura & Martínez-Millán, 2000; Table A1) generated using the R package NLMR (Sciaini et al., 2018). In homogeneous landscapes, one boar family group was allocated to each cell with an average breeding capacity B of 4.5 females, resulting in the reported density of approximately 20 boars per cell or 5 boars per km² (European Food Safety Authority, 2009; Howells & Edwards-Jones, 1997; Melis et al., 2006; Sodeikat & Pohlmeyer, 2003). In heterogeneous landscapes a breeding capacity B between 0 and 9 was assigned to each of the 2500 grid cells ($B \in \{0;9\}$). In case B is a floating point number, the number of individuals is determined stochastically based on the remainder. Initial age distribution was obtained from the results of a 100-year model run conducted by (Kramer-Schadt et al., 2009); Table A2), the sex ratio was balanced (i.e. probability of 0.5 to be either male or female). Wild boar density reflects long-term average values of densely populated Central European habitats (European Food Safety Authority, 2009; Howells & Edwards-Jones, 1997; Melis et al., 2006; Sodeikat & Pohlmeyer, 2003). Group size was initialised according to the cells carrying capacity K_i that is 4.5 times its breeding capacity B_i.

6 Input

M1 & M2: The model does not include external input.

7 Submodels

Initial infection (pathogen release)

M1 & M2: The virus is released to the population by infection of one wild boar group (i.e. cell) in middle of the upper row of home ranges (i.e. cell with the coordinates x = 1 and y = 13) to allow for comparison between runs. The release is scheduled in a random week of the second year of the model run.

Pathogen transmission

M1 & M2: Virus transmission is modelled stochastically. The transmission parameter determines the weekly probability of being infected by an infectious group mate β_w.

In the model without movement (afterwards referred to as the "classical model"), weekly infection pressure λ_i for each susceptible individual in cell i is determined by the probability of being infected by an infectious group mate β_w (within-group transmission probability) and the probability of being infected by an infectious individual in one of the eight neighbouring cells β_e (between-group transmission probability):

$$\lambda_i = 1 - (1 - \beta_w)^{I_i} \cdot (1 - \beta_e)^{\Sigma_i I_j} \quad [A1]$$

where I_i is the number of infectious group mates and I_j is the numbers of infectious hosts in the j^{th} adjacent cell. The resulting probability value λ_i provides the parameter of a binomial chance process to decide whether a susceptible animal will be infected.

The transmission parameters β_w (and thereby β_e since it was fixed as one tenth of β_w) was calibrated in order to reproduce the spreading velocity observed in France (Rossi et al., 2010) with the constant parameter value β_w = 0.0208 within and, hence, β_e = 0.00208 between groups (Kramer-Schadt et al., 2009).

In the model version involving explicit movements presented here, infection might be translocated within the host population. Because ranging movements are performed by adult males only, the homogeneous transmission probability λ_i was transformed to account for these sex-and age-dependent transmission probabilities. Therefore, for all individuals but adult males the weekly probability of being infected by infectious group mates (but not by infectious ranging males) is simply β_w since females and their group follow a staying rule with the almost all contacts within the group (Pepin et al., 2016; Spitz & Janeau, 1990). The accumulated probability λ_i for susceptible non-ranging individuals is thus reduced to:

$$\lambda_i = 1 - (1 - \beta_w)^{I_i} \quad [A2]$$

where is the number of infectious group mates (but not infectious ranging males which do not belong to any group). For adult, ranging males, the individual probability of virus transmission during movements β_m (i.e. being infected by an infectious animal in a cell moving through as well as the probability of infecting a susceptible individual while passing the cell) was fitted to account for the resuming transmission probabilities (i.e. the remaining within- and between-group transmission probabilities of the classical model, see Eq. A2). We calibrated one constant transmission probability (i.e. $\beta_w = \beta_m$, afterwards just referred to as simply β) to result in the comparable distributions of the basic reproduction number (R_0, number of secondary infections) as in the classical model. Using a Kolmogorov-Smirnov test, the constant parameter value β = 0.022 gave the best results for different scenarios of infection and movement rules (Scherer et. al., 2020). Individual per step transmission probability $\beta_{m,i}$ is related to the number of steps the animal makes. Therefore, the infection probability for cells passed by infected individuals is scaled to the individual movement distance $d_{m,i}$ (see section "Ranging movement"):

$$\beta_{m,i} = \frac{\beta}{d_{m,i}}. \qquad [A3]$$

By doing so, infection probability decreases with increasing movement distance which relates to the time an animal is able to spend within each cell and thus to transmit the virus on its way.

CSF shows a variety of disease courses on the individual level (Depner et al., 1997; Liess, 1987). Therefore, in our model the disease course is stochastically specified for each individual. The disease course submodel is described by two parameters: individual case mortality M and the mean infectious period of lethally infected hosts μ. Upon infection the host is stochastically assigned either as lethally infected (with probability M) or as transiently infected (1 - M). M is age-specific (Dahle & Liess 1992): for adults the probability is decreased to $M_a = M^2$ and for piglets increased to $M_p = \sqrt{M}$ while it is unchanged for subadults $M_s = M$. Transiently infected wild boars first pass through an infectious period of one week and subsequently becomes non-infectious and gain life-long immunity (Artois et al. 2002; Moennig et al. 2003; European Food Safety Authority, 2009). The individual infectious period (m_i in weeks) of lethally infected hosts is drawn from an exponential distribution with the mean specified by parameter μ:

$$m_i = 1 + floor(-(\mu - 0.5) \cdot ln(U(0,1))) \qquad [A4]$$

where $U(0,1)$ is a uniformly distributed random number between 0 and 1. To avoid unrealistically long infections, m_i was stochastically assigned until $m_i \leq 10 \times \mu$. Lethally infected hosts remain infectious until death. Offspring from immune female breeders gets maternal antibodies and is thus immune for

the first eight to twelve weeks after birth (t_{anti}). The number of weeks of immunisation due to maternal antibodies is randomly assigned for those piglets.

Ranging movement

M1 & M2: While adult females move mainly within their family group (*staying strategy*), adult males follow a *ranging strategy* and move solitary (Spitz & Janeau 1990, Figure A2). Ranging distances vary between males with a mean distance of 24 km per week and rare long-distance behaviour with up to 84 km per week (Morelle et al. 2015). For each adult male i, an individual movement distance $d_{m,i}$ was drawn from the median of the Weibull distribution given by $b*(1 - ln(1 - U[0,1]))^k$ with a scale of b = 26 and a shape of k = 1.3, resulting in a mean of 12 cells and truncated to the maximum movement distance D_{max} of 42 cells (with a cell being 2 km in diameter). To study effects of inter-cell movement on disease dynamics, Scherer et al., (2020) implemented three different movement strategies. In general, ranging individuals move until the individual weekly movement distance is reached or there is no better decision to make and only into cells with a positive habitat quality ($B > 0$). Individuals stop moving if there is no cell available. If there is a tie (i.e. two or more cells with equal attractiveness), one of those cells is chosen randomly.

M1 & M2: *(a) Correlated Random Walk (CRW):* In a CRW, subsequent movement directions are correlated such that highly correlated movement paths are nearly straight (Turchin 1998; Figure A3a). This movement model improves the RW approach by incorporating directional persistence that moving animals very frequently exhibit (Figure A3; Kareiva & Shigesada 1983). The direction of a step is drawn from a wrapped Cauchy distribution with a mean direction equal to the previous direction (Fletcher 2006):

$$\theta_{t,i} = \theta_{t-1,i} + 2 \cdot arctan\left(\frac{1-\rho}{1+\rho} \cdot \pi \cdot U(-0.5,0.5)\right) \quad [A5]$$

Where $\theta_{t,i}$ and $\theta_{t-1,i}$ are the headings of individual i of the next or previous step, respectively, ρ is a parameter related to the concentration around the mean direction (i.e. ρ = 1 results in a straight line and ρ = 0 equals a RW), and U(-0.5,0.5) is a uniformly distributed random number between -0.5 and 0.5. In case individuals reach the border of the simulated landscape, the Individual is reflected in a 90° angle followed by reset and recalculation of $\theta_{t,I}$ to avoid aggregation around the landscape borders.

M1 & M2: *(b) Habitat-Dependent Movement (HDM):* A reasonable hypothesis is that a selective animal should choose high quality cells for its home range. The distribution and abundance of resources greatly affect movement patterns of several animal species and has also been reported for wild boars (Morelle

et al. 2015). Assuming higher food resources and better shelter in high quality habitat, individuals decide among their neighbouring cells based on the habitat quality (Figure A3b). The parameter ρ here relates to the accuracy of an individual estimating the quality of the focal and neighbouring cells, with the movement decision in ρ-1 cases being purely random.

[1]M1: *(c) Competition-Driven Movement (CDM):* Effective habitat quality might be lower due to competition with conspecifics. Thus, competition-driven movement is biased to cells with higher net habitat quality and was implemented as negative density dependence. Movement weights were calculated as the ratio of number of conspecifics in the focal cell and the carrying capacity (*K*), i.e. the potential maximum group size of the cell (Figure A3c).

For all movement strategies, ρ was fixed as 0.7, i.e. 30% of the decisions were made randomly.

Natal dispersal

M1 & M2: Herd splitting, where subadult individuals may move together to search for or form new groups, is performed in specified weeks of the. The timing of these events is sex-dependent: Subadult females without offspring perform their natal dispersal in the 29th week of the year, while subadult males disperse during the 17th week. In the given week of the year, all herds to split are extracted, matching the conditions of containing at least a specified number of subadults N_{disp} to move (either male or female). For female dispersal, only cells exceeding the breeding capacity *B* are evaluated. For each of them, a habitat cell not exceeding carrying capacity *K* (for males) or without any family group (for females) within a Euclidean distance d_{disp} is selected randomly as new cell for the group, excluding the source cell (Figure A2). If there is no cell fulfilling these conditions, subadults stay within their group's cell.

Reproduction

M1 & M2: Females reproduce once a year, depending on their age class. Individual females, which are at least subadult, reproduce depending on the season with a peak in March and no reproduction in winter from October to December (Boitani et al. 1995) (Table A2).

M1 & M2: In the first week of the year, female individuals are checked for their breeding status; female individuals are checked for their breeding status on a weekly basis. All females not exceeding their habitat cells breeding capacity, starting with the oldest individuals, are allowed to breed.

[1] This ODD describes M2, so that 'Competition-Driven Movement (CDM)' for M1 is obsolete. It is kept in the ODD to better understand how the design of the model developed

M1: The week of the year to breed is assigned in the first week of each year according to weekly reproduction probabilities, derived from monthly probabilities and the number of weeks in the month (Table A2).

M2: If an individual was assigned to breed the chance of reproduction at that time is drawn from monthly probabilities and the number of weeks in the month (Table A2).

M1 & M2: Litter size is drawn from a pre-calculated truncated normal distribution (Table A1,3) and reduced to a constant fraction for infected individuals. Litter size of transient shedders and lethally infected hosts is multiplied with the reduction factor α_f.

M1 & M2: Depending on the disease state of the breeding individual, its piglet's disease states are adjusted. Susceptible individuals produce susceptible offspring, immune individuals produce immune offspring with maternal antibodies (see section "Pathogen state transition"). Transient shedders and lethally infected individuals yield offspring, each one lethally infected with a given probability of prenatal infection p_{pi}.

Mortality

M1 & M2: Stochastic baseline mortality is age-dependent and adjusted to annual survival estimates found in the literature (Table A1). Per time step we apply the adjusted age-dependent mortality (m_{week}) to the individual:

$$m_{week} = 1 - (s_{year})^{1/52}. \quad [A6]$$

In addition to the stochastic baseline mortality, each individual may die due to reaching a certain maximum age, or due to a lethal infection after a certain infection time span m (see section "Pathogen transmission").

M2: A selected number of individuals K_{over} (see 7.10 Resource response for the selection) are subject to a variable, resource-based mortality with an increasing chance of mortality dependent on how long the individual is subject to low resource conditions up to a variable time limit S_{max} as well as the number of individuals (g_{act}) in relation to maximum group (g_{sus}) size and age a.

$$m_{resource} = \frac{(g_{act} - g_{sus})}{100} * a * t_{over} \quad [A7]$$

With a being an age factor corresponding to the individuals being a piglet or adult/subadult and t_{over} the time the individual is part of the K_{over} individual pool. As well as a 100% mortality when t_{over} equals S_{max}.

Ageing

M1 & M2: The ageing process iterates over all individuals. For each individual k, age T_k is incremented one week, and disease state transitions are performed. Females become subadult and adult at an age of 34 and 52 weeks, respectively, while males enter the subadult and adult age groups at an age of 21 and 104 week, respectively.

Disease course (pathogen state transition)

M1 & M2: Transient shedders convert to immune after a certain latency period t_{latent}. An individual i protected by maternal antibodies turns susceptible if reaching an age T_i of the protection time of t_{anti} (see section "Pathogen transmission"). After disease state transition the age of the infection is incremented by one week if the individual is not susceptible.

Landscape dynamic

M2: The autocorrelated landscape dynamic is superimposed over the different types of heterogeneous starting landscapes. Throughout each simulated year, resource availability in each cell increases in 5-weeks intervals for approximately 25 weeks and then declines in 5-weeks intervals for the next 25 weeks. The resource availability translates directly into the breeding capacity for each cell and for each increase or decrease the value of the breeding capacity is changed by one. During the increase, the breeding capacity cannot exceed the maximum breeding capacity of 9 and cannot fall below 1 during the decrease i.e. the breeding capacity in a cell designated as habitat cannot become 0 during the course of a year. Additionally, barriers and matrix which have an assigned breeding capacity of 0 cannot become habitat i.e. matrix/barrier cells will always have a breeding capacity of 0. The default landscape dynamic is implemented to follow the host individual's monthly reproduction probabilities (see table A2), where the peak reproduction probability matches in time with the peak resource availability. Furthermore, the landscape dynamic can be temporally shifted away from the peak host reproduction probability in 25% increments (0% – match, 25% mismatch, 50% mismatch, 75% mismatch, 100% – full mismatch). In this case, a full mismatch would mean that the resource availability is at its lowest when the host reproduction probability is at its highest.

The random landscape dynamic functions similar to the autocorrelated variant without a temporal shift. Throughout each simulated year, resource availability in each cell changes randomly in 5-weeks intervals for approximately 50 weeks whereby each cell is allocated a random integer between 1 and 9. At the end of each year, the landscape resets to the original starting landscape.

Resource responses

M2: If the group size exceeds the carrying capacity K in a cell, a dispersal event will be triggered. The likelihood of dispersal follows an age gradient where older females will try to disperse last. For male individuals, a random habitat cell not exceeding the carrying capacity K will be randomly selected within a Euclidean distance d_{disp} as new cell. For female individuals, the randomly selected habitat cell must fulfil the prerequisite of not hosting another family group. However, if an individual currently has offspring it and the offspring will stay at in their current cell. If there is no suitable habitat cell fulfilling these prerequisites within the distance d_{disp} the individuals will stay. Individuals are continuously selected for dispersal until the group size no longer exceeds the carrying capacity K or no more suitable habitat within the distance d_{disp} can be found. For a secondary response after the dispersal event (if applicable), a cell specific number of individuals K_{over} that is the difference between carrying capacity K and group size will be selected. The selection of these individuals is age dependant where the oldest females are selected last. All selected individuals are subjected to an increasing age-dependant mortality (see mortality).

Figures

Flow chart of the SwiFCoIBMove model and its submodels

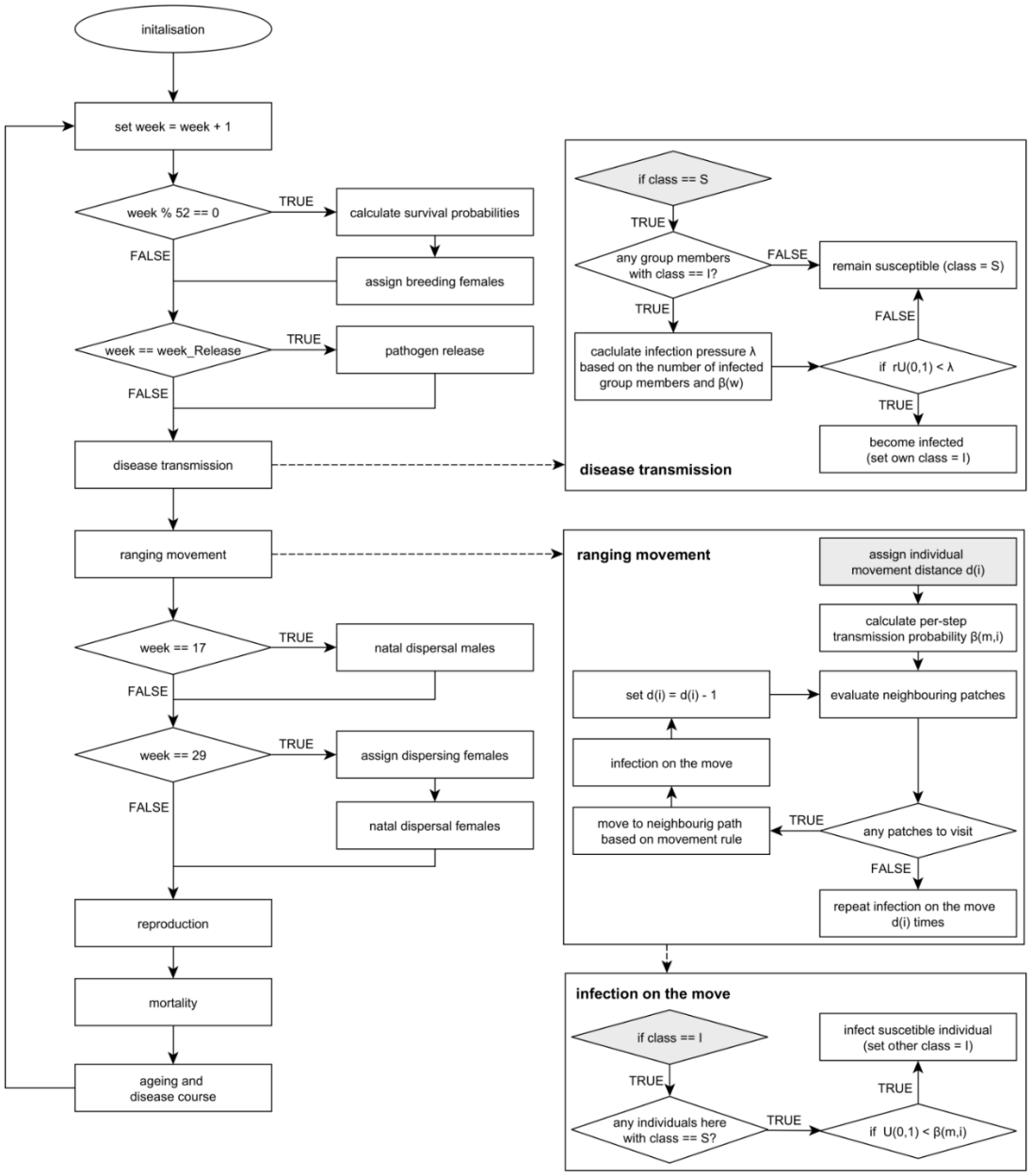

Figure A1: Flow chart of the agent-based, spatially explicit host-pathogen model "SwiFCoIBMove" and its submodels.

Flow chart of the SwiFCoIBM_dynamic model

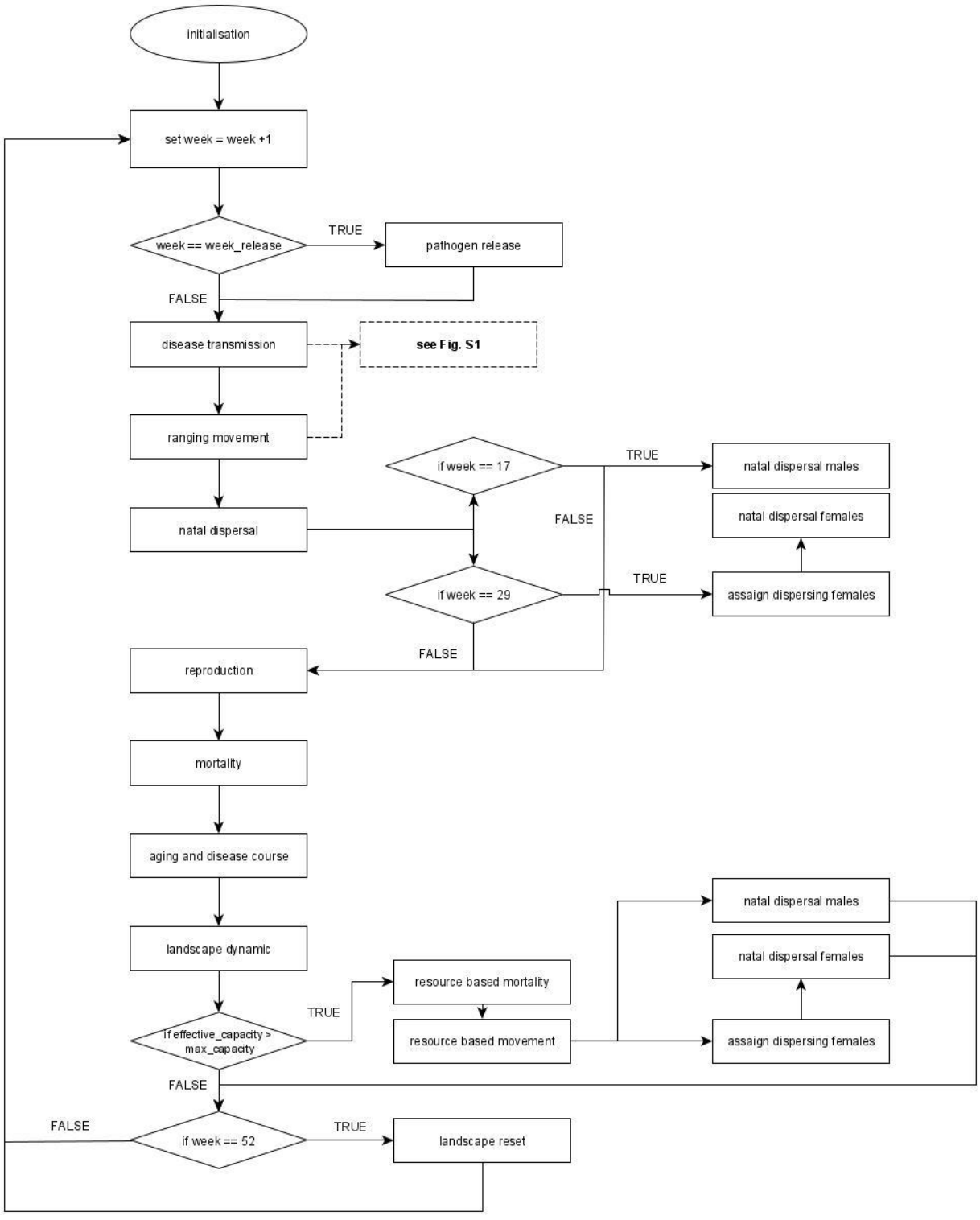

Figure A1.1: Flow chart of the agent-based, spatially explicit host-pathogen model "SwiFCoIB_dynamic"

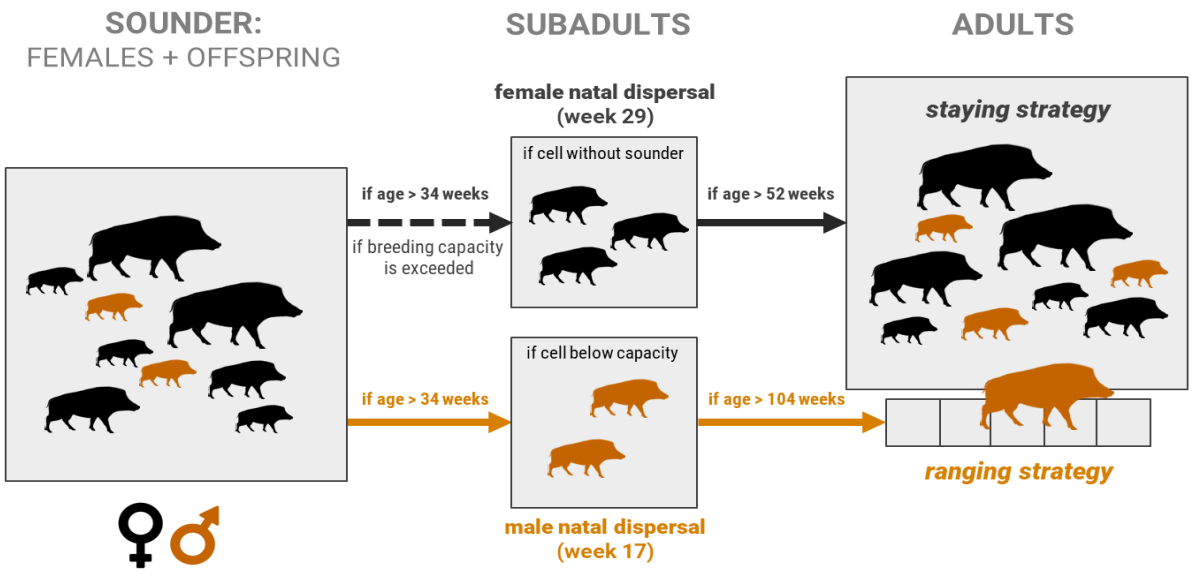

Figure A2: Schematic representation of different natal dispersal events of subadult wild boars and movement strategies of adult wild boars. The group of adult and subadult females and their offspring is called a sounder. If the breeding capacity of the sounders cell is exceeded, subadult females search in groups of 3 or more individuals for an unoccupied cell in a radius of three cells. Female wild boars reach their adulthood earlier (model assumption: if older than 1 year) and follow a staying strategy, thus not moving outside of the sounders cell (grey squares). Male wild boars always separate from the sounder when reaching the subadult age and move in groups of 2 or more to one of the cells below capacity in a radius of 3 cells. When becoming adult, male wild boars move solitary between home ranges.

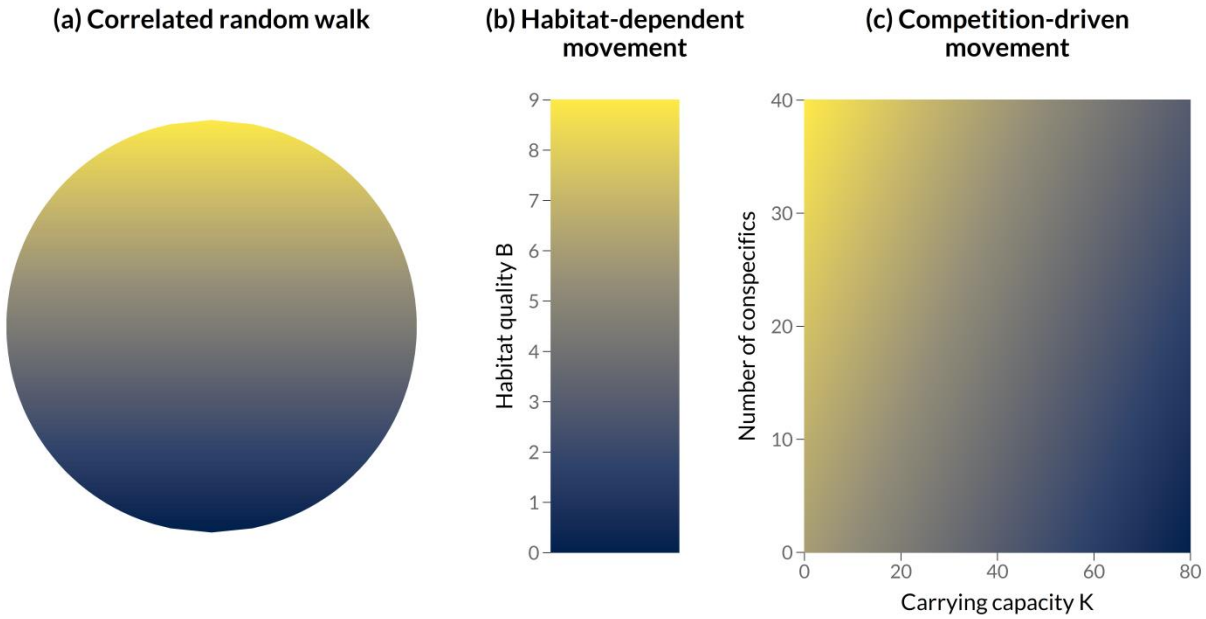

Figure A3: Movement assumptions used to model ranging behaviour of adult males. Probability of movement depends on the **(a)** direction of previous steps (Correlated Random Walk), **(b)** habitat quality B or **(c)** carrying capacity K in relation to the number of conspecifics. The lighter the colour, the higher the probability the individual chooses this cell. Movement decisions are furthermore driven by a random component determined by ρ.

Table A1: Parameter setup used in the spatially-explicit classical swine fever-wild boar model. M1: Each of the 60 combinations (3 movement strategies × 4 landscape scenarios × 5 case fatality ratios) was repeated 200 times while generating new underlying landscapes depending on the scenario input, resulting in 12.000 runs in total. M2: Each of the 300 combinations (3 movement strategies 3 × landscape dynamic × 4 landscape scenarios × 5 max survival time under low resources × 5 level of resource mismatch) was repeated 25 times, resulting in 22.500 runs in total.

Parameter	Values	Reference(s)
Longevity	11 years (572 weeks)	(Jezierski, 1977)
Sex ratio	1:1	(e.g. Durio et al., 2014; Fernández-Llario et al., 1999; Moretti, 2014)
Survival probability of adults and subadults	s_{mean}= 0.6; s_{min} = 0.4	(Focardi et al., 1996; Gaillard et al., 1987)
Survival probability of piglets	s_{mean}= 0.5; s_{min} = 0.1	(Focardi et al., 1996)
Reproduction probability	see Table A2	(Boitani et al., 1995)
Breed count distribution	see Table A3	(Bieber & Ruf, 2005)
Movement rule	CRW M1,M2; HDM M1,M2; CDM M1	(Fletcher, 2006)
Tendency to move randomly ρ	0.3	
Mean movement distance D_{mean}	24 km (12 cells) per week	(Morelle et al., 2015)
Maximum movement distance D_{max}	84 km (42 cells) per week	(Morelle et al., 2015)
Individual weekly ranging distance $D_{m,i}$	D_i {1, D_{max}} ~ Wei(26, 1.3)	
Maximal natal dispersal distance d_{disp}	3 cells (6 km)	(Sodeikat & Pohlmeyer, 2003)
Minimum number of dispersers N_{disp}	2 for females; 3 for males	
Case fatality ratio M	{0, 0.25, 0.5, 0.75, 1} 0.5	
Mean infectious period μ	4 weeks 6 weeks	
Transmission probability β	0.022	
Fertility reduction due to infection	0.625	(Kramer-Schadt et al., 2009)
Probability of prenatal infection	0.5	(Kramer-Schadt et al., 2009)
Transient period t_{trans}	1 week	(Artois et al., 2002; Moennig et al., 2003)
Period of maternal antibodies t_{anti}	12 weeks	(Depner et al., 2000)
Simulated years	12 (624 weeks) 50 (260 weeks)	

*Continued on the next page

Table A1: Parameter setup – continuation

Parameter	Values	Reference(s)
Pathogen release	random week of the 2nd year	
Mean number of reproductive females	4.5	(European Food Safety Authority, 2009; Howells & Edwards-Jones, 1997; Sodeikat & Pohlmeyer, 2003)
Habitat quality range	[0, 9]	
Initial mean density	5 individuals/km²	(Kramer-Schadt et al., 2009)
Initial age distribution	see Table A4	(Kramer-Schadt et al., 2009)
Age blur in initial individuals	± 3 weeks	
Landscape dynamic	Autocorrelated, Random No dynamic	
Max survival time under low resources S_{max}	{5,10,15,20,25} weeks	
Level of resource mismatch	{0,25,50,75,100} %	

Table A2: Monthly reproduction probabilities (Boitani et al., 1995) used to stochastically determine the number of breeding females.

Month	Jan	Feb	Mar	Apr	May	Jun	Jul	Aug	Sep	Oct	Nov	Dec
Number of weeks	4	4	5	4	4	5	4	4	5	5	4	4
Reproduction probability	0.0	0.1	0.23	0.34	0.07	0.08	0.06	0.03	0.03	0.0	0.0	0.0

Table A3: Breed count distribution (Bieber & Ruf, 2005) used to estimate litter sizes.

Litter size	0	1	2	3	4	5	6	7	8	9	10	0
Probability	.01306	.06915	.01629	.24994	.24994	.01629	.06915	.01910	.00343	.0004	.00002	.01306

Table A4: Initial age distribution (Kramer-Schadt et al., 2009) used to initialize each model run.

Age (years)	1	2	3	4	5	6	7	8	9	10
Proportion	0.38	0.24	0.15	0.09	0.06	0.03	0.02	0.01	0.01	0.01

References

Artois, M., Depner, K.R., Guberti, V., Hars, J., Rossi, S., Rutili, D., 2002. Classical swine fever (hog cholera) in wild boar in Europe. Rev. Sci. Tech. OIE 21, 287–303. https://doi.org/10.20506/rst.21.2.1332

Bieber, C., Ruf, T., 2005. Population dynamics in wild boar *Sus scrofa* : ecology, elasticity of growth rate and implications for the management of pulsed resource consumers: *Population dynamics in wild boar*. Journal of Applied Ecology 42, 1203–1213. https://doi.org/10.1111/j.1365-2664.2005.01094.x

Boitani, L., Mattei, L., Nonis, D., Corsi, F., 1994. Spatial and Activity Patterns of Wild Boars in Tuscany, Italy. Journal of Mammalogy 75, 600–612. https://doi.org/10.2307/1382507

Depner, K.R., Hinrichs, U., Bickhardt, K., Greiser-Wilke, I., Pohlenz, J., Moennig, V., Liess, B., 1997. Influence of breed-related factors on the course of classical swine fever virus infection. Veterinary Record 140, 506–507. https://doi.org/10.1136/vr.140.19.506

Depner, K.R., Müller, T., Lange, E., Staubach, C., Teuffert, J., 2000. Transient classical swine fever virus infection in wild boar piglets partially protected by maternal antibodies. Dtsch Tierarztl Wochenschr 107, 66–68.

Durio, P., Gallo Orsi, U., Macchi, E., & Perrone, A. (2014). Structure and monthly birth distribution of a wild boar population living in mountainous environment. Journal of Mountain Ecology, 3(0). Retrieved from http://www.mountainecology.org/index.php/me/article/view/112

EFSA (European Food Safety Authority). (2009). Control and eradication of Classical Swine Fever in wild boar. European Food Safety Authority Journal, 932(EFSA-Q-2007-200), 1–18. Retrieved from https://efsa.onlinelibrary.wiley.com/doi/abs/10.2903/j.efsa.2009.932

Fernández, N., Kramer-Schadt, S., Thulke, H.-H., 2006. Viability and Risk Assessment in Species Restoration: Planning Reintroductions for the Wild Boar, a Potential Disease Reservoir. E&S 11, art6. https://doi.org/10.5751/ES-01560-110106

Fernández-Llario, P., Carranza, J., Mateos-Quesada, P., 1999. Sex allocation in a polygynous mammal with large litters: the wild boar. Animal Behaviour 58, 1079–1084. https://doi.org/10.1006/anbe.1999.1234

Fletcher, R.J., 2006. Emergent properties of conspecific attraction in fragmented landscapes. The American naturalist 168, 207–219. https://doi.org/10.1086/505764

Focardi, S., Toso, S., Pecchioli, E., 1996. The population modelling of fallow deer and wild boar in a Mediterranean ecosystem. Forest Ecology and Management 88, 7–14. https://doi.org/10.1016/S0378-1127(96)03804-2

Gaillard, J. M., Vassant, J., & Klein, F. (1987). Quelques caractéristiques de la dynamique des populations de sangliers (Sus scrofa scrofa) en milieu chassé. Gibier, Faune Sauvage / ONC, Office National de La Chasse, 4, 31–47.

Grimm, V., Berger, U., Bastiansen, F., Eliassen, S., Ginot, V., Giske, J., Goss-Custard, J., Grand, T., Heinz, S.K., Huse, G., Huth, A., Jepsen, J.U., Jørgensen, C., Mooij, W.M., Müller, B., Pe'er, G., Piou, C., Railsback, S.F., Robbins, A.M., Robbins, M.M., Rossmanith, E., Rüger, N., Strand, E., Souissi, S., Stillman, R.A., Vabø, R., Visser, U., DeAngelis, D.L., 2006. A standard protocol for describing individual-based and agent-based models. Ecological Modelling 198, 115–126. https://doi.org/10.1016/j.ecolmodel.2006.04.023

Grimm, V., Berger, U., DeAngelis, D.L., Polhill, J.G., Giske, J., Railsback, S.F., 2010. The ODD protocol: A review and first update. Ecological Modelling 221, 2760–2768. https://doi.org/10.1016/j.ecolmodel.2010.08.019

Grimm, V., Railsback, S.F., Vincenot, C.E., Berger, U., Gallagher, C., DeAngelis, D.L., Edmonds, B., Ge, J., Giske, J., Groeneveld, J., Johnston, A.S.A., Milles, A., Nabe-Nielsen, J., Polhill, J.G., Radchuk, V., Rohwäder, M.-S., Stillman, R.A., Thiele, J.C., Ayllón, D., 2020. The ODD Protocol for Describing Agent-Based and Other Simulation Models: A Second Update to Improve Clarity, Replication, and Structural Realism. JASSS 23, 7. https://doi.org/10.18564/jasss.4259

Howells, O., Edwards-Jones, G., 1997. A feasibility study of reintroducing wild boar Sus scrofa to Scotland: Are existing woodlands large enough to support minimum viable populations. Biological Conservation 81, 77–89. https://doi.org/10.1016/S0006-3207(96)00134-6

Jędrzejewska, B., Jędrzejewski, W., Bunevich, A.N., Miłkowski, L., Krasiński, Z.A., 1997. Factors shaping population densities and increase rates of ungulates in Bialowieza Primeval Forest (Poland and Belarus) in the 19th and 20th centuries. Acta Theriologica.
Jezierski W., 1977: Longevity and mortality rate in a population of wild boar. Acta theriol., 22, 24: 337—348

Kramer-Schadt, S., Fernández, N., Eisinger, D., Grimm, V., Thulke, H.-H., 2009. Individual variations in infectiousness explain long-term disease persistence in wildlife populations. Oikos 118, 199–208. https://doi.org/10.1111/j.1600-0706.2008.16582.x

Leaper, R., Massei, G., Gorman, M.L., Aspinall, R., 1999. The feasibility of reintroducing Wild Boar (Sus scrofa) to Scotland. Mammal Review 29, 239–258. https://doi.org/10.1046/j.1365-2907.1999.2940239.x

Liess, B., 1987. Pathogenesis and epidemiology of hog cholera. Ann Rech Vet 18, 139–145.

Melis, C., Szafranska, P.A., Jedrzejewska, B., Barton, K., 2006. Biogeographical variation in the population density of wild boar (Sus scrofa) in western Eurasia. J Biogeography 33, 803–811. https://doi.org/10.1111/j.1365-2699.2006.01434.x

Moennig, V., Floegel-Niesmann, G., Greiser-Wilke, I., 2003. Clinical signs and epidemiology of classical swine fever: a review of new knowledge. Vet J 165, 11–20. https://doi.org/10.1016/s1090-0233(02)00112-0

Morelle, K., Podgórski, T., Prévot, C., Keuling, O., Lehaire, F., Lejeune, P., 2015. Towards understanding wild boar *S us scrofa* movement: a synthetic movement ecology approach: A review of wild boar *Sus scrofa* movement ecology. Mammal Review 45, 15–29. https://doi.org/10.1111/mam.12028

Moretti, M., 2014. Birth distribution, structure and dynamics of a hunted mountain population of Wild boars (Sus scrofa L.), Ticino, Switzerland. Journal of Mountain Ecology 3.

Pepin, K.M., Davis, A.J., Beasley, J., Boughton, R., Campbell, T., Cooper, S.M., Gaston, W., Hartley, S., Kilgo, J.C., Wisely, S.M., Wyckoff, C., VerCauteren, K.C., 2016. Contact heterogeneities in feral swine: implications for disease management and future research. Ecosphere 7. https://doi.org/10.1002/ecs2.1230

Rossi, S., Pol, F., Forot, B., Masse-provin, N., Rigaux, S., Bronner, A., Le Potier, M.-F., 2010. Preventive vaccination contributes to control classical swine fever in wild boar (*Sus scrofa* sp.). Veterinary Microbiology 142, 99–107. https://doi.org/10.1016/j.vetmic.2009.09.050

Saura, S., Martínez-Millán, J., 2000. Landscape patterns simulation with a modified random clusters method. Landscape Ecology 15, 661–678. https://doi.org/10.1023/A:1008107902848

Sodeikat, G., Pohlmeyer, K., 2003. Escape movements of family groups of wild boar *Sus scrofa* influenced by drive hunts in Lower Saxony, Germany. Wildlife Biology 9, 43–49. https://doi.org/10.2981/wlb.2003.063

Spitz, F., Janeau, G., 1990. Spatial strategies: an attempt to classify daily movements of wild boar. Acta Theriologica 35, 129–149.

Wilensky, U. (1999). NetLogo (Version 6.1.0). Retrieved from http://ccl.northwestern.edu/netlogo/

A2 Additional figures

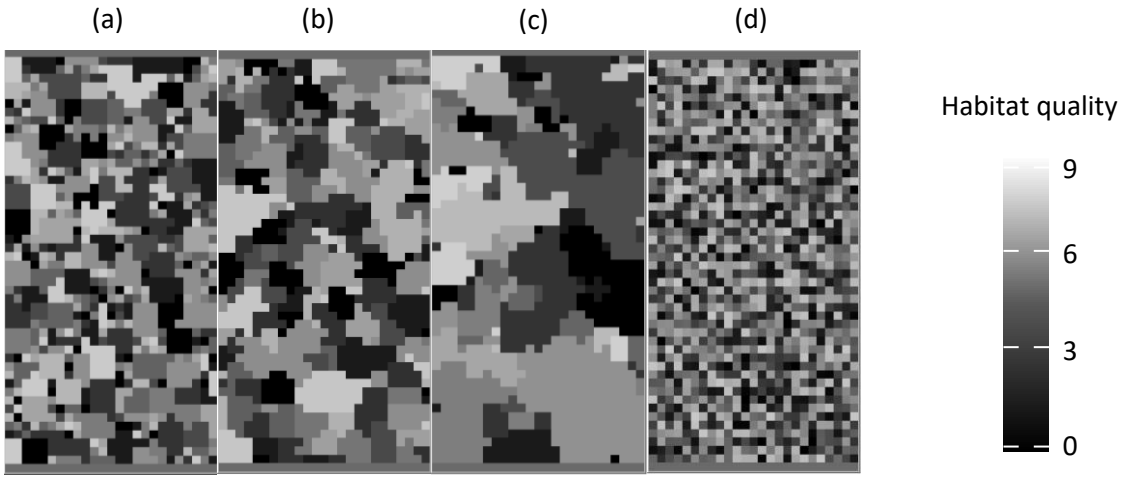

Figure A4: Example landscape configurations and habitat clustering used in the model, with (a) small clusters, (b) medium clusters, (c) large clusters of similar habitat quality and (d) randomly distributed habitat cells. The colour gradient shows the habitat quality (i.e. the maximum number of breeding females supported by the individual landscape cells).

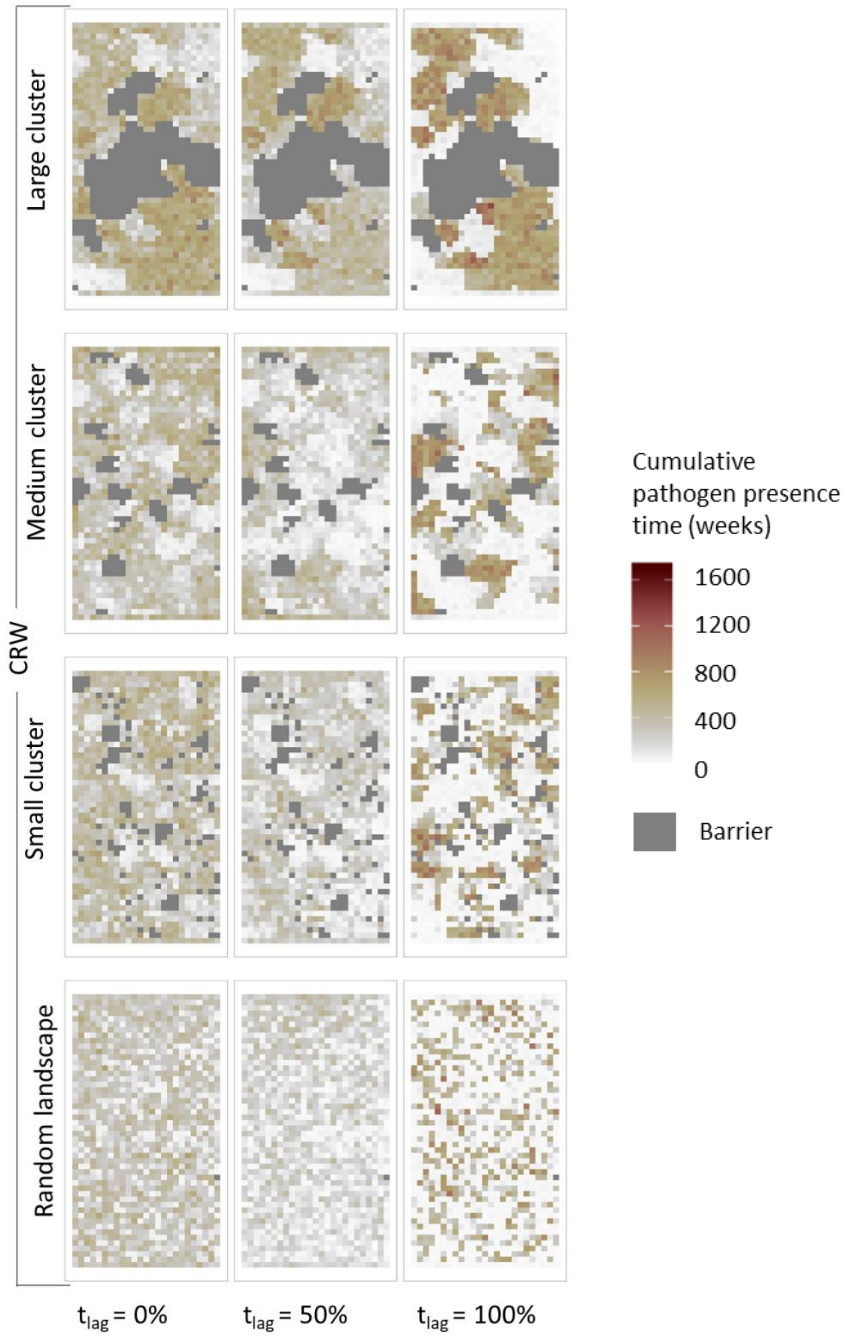

Figure A5: Spatial distribution of infected host individuals in the correlated random walk (CRW) movement scenarios throughout all landscape configurations (top to bottom: large clusters, medium clusters, small clusters, and a random configuration). The distribution is recorded as the cumulative time in weeks of infected hosts being present in the individual habitat cells at the end of a simulation run (colour gradient). Areas without any infected hosts at the end of a simulation run are further highlighted as barriers (dark grey). The distributions are further shown for three temporal shift scenarios (left to right t_{lag} 0%, t_{lag} 50% and t_{lag} 100%).

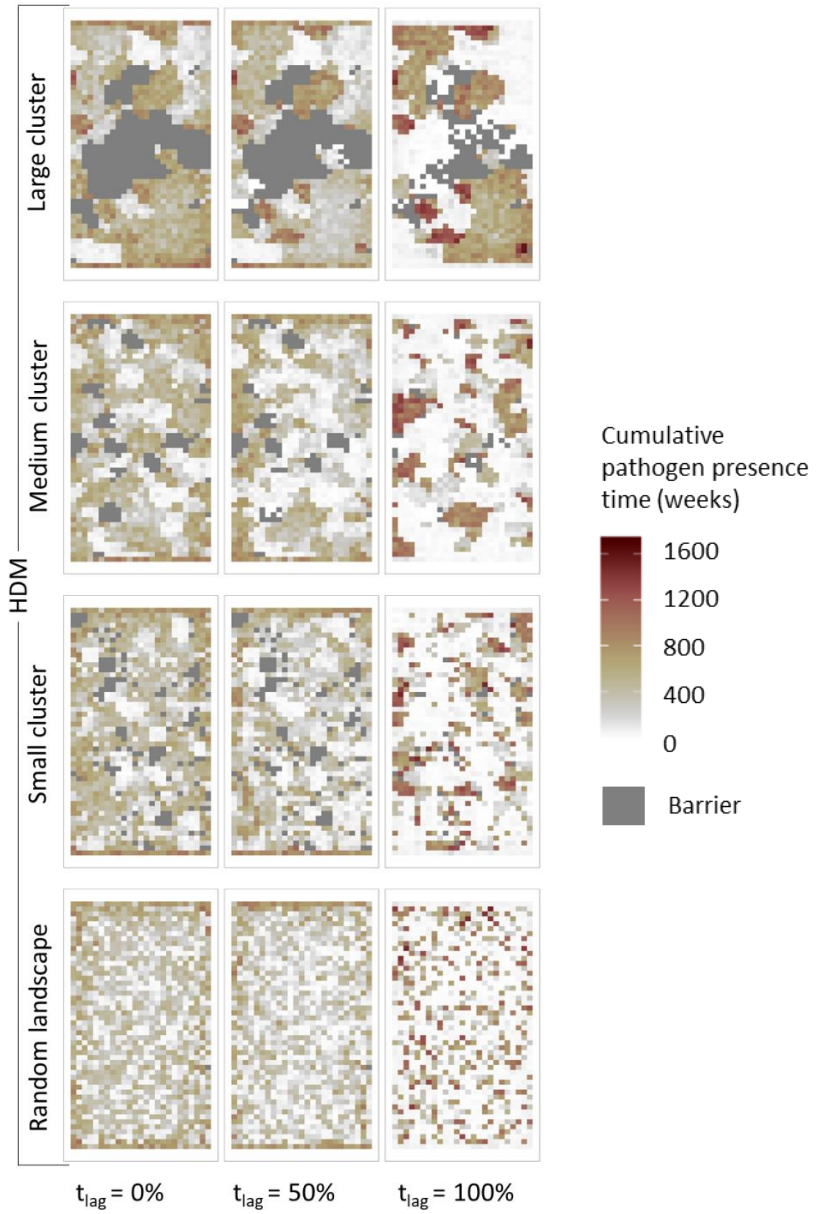

Figure A6: Spatial distribution of infected host individuals in habitat dependent movement (HDM) scenarios throughout all landscape configurations (top to bottom: large clusters, medium clusters, small clusters, and a random configuration). The distribution is recorded as the cumulative time in weeks of infected hosts being present in the individual habitat cells at the end of a simulation run (colour gradient). Areas without any infected hosts at the end of a simulation run are further highlighted as barriers (dark grey). The distributions are further shown for three temporal shift scenarios (left to right t_{lag} 0%, t_{lag} 50% and t_{lag} 100%).

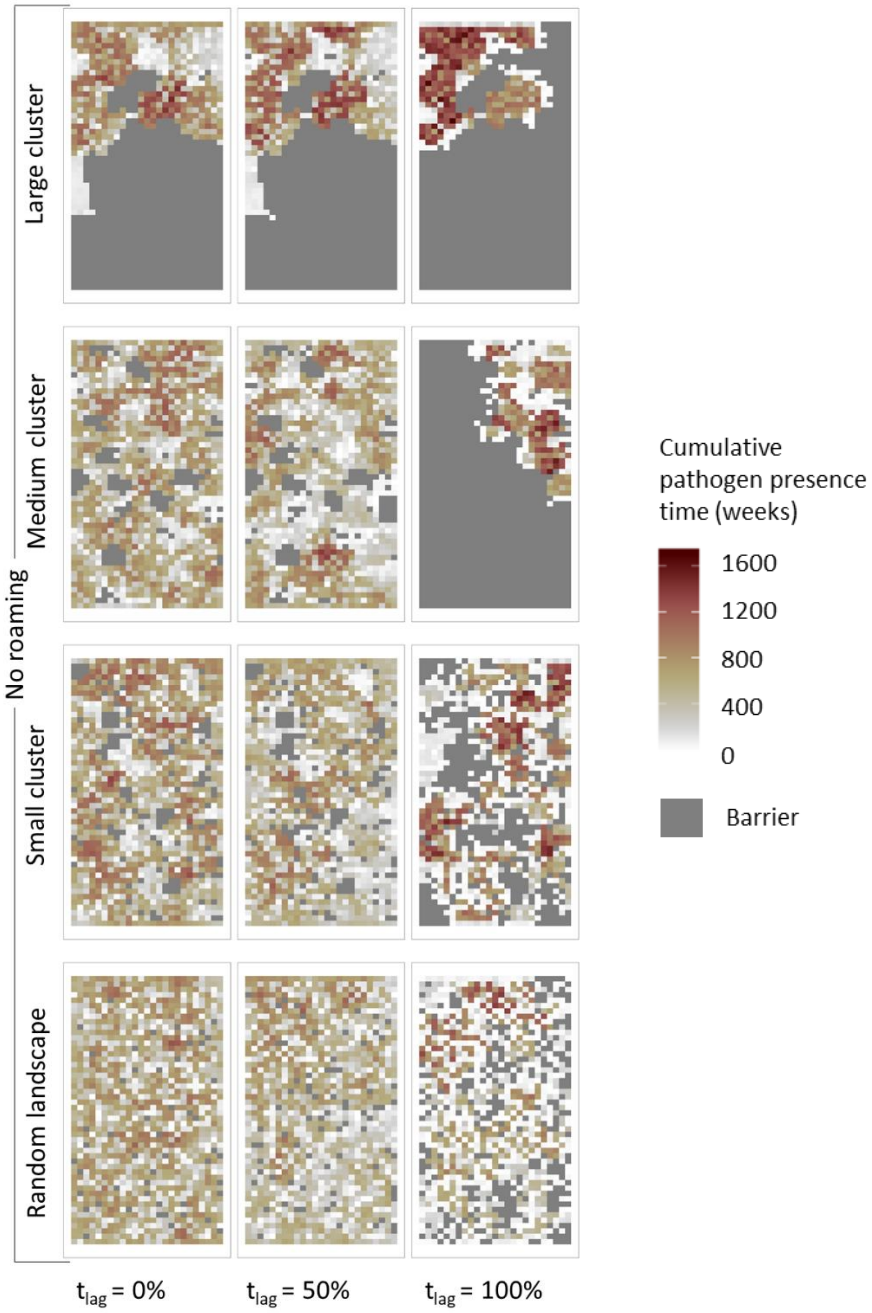

Figure A7: Spatial distribution of infected host individuals in scenarios without explicit host movement (neighbourhood infection) throughout all landscape configurations (top to bottom: large clusters, medium clusters, small clusters, and a random configuration). The distribution is recorded as the cumulative time in weeks of infected hosts being present in the individual habitat cells at the end of a simulation run (colour gradient). Areas without any infected hosts at the end of a simulation run are further highlighted as barriers (dark grey). The distributions are further shown for three temporal shift scenarios (left to right t_{lag} 0%, t_{lag} 50% and t_{lag} 100%).

APPENDIX B
SUPPLEMENTARY MATERIAL FOR CHAPTER 3

B1 Model description (ODD protocol)

The classical swine fever (CSF) wild boar model is a combination of a spatially explicit, stochastic, agent-based model for wild boars (*Sus scrofa* L.) and an epidemiological model for the CSF virus. The model was implemented in NetLogo (Wilensky, 1999) and is documented following the ODD protocol (Grimm et al., 2006, 2010, 2020).

The ODD protocol below includes changes in model description across three wild boar / CSF eco-epidemiological models. The first model SwiFCoIBMove (M1 and black text throughout, Scherer et al. 2020) was developed to assess the effects of host movement and landscape structure on disease dynamics, SwiFCoIBM_dynamic (M2 and blue text throughout, Kürschner et al. 2021) was developed to assess the role of a dynamic resource landscape and temporal mismatches on disease dynamics and SwiFCoIBM_Evo (M3 and green text throughout) was developed to investigate the effect of evolving pathogenic virulence. As a note, while in some instance (as seen for example in 1. Purpose) parts of the previous models are replaced, in other instances and submodels (as seen in 4– *Emergence*) M3 is a mixture of old and new versions. As a second note, specific changes to M1 that are in both M2 and M3 are marked with an orange colour in the text.

1 Purpose

[1]M1: The model aims to assess the role of host movement based on individual movement decisions (imposed, i.e. a correlated random walk, or based on external factors such as habitat and conspecifics) and landscape structure in driving on-going disease dynamics as pathogen persistence and patterns of spread. Specifically, the question will be addressed to what degree a high-resolution representation of the interaction between moving vectors and landscape features is required to capture spatiotemporal disease dynamics in a predictive way.

[1]M2: The model aims to assess the role of a dynamic resource landscape and temporal shifts in resources on disease dynamics as pathogen persistence and patterns of spread through individual movement. Specifically, how seasonal resource availability and the decoupling of resource availability and reproduction alter disease dynamics.

M3: The model investigates the effect dynamic resource landscape and temporal shifts on a multi-strain pathogen system, pathogen evolution and pathogen trade-offs. Particularly, how temporal mismatches

[1]This ODD describes M3, so that 'Purpose' for M1 and M2 is obsolete. It is kept in the ODD to better understand how the design of the model developed

between optimal resource availability and biological events affect host-pathogen coexistence and pathogen spread.

2 Entities, state variables and scales

The model entities are spatial units, or grid cells, and wild boars. Grid cells are characterized by habitat quality in terms of breeding capacity, i.e. the number of female boars that are allowed to have offspring (Jedrzejewska et al., 1997). Thereby, local host density is in the model, i.e. increasing numbers of fertile females can breed only until breeding capacity is reached. A grid cell represents about 2 km × 2 km, encompassing an average home range area of a boar group (Leaper et al., 1999).

Wild boars are characterized by sex, age in weeks, location, demographic status (e.g. breeding, dispersing and ranging) and health status. Three age classes are distinguished: piglet (< 34 weeks), subadult (between 34 weeks and < 1 year for females and < 2 years for males) and adult. Location is defined by the grid cell the wild boar inhabits. The health status of the individuals is described by an SIR epidemiological classification (susceptible; transiently infected; lethally infected with individual infectious period; immune by surviving the infection or by maternal antibodies). Females, which are at least subadult, may be assigned as breeders according to the breeding capacity of their family group's cell. Subadult wild boars may disperse during the dispersal period dependent on their sex and demographic status (disperser or non-disperser). In the model versions simulating explicit movement, males become ranging individuals (i.e. move solely) once they are adult and thereby change their locations every time step.

M1, M2, M3: One time step corresponds to the approximate CSF incubation time of one week (Artois et al., 2002; Moennig et al., 2003) while simulations usually run for 12 years (624 weeks), 50 years (2600 weeks) or 100 years (5200 weeks) with the virus being released in the second year (week 53-104) to a defined boar group to ensure the same distance to the model borders or the centre of the landscape and an established spatial population structure. The model landscape consists of 100 km × 50 km (50 × 25 grid cells).

3 Process overview and scheduling

[1]M1: Each time step, the following procedures are executed by the wild boars in the given order: pathogen transmission, ranging movement, natal dispersal of males and females, respectively, reproduction, mortality, ageing, and disease course (Figure B1)

In the first week of each year, females are assigned to breed. Natal dispersal of males and females was limited to week 17 and week 29 of the year, respectively.

M2 & M3: Each time step, the following procedures are executed by the wild boars in the given order: pathogen transmission, ranging movement, natal dispersal of males and females, resource-based host movement, host reproduction, general host mortality, resource-based host mortality, ageing, and disease course (Figure B1.1 (M2) B1.2 (M3)).

M2 & M3: Females are assigned to breed on a week to week basis, with the prerequisite that they have not bread previously in the current year.

4 Design concepts

Basic principles

M1, M2 & M3: Both processes of the host and the pathogen are simulated with a given stochasticity which resembles natural conditions. Disease transmission for groups is modelled density-dependent (see Eq. B1 and B2). Heterogeneous landscape scenarios were simulated using neutral landscape model algorithms.

Emergence

M1, M2 & M3: Wild boar population dynamics emerge from individual behaviour, resulting from age- and sex-dependent movement behaviours (natal dispersal and ranging) as well as age-dependent seasonal reproduction, survival probabilities and is mitigated by the underlying dynamic resource landscape. The epidemic course emerges from different virus transmission probabilities, wild boar movement behaviours (only M1 & M2) as well as individual stochastic disease courses and infectious periods.

[1] This ODD describes M3, so that 'Process overview and scheduling' for M1 is obsolete. It is kept in the ODD to better understand how the design of the model developed

Adaptation

M1 & M2: Movement rules either reproduce observed movement behaviours (phenomenological approach, e.g. correlated random walk with a given directional persistence) or are based on decisions in response to spatial structure or conspecifics (mechanistic approach, e.g. the competition-driven movement rule implicitly seeks to increase habitat quality in relation to conspecifics).

M1, M2 & M3: The number of breeding females per cell is determined by (a) the habitat quality of the cell and M1: (b) the number and age of the reproductive females within the cell.

Objectives

M1 & M2: The exact way individuals decide where to move depend on the applied movement rule (see section "Ranging movement"). In general, ranging individuals (i.e. adult males) using decision-based movement rules move into the neighbouring cell with the highest weight (which is defined by the applied movement rule). Individuals' decisions are not perfect but may be a random direction depending on the directional persistence ρ (probability to move randomly = 1 - ρ, set to 0.7).

M1, M2 & M3: Dispersing individuals search for empty (unoccupied) cells (in case of female dispersers) or join other groups that are below their cells' carrying capacity (in case of male dispersers).

Learning

M1, M2 & M3: There is no learning implemented in our model.

Prediction

M1, M2 & M3: There is no need to predict future environmental conditions.

Sensing

M1, M2 & M3: Individuals moving through the landscape may base their decisions on the underlying landscape structure in terms of habitat quality (or, synonymously, breeding capacity B) or number of conspecifics. Moving individuals can sense all that information from their own cell and surrounding cells but the decision might be random (implicitly due to insufficient information) depending on the assumed directional persistence ρ.

Interaction

M1, M2 & M3: Based on the transmission rates, interactions between individuals might lead to virus transmission from an infected to a susceptible individual. Reproduction is density-and age-dependent

with the oldest females giving birth first. Thus, if the number of reproducible females exceeds a cell's breeding capacity, interaction leads to repressed reproduction.

Stochasticity

M1, M2 & M3: Demographic and behavioural parameters are imposed via probability distributions to account for variation in the biological processes. Stochastic individual disease courses and infectious periods are modelled explicitly because variation in the disease outcome between individuals was identified to be essential for virus endemicity without reservoirs (Kramer-Schadt et al., 2009). Movement decisions are based on a random component (with 30% of the decisions being random).

Collectives

M1, M2 & M3: Individuals that are not ranging between home ranges (i.e. all individuals but adult males) form groups within their cell that experience density-dependent transmission probabilities. These groups are formed by reproducible females and their offspring. During natal dispersal, male subadults may join those groups while female subadults may form new groups.

Observation

M1, M2 & M3: To evaluate model outcomes, we measure several properties of the host-virus system at each time step of the simulation. These outputs include number of individuals for each class of age (piglet, subadult, adult), demographic (resident, ranging) and health status (susceptible, infected, recovered) and their combinations. Furthermore, sex ratio, number of new infections (transient and lethal), number of cells with infectious individuals, the last week of infection and the cumulative time (i.e. how many weeks in total) of infected hosts per habitat cell are recorded. From this output, duration of an outbreak, probability of disease persistence (i.e. the virus being present in the system until the end of simulations), outbreak size for different classes, as well as density distribution of infected hosts can be estimated. Furthermore, we recorded the number of infected individuals separately for each strain of the pathogen and the mean landscape-wide virulence of all infected individuals.

5 Initialization

M1, M2 & M3: We simulate landscapes with four different levels of spatial heterogeneity in habitat quality: homogeneous (only M1 & M3), random, and two or four clustered landscape scenarios using a random cluster algorithm (very small, small, medium and large clusters, respectively; Saura & Martínez-Millán, 2000; Table B1) generated using the R package NLMR (Sciaini et al., 2018). In homogeneous landscapes, one boar family group was allocated to each cell with an average breeding capacity B of 4.5

females, resulting in the reported density of approximately 20 boars per cell or 5 boars per km² (European Food Safety Authority, 2009; Howells & Edwards-Jones, 1997; Melis et al., 2006; Sodeikat & Pohlmeyer, 2003). In heterogeneous landscapes a breeding capacity B between 0 and 9 was assigned to each of the 2500 grid cells ($B \in \{0;9\}$). In case B is a floating point number, the number of individuals is determined stochastically based on the remainder. Initial age distribution was obtained from the results of a 100-year model run conducted by (Kramer-Schadt et al., 2009); Table B2), the sex ratio was balanced (i.e. probability of 0.5 to be either male or female). Wild boar density reflects long-term average values of densely populated Central European habitats (European Food Safety Authority, 2009; Howells & Edwards-Jones, 1997; Melis et al., 2006; Sodeikat & Pohlmeyer, 2003). Group size was initialised according to the cells carrying capacity K_i that is 4.5 times its breeding capacity B_i.

6 Input

M1, M2 & M3: The model does not include external input representing environmental conditions changing over time.

7 Submodels

Initial infection (pathogen release)

M1 & M2: The virus is released to the population by infection of one wild boar group (i.e. cell) in middle of the upper row of home ranges (i.e. cell with the coordinates x = 1 and y = 13) to allow for comparison between runs. The release is scheduled in a random week of the second year of the model run.

M3: The virus is released to the population by infection of several wild boar groups (i.e., cells), starting with the centre of the landscape (i.e., cell with the coordinates x = 24 and y = 13) as well as three randomly selected cells in the vicinity. The release is scheduled in a random week of the second year of the model run.

Pathogen transmission

[1]M1 & M2: Virus transmission is modelled stochastically. The transmission parameter determines the weekly probability of being infected by an infectious group mate β_w.

[1]This ODD describes M3, so that '7.2.Pathogen transmission' for M1 and M2 is obsolete. It is kept in the ODD to better understand how the design of the model developed

In the model without movement (afterwards referred to as the "classical model"), weekly infection pressure λ_i for each susceptible individual in cell i is determined by the probability of being infected by an infectious group mate β_w (within-group transmission probability) and the probability of being infected by an infectious individual in one of the eight neighbouring cells β_e (between-group transmission probability):

$$\lambda_i = 1 - (1 - \beta_w)^{I_i} \cdot (1 - \beta_e)^{\Sigma_i I_j} \quad [B1]$$

where I_i is the number of infectious group mates and I_j is the numbers of infectious hosts in the j^{th} adjacent cell. The resulting probability value λ_i provides the parameter of a binomial chance process to decide whether a susceptible animal will be infected.

The transmission parameters β_w (and thereby β_e since it was fixed as one tenth of β_w) was calibrated in order to reproduce the spreading velocity observed in France (Rossi et al., 2010) with the constant parameter value β_w = 0.0208 within and, hence, β_e = 0.00208 between groups (Kramer-Schadt et al., 2009).

In the model version involving explicit movements presented here, infection might be translocated within the host population. Because ranging movements are performed by adult males only, the homogeneous transmission probability λ_i was transformed to account for these sex-and age-dependent transmission probabilities. Therefore, for all individuals but adult males the weekly probability of being infected by infectious group mates (but not by infectious ranging males) is simply β_w since females and their group follow a staying rule with the almost all contacts within the group (Pepin et al., 2016; Spitz & Janeau, 1990). The accumulated probability λ_i for susceptible non-ranging individuals is thus reduced to:

$$\lambda_i = 1 - (1 - \beta_w)^{I_i} \quad [B2]$$

where is the number of infectious group mates (but not infectious ranging males which do not belong to any group). For adult, ranging males, the individual probability of virus transmission during movements β_m (i.e. being infected by an infectious animal in a cell moving through as well as the probability of infecting a susceptible individual while passing the cell) was fitted to account for the resuming transmission probabilities (i.e. the remaining within- and between-group transmission probabilities of the classical model, see Eq. B2). We calibrated one constant transmission probability (i.e. $\beta_w = \beta_m$, afterwards just referred to as simply β) to result in the comparable distributions of the basic reproduction number (R_o, number of secondary infections) as in the classical model. Using a Kolmogorov-Smirnov test, the constant parameter value β = 0.022 gave the best results for different scenarios of infection and movement rules (Scherer et al., 2020). Individual per step transmission probability $\beta_{m,i}$ is related to the

number of steps the animal makes. Therefore, the infection probability for cells passed by infected individuals is scaled to the individual movement distance $d_{m,i}$ (see section "Ranging movement"):

$$\beta_{m,i} = \frac{\beta}{d_{m,i}}. \quad [B3]$$

By doing so, infection probability decreases with increasing movement distance which relates to the time an animal is able to spend within each cell and thus to transmit the virus on its way.

CSF shows a variety of disease courses on the individual level (Depner et al., 1997; Liess, 1987). Therefore, in our model the disease course is stochastically specified for each individual. The disease course submodel is described by two parameters: individual case mortality M and the mean infectious period of lethally infected hosts μ. Upon infection the host is stochastically assigned either as lethally infected (with probability M) or as transiently infected (1 - M). M is age-specific (Dahle & Liess 1992): for adults the probability is decreased to $M_a = M^2$ and for piglets increased to $M_p = \sqrt{M}$ while it is unchanged for subadults $M_s = M$. Transiently infected wild boars first pass through an infectious period of one week and subsequently becomes non-infectious and gain life-long immunity (Artois et al. 2002; Moennig et al. 2003; European Food Safety Authority, 2009). The individual infectious period (m_i in weeks) of lethally infected hosts is drawn from an exponential distribution with the mean specified by parameter μ:

$$m_i = 1 + floor(-(\mu - 0.5) \cdot ln(U(0,1))) \quad [B4]$$

where *U(0,1)* is a uniformly distributed random number between 0 and 1. To avoid unrealistically long infections, m_i was stochastically assigned until $m_i \leq 10 \times \mu$. Lethally infected hosts remain infectious until death. Offspring from immune female breeders gets maternal antibodies and is thus immune for the first eight to twelve weeks after birth (t_{anti}). The number of weeks of immunisation due to maternal antibodies is randomly assigned for those piglets.

M3: In the model, instead of one single viral strain like in M1 and M2, we added 12 arbitrarily categorized viral strains that differ in their transmission potential and the survival time of the host they infect (Table B5). Similar to the previous model version, weekly infection pressure λ_{is} for each susceptible individual in cell i is determined by the probability of being infected by an infectious group mate β_w (within-group transmission probability) and the probability of being infected by an infectious individual in one of the eight neighbouring cells $\frac{\beta_w}{10}$ (between-group transmission probability):

$$\lambda_{is} = 1 - (1 - (\beta_w + T_s))^{I_s} \cdot (1 - \frac{(\beta_w + T_s)}{10})^{\Sigma_i I_{js}} \quad [B6]$$

where I_i is the number of infectious group mates and I_j is the numbers of infectious hosts in the j^{th} adjacent cell. The resulting probability value λ_{is} provides the parameter of a binomial chance process to decide whether a susceptible animal will be infected. Due to the model now having multiple strains with different infection probabilities, there is now the subscript s added to all relevant terms, indicating that those values are now strain specific. Therefore, we calculate infection pressures for all strains separately and only take individuals with the respective strains into consideration when determining I_s for within group or I_{js} for between group transmission. We added a strain specific factor T_s (Table B5) to infection pressure calculation so ensure transmissibility differences of the individual strains along a trade-off (Table B5), while the base transmission probability β_w (0.0208) remained unchanged from model M1 and M2.

CSF shows a variety of disease courses on the individual level (Depner et al., 1997; Liess, 1987). Therefore, in our model the disease course is specified for each individual. The disease course sub model is described by two parameters: individual case mortality M and the infectious period of lethally infected hosts. One week after infection the host is stochastically assigned either as lethally infected (with probability M) or as transiently infected (1 - M) in which case it becomes non-infectious and gains life-long immunity. M is age specific (Dahle & Liess 1992): for adults the probability is decreased to $M_a=M^2$ and for piglets increased to $M_p=\sqrt{M}$ while it is unchanged for subadults $M_s=M$. The individual infectious period is strain specific and selected from table B5.

Lethally infected hosts remain infectious until death. Offspring from immune female breeders get maternal antibodies and is thus immune for the first eight to twelve weeks after birth (t_{anti}). The number of weeks of immunisation due to maternal antibodies is randomly assigned for those piglets.

Pathogen evolution

During every transmission event, the pathogen can evolve into a different strain with different strain specific variables compared to the parental strain. Once a host individual is becoming infected by a specific strain, an evolution check is applied, whereby with a mutation rate of 0.01 (table B1) the strain can evolve. If the strain evolves, the new strain is selected from a normal distribution with a standard deviation of 1 around the parental strain. The resulting strain will be closely related to the parental strain. If the transmitted strain does not evolve, it is transmitted directly without any changes to a new host.

Ranging movement

[1]M1 & M2: While adult females move mainly within their family group (*staying strategy*), adult males follow a *ranging strategy* and move solitary (Spitz & Janeau 1990, Figure B2). Ranging distances vary between males with a mean distance of 24 km per week and rare long-distance behaviour with up to 84 km per week (Morelle et al. 2015). For each adult male *i*, an individual movement distance $d_{m,i}$ was drawn from the median of the Weibull distribution given by $b*(1 - ln(1 - U[0,1]))^k$ with a scale of b = 26 and a shape of k = 1.3, resulting in a mean of 12 cells and truncated to the maximum movement distance D_{max} of 42 cells (with a cell being 2 km in diameter). To study effects of inter-cell movement on disease dynamics, we implemented three different movement strategies. In general, ranging individuals move until the individual weekly movement distance is reached or there is no better decision to make and only into cells with a positive habitat quality (B > 0). Individuals stop moving if there is no cell available. If there is a tie (i.e. two or more cells with equal attractiveness), one of those cells is chosen randomly.

M1 & M2: *(a) Correlated Random Walk (CRW):* In a CRW, subsequent movement directions are correlated such that highly correlated movement paths are nearly straight (Turchin 1998; Figure B3a). This movement model improves the RW approach by incorporating directional persistence that moving animals very frequently exhibit (Figure B3; Kareiva & Shigesada 1983). The direction of a step is drawn from a wrapped Cauchy distribution with a mean direction equal to the previous direction (Fletcher 2006):

$$\theta_{t,i} = \theta_{t-1,i} + 2 \cdot arctan\left(\frac{1-\rho}{1+\rho} \cdot \pi \cdot U(-0.5,0.5)\right) \quad [B5]$$

Where $\theta_{t,i}$ and $\theta_{t-1,i}$ are the headings of individual *i* of the next or previous step, respectively, ρ is a parameter related to the concentration around the mean direction (i.e. ρ = 1 results in a straight line and ρ = 0 equals a RW), and U(-0.5,0.5) is a uniformly distributed random number between -0.5 and 0.5. In case individuals reach the border of the simulated landscape, the Individual is reflected in a 90° angle followed by reset and recalculation of $\theta_{t,I}$ to avoid aggregation around the landscape borders.

M1 & M2: *(b) Habitat-Dependent Movement (HDM):* A reasonable hypothesis is that a selective animal should choose high quality cells for its home range. The distribution and abundance of resources greatly affect movement patterns of several animal species and has also been reported for wild boars (Morelle

[1]This ODD describes M3, so that '7.3.Ranging movement' for M1 and M2 is obsolete. It is kept in the ODD to better understand how the design of the model developed

et al. 2015). Assuming higher food resources and better shelter in high quality habitat, individuals decide among their neighbouring cells based on the habitat quality (Figure B3b). The parameter ρ here relates to the accuracy of an individual estimating the quality of the focal and neighbouring cells, with the movement decision in ρ-1 cases being purely random.

M1: *(c) Competition-Driven Movement (CDM):* Effective habitat quality might be lower due to competition with conspecifics. Thus, competition-driven movement is biased to cells with higher net habitat quality and was implemented as negative density dependence. Movement weights were calculated as the ratio of number of conspecifics in the focal cell and the carrying capacity (*K*), i.e. the potential maximum group size of the cell (Figure B3c).

For all movement strategies, ρ was fixed as 0.7, i.e. 30% of the decisions were made randomly.

M3: No ranging movement was applied.

Natal dispersal

M1, M2 & M3: Herd splitting, where subadult individuals may move together to search for or form new groups, is performed in specified weeks of the. The timing of these events is sex-dependent: Subadult females without offspring perform their natal dispersal in the 29th week of the year, while subadult males disperse during the 17th week. In the given week of the year, all herds to split are extracted, matching the conditions of containing at least a specified number of subadults N_{disp} to move (either male or female). For female dispersal, only cells exceeding the breeding capacity *B* are evaluated. For each of them, a habitat cell not exceeding carrying capacity *K* (for males) or without any family group (for females) within a Euclidean distance d_{disp} is selected randomly as new cell for the group, excluding the source cell (Figure B2). If there is no cell fulfilling these conditions, subadults stay within their group's cell.

Reproduction

M1, M2 & M3: Females reproduce once a year, depending on their age class. Individual females, which are at least subadult, reproduce depending on the season with a peak in March and no reproduction in winter from October to December (Boitani et al. 1995) (Table B2).

M1, M2 & M3: In the first week of the year, female individuals are checked for their breeding status; female individuals are checked for their breeding status on a weekly basis. All females not exceeding their habitat cells breeding capacity, starting with the oldest individuals, are allowed to breed.

M1: The week of the year to breed is assigned in the first week of each year according to weekly reproduction probabilities, derived from monthly probabilities and the number of weeks in the month (Table B2).

M2 & M3: If an individual was assigned to breed the chance of reproduction at that time is drawn from monthly probabilities and the number of weeks in the month (Table B2).

M1, M2 & M3: Litter size is drawn from a pre-calculated truncated normal distribution (Table B1,3) and reduced to a constant fraction for infected individuals. Litter size of transient shedders and lethally infected hosts is multiplied with the reduction factor α_f.

M1, M2 & M3: Depending on the disease state of the breeding individual, its piglets disease states are adjusted. Susceptible individuals produce susceptible offspring, immune individuals produce immune offspring with maternal antibodies (see section "Pathogen state transition"). Transient shedders and lethally infected individuals yield offspring, each one lethally infected with a given probability of prenatal infection p_{pi}.

Mortality

M1, M2 & M3: Stochastic baseline mortality is age-dependent and adjusted to annual survival estimates found in the literature (Table B1). Per time step we apply the adjusted age-dependent mortality (m_{week}) to the individual:

$$m_{week} = 1 - (s_{year})^{1/52}. \quad [B6]$$

In addition to the stochastic baseline mortality, each individual may die due to reaching a certain maximum age, or due to a lethal infection after a certain infection time span m (see section "Pathogen transmission").

M2 & M3: A selected number of individuals K_{over} (see Resource response for the selection) are subject to a variable, resource-based mortality with an increasing chance of mortality dependent on how long the individual is subject to low resource conditions up to a variable time limit S_{max} as well as the number of individuals (g_{act}) in relation to maximum group (g_{sus}) size and age.

$$m_{resource} = \frac{(g_{act} - g_{sus})}{100} * a * t_{over} \quad [B7]$$

With a being an age factor corresponding to the individuals being a piglet or adult/subadult and t_{over} the time the individual is part of the K_{over} individual pool. As well as a 100% mortality when t_{over} equals S_{max}.

Ageing

M1, M2 & M3: The ageing process iterates over all individuals. For each individual k, age T_k is incremented one week and disease state transitions are performed. Females become subadult and adult at an age of 34 and 52 weeks, respectively, while males enter the subadult and adult age groups at an age of 21 and 104 week, respectively.

Disease course (pathogen state transition)

M1 & M2: Transient shedders convert to immune after a certain latency period t_{latent}. An individual i protected by maternal antibodies turns susceptible if reaching an age T_i of the protection time of t_{anti} (see section "Pathogen transmission"). After disease state transition the age of the infection is incremented by one week if the individual is not susceptible.

M3: An individual i protected by maternal antibodies turns susceptible if reaching an age T_i of the protection time of t_{anti} (see section "Pathogen transmission"). After disease state transition the age of the infection is incremented by one week if the individual is not susceptible.

Landscape dynamic

M2 & M3: The autocorrelated landscape dynamic is superimposed over the different types of heterogeneous starting landscapes. Throughout each simulated year, resource availability in each cell increases in 5-weeks intervals for approximately 25 weeks and then declines in 5-weeks intervals for the next 25 weeks. The resource availability translates directly into the breeding capacity for each cell and for each increase or decrease the value of the breeding capacity is changed by one. During the increase, the breeding capacity cannot exceed the maximum breeding capacity of 9 and cannot fall below 1 during the decrease i.e. the breeding capacity in a cell designated as habitat cannot become 0 during the course of a year. Additionally, barriers and matrix which have an assigned breeding capacity of 0 cannot become habitat i.e. matrix/barrier cells will always have a breeding capacity of 0. The default landscape dynamic is implemented to follow the host individual's monthly reproduction probabilities (see table B2), where the peak reproduction probability matches in time with the peak resource availability. Furthermore, the landscape dynamic can be temporally shifted away from the peak host reproduction probability in 25% increments (0% – match, 25% mismatch, 50% mismatch, 75% mismatch, 100% – full mismatch). In this case, a full mismatch would mean that the resource availability is at its lowest when the host reproduction probability is at its highest.

The random landscape dynamic functions similar to the autocorrelated variant without a temporal shift. Throughout each simulated year, resource availability in each cell changes randomly in 5-weeks intervals

for approximately 50 weeks whereby each cell is allocated a random integer between 1 and 9. At the end of each year, the landscape resets to the original starting landscape.

Resource responses

M2 & M3: If the group size exceeds the carrying capacity K in a cell, a dispersal event will be triggered. The likelihood of dispersal follows an age gradient where older females will try to disperse last. For male individuals, a random habitat cell not exceeding the carrying capacity K will be randomly selected within a Euclidean distance d_{disp} as new cell. For female individuals, the randomly selected habitat cell must fulfil the prerequisite of not hosting another family group. However, if an individual currently has offspring it and the offspring will stay at in their current cell. If there is no suitable habitat cell fulfilling these prerequisites within the distance d_{disp} the individuals will stay. Individuals are continuously selected for dispersal until the group size no longer exceeds the carrying capacity K. For a secondary response after the dispersal event (if applicable), a cell specific number of individuals K_{over} that is the difference between carrying capacity K and group size will be selected. The selection of these individuals is age dependant where the oldest females are selected last. All selected individuals are subjected to an increasing age-dependant mortality (see mortality).

Figures

Flow chart of the SwiFCoIBMove model and its submodels

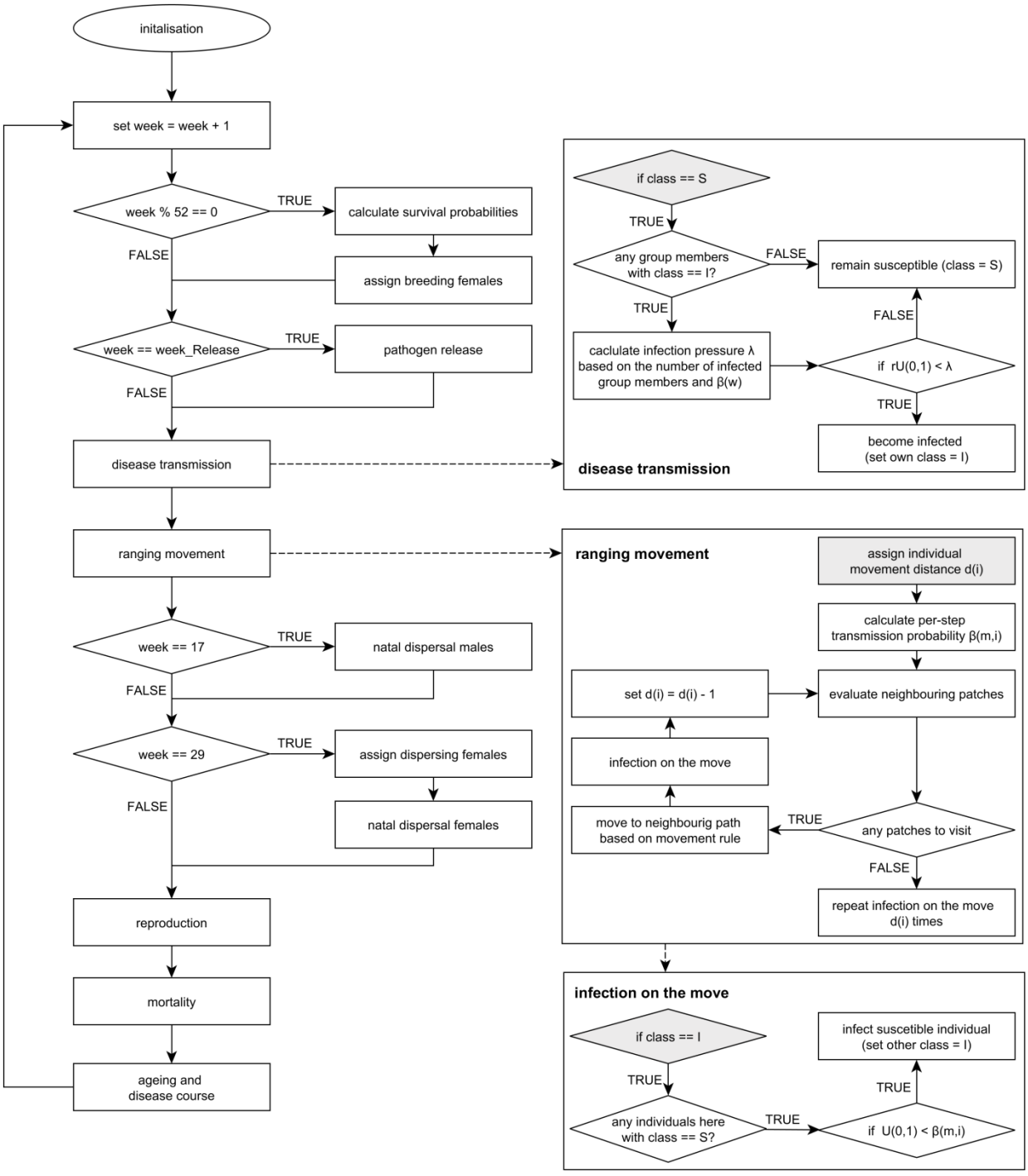

Figure B1: Flow chart of the agent-based, spatially explicit host-pathogen model "SwiFCoIBMove" and its submodels.

Flow chart of the SwiFCoIBM_dynamic model

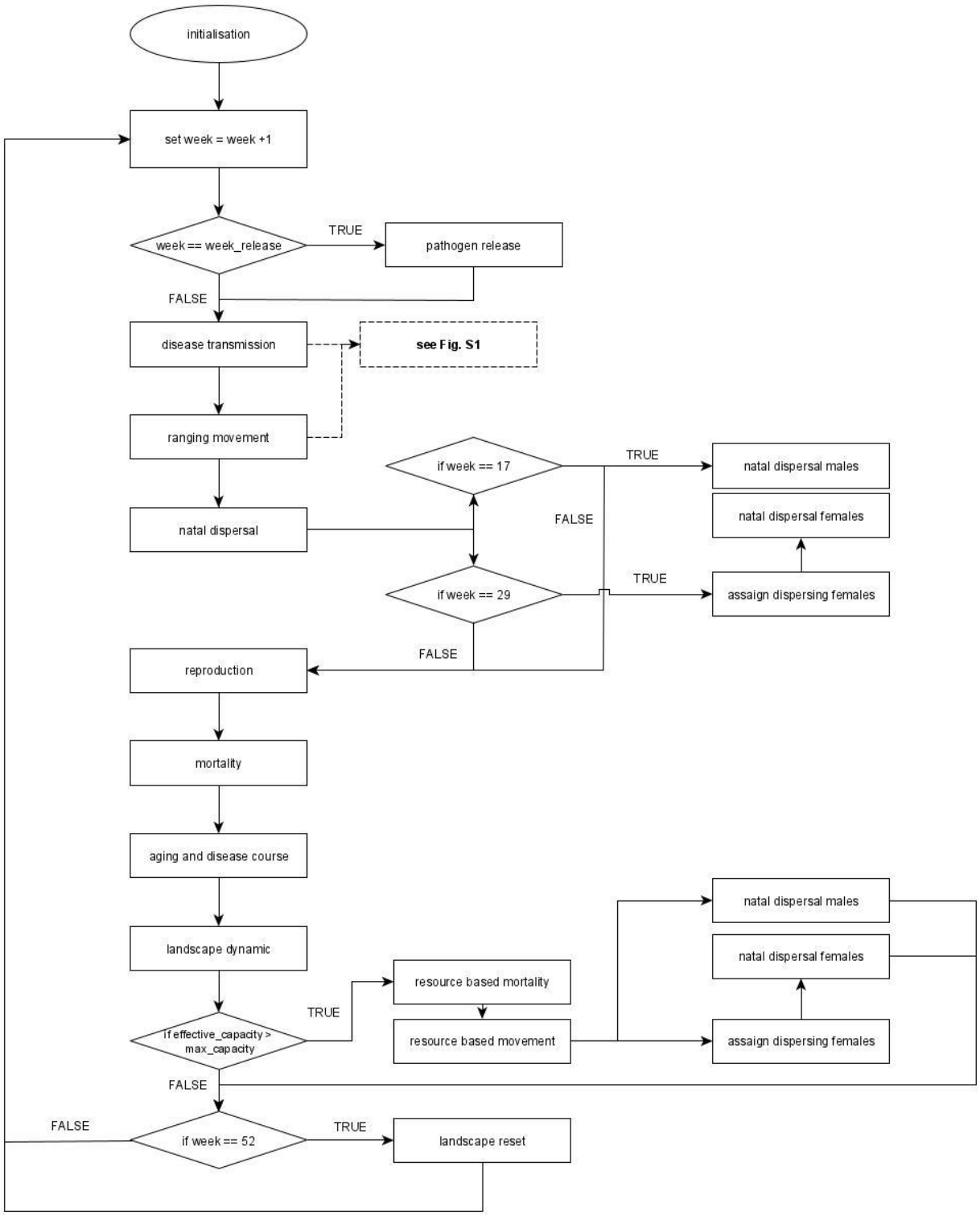

Figure B1.1: Flow chart of the agent-based, spatially explicit host-pathogen model "SwiFCoIB_dynamic"

Flow chart of the SwiFCoIBM_evo model

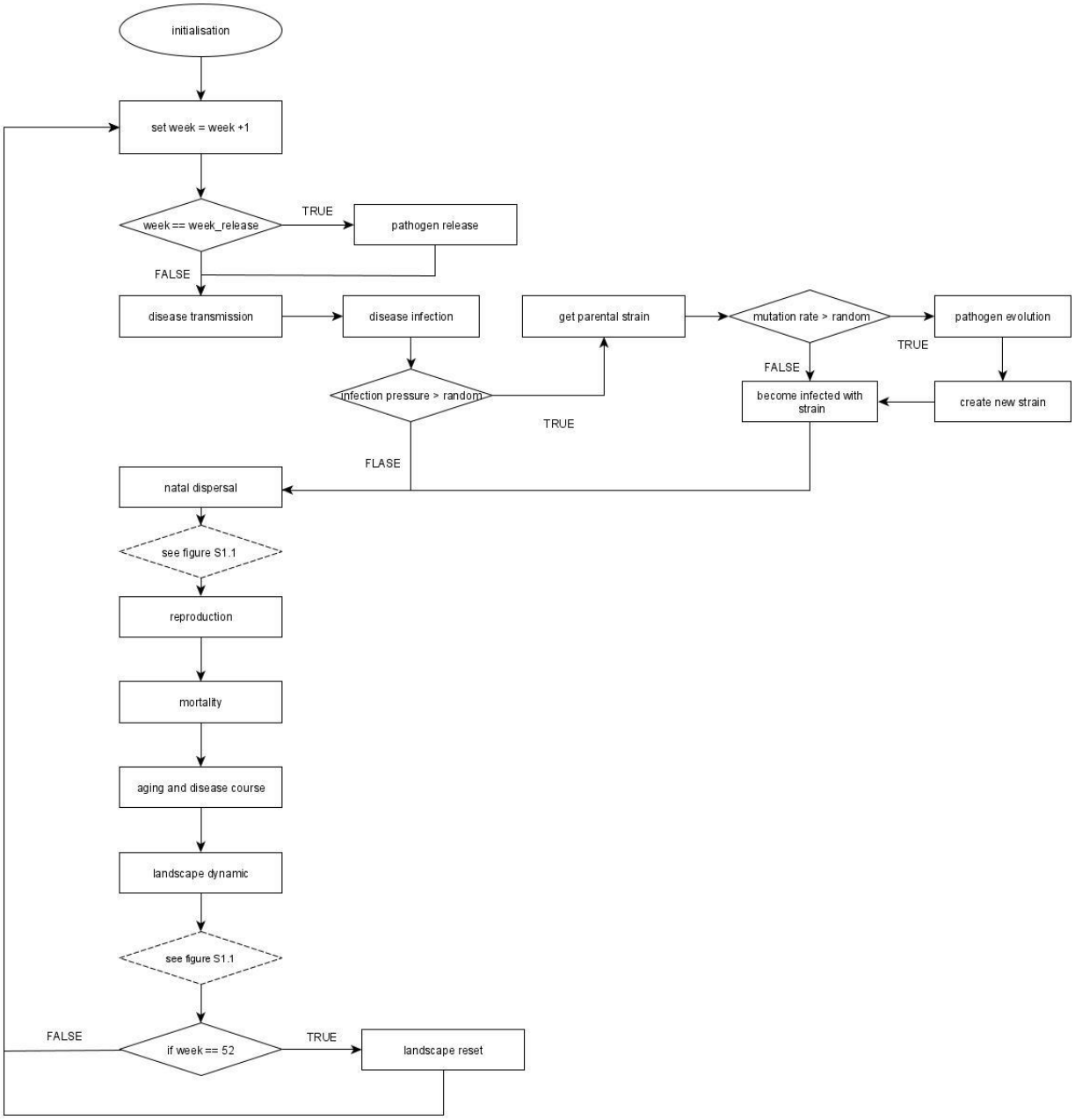

Figure B1.2: Flow chart of the agent-based, spatially explicit host-pathogen model "SwiFCoIB_evo"

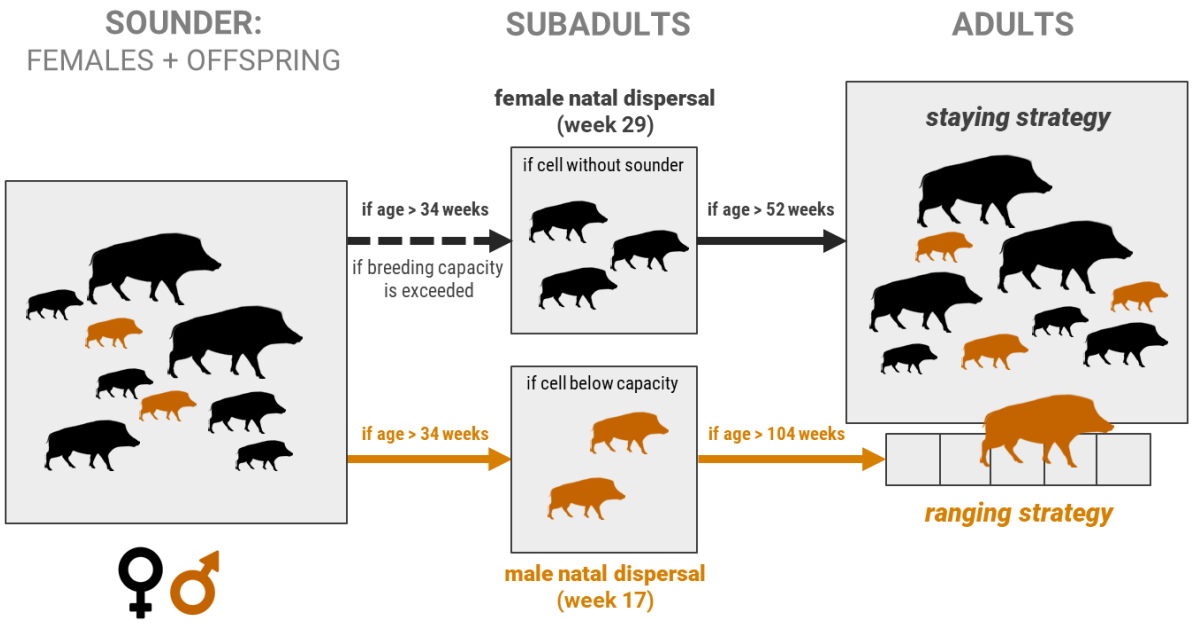

Figure B2: Schematic representation of different natal dispersal events of subadult wild boars and movement strategies of adult wild boars. The group of adult and subadult females and their offspring is called a sounder. If the breeding capacity of the sounders cell is exceeded, subadult females search in groups of 3 or more individuals for an unoccupied cell in a radius of three cells. Female wild boars reach their adulthood earlier (model assumption: if older than 1 year) and follow a staying strategy, thus not moving outside of the sounders cell (grey squares). Male wild boars always separate from the sounder when reaching the subadult age and move in groups of 2 or more to one of the cells below capacity in a radius of 3 cells. When becoming adult, male wild boars move solitary between home ranges.

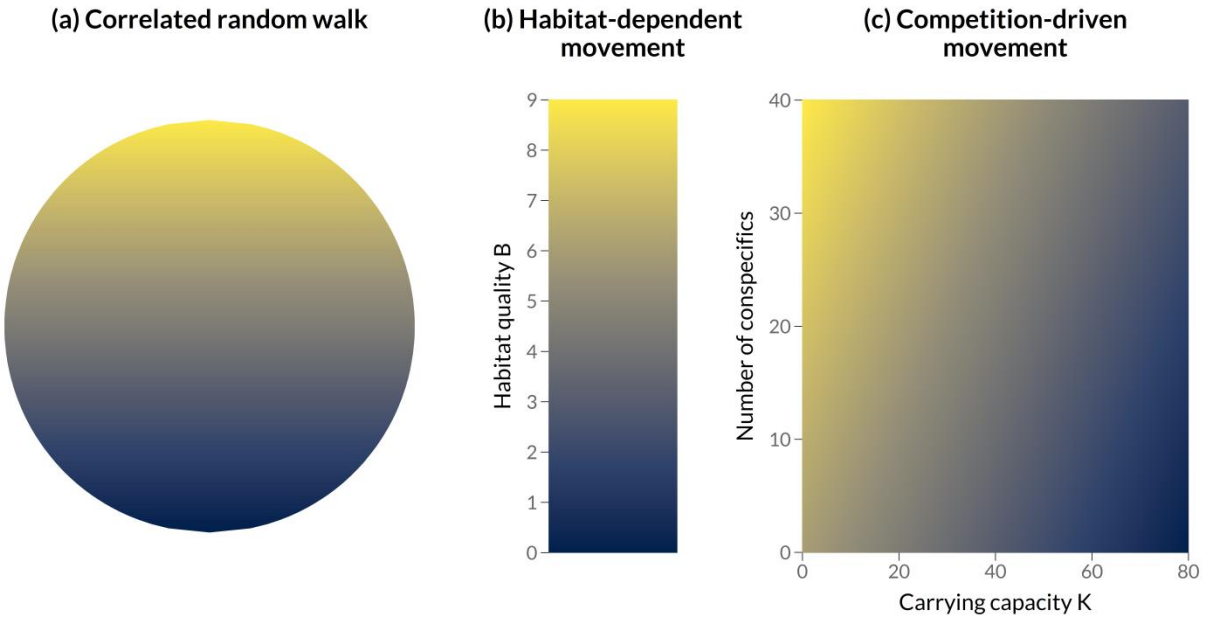

Figure B3: Movement assumptions used to model ranging behaviour of adult males. Probability of movement depends on the **(a)** direction of previous steps (Correlated Random Walk), **(b)** habitat quality B or **(c)** carrying capacity K in relation to the number of conspecifics. The lighter the colour, the higher the probability the individual chooses this cell. Movement decisions are furthermore driven by a random component determined by ρ.

Table B1: Parameter setup used in the spatially-explicit classical swine fever-wild boar model. M1: Each of the 60 combinations (3 movement strategies × 4 landscape scenarios × 5 case fatality ratios) was repeated 200 times while generating new underlying landscapes depending on the scenario input, resulting in 12.000 runs in total. M2: Each of the 300 combinations (3 movement strategies 3 × landscape dynamic × 4 landscape scenarios × 5 max survival time under low resources × 5 level of resource mismatch) was repeated 25 times, resulting in 22.500 runs in total. M3: Each of the 10 combinations (5 landscape scenarios × 2 landscape dynamic) was repeated 25 times, resulting in 250 runs in total

Parameter	Values	Reference(s)
Longevity	11 years (572 weeks)	(Jezierski, 1977)
Sex ratio	1:1	(e.g. Durio et al., 2014; Fernández-Llario et al., 1999; Moretti, 2014)
Survival probability of adults and subadults	s_{mean}= 0.6; s_{min} = 0.4	(Focardi et al., 1996; Gaillard et al., 1987)
Survival probability of piglets	s_{mean}= 0.5; s_{min} = 0.1	(Focardi et al., 1996)
Reproduction probability	see Table B2	(Boitani et al., 1995)
Breed count distribution	see Table B3	(Bieber & Ruf, 2005)
Movement rule (M1, M2)	CRW (M1,M2) HDM (M1,M2) CDM (M1)	(Fletcher, 2006)
Tendency to move randomly ρ (M1, M2)	0.3	
Mean movement distance D_{mean} (M1, M2)	24 km (12 cells) per week	(Morelle et al., 2015)
Maximum movement distance D_{max} (M1, M2)	84 km (42 cells) per week	(Morelle et al., 2015)
Indiv. weekly ranging distance $D_{m,I}$ (M1, M2)	D_i {1, D_{max}} ~ Wei(26, 1.3)	
Maximal natal dispersal distance d_{disp}	3 cells (6 km)	(Sodeikat & Pohlmeyer, 2003)
Minimum number of dispersers N_{disp}	2 for females; 3 for males	
Case fatality ratio M	{0, 0.25, 0.5, 0.75, 1} 0.5, 0.5	
Mean infectious period μ (M1, M2)	4 weeks, 6 weeks	
Transmission probability β (M1, M2)	0.022	
Fertility reduction due to infection	0.625	(Kramer-Schadt et al., 2009)
Probability of prenatal infection	0.5	(Kramer-Schadt et al., 2009)
Transient period t_{trans}	1 week	(Artois et al., 2002; Moennig et al., 2003)
Period of maternal antibodies t_{anti}	12 weeks	(Depner et al., 2000)
Simulated years	12 (624 weeks), 50 (260 weeks), 100 (5200 weeks)	

*Continued on the next page

Table B1: Parameter setup – continuation

Parameter	Values	Reference(s)
Pathogen release	random week of the 2nd year	
Mean number of reproductive females	4.5	(European Food Safety Authority, 2009; Howells & Edwards-Jones, 1997; Sodeikat & Pohlmeyer, 2003)
Habitat quality range	[0, 9]	
Initial mean density	5 individuals/km²	(Kramer-Schadt et al., 2009)
Initial age distribution	see Table B4	(Kramer-Schadt et al., 2009)
Age blur in initial individuals	± 3 weeks	
Landscape dynamic (M2, M3)	Autocorrelated, Random No dynamic	
Max survival time under low resources S_{max}	{5,10,15,20,25} weeks 10 weeks	
Level of resource mismatch	{0,25,50,75,100} % {0,100} %	
Mutation rate	0.01	
Transmission factor	See table B5	
Survival times	See table B5	

Table B2: Monthly reproduction probabilities (Boitani et al., 1995) used to stochastically determine the number of breeding females.

Month	Jan	Feb	Mar	Apr	May	Jun	Jul	Aug	Sep	Oct	Nov	Dec
Number of weeks	4	4	5	4	4	5	4	4	5	5	4	4
Reproduction probability	0.0	0.1	0.23	0.34	0.07	0.08	0.06	0.03	0.03	0.0	0.0	0.0

Table B3: Breed count distribution (Bieber & Ruf, 2005) used to estimate litter sizes.

Litter size	0	1	2	3	4	5	6	7	8	9	10	0
Probability	.01306	.06915	.01629	.24994	.24994	.01629	.06915	.01910	.00343	.0004	.00002	.01306

Table B4: Initial age distribution (Kramer-Schadt et al., 2009) used to initialize each model run.

Age (years)	1	2	3	4	5	6	7	8	9	10
Proportion	0.38	0.24	0.15	0.09	0.06	0.03	0.02	0.01	0.01	0.01

Table B5: Pathogen strains with their respective transmission factor and the survival time (weeks) they impose on infected hosts.

Strain	1	2	3	4	5	6	7	8	9	10	11	12
Transmission factor	.0006	.0007	.0008	.0009	.001	.002	.003	.004	.006	.007	.007	.007
Survival time (weeks)	14	13	11	11	10	9	8	6	3	3	2	1

References

Artois, M., Depner, K.R., Guberti, V., Hars, J., Rossi, S., Rutili, D., 2002. Classical swine fever (hog cholera) in wild boar in Europe. Rev. Sci. Tech. OIE 21, 287–303. https://doi.org/10.20506/rst.21.2.1332

Bieber, C., Ruf, T., 2005. Population dynamics in wild boar *Sus scrofa* : ecology, elasticity of growth rate and implications for the management of pulsed resource consumers: *Population dynamics in wild boar*. Journal of Applied Ecology 42, 1203–1213. https://doi.org/10.1111/j.1365-2664.2005.01094.x

Boitani, L., Mattei, L., Nonis, D., Corsi, F., 1994. Spatial and Activity Patterns of Wild Boars in Tuscany, Italy. Journal of Mammalogy 75, 600–612. https://doi.org/10.2307/1382507

Depner, K.R., Hinrichs, U., Bickhardt, K., Greiser-Wilke, I., Pohlenz, J., Moennig, V., Liess, B., 1997. Influence of breed-related factors on the course of classical swine fever virus infection. Veterinary Record 140, 506–507. https://doi.org/10.1136/vr.140.19.506

Depner, K.R., Müller, T., Lange, E., Staubach, C., Teuffert, J., 2000. Transient classical swine fever virus infection in wild boar piglets partially protected by maternal antibodies. Dtsch Tierarztl Wochenschr 107, 66–68.

Durio, P., Gallo Orsi, U., Macchi, E., & Perrone, A. (2014). Structure and monthly birth distribution of a wild boar population living in mountainous environment. Journal of Mountain Ecology, 3(0). Retrieved from http://www.mountainecology.org/index.php/me/article/view/112

EFSA (European Food Safety Authority). (2009). Control and eradication of Classical Swine Fever in wild boar. European Food Safety Authority Journal, 932(EFSA-Q-2007-200), 1–18. Retrieved from https://efsa.onlinelibrary.wiley.com/doi/abs/10.2903/j.efsa.2009.932

Fernández, N., Kramer-Schadt, S., Thulke, H.-H., 2006. Viability and Risk Assessment in Species Restoration: Planning Reintroductions for the Wild Boar, a Potential Disease Reservoir. E&S 11, art6. https://doi.org/10.5751/ES-01560-110106

Fernández-Llario, P., Carranza, J., Mateos-Quesada, P., 1999. Sex allocation in a polygynous mammal with large litters: the wild boar. Animal Behaviour 58, 1079–1084. https://doi.org/10.1006/anbe.1999.1234

Fletcher, R.J., 2006. Emergent properties of conspecific attraction in fragmented landscapes. The American naturalist 168, 207–219. https://doi.org/10.1086/505764

Focardi, S., Toso, S., Pecchioli, E., 1996. The population modelling of fallow deer and wild boar in a Mediterranean ecosystem. Forest Ecology and Management 88, 7–14. https://doi.org/10.1016/S0378-1127(96)03804-2

Gaillard, J. M., Vassant, J., & Klein, F. (1987). Quelques caractéristiques de la dynamique des populations de sangliers (Sus scrofa scrofa) en milieu chassé. Gibier, Faune Sauvage / ONC, Office National de La Chasse, 4, 31–47.

Grimm, V., Berger, U., Bastiansen, F., Eliassen, S., Ginot, V., Giske, J., Goss-Custard, J., Grand, T., Heinz, S.K., Huse, G., Huth, A., Jepsen, J.U., Jørgensen, C., Mooij, W.M., Müller, B., Pe'er, G., Piou, C., Railsback, S.F., Robbins, A.M., Robbins, M.M., Rossmanith, E., Rüger, N., Strand, E., Souissi, S., Stillman, R.A., Vabø, R., Visser, U., DeAngelis, D.L., 2006. A standard protocol for describing individual-based and agent-based models. Ecological Modelling 198, 115–126. https://doi.org/10.1016/j.ecolmodel.2006.04.023

Grimm, V., Berger, U., DeAngelis, D.L., Polhill, J.G., Giske, J., Railsback, S.F., 2010. The ODD protocol: A review and first update. Ecological Modelling 221, 2760–2768. https://doi.org/10.1016/j.ecolmodel.2010.08.019

Grimm, V., Railsback, S.F., Vincenot, C.E., Berger, U., Gallagher, C., DeAngelis, D.L., Edmonds, B., Ge, J., Giske, J., Groeneveld, J., Johnston, A.S.A., Milles, A., Nabe-Nielsen, J., Polhill, J.G., Radchuk, V., Rohwäder, M.-S., Stillman, R.A., Thiele, J.C., Ayllón, D., 2020. The ODD Protocol for Describing Agent-Based and Other Simulation Models: A Second Update to Improve Clarity, Replication, and Structural Realism. JASSS 23, 7. https://doi.org/10.18564/jasss.4259

Howells, O., Edwards-Jones, G., 1997. A feasibility study of reintroducing wild boar Sus scrofa to Scotland: Are existing woodlands large enough to support minimum viable populations. Biological Conservation 81, 77–89. https://doi.org/10.1016/S0006-3207(96)00134-6

Jędrzejewska, B., Jędrzejewski, W., Bunevich, A.N., Miłkowski, L., Krasiński, Z.A., 1997. Factors shaping population densities and increase rates of ungulates in Bialowieza Primeval Forest (Poland and Belarus) in the 19th and 20th centuries. Acta Theriologica.
Jezierski W., 1977: Longevity and mortality rate in a population of wild boar. Acta theriol., 22, 24: 337—348

Kramer-Schadt, S., Fernández, N., Eisinger, D., Grimm, V., Thulke, H.-H., 2009. Individual variations in infectiousness explain long-term disease persistence in wildlife populations. Oikos 118, 199–208. https://doi.org/10.1111/j.1600-0706.2008.16582.x

Kürschner, T., Scherer, C., Radchuk, V., Blaum, N., Kramer-Schadt, S., 2021. Movement can mediate temporal mismatches between resource availability and biological events in host–pathogen interactions. Ecol. Evol. 11, 5728–5741. https://doi.org/10.1002/ece3.7478

Leaper, R., Massei, G., Gorman, M.L., Aspinall, R., 1999. The feasibility of reintroducing Wild Boar (Sus scrofa) to Scotland. Mammal Review 29, 239–258. https://doi.org/10.1046/j.1365-2907.1999.2940239.x

Liess, B., 1987. Pathogenesis and epidemiology of hog cholera. Ann Rech Vet 18, 139–145.

Melis, C., Szafranska, P.A., Jedrzejewska, B., Barton, K., 2006. Biogeographical variation in the population density of wild boar (Sus scrofa) in western Eurasia. J Biogeography 33, 803–811. https://doi.org/10.1111/j.1365-2699.2006.01434.x

Moennig, V., Floegel-Niesmann, G., Greiser-Wilke, I., 2003. Clinical signs and epidemiology of classical swine fever: a review of new knowledge. Vet J 165, 11–20. https://doi.org/10.1016/s1090-0233(02)00112-0

Morelle, K., Podgórski, T., Prévot, C., Keuling, O., Lehaire, F., Lejeune, P., 2015. Towards understanding wild boar *S us scrofa* movement: a synthetic movement ecology approach: A review of wild boar *Sus scrofa* movement ecology. Mammal Review 45, 15–29. https://doi.org/10.1111/mam.12028

Moretti, M., 2014. Birth distribution, structure and dynamics of a hunted mountain population of Wild boars (Sus scrofa L.), Ticino, Switzerland. Journal of Mountain Ecology 3.

Pepin, K.M., Davis, A.J., Beasley, J., Boughton, R., Campbell, T., Cooper, S.M., Gaston, W., Hartley, S., Kilgo, J.C., Wisely, S.M., Wyckoff, C., VerCauteren, K.C., 2016. Contact heterogeneities in feral swine: implications for disease management and future research. Ecosphere 7. https://doi.org/10.1002/ecs2.1230

Rossi, S., Pol, F., Forot, B., Masse-provin, N., Rigaux, S., Bronner, A., Le Potier, M.-F., 2010. Preventive vaccination contributes to control classical swine fever in wild boar (*Sus scrofa* sp.). Veterinary Microbiology 142, 99–107. https://doi.org/10.1016/j.vetmic.2009.09.050

Saura, S., Martínez-Millán, J., 2000. Landscape patterns simulation with a modified random clusters method. Landscape Ecology 15, 661–678. https://doi.org/10.1023/A:1008107902848

Sodeikat, G., Pohlmeyer, K., 2003. Escape movements of family groups of wild boar *Sus scrofa* influenced by drive hunts in Lower Saxony, Germany. Wildlife Biology 9, 43–49. https://doi.org/10.2981/wlb.2003.063

Spitz, F., Janeau, G., 1990. Spatial strategies: an attempt to classify daily movements of wild boar. Acta Theriologica 35, 129–149.

Wilensky, U. (1999). NetLogo (Version 6.0.4). Retrieved from http://ccl.northwestern.edu/netlogo/

B2 Additional figures

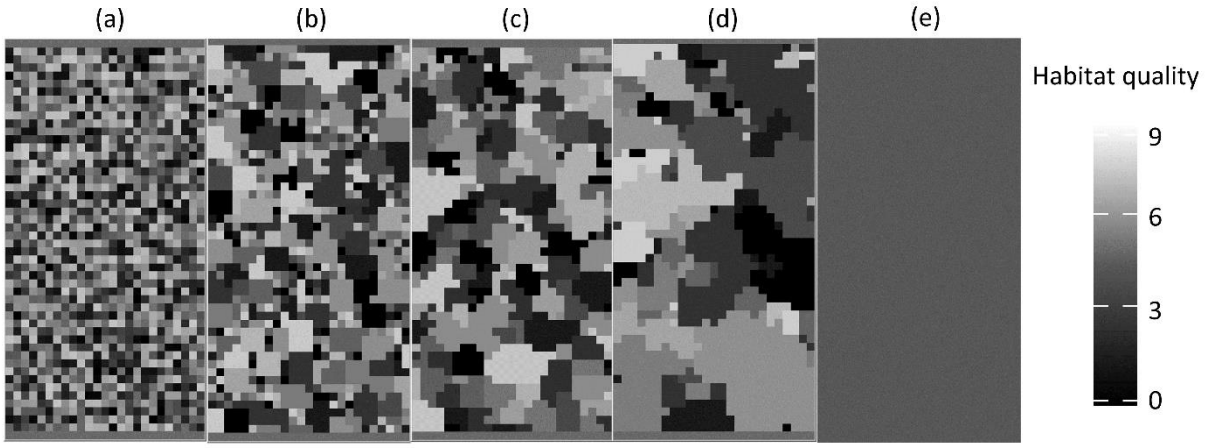

Figure B4: Example landscape configurations and habitat clustering used in the model, with (a) randomly distributed habitat cells, (b) small clusters, (c) medium clusters, (d) large clusters, and (e) a homogenous landscape. The colour gradient shows the habitat quality (i.e. the number of breeding females supported by the individuals landscape cells).

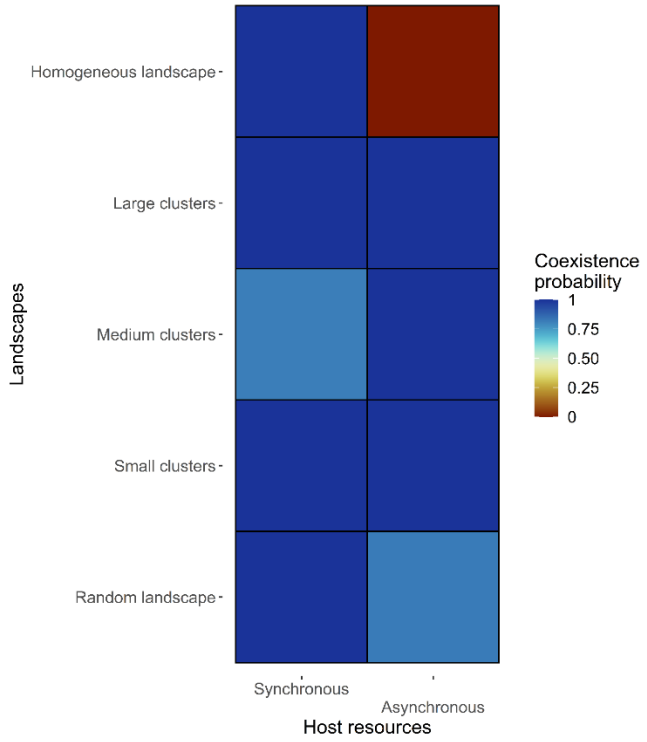

Figure B5: Coexistence probability for host and pathogen (colour gradient) for all landscape scenarios and separated for synchronous and asynchronous host resources. In homogenous landscapes, due to a collapse of the host population, host-pathogen coexistence was not achievable in the current model-framework and therefore excluded.

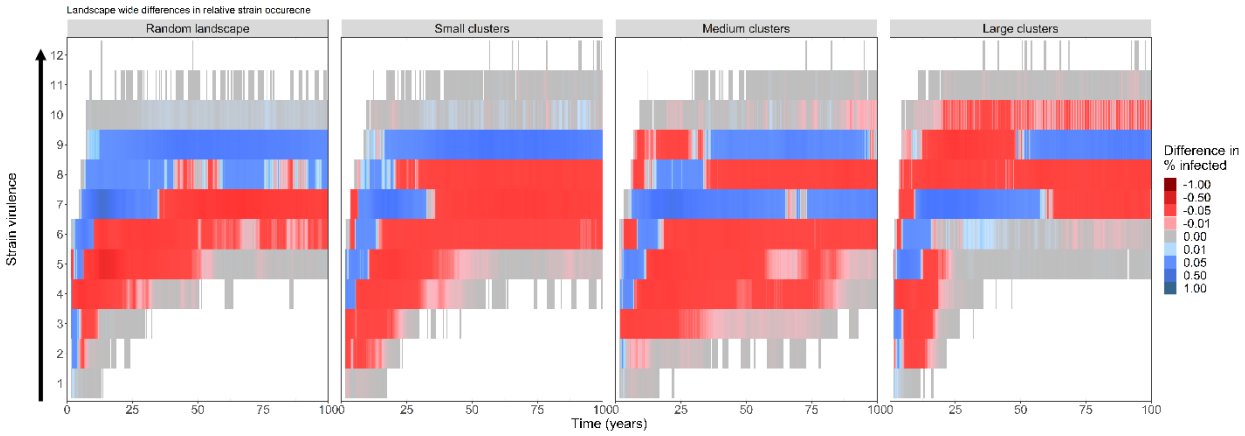

Figure B6: Differences in the proportion of infected individuals with each strain in the landscape to highlight the effect of asynchronous scenarios. The blue colour gradient means that a strain was more dominant in synchronous (T_{lag} = 0) scenarios while the red colour gradient shows that a strain was more dominan in asynchronous scenarios (T_{lag} = 100). Gray means there was no difference in strain proportions between both scenarios.

L

APPENDIX C
SUPPLEMENTARY MATERIAL FOR CHAPTER 4

C1 Model description (ODD protocol)

The classical swine fever (CSF) wild boar model is a combination of a spatially explicit, stochastic, agent-based model for wild boars (*Sus scrofa* L.) and an epidemiological model for the CSF virus. The model was implemented in NetLogo (Wilensky, 1999) and is documented following the ODD protocol (Grimm et al., 2006, 2010, 2020).

The ODD protocol below includes changes in model description across three wild boar / CSF eco-epidemiological models. The main basis is the model "SwiFCoIBM_Evo" (M1 and black text throughout, Kürschner et al. 2022 under review) was developed to assess the effects of host movement and landscape structure, dynamic and evolution of traits on disease dynamic. It is based on previous model iterations and ODD protocols by Scherer et al., (2020) and Kürschner et al., (2021).

The model described in this protocol ("SwiFCoIBM_Emp"; M2 and blue text throughout) was developed to apply previous model implementations to realistic landscapes and empirical outbreak data, for example a CSF outbreak in the Nort-East German state Mecklenburg-Vorpommern (Scherer et al., 2019). Many processes, submodels and their descriptions such as movement behaviour and basic pathogen transmission used in M2 remain mostly unaltered from previous implementations and ODD protocols in Scherer et al., (2020).

As a note, while in some instance (as seen for example in 1. Purpose) parts of the previous models are replaced, in other instances and submodels (as seen in 2. Entities, state variables and scales) M2 is a mixture of old and new versions.

1 Purpose

[1]M1: The model investigates the effect dynamic resource landscape and temporal shifts on a multi-strain pathogen system, pathogen evolution and pathogen trade-offs. Particularly, how temporal mismatches between optimal resource availability and biological events affect host-pathogen coexistence and pathogen spread.

M2: The model aims to match patterns observed in CSF outbreak in Mecklenburg-Vorpommern (Scherer et al., 2019) with simulated data using habitat suitability map of Mecklenburg-Vorpommern as a basis for initial wild boar distribution and density. Specifically, we wanted to analyse the effect of

[1]This ODD describes M2, so that 'Purpose' for M1 is obsolete. It is kept in the ODD to better understand how the design of the model developed

different decision-making processes in host movement on disease outbreak patterns, pathogen persistence, and transmission.

2 Entities, state variables and scales

The model entities are spatial units, or grid cells, and wild boars. Grid cells are characterized by habitat quality in terms of breeding capacity, i.e., the number of female boars that are allowed to have offspring (Jedrzejewska et al., 1997). Thereby, local host density is in the model, i.e., increasing numbers of fertile females can breed only until breeding capacity is reached. A grid cell represents about 2 km × 2 km, encompassing an average home range area of a boar group (Leaper et al., 1999).

Wild boars are characterized by sex, age in weeks, location, demographic status (e.g., breeding, dispersing and ranging) and health status. Three age classes are distinguished: piglet (< 34 weeks), subadult (between 34 weeks and < 1 year for females and < 2 years for males) and adult. Location is defined by the grid cell the wild boar inhabits. The health status of the individuals is described by an SIR epidemiological classification (susceptible; transiently infected; lethally infected with individual infectious period; immune by surviving the infection or by maternal antibodies). Females, which are at least subadult, may be assigned as breeders according to the breeding capacity of their family group's cell. Subadult wild boars may disperse during the dispersal period dependent on their sex and demographic status (disperser or non-disperser). In the model versions simulating explicit movement, males become ranging individuals (i.e., move solely) once they are adult and thereby change their locations every time step.

M1, M2: One time step corresponds to the approximate CSF incubation time of one week (Artois et al., 2002; Moennig et al., 2003) while simulations usually run for 100 years (5200 weeks) or 11 years (572 weeks) with the virus being released in the second year (week 53-104) to a defined boar group to ensure the same distance to the centre of the landscape and an established spatial population structure. The model landscape consists of 100 km × 50 km (50 × 25 grid cells) or a 128 x 90 grid cell approximation of Mecklenburg-Vorpommern and the surrounding area (Fernández et al., 2006; Scherer et al., 2019).

3 Process overview and scheduling

Each time step, the following procedures are executed by the wild boars in the given order: pathogen transmission, ranging movement, natal dispersal of males and females, resource-based host movement, host reproduction, general host mortality, resource-based host mortality, ageing, and disease course

(Figure C1). Females are assigned to breed on a week to week basis, with the prerequisite that they have not bread previously in the current year.

4 Design concepts

Basic principles

Both processes of the host and the pathogen are simulated with a given stochasticity which resembles natural conditions. Disease transmission for groups is modelled density-dependent (see Eq. C1 and C2). Heterogeneous landscape scenarios were simulated using neutral landscape model algorithms.

Emergence

Wild boar population dynamics emerge from individual behaviour, resulting from age- and sex-dependent movement behaviours (natal dispersal and ranging) as well as age-dependent seasonal reproduction, survival probabilities and is mitigated by the underlying dynamic resource landscape. The epidemic course emerges from different virus transmission probabilities, infectious periods wild boar movement behaviours (only M2) as well as individual stochastic disease courses.

Adaptation

Movement rules either reproduce observed movement behaviours (phenomenological approach, e.g., correlated random walk with a given directional persistence) or are based on decisions in response to spatial structure or conspecifics (mechanistic approach, e.g., the competition-driven movement rule implicitly seeks to increase habitat quality in relation to conspecifics).

The number of breeding females per cell is determined by the habitat quality of the cell and the number and age of the reproductive females within the cell.

Objectives

The exact way individuals decide where to move depend on the applied movement rule (see section "Ranging movement"). In general, ranging individuals (i.e., adult males) using decision-based movement rules move into the neighbouring cell with the highest weight (which is defined by the applied movement rule). Individuals' decisions are not perfect but may be a random direction depending on the directional persistence ρ (probability to move randomly = 1 - ρ, set to 0.7).

Dispersing individuals search for empty (unoccupied) cells (in case of female dispersers) or join other groups that are below their cells' carrying capacity (in case of male dispersers).

Learning

There is no learning implemented in our model.

Prediction

There is no need to predict future environmental conditions.

Sensing

Individuals moving through the landscape may base their decisions on the underlying landscape structure in terms of habitat quality (or, synonymously, breeding capacity B) or number of conspecifics. Moving individuals can sense all that information from their own cell and surrounding cells but the decision might be random (implicitly due to insufficient information) depending on the assumed directional persistence ρ.

Interaction

Based on the transmission rates, interactions between individuals might lead to virus transmission from an infected to a susceptible individual. Reproduction is density-and age-dependent with the oldest females giving birth first. Thus, if the number of reproducible females exceeds a cell's breeding capacity, interaction leads to repressed reproduction.

Stochasticity

Demographic and behavioural parameters are imposed via probability distributions to account for variation in the biological processes. Stochastic individual disease courses and infectious periods are modelled explicitly because variation in the disease outcome between individuals was identified to be essential for virus endemicity without reservoirs (Kramer-Schadt et al., 2009). Movement decisions are based on a random component (with 30% of the decisions being random).

Collectives

Individuals that are not ranging between home ranges (i.e., all individuals but adult males) form groups within their cell that experience density-dependent transmission probabilities. These groups are formed by reproducible females and their offspring. During natal dispersal, male subadults may join those groups while female subadults may form new groups.

Observation

M1 & M2: To evaluate model outcomes, we measure several properties of the host-virus system at each time step of the simulation. These outputs include number of individuals for each class of age (piglet, subadult, adult), demographic (resident, ranging) and health status (susceptible, infected, recovered) and their combinations. Furthermore, sex ratio, number of new infections, number of cells with infectious individuals, the last week of infection and the cumulative time (i.e., how many weeks in total) of infected hosts per habitat cell are recorded. From this output, duration of an outbreak, probability of disease persistence (i.e., the virus being present in the system until the end of simulations), outbreak size for different classes, as well as density distribution of infected hosts can be estimated. Further recorded outputs were the strain carried by individuals hosts in total and per cell, number of infected, immune and susceptible per cell and time, cumulative per cell, dead individuals per cell and time, health status of dead individuals per cell and cause of host death per cell.

5 Initialization

M1 & M2: We simulate landscapes with four different levels of spatial heterogeneity in habitat quality: homogeneous, random, four clustered landscape scenarios using a random cluster algorithm (very small, small, medium and large clusters, respectively; Saura & Martínez-Millán, 2000; Table C1) generated using the R package NLMR (Sciaini et al., 2018). In homogeneous landscapes, one boar family group was allocated to each cell with an average breeding capacity B of 4.5 females, resulting in the reported density of approximately 20 boars per cell or 5 boars per km² (European Food Safety Authority, 2009; Howells & Edwards-Jones, 1997; Melis et al., 2006; Sodeikat & Pohlmeyer, 2003). In heterogeneous landscapes a breeding capacity B between 0 and 9 was assigned to each of the 2500 grid cells ($B \in \{0;9\}$). In case B is a floating point number, the number of individuals is determined stochastically based on the remainder. In M2, the habitat suitability map of MVP is loaded as a basis for the breeding capacity B ranging from 0 to 9. Initial age distribution was obtained from the results of a 100-year model run conducted by (Kramer-Schadt et al., 2009); Table C2), the sex ratio was balanced (i.e. probability of 0.5 to be either male or female). Wild boar density reflects long-term average values of densely populated Central European habitats (European Food Safety Authority, 2009; Howells & Edwards-Jones, 1997; Melis et al., 2006; Sodeikat & Pohlmeyer, 2003). Group size was initialised according to the cells carrying capacity K_i that is 4.5 times its breeding capacity B_i.

6 Input

[1]M1: The model does not include external input representing environmental conditions changing over time.

M2: The model uses a wild boar habitat suitability map of Mecklenburg-Vorpommern (Scherer et al. 2019, Fernandez et al. 2006).

7 Submodels

Initial infection (pathogen release)

M1: The virus is released to the population by infection of several wild boar groups (i.e., cells), starting with the centre of the landscape (i.e., cell with the coordinates x = 24 and y = 13) as well as three randomly selected cells in the vicinity. The release is scheduled in a random week of the second year of the model run.

M2: The virus is released to the population by infection of several wild boar groups (i.e., cells), in the central northern area of Mecklenburg-Vorpommern as well as three randomly selected cells in the vicinity. The release is scheduled in a random week of the second year of the model run.

Pathogen transmission

M1: This model uses 12 arbitrarily categorized viral strains that differ in their transmission potential and the survival time of the host they infect (Table C5). Weekly infection pressure λ_{is} for each susceptible individual in cell i is determined by the probability of being infected by an infectious group mate β_w (within-group transmission probability) and the probability of being infected by an infectious individual in one of the eight neighbouring cells $\frac{\beta_w}{10}$ (between-group transmission probability):

$$\lambda_{is} = 1 - (1 - (\beta_w + T_s))^{I_s} \cdot (1 - \frac{(\beta_w + T_s)}{10})^{\Sigma_i I_{js}} \quad [C1]$$

where I_i is the number of infectious group mates and I_j is the numbers of infectious hosts in the j^{th} adjacent cell. The resulting probability value λ_{is} provides the parameter of a binomial chance process to decide whether a susceptible animal will be infected. Due to the model now having multiple strains with different infection probabilities, there is now the subscript s added to all relevant terms, indicating that those values are now strain specific. Therefore, we calculate infection pressures for all strains separately and only take individuals with the respective strains into consideration when determining I_s for within

[1] This ODD describes M2, so that '6 Input' for M1 is obsolete. It is kept in the ODD to better understand how the design of the model developed

group or I_{Js} for between group transmission. Since the number of infected hosts per strain can be significantly smaller than the sum of all infected host individuals, we added a strain specific factor T_s (Table C5) to infection pressure calculation so ensure transmissibility of the individual strains, while the base transmission probability β_w (0.0208) remained unchanged from model M1 and M2.

CSF shows a variety of disease courses on the individual level (Depner et al., 1997; Liess, 1987). Therefore, in our model the disease course is specified for each individual. The disease course sub model is described by two parameters: individual case mortality M and the infectious period of lethally infected hosts. One week after infection the host is stochastically assigned as lethally infected, with a probability M an individual can become non-infectious and gains life-long immunity. M is age specific (Dahle & Liess 1992): for adults the probability is decreased to $M_a=M^2$ and for piglets increased to $M_p=\sqrt{M}$ while it is unchanged for subadults $M_s=M$. The individual infectious period is strain specific and selected from table C5.

Lethally infected hosts remain infectious until death. Offspring from immune female breeders gets maternal antibodies and is thus immune for the first eight to twelve weeks after birth (t_{anti}). The number of weeks of immunisation due to maternal antibodies is randomly assigned for those piglets.

M2: In this model version, presented here, infection might be translocated within the host population. Because ranging movements are performed by adult males only, the strain specific transmission probability λ_{is} was transformed to account for these sex-and age-dependent transmission probabilities. Therefore, for all individuals but adult males the weekly probability of being infected by infectious group mates (but not by infectious ranging males) is simply β_{ws} adjusted for a strain specific transmission probability T_S since females and their group follow a staying rule with the almost all contacts within the group (Pepin et al., 2016; Spitz & Janeau, 1990). The accumulated probability λ_{is} for susceptible non-ranging individuals is thus reduced to:

$$\lambda_i = 1 - (1 - \beta_w + T_S)^{I_i} \qquad [C2]$$

Where I is the number of infectious group mates (but not infectious ranging males which do not belong to any group).

For adult, ranging males, the individual probability of virus transmission during movements β_m (i.e. being infected by an infectious animal in a cell moving through as well as the probability of infecting a susceptible individual while passing the cell) was fitted to account for the resuming transmission probabilities (i.e. the remaining within- and between-group transmission probabilities of the classical

model, see Eq. C2). We calibrated one constant transmission probability (i.e. $\beta_w = \beta_m$, afterwards just referred to as simply β) to result in the comparable distributions of the basic reproduction number (R_0, number of secondary infections) as in the classical model. The previous model implementation by Scherer et al. (2020), that included explicit host movement and transmission estimated $\beta = 0.022$ as the best results for different scenarios of infection and movement rules. Individual per step transmission probability $\beta_{m,i}$ is related to the number of steps the animal makes. Therefore, the infection probability for cells passed by infected individuals is scaled to the individual movement distance $d_{m,i}$ (see section "Ranging movement") and was adjusted for strain specific transmission through T_s:

$$\beta_{m,i} = \frac{\beta + T_s}{d_{m,i}}. \quad [C3]$$

By doing so, infection probability decreases with increasing movement distance which relates to the time an animal is able to spend within each cell and thus to transmit the virus on its way.

CSF shows a variety of disease courses on the individual level (Depner et al., 1997; Liess, 1987). Therefore, in our model the disease course is specified for each individual. The disease course sub model is described by two parameters: individual case mortality M and the infectious period of lethally infected hosts. One week after infection the host is stochastically assigned as lethally infected, with a probability M an individual can become non-infectious and gains life-long immunity. M is age specific (Dahle & Liess 1992): for adults the probability is decreased to $M_a=M^2$ and for piglets increased to $M_p=\sqrt{M}$ while it is unchanged for subadults $M_s=M$. The individual infectious period is strain specific and selected from table C5.

Pathogen evolution

During every transmission event, the pathogen can evolve into a different strain with different strain specific variables compared to the parental strain. Once a host individual is becoming infected by a specific strain, an evolution check is applied, whereby with a mutation rate of 0.01 (table C1) the strain can evolve. If the strain evolves, the new strain is selected from a normal distribution with a standard deviation of 1 around the parental strain. The resulting strain will be closely related to the parental strain. If the transmitted strain does not evolve, it is transmitted directly without any changes to a new host.

Vaccination

All cells that are overlapping with the "vaccination area" (Figure C4) are designated vaccination cells. Starting 52 timesteps after pathogen release a percentage of susceptible adults (vc_adult) and susceptible subadults (vc_subadult) are set to immune (Table C1). This process is repeated every 13 timesteps.

Ranging movement

only M2; adapted from Scherer et al., (2020): While adult females move mainly within their family group (*staying strategy*), adult males follow a *ranging strategy* and move solitary (Spitz & Janeau 1990, Figure C2). Ranging distances vary between males with a mean distance of 24 km per week and capability for long-distance behaviour with up to 84 km per week (Morelle et al. 2015). For each adult male *i*, an individual movement distance $d_{m,i}$ was drawn from the median of the Weibull distribution given by *b*(1 - ln(1 - U[0,1]))^k* with a scale of b = 26 and a shape of k = 1.3, resulting in a mean of 12 cells and truncated to the maximum movement distance D_{max} of 42 cells (with a cell being 2 km in diameter). To study effects of inter-cell movement on disease dynamics, we implemented three different movement strategies. In general, ranging individuals move until the individual weekly movement distance is reached or there is no better decision to make and only into cells with a positive habitat quality (B > 0). Individuals stop moving if there is no cell available. If there is a tie (i.e., two or more cells with equal attractiveness), one of those cells is chosen randomly.

(a) Habitat-Driven Correlated Random Walk (HDCRW): In a basic CRW, subsequent movement directions are correlated such that highly correlated movement paths are nearly straight (Turchin 1998; Figure C3a). This movement model improves the RW approach by incorporating directional persistence that moving animals very frequently exhibit (Figure C3; Kareiva & Shigesada 1983). The direction of a step is drawn from a wrapped Cauchy distribution with a mean direction equal to the previous direction (Fletcher, 2006):

$$\theta_{t,i} = \theta_{t-1,i} + 2 \cdot arctan\left(\frac{1-\rho}{1+\rho} \cdot \pi \cdot U(-0.5,0.5)\right) \quad [C_5]$$

Where $\theta_{t,i}$ and $\theta_{t-1,i}$ are the headings of individual *i* of the next or previous step, respectively, ρ is a parameter related to the concentration around the mean direction (i.e., ρ = 1 results in a straight line and ρ = 0 equals a RW), and U(-0.5,0.5) is a uniformly distributed random number between -0.5 and 0.5. In the habitat-driven CRW, individuals decide among their target cells based on the habitat quality by selecting the best possible habitat cell and perform a CRW for long-distance movement.In case individuals reach the border of the simulated landscape, the Individual is reflected in a 90° angle followed by reset and recalculation of $\theta_{t,I}$ to avoid aggregation around the landscape borders.

(b) Habitat-Driven Movement (HDM): A reasonable hypothesis is that a selective animal should choose high quality cells for its home range. The distribution and abundance of resources greatly affect movement patterns of several animal species and has also been reported for wild boars (Morelle et al. 2015). Assuming higher food resources and better shelter in high quality habitat, individuals decide

among their neighbouring cells based on the habitat quality (Figure C3b). The parameter ρ here relates to the accuracy of an individual estimating the quality of the focal and neighbouring cells, with the movement decision in ρ-1 cases being purely random.

(c) Competition-Driven Movement (CDM): Effective habitat quality might be lower due to competition with conspecifics. Thus, competition-driven movement is biased to cells with higher net habitat quality and was implemented as negative density dependence. Movement weights were calculated as the ratio of number of conspecifics in the focal cell and the carrying capacity (*K*), i.e., the potential maximum group size of the cell (Figure C3c).

For all movement strategies, ρ was fixed as 0.7, i.e., 30% of the decisions were made randomly.

Natal dispersal

Herd splitting, where subadult individuals may move together to search for or form new groups, is performed in specified weeks of the. The timing of these events is sex-dependent: Subadult females without offspring perform their natal dispersal in the 29th week of the year, while subadult males disperse during the 17th week. In the given week of the year, all herds to split are extracted, matching the conditions of containing at least a specified number of subadults N_{disp} to move (either male or female). For female dispersal, only cells exceeding the breeding capacity *B* are evaluated. For each of them, a habitat cell not exceeding carrying capacity *K* (for males) or without any family group (for females) within a Euclidean distance d_{disp} is selected randomly as new cell for the group, excluding the source cell (Figure C2). If there is no cell fulfilling these conditions, subadults stay within their group's cell.

Reproduction

Females reproduce once a year, depending on their age class. Individual females, which are at least subadult, reproduce depending on the season with a peak in March and no reproduction in winter from October to December (Boitani et al. 1995) (Table C2). Female individuals are checked for their breeding status on a weekly basis. All females not exceeding their habitat cells breeding capacity, starting with the oldest individuals, are allowed to breed. If an individual was assigned to breed the chance of reproduction at that time is drawn from monthly probabilities and the number of weeks in the month (Table C2).

Litter size is drawn from a pre-calculated truncated normal distribution (Table C1,3) and reduced to a constant fraction for infected individuals. Litter size of transient shedders and lethally infected hosts is multiplied with the reduction factor α_f.

Depending on the disease state of the breeding individual, its piglets disease states are adjusted. Susceptible individuals produce susceptible offspring, immune individuals produce immune offspring with maternal antibodies (see section "Pathogen state transition"). Transient shedders and lethally infected individuals yield offspring, each one lethally infected with a given probability of prenatal infection p_{pi}.

Mortality

Stochastic baseline mortality is age-dependent and adjusted to annual survival estimates found in the literature (Table C1). Per time step we apply the adjusted age-dependent mortality (m_{week}) to the individual:

$$m_{week} = 1 - (s_{year})^{1/52} \quad [C6]$$

In addition to the stochastic baseline mortality, each individual may die due to reaching a certain maximum age, or due to a lethal infection after a certain infection time span m (see section "Pathogen transmission").

A selected number of individuals K_{over} (see 7.10 Resource response for the selection) are subject to a variable, resource-based mortality with an increasing chance of mortality dependent on how long the individual is subject to low resource conditions up to a variable time limit S_{max} as well as the number of individuals (g_{act}) in relation to maximum group (g_{sus}) size and age.

$$m_{resource} = \frac{(g_{act} - g_{sus})}{100} * a * t_{over} \quad [C7]$$

With a being an age factor corresponding to the individuals being a piglet or adult/subadult and t_{over} the time the individual is part of the K_{over} individual pool. As well as a 100% mortality when t_{over} equals S_{max}.

Ageing

The ageing process iterates over all individuals. For each individual k, age T_k is incremented one week, and disease state transitions are performed. Females become subadult and adult at an age of 34 and 52 weeks, respectively, while males enter the subadult and adult age groups at an age of 21 and 104 week, respectively.

Disease course (pathogen state transition)

An individual i protected by maternal antibodies turns susceptible if reaching an age T_i of the protection time of t_{anti} (see section "Pathogen transmission"). After disease state transition the age of the infection is incremented by one week if the individual is not susceptible.

Landscape dynamic

M1: The autocorrelated landscape dynamic is superimposed over the different types of starting landscapes. Throughout each simulated year, resource availability in each cell increases in 5-weeks intervals for approximately 25 weeks and then declines in 5-weeks intervals for the next 25 weeks. The resource availability translates directly into the breeding capacity for each cell and can during the increase not exceed the maximum breeding capacity of 9 and cannot fall below 1 i.e., the habitat cannot become 0 during the course of a year. Additionally, barriers and matrix which have an assigned breeding capacity of 0 cannot become habitat.

The first week of the dynamic can be set fixed or can be set to also increment for each subsequent simulation run. The random landscape dynamic functions similar to the autocorrelated variant. Throughout each simulated year, resource availability in each cell changes randomly in 5-weeks intervals for approximately 50 weeks whereby each cell is allocated a random integer between 1 and 9. At the end of each year, the landscape resets to the original starting landscape.

M2: No landscape dynamic was applied.

Resource responses

If the group size exceeds the carrying capacity K in a cell, a dispersal event will be triggered. The likelihood of dispersal follows an age gradient where older females will try to disperse last. For male individuals, a random habitat cell not exceeding the carrying capacity K will be randomly selected within a Euclidean distance d_{disp} as new cell. For female individuals, the randomly selected habitat cell must fulfil the prerequisite of not hosting another family group. However, if an individual currently has offspring it and the offspring will stay at in their current cell. If there is no suitable habitat cell fulfilling these prerequisites within the distance d_{disp} the individuals will stay. Individuals are continuously selected for dispersal until the group size no longer exceeds the carrying capacity K. For a secondary response after the dispersal event (if applicable), a cell specific number of individuals K_{over} that is the difference between carrying capacity K and group size will be selected. The selection of these individuals

is age dependant where the oldest females are selected last. All selected individuals are subjected to an increasing age-dependant mortality (see mortality).

Figures

Flow chart of the SwiFCoIBM* models and its submodels (M1 & M2)

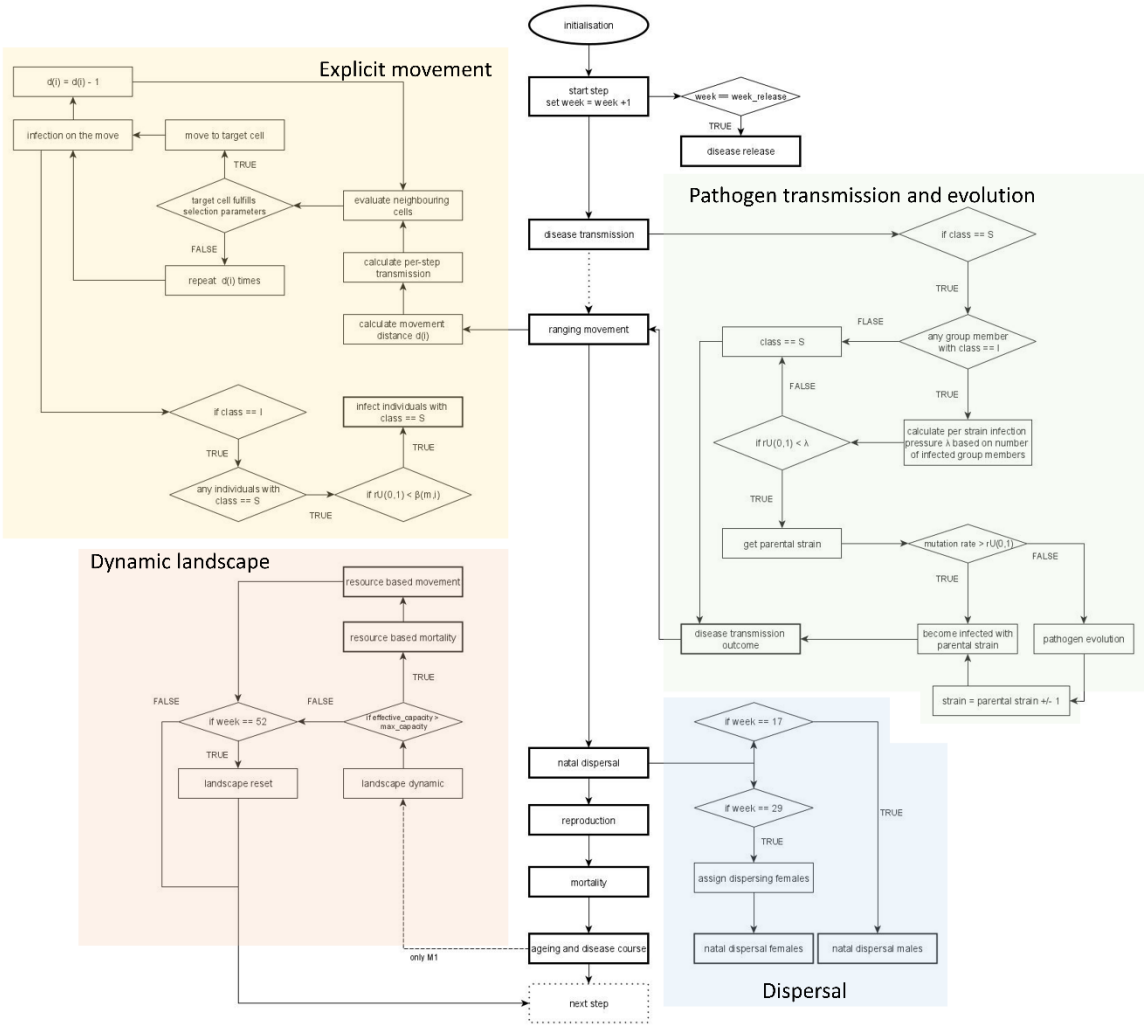

Figure C1: Flow chart of the agent-based, spatially explicit host-pathogen model "SwiFCoIBM*" and its submodels. This flow chart includes all previous model iterations and is visually compartmentalized (colours) into 4 branch-processes: Yellow – Processes for explicit host movement; Green – Pathogen transmission and evolution processes; Orange – Processes related to landscape and landscape dynamic; Blue – Dispersal processes.

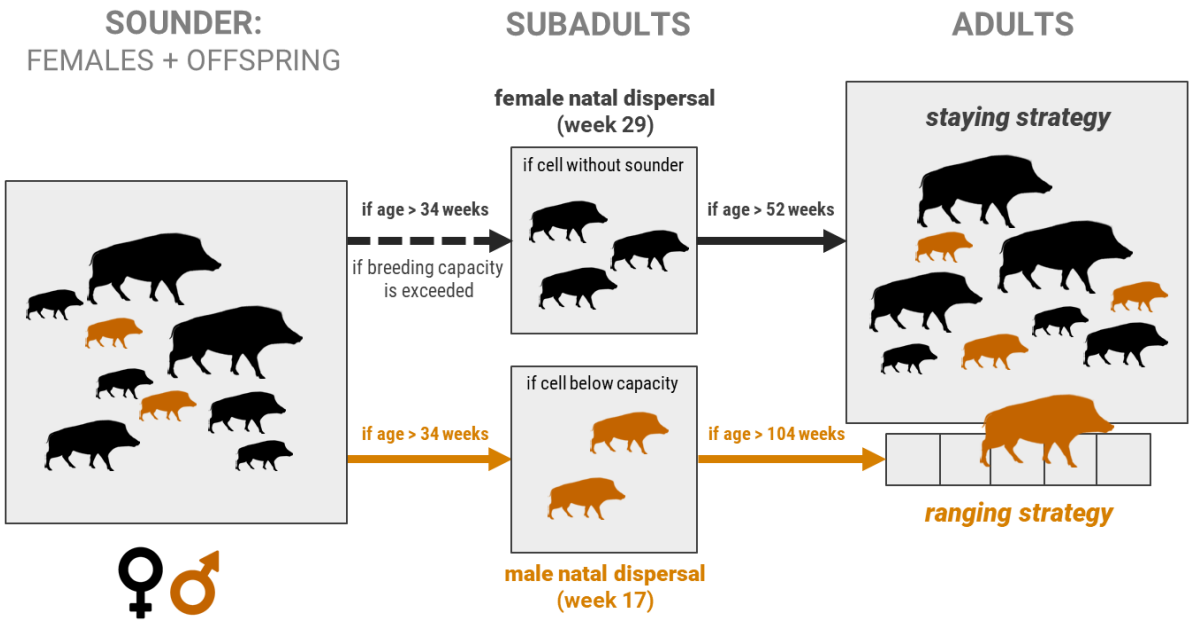

Figure C2 (Scherer et al., 2020): Schematic representation of different natal dispersal events of subadult wild boars and movement strategies of adult wild boars. The group of adult and subadult females and their offspring is called a sounder. If the breeding capacity of the sounders cell is exceeded, subadult females search in groups of 3 or more individuals for an unoccupied cell in a radius of three cells. Female wild boars reach their adulthood earlier (model assumption: if older than 1 year) and follow a staying strategy, thus not moving outside of the sounders cell (grey squares). Male wild boars always separate from the sounder when reaching the subadult age and move in groups of 2 or more to one of the cells below capacity in a radius of 3 cells. When becoming adult, male wild boars move solitary between home ranges.

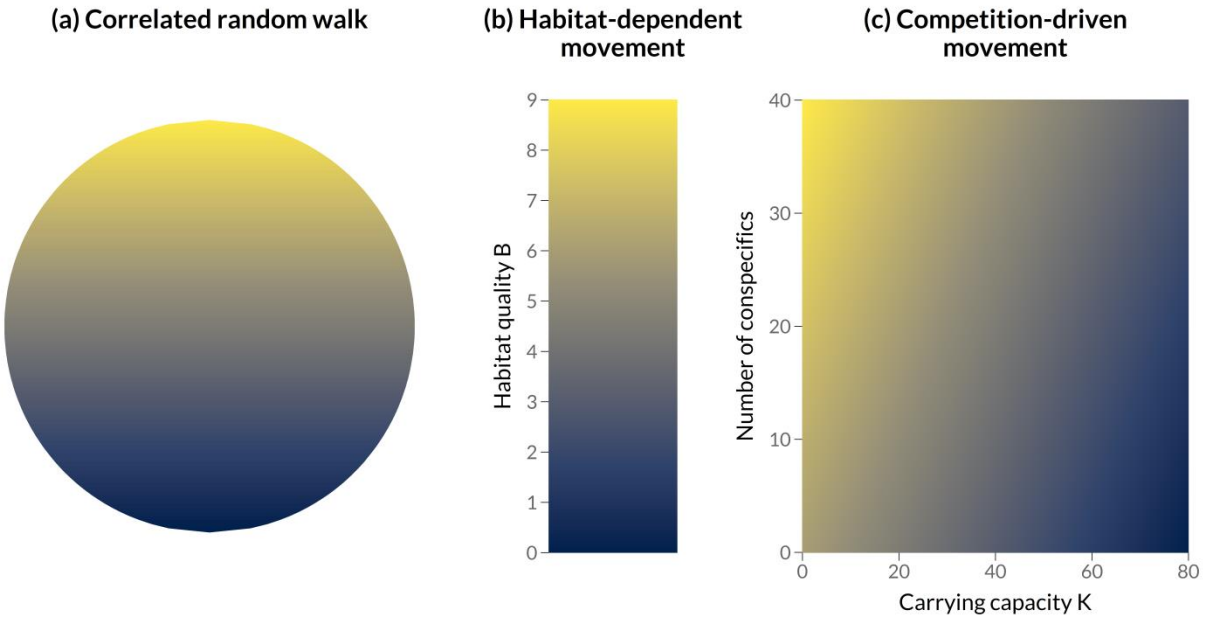

Figure C3 (Scherer et al., 2020): Movement assumptions used to model ranging behaviour of adult males. Probability of movement depends on the **(a)** direction of previous steps (Correlated Random Walk), **(b)** habitat quality B or **(c)** carrying capacity K in relation to the number of conspecifics. The lighter the colour, the higher the probability the individual chooses this cell. Movement decisions are furthermore driven by a random component determined by ρ.

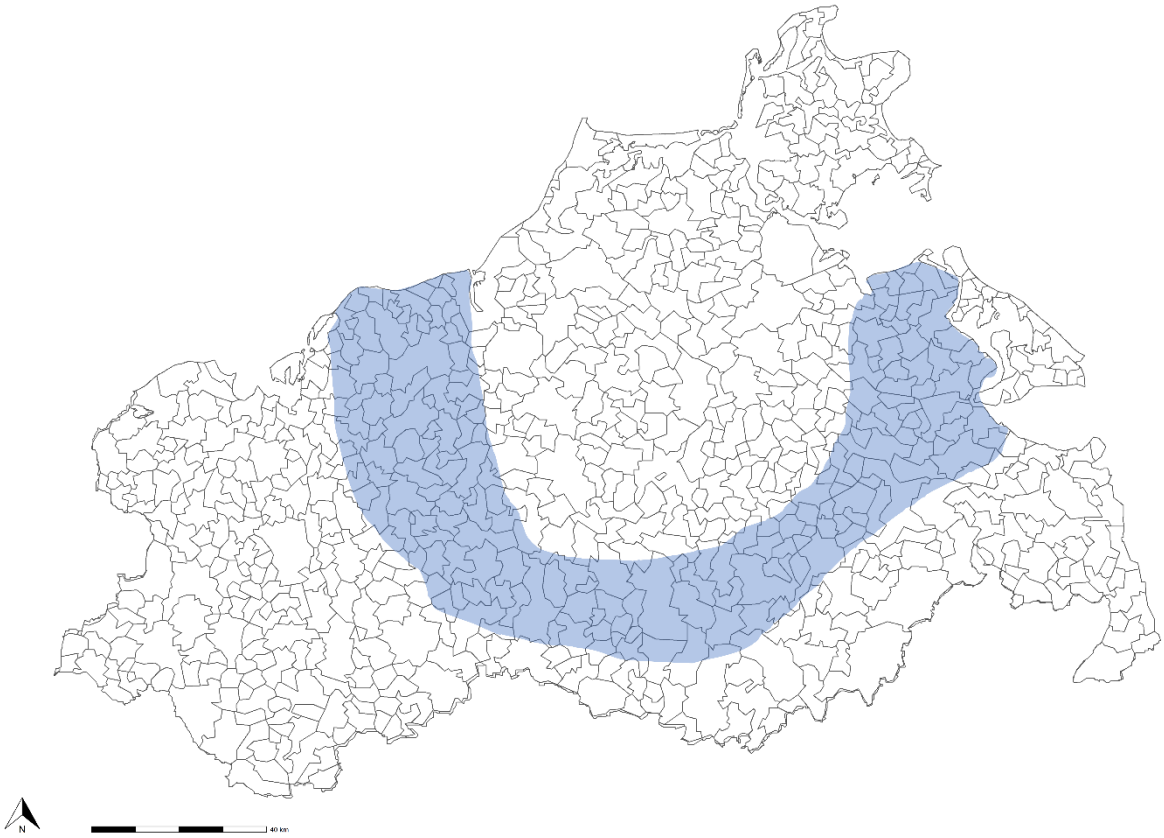

Figure C4: Municipality map of Mecklenburg-Vorpommern, highlighting the area of vaccination (blue). All landscape cells within the blue band were used for vaccination where 30% of susceptible hosts and 15% of susceptible subadults are set to immune every 13 timesteps starting 52 timesteps after the initial outbreak.

Table C1: Parameter setup used in the spatially-explicit classical swine fever-wild boar model. M1: Each of the 10 combinations (5 landscape scenarios × 2 landscape dynamic) was repeated 25 times, resulting in 250 runs in total. M2: Each of the 12 combinations (4 movement strategies × 3 sampling scheme) was repeated 5 times, resulting in 120 runs in total.

Parameter	Values	Reference(s)
Longevity	11 years (572 weeks)	(Jezierski, 1977)
Sex ratio	1:1	(e.g. Durio et al., 2014; Fernández-Llario et al., 1999; Moretti, 2014)
Survival probability of adults and subadults	s_{mean}= 0.6; s_{min} = 0.4	(Focardi et al., 1996; Gaillard et al., 1987)
Survival probability of piglets	s_{mean}= 0.5; s_{min} = 0.1	(Focardi et al., 1996)
Reproduction probability	see Table C2	(Boitani et al., 1995)
Breed count distribution	see Table C3	(Bieber & Ruf, 2005)
Movement rule	HDCRW, HDM, CDM	(Fletcher, 2006)
Tendency to move randomly ρ	0.3	
Mean movement distance D_{mean}	24 km (12 cells) per week	(Morelle et al., 2015)
Maximum movement distance D_{max}	84 km (42 cells) per week	(Morelle et al., 2015)
Individual weekly ranging distance $D_{m,I}$	D_i {1, D_{max}} ~ Wei(26, 1.3)	
Maximal natal dispersal distance d_{disp}	3 cells (6 km)	(Sodeikat & Pohlmeyer, 2003)
Minimum number of dispersers N_{disp}	2 for females; 3 for males	
Case fatality ratio M	0.5	
Mean infectious period μ	4 weeks, 6 weeks	
Transmission probability β	0.022 (base)	
Fertility reduction due to infection	0.625	(Kramer-Schadt et al., 2009)
Probability of prenatal infection	0.5	(Kramer-Schadt et al., 2009)
Transient period t_{trans}	1 week	(Artois et al., 2002; Moennig et al., 2003)
Period of maternal antibodies t_{anti}	12 weeks	(Depner et al., 2000)
Simulated years	100 (5200 weeks), 11 (572 weeks)	
Vaccinated adults (vc_adult)	30 (%)	
Vaccinated subadults (vc_subadult)	15 (%)	

*Continued on the next page

Table C1: Parameter setup - continuation

Parameter	Values	Reference(s)
Pathogen release	random week of the 2nd year	
Mean number of reproductive females	4.5	(European Food Safety Authority, 2009; Howells & Edwards-Jones, 1997; Sodeikat & Pohlmeyer, 2003)
Habitat quality range	[0, 9]	
Initial mean density	5 individuals/km²	(Kramer-Schadt et al., 2009)
Initial age distribution	see Table C4	(Kramer-Schadt et al., 2009)
Age blur in initial individuals	± 3 weeks	
Landscape dynamic	Autocorrelated No dynamic	
Max survival time under low resources S_{max}	10 weeks	
Level of resource mismatch (only M1)	{0,100} %	
Mutation rate	0.01	
Transmission factor	See table C5	
Survival times	See table C5	
Sampling	All individuals, 5 per cell, 5 per municipality	

Table A2: Monthly reproduction probabilities (Boitani et al., 1995) used to stochastically determine the number of breeding females.

Month	Jan	Feb	Mar	Apr	May	Jun	Jul	Aug	Sep	Oct	Nov	Dec
Number of weeks	4	4	5	4	4	5	4	4	5	5	4	4
Reproduction probability	0.0	0.1	0.23	0.34	0.07	0.08	0.06	0.03	0.03	0.0	0.0	0.0

Table A3: Breed count distribution (Bieber & Ruf, 2005) used to estimate litter sizes.

Litter size	0	1	2	3	4	5	6	7	8	9	10	0
Probability	.01306	.06915	.01629	.24994	.24994	.01629	.06915	.01910	.00343	.0004	.00002	.01306

Table A4: Initial age distribution (Kramer-Schadt et al., 2009) used to initialize each model run.

Age (years)	1	2	3	4	5	6	7	8	9	10
Proportion	0.38	0.24	0.15	0.09	0.06	0.03	0.02	0.01	0.01	0.01

Table B5: Pathogen strains with their respective transmission factor and the survival time they impose on infected hosts.

Strain	1	2	3	4	5	6	7	8	9	10	11	12
Transmission factor	.0006	.0007	.0008	.0009	.001	.002	.003	.004	.006	.007	.007	.007
Survival time (weeks)	14	13	11	11	10	9	8	6	3	3	2	1

References

Artois, M., Depner, K.R., Guberti, V., Hars, J., Rossi, S., Rutili, D., 2002. Classical swine fever (hog cholera) in wild boar in Europe. Rev. Sci. Tech. OIE 21, 287–303. https://doi.org/10.20506/rst.21.2.1332

Bieber, C., Ruf, T., 2005. Population dynamics in wild boar *Sus scrofa* : ecology, elasticity of growth rate and implications for the management of pulsed resource consumers: *Population dynamics in wild boar*. Journal of Applied Ecology 42, 1203–1213. https://doi.org/10.1111/j.1365-2664.2005.01094.x

Boitani, L., Mattei, L., Nonis, D., Corsi, F., 1994. Spatial and Activity Patterns of Wild Boars in Tuscany, Italy. Journal of Mammalogy 75, 600–612. https://doi.org/10.2307/1382507

Depner, K.R., Hinrichs, U., Bickhardt, K., Greiser-Wilke, I., Pohlenz, J., Moennig, V., Liess, B., 1997. Influence of breed-related factors on the course of classical swine fever virus infection. Veterinary Record 140, 506–507. https://doi.org/10.1136/vr.140.19.506

Depner, K.R., Müller, T., Lange, E., Staubach, C., Teuffert, J., 2000. Transient classical swine fever virus infection in wild boar piglets partially protected by maternal antibodies. Dtsch Tierarztl Wochenschr 107, 66–68.

Durio, P., Gallo Orsi, U., Macchi, E., & Perrone, A. (2014). Structure and monthly birth distribution of a wild boar population living in mountainous environment. Journal of Mountain Ecology, 3(0). Retrieved from http://www.mountainecology.org/index.php/me/article/view/112

EFSA (European Food Safety Authority). (2009). Control and eradication of Classical Swine Fever in wild boar. European Food Safety Authority Journal, 932(EFSA-Q-2007-200), 1–18. Retrieved from https://efsa.onlinelibrary.wiley.com/doi/abs/10.2903/j.efsa.2009.932

Fernández, N., Kramer-Schadt, S., Thulke, H.-H., 2006. Viability and Risk Assessment in Species Restoration: Planning Reintroductions for the Wild Boar, a Potential Disease Reservoir. E&S 11, art6. https://doi.org/10.5751/ES-01560-110106

Fernández-Llario, P., Carranza, J., Mateos-Quesada, P., 1999. Sex allocation in a polygynous mammal with large litters: the wild boar. Animal Behaviour 58, 1079–1084. https://doi.org/10.1006/anbe.1999.1234

Fletcher, R.J., 2006. Emergent properties of conspecific attraction in fragmented landscapes. The American naturalist 168, 207–219. https://doi.org/10.1086/505764

Focardi, S., Toso, S., Pecchioli, E., 1996. The population modelling of fallow deer and wild boar in a Mediterranean ecosystem. Forest Ecology and Management 88, 7–14. https://doi.org/10.1016/S0378-1127(96)03804-2

Gaillard, J. M., Vassant, J., & Klein, F. (1987). Quelques caractéristiques de la dynamique des populations de sangliers (Sus scrofa scrofa) en milieu chassé. Gibier, Faune Sauvage / ONC, Office National de La Chasse, 4, 31–47.

Grimm, V., Berger, U., Bastiansen, F., Eliassen, S., Ginot, V., Giske, J., Goss-Custard, J., Grand, T., Heinz, S.K., Huse, G., Huth, A., Jepsen, J.U., Jørgensen, C., Mooij, W.M., Müller, B., Pe'er, G., Piou, C., Railsback, S.F., Robbins, A.M., Robbins, M.M., Rossmanith, E., Rüger, N., Strand, E., Souissi, S., Stillman, R.A., Vabø, R., Visser, U., DeAngelis, D.L., 2006. A standard protocol for describing individual-based and agent-based models. Ecological Modelling 198, 115–126. https://doi.org/10.1016/j.ecolmodel.2006.04.023

Grimm, V., Berger, U., DeAngelis, D.L., Polhill, J.G., Giske, J., Railsback, S.F., 2010. The ODD protocol: A review and first update. Ecological Modelling 221, 2760–2768. https://doi.org/10.1016/j.ecolmodel.2010.08.019

Grimm, V., Railsback, S.F., Vincenot, C.E., Berger, U., Gallagher, C., DeAngelis, D.L., Edmonds, B., Ge, J., Giske, J., Groeneveld, J., Johnston, A.S.A., Milles, A., Nabe-Nielsen, J., Polhill, J.G., Radchuk, V., Rohwäder, M.-S., Stillman, R.A., Thiele, J.C., Ayllón, D., 2020. The ODD Protocol for Describing Agent-Based and Other Simulation Models: A Second Update to Improve Clarity, Replication, and Structural Realism. JASSS 23, 7. https://doi.org/10.18564/jasss.4259

Howells, O., Edwards-Jones, G., 1997. A feasibility study of reintroducing wild boar Sus scrofa to Scotland: Are existing woodlands large enough to support minimum viable populations. Biological Conservation 81, 77–89. https://doi.org/10.1016/S0006-3207(96)00134-6

Jędrzejewska, B., Jędrzejewski, W., Bunevich, A.N., Miłkowski, L., Krasiński, Z.A., 1997. Factors shaping population densities and increase rates of ungulates in Bialowieza Primeval Forest (Poland and Belarus) in the 19th and 20th centuries. Acta Theriologica.
Jezierski W., 1977: Longevity and mortality rate in a population of wild boar. Acta theriol., 22, 24: 337—348

Kramer-Schadt, S., Fernández, N., Eisinger, D., Grimm, V., Thulke, H.-H., 2009. Individual variations in infectiousness explain long-term disease persistence in wildlife populations. Oikos 118, 199–208. https://doi.org/10.1111/j.1600-0706.2008.16582.x

Kürschner, T., Scherer, C., Radchuk, V., Blaum, N., Kramer-Schadt, S., 2021. Movement can mediate temporal mismatches between resource availability and biological events in host–pathogen interactions. Ecol. Evol. 11, 5728–5741. https://doi.org/10.1002/ece3.7478

Kürschner T, Scherer C, Radchuk V, Blaum N, Kramer-Schadt S. 2022. Resource asynchrony and landscape homogenization as drivers of virulence evolution. Under review.

Leaper, R., Massei, G., Gorman, M.L., Aspinall, R., 1999. The feasibility of reintroducing Wild Boar (Sus scrofa) to Scotland. Mammal Review 29, 239–258. https://doi.org/10.1046/j.1365-2907.1999.2940239.x

Liess, B., 1987. Pathogenesis and epidemiology of hog cholera. Ann Rech Vet 18, 139–145.

Melis, C., Szafranska, P.A., Jedrzejewska, B., Barton, K., 2006. Biogeographical variation in the population density of wild boar (Sus scrofa) in western Eurasia. J Biogeography 33, 803–811. https://doi.org/10.1111/j.1365-2699.2006.01434.x

Moennig, V., Floegel-Niesmann, G., Greiser-Wilke, I., 2003. Clinical signs and epidemiology of classical swine fever: a review of new knowledge. Vet J 165, 11–20. https://doi.org/10.1016/s1090-0233(02)00112-0

Morelle, K., Podgórski, T., Prévot, C., Keuling, O., Lehaire, F., Lejeune, P., 2015. Towards understanding wild boar *S us scrofa* movement: a synthetic movement ecology approach: A review of wild boar *Sus scrofa* movement ecology. Mammal Review 45, 15–29. https://doi.org/10.1111/mam.12028

Moretti, M., 2014. Birth distribution, structure and dynamics of a hunted mountain population of Wild boars (Sus scrofa L.), Ticino, Switzerland. Journal of Mountain Ecology 3.

Pepin, K.M., Davis, A.J., Beasley, J., Boughton, R., Campbell, T., Cooper, S.M., Gaston, W., Hartley, S., Kilgo, J.C., Wisely, S.M., Wyckoff, C., VerCauteren, K.C., 2016. Contact heterogeneities in feral swine: implications for disease management and future research. Ecosphere 7. https://doi.org/10.1002/ecs2.1230

Rossi, S., Pol, F., Forot, B., Masse-provin, N., Rigaux, S., Bronner, A., Le Potier, M.-F., 2010. Preventive vaccination contributes to control classical swine fever in wild boar (*Sus scrofa* sp.). Veterinary Microbiology 142, 99–107. https://doi.org/10.1016/j.vetmic.2009.09.050

Saura, S., Martínez-Millán, J., 2000. Landscape patterns simulation with a modified random clusters method. Landscape Ecology 15, 661–678. https://doi.org/10.1023/A:1008107902848

Sodeikat, G., Pohlmeyer, K., 2003. Escape movements of family groups of wild boar *Sus scrofa* influenced by drive hunts in Lower Saxony, Germany. Wildlife Biology 9, 43–49. https://doi.org/10.2981/wlb.2003.063

Spitz, F., Janeau, G., 1990. Spatial strategies: an attempt to classify daily movements of wild boar. Acta Theriologica 35, 129–149.

Wilensky, U. (1999). NetLogo (Version 6.2.0). Retrieved from http://ccl.northwestern.edu/netlogo/

C2 Additional figures

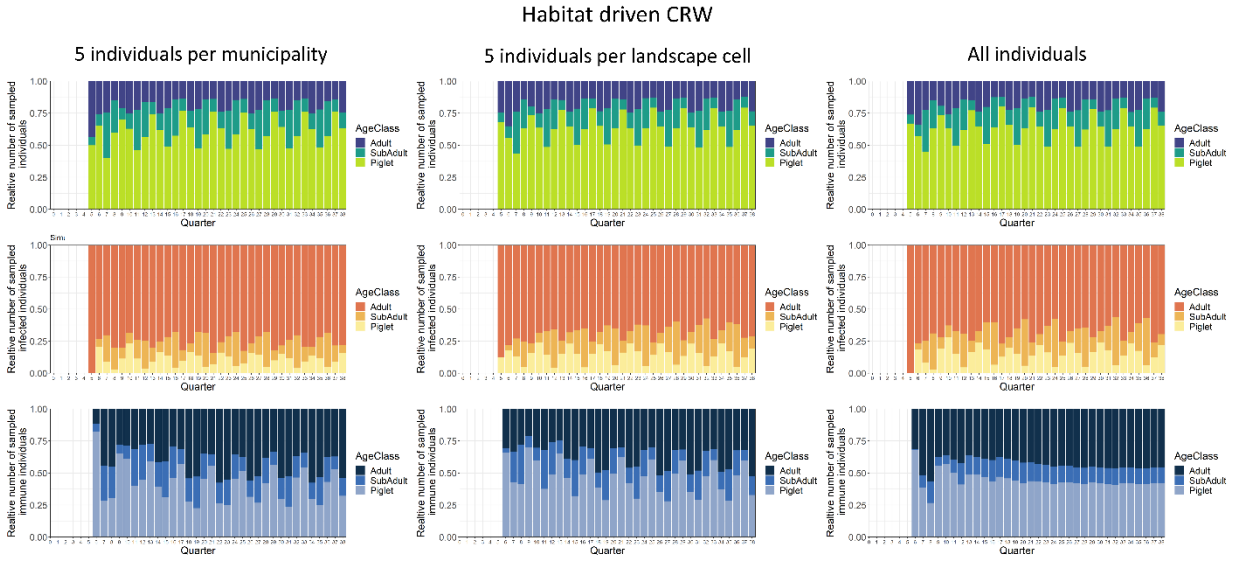

Figure C5: Relative number of sampled individuals per age class (adult, subadult, piglet, colour) in the HDCRW scenario with the sampling schemes (left to right) for all susceptible individuals (top), infected individuals (middle) and immune individuals (bottom).

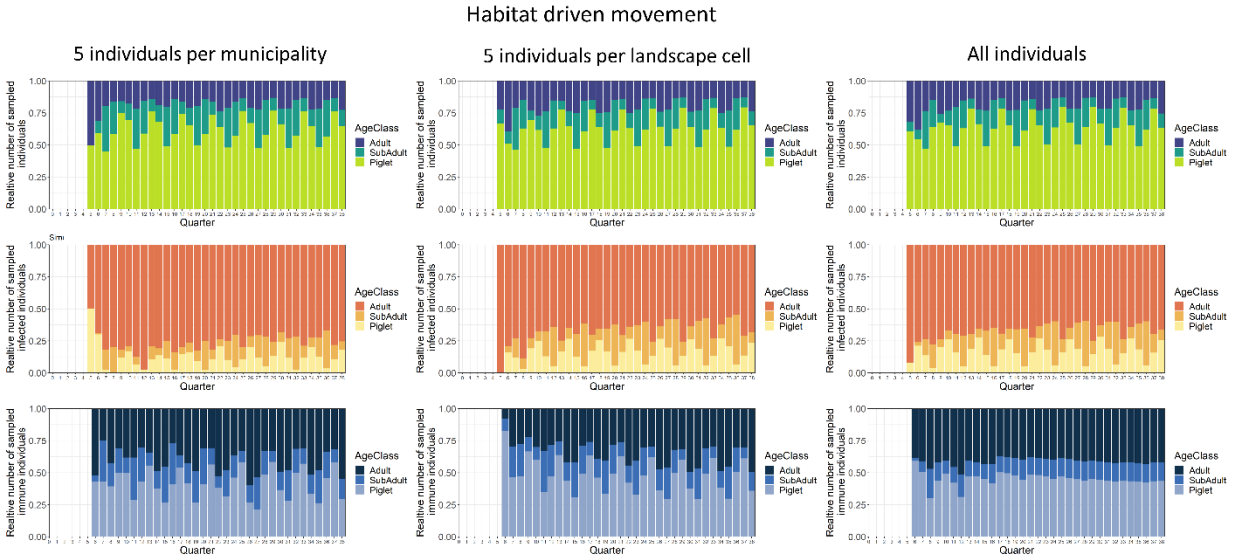

Figure C6: Relative number of sampled individuals per age class (adult, subadult, piglet, colour) in the HDM scenario with the sampling schemes (left to right) for all susceptible individuals (top), infected individuals (middle) and immune individuals (bottom).

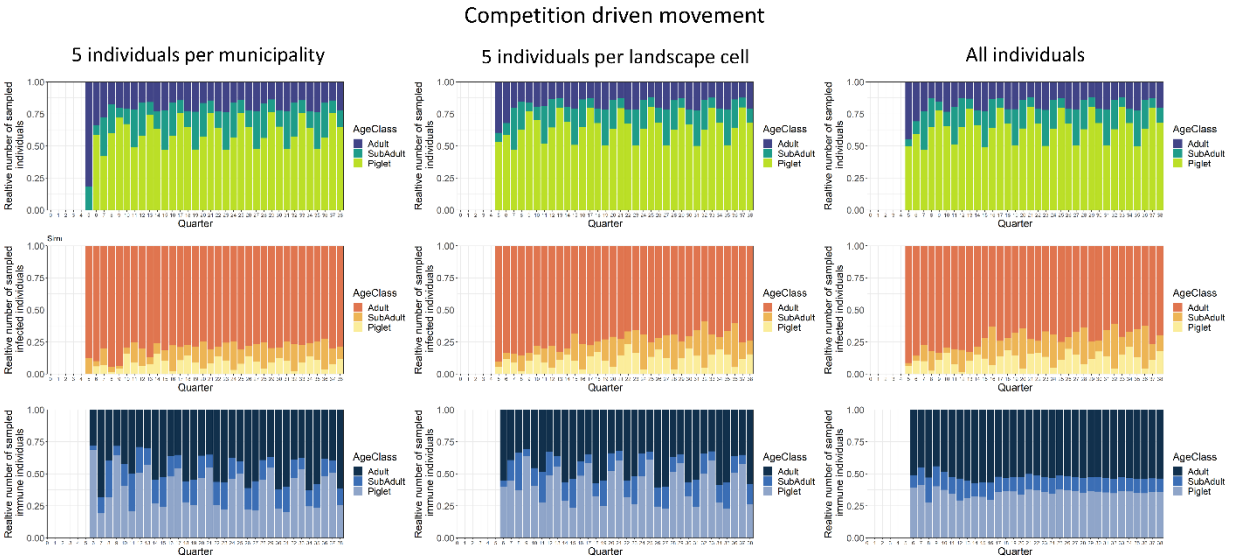

Figure C7: Relative number of sampled individuals per age class (adult, subadult, piglet, colour) in the CDM scenario with the sampling schemes (left to right) for all susceptible individuals (top), infected individuals (middle) and immune individuals (bottom).

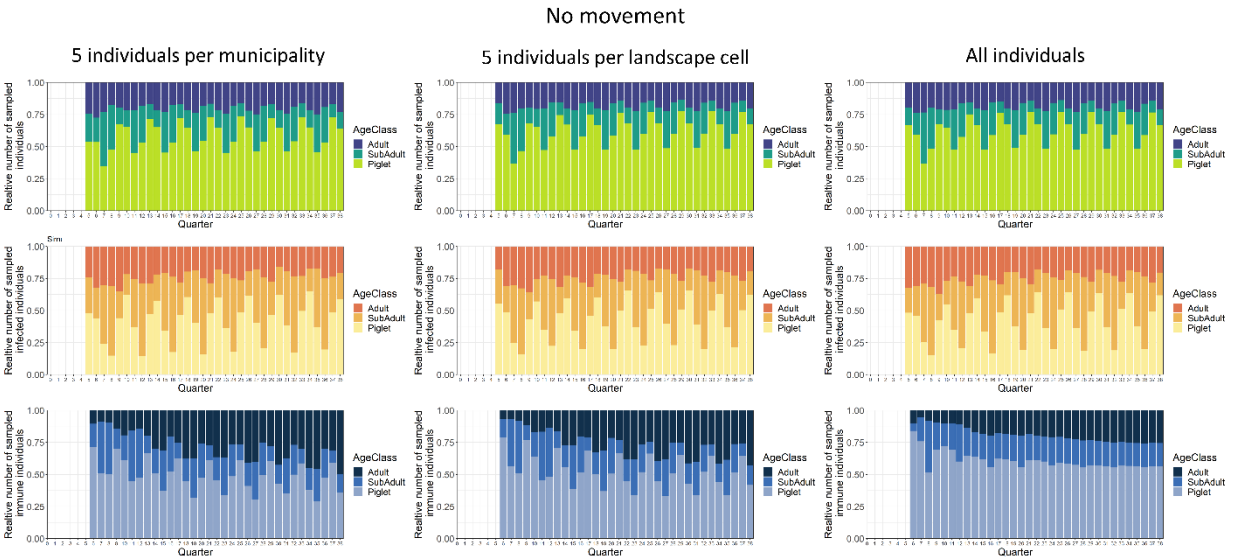

Figure C8: Relative number of sampled individuals per age class (adult, subadult, piglet, colour) in the no movement scenario with the sampling schemes (left to right) for all susceptible individuals (top), infected individuals (middle) and immune individuals (bottom).

Declaration of Authorship

I hereby declare to have prepared this dissertation independently under the commonly accepted help of my supervisors. All direct or indirect sources used are given as references. All contributions of co-authors are acknowledged. This thesis has not been submitted to any other university or institution before.

Potsdam,

_____

Tobias Kürschner